Wind climate and urban geometry

Document Version:
Publisher's PDF, also known as Version of Record (includes final page, issue and volume numbers)

Please check the document version of this publication:

WIND CLIMATE
AND
URBAN GEOMETRY

Marcel Bottema

WIND CLIMATE

AND

URBAN GEOMETRY

WIND CLIMATE
AND
URBAN GEOMETRY

PROEFSCHRIFT

ter verkrijging van de graad van doctor aan de
Technische Universiteit Eindhoven, op gezag van
de Rector Magnificus, prof. dr. J.H. van Lint,
voor een commissie aangewezen door het College
van Dekanen in het openbaar te verdedigen op
dinsdag 12 januari 1993 te 16.00 uur

door

MARCEL BOTTEMA

geboren te Utrecht

Dit proefschrift is goedgekeurd
door de promotoren

prof. ir. J.A. Wisse
prof. ir. R.H.M. Uytenhaak

VOORWOORD

Bij het totstandkomen van dit proefschrift, en bij het onderzoek, zijn een groot aantal mensen betrokken geweest.

CONTENTS

NOTATION

a	Velocity scale in Weibull distribution (eq. 3.9) [m/s]
A	Area [m^2]
A_{Du}	Total body area (DuBois area) (eq. 3.3) [m^2]
A_f	Frontal area of body (eq. 3.2) [m^2]
A_p	Projected area (of body) [m^2]
A_s	Side wind area of body (eq. 3.2)[m^2]
A	Constant [-] in eq. 2.4 (geostrophic drag law); A = 1.8 in neutral ABL
B	Constant [-] in eq. 2.4 (geostrophic drag law); A = 4.5 in neutral ABL
c_p	Specific heat of air (1004 J kg^{-1} K^{-1})
C_p	Pressure coefficient (eq. 2.20) [-]
C_{pHo}	Pressure coefficient with U_{Ho} as reference speed [-]
C_μ	K-ϵ model constant [-]
d_x	distance between obstacle faces (x-direction; fig. 4.6) [m]
d_y	distance between obstacle faces (y-direction; fig. 4.6) [m]
D_x, D_y	As d_x and $_y$, but for high rise buildings (fig. 4.18) [m]
D/Dt	Material or total derivative along a streamline [1/s], eq. 2.17
e_t	Truncation error
E'	Constant in FLUENT wall function [-]
f	Coriolis parameter (1.146 /s for 52° NB)
f	Frequency (in section 2.3) [1/s]
F	Force [N]
g	Gravitational acceleration [m/s^2]
h	Height of low rise buildings [m]
h	Body height (in chapter 3) [m]
h_{IBL}	Height of internal boundary layer (eq. 2.13 or eq. 4.4) [m]
G	Macro wind at top of boundary layer (eq. 2.4) [m/s]
H	Building height [m]
H_o	Sensible heat flux from surface [W/m^2]
k	Peak factor in eq. 2.12 and eq. 3.7 [-]
k	Shape factor in Weibull distribution (eq. 3.9) [-]
K	Kinetic energy of turbulence per unit mass (eq. 2.9) [m^2/s^2]
K_0	or $K_0(z)$: Approach flow turbulent kinetic energy [m^2/s^2]
$K_{0,loc}$	As K_0, but in absence of building (x,y = 0) [m^2/s^2]
L	Building length or thickness (fig. 4.7) [m]
L	Length scale [m], e.g. of building influence
L	Length of hill slope, roughness strip etc. [m]
L_a	Actual wake length (eq. 4.7) [m]
L_F	Length of frontal vortex [m]
L_g	Length scale of gust (chapter 3) [m]
L_g	Geometrical influence scale (eq. 4.8) [m]
L_0	Wake length for standard conditions (eq. 4.7) [m]
L_P	Podium length (fig. 4.25) [m]
L_R	Length of recirculation zone [m]
L_s	Length parameter of area with decreased discomfort probability [m]
m	Mass [kg]
M	Metabolism [W]

M	Wind speed parameter in eq. 3.9 [m/s]
p	Pressure [N/m^2]
p	Fluctuating part of pressure (eq. 2.26 only) [N/m^2]
p_0	Ambient pressure [N/m^2]
p(u)	Probability density funtion of u (eq. 2.11)
P	Discomfort or danger probability [%] (in chapter 6: days per year)
P_{max}	Maximum acceptable P (chapter 3) [%]
P_{max}	Maximum discomfort probability near building (chapter 5) [%]
$P_{max,d}$	Maximum danger probability near building (chapter 5) [%]
P_o	Discomfort or danger probability in approach flow [%]
r	Length over which building corner is rounded, stepped, etc. (fig. 4.26) [m]
R	Radius of corner stream 'circle' [m]
R_D	Radius of circle of increased discomfort probability (chapter 5) [m]
R_{dan}	Radius of circle of unacceptable danger probability (chapter 7) [m]
S	Clear spacing or street dimension [m]
S_x	Clear spacing in x direction (fig. 4.6; fig. 4.18) [m]
S_x	Street length [m]
S_y	Clear spacing in y direction (fig. 4.6; fig. 4.18) [m]
S_y	Street width [m]
t	Time [s]
t_g	Time over which gust speed is approx. constant [s]
T	Air temperature [K]
T_i	Turbulence intensity σ_i/U for fluctuating component i (u,v,w) (eq. 2.8) [-]
u	or u': Fluctuating part of U-velocity [m/s]
u_i	Fluctuating velocity component (i = 1,2,3) [m/s]
u_iu_j	Kinematic Reynolds stress (i,j = 1,2,3) [m^2/s^2]
U	Velocity scale (chapter 2) [m/s]
U	Mean streamwise velocity component (chapter 2) [m/s]
U	Mean wind speed (default: at pedestrian level = 1.75 m height) [m/s]
U_e	Equivalent wind speed (eq. 3.7) [m/s]
U_g	Gust speed [m/s]
U_i	Mean velocity component for i-directon (i = 1,2,3) in chapter 2; instantaneous velocity for eq. 2.16 through 2.20 [m/s]
U_{pot}	Potential wind speed (z_0 = 0.03 m; z = 10 m) [m/s]
U_{Ho}	Approach flow wind speed at height H [m/s]
U_o	or $U_o(z)$: Approach flow wind speed at height z [m/s]
$U_{o,loc}$	As for U_o, but in absence of building (x,y = 0) [m/s]
U_t	Momentary streamwise velocity U(t) [m/s]
$U_{2.5h}$	Reference speed for low rise building groups at 2.5 building heights [m/s]
U_3	Gust speed with t_g = 3 sec (chapter 3) [m/s]
U_{10}	As U_3 but with t_g = 10 sec (chapter 3) [m/s]
U^*	Friction velocity (eq. 2.2) [m/s]
v	or v': Fluctuating part of V-velocity [m/s]
V	Mean lateral velocity component [m/s]
V	Walking or cycling speed (chapter 3) [m/s]
w	or w': Fluctuating part of W-velocity [m/s]
W	Building width (fig. 4.7) [m]
x	Streamwise coordinate [m]

x	fetch (over new terrain) [m]
x_i	Coordinate (chapter 2) (i = 1,2,3) [m]
x_{loc}	Fetch over terrain with $z_0 = z_{0,loc}$ [-]
x_{ref}	Upstream reference location [m]
y	Lateral coordinate [m]
z	Vertical coordinate [m]
z_d	displacement length [m]
z_L	Monin Obukhov length [m]
z_0	Aerodynamic roughness length [m]
	z_0^+ is the larger of two roughness lengths
$z_{0,b}$	z_0 of building surface [m]
$z_{0,loc}$	z_0 of local ground surface (near building) [m]
$z_{0,s}$	z_0 of street surface [m]

α	angle between surface wind and macro wind (eq. 2.5)
α	Power law exponent [-]
γ	Wind amplification factor U/U_{pot} [-]
γ_e	'effective' γ: direction independent γ which yields the same wind climate as in reality.
γ_{min}	direction independant γ for which discomfort probability ≈ 0 [-]
γ_{max}	direction independant γ for which local wind climate starts to be unacceptable [-]
δ	Boundary layer height [m]
δ_{ij}	Kronecker delta tensor [-]: $\delta_{ij} = 1$ for i=j, else $\delta_{ij} = 0$
Δ	difference between / in
Δf	Frequency shift in LDA [1/s]
ΔS	Fractional speed up factor S [-]
ε	Dissipation rate of K [m^2/s^3]
η_e	Efficiency for Extra Work $EW/(M-M_0)$ [-]
η_t	Total efficiency EW/M [-]
θ	Equilibrium angle for 'hanging' in the wind (fig. 3.1)
θ	Wind direction (fig. 4.7)
θ_{max}	Wind direction with maximum U/U_{Ho}
κ	von Karman constant (0.4) [-]
λ	Relative increment in spacing of neighbouring grid lines (chapter 2) [-]
λ_e	Wake length correction factor; end effect (fig. 4.14) [-]
λ_f	Frontal area density (w h) / ($d_x d_y$) [-]
λ_r	Wake length correction factor [-]; effect of approach flow roughness (fig. 4.14, fig. 4.28)
λ_S	Scale factor: L_m/L_{fs} (chapter 2) [-]
λ_W	Wake length correction factor; effect of obstacle width (fig. 4.14) [-]
λ_θ	Wake length correction factor; effect of approach flow angle (fig. 4.14) [-]
ν	Kinematic viscosity (1.3-1.5 m^2/s for air)
ν_t	Turbulent viscosity or eddy viscosity [m^2/s]
ϕ	porosity [-]
ρ	air density (1.293 kg/m^3 in FLUENT)
σ	Standard deviation or standard error (uncertainty)

σ_i Standard deviation in velocity component i (i = u,v,w) [m/s]
$\sigma(x,y)$ Dimensionless solution function for ΔS (fig. 4.4) [-]
σ_Δ 'standard difference' between estimated and measured γ (eq. 6.1)
τ Turbulent shear stress $\rho u'w'$ [N/m^2]
ψ Stability correction [-]

Subscripts:

det   of detail
fs   full scale
gap   of gap
H   At height H
Ho   Of approach flow at height H
i   The three coordinate directions: i=1: streamwise, i=2: lateral, i=3: vertical
j,k,l As i
loc   local ($z_{0,loc}$ for local surface roughness)
min   minimum / the smallest of
max   maximum / the largest of
m   model scale
o   Of approach flow
o   Of surface (for z_0, τ_0, H_0)
t   turbulent (except U_t)

Superscripts

+   The largest of

Abbreviations:

ABL   Atmospheric boundary layer
EW   Extra work
Fr   Froude number [-] (section 2.3.1.1)
HWA   Hot wire anemometer
IBL   Internal boundary layer
LDA   Laser Doppler anemometer
min(a,b)   The lesser of a and b
max(a,b)   The larger of a and b
Re   Reynolds number UL/ν [-]
St   Strouhal number Ut/L [-]
|u| Absolute value of u(t)-component

1   Introduction

1.1   Design and outdoor climate

Buildings should provide shelter for human activities. In too many cases, this
shelter is only provided indoors. However, outdoor climate is influenced by men
as well. Too little attention for outdoor climate may cause increased levels of
air pollution, too much or too little sunshine and daylighting, energy losses
because of excessive ventilation of buildings, wind nuisance in streets around
buildings, and in some cases even structural damage.
The effects of outdoor climate can be divided into three classes, as is shown in
figure 1.1:

```
                        ┌──────────────────┐
            ┌───────────│  outdoor climate  │───────────┐
            │           └──────────────────┘           │
            │                    │                      │
  ┌──────────────────┐  ┌──────────────────┐  ┌──────────────────┐
  │ preconditions for │  │ building:         │  │ interference with │
  │ indoor climate    │  │ construction      │  │ outdoor activities│
  │                   │  │ maintenance       │  │                   │
  └──────────────────┘  └──────────────────┘  └──────────────────┘
            │                    │                      │
  ┌──────────────────┐  ┌──────────────────┐  ┌──────────────────┐
  │ noise             │  │ wind forces       │  │ noise             │
  │ air pollution     │  │ air pollution     │  │ air pollution     │
  │ ventilation       │  │ driving rain      │  │ wind nuisance     │
  │ temperature       │  │ frost             │  │ temperature       │
  │ daylight          │  │ snow loading      │  │ daylight          │
  │ sun/radiation     │  └──────────────────┘  │ sun/radiation     │
  │ moisture          │                        │ moisture          │
  └──────────────────┘                        │ rain              │
                                               └──────────────────┘
```
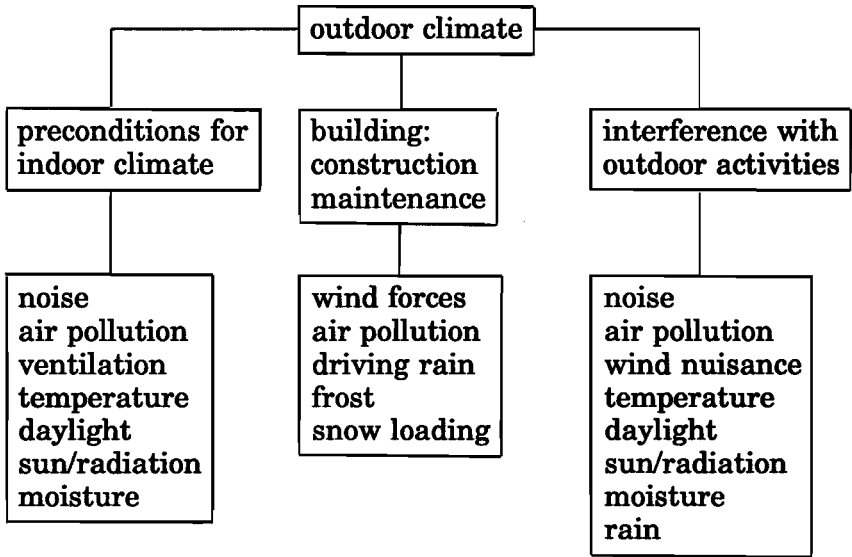
Figure 1.1:   *Classification of effects of outdoor climate*

First of all, outdoor climate determines the buildings' life time, its
maintenance, and its appearance. The buildings' maintenance and the
buildings' appearance are influenced by air pollution, rain penetration and
frost. Stability and strength of a building should be sufficient to withstand
wind loading (both static and dynamic) and snow and water loading during its
lifetime.

Outdoor climate should also be taken into account when designing for indoor climate. The required sound insulation, indoor lighting, and heating/cooling depends on outdoor levels of sound, daylight, solar radiation, and outdoor temperature.

Finally it is important to note that outdoor areas (pedestrian walkways, roads, parks etc.) should be suitable and comfortable for human activities. Many properties of outdoor climate (wind, noise, air pollution, daylight, radiation) are influenced by men, and by the way they build. Designing for outdoor climate is a logical and necessary step in order to create a comfortable outdoor environment.

Different properties of outdoor climate yield different consequences for urban design. This may give rise to conflicting requirements (see Oke, 1988): Too much shelter may lead to local accumulation of air pollution, whereas too little shelter leads to uncomfortable or even dangerous situations for pedestrians. These conflicting requirements call for integrated advice on all issues of outdoor climate. By now, this is not feasible because knowledge on many issues is far too limited.

1.	Requirements	
2.	Information phase	Handbook / design rules
3.	Sketch design	Wind expert / expert model
4.	Towards a final design	Wind tunnel test
5.	Construction	
6.	Evaluation	Wind expert
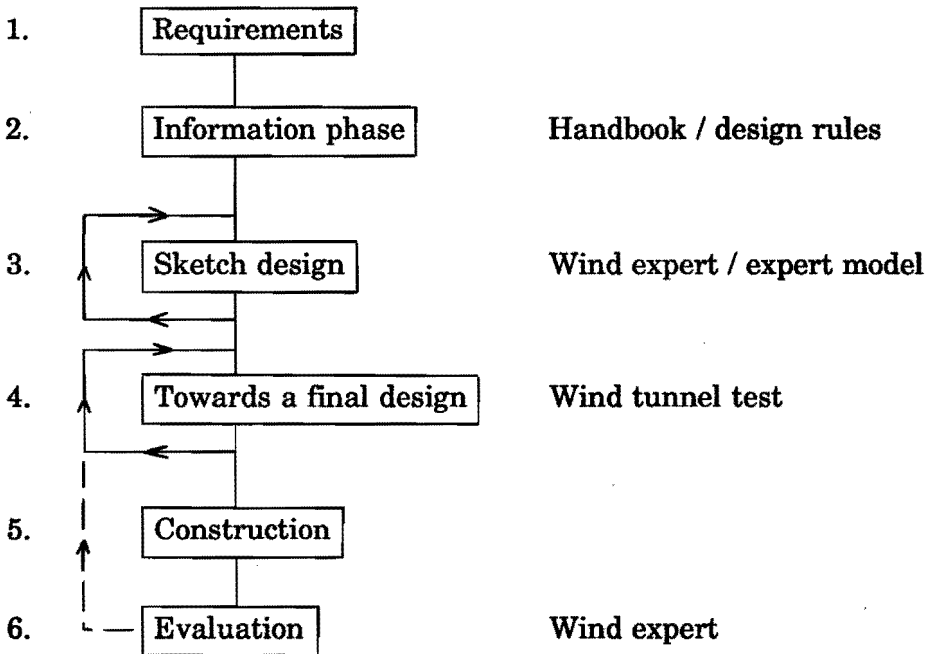
Figure 1.2:   *Incorporation of wind climate forecasts (on the right) into the design process. See text for explanation of the above key words.*

Especially prediction of the relation between air pollution levels and urban geometry is very difficult. The same applies to incorporation of this knowledge into the early stages of design. Prospects are much better for early prediction of wind climate, i.e. pedestrian comfort and safety. This is the subject of the present study.

Figure 1.2 shows how wind climate forecasts can be incorporated into the design process. It is of great importance that wind climate forecasts are available before or in the sketch design stage. In later stages, building dimensions, orientation, and use of outdoor space are almost fixed and little can be done to improve an already uncomfortable wind climate.

In the first design stage, it should be made explicit which human activities are foreseen, both indoors and outdoors. For each of the outdoor activities, requirements can be formulated in terms of outdoor (wind) climate.

The next stage is one of gathering and analyzing information. In the case of wind comfort, design rules and hand books can be consulted in order to get a first impression of building types which will yield the required wind climate. A similar approach can, and should, be taken for other environmental aspects as given in figure 1.1.

If (or before) a first sketch design is available, the architect can consult a wind expert. The expected wind climate can be judged, the sketch design can be improved and the effects of improvements can be analyzed.

When the design is almost finished, a wind tunnel test can be carried out in order to check whether wind climate meets requirements as set by the planned outdoor human activities. Eventually, some (minor) design modifications must result in the desired improvement in wind climate.

A final issue in 'wind conscious design' is evaluation: is the acceptability of outdoor conditions as expected?

1.2 Wind comfort; state of the art

Planning with wind is not limited to modern times. There are several examples of wind conscious design in antiquity (see Aynsley et al, 1977). Vitruvius' (75-26 B.C.) works are probably the best known, but not the oldest. Vitruvius suggests that house blocks should be oriented at an angle of 45⁰ to prevailing winds, so that 'winds strike against the angles of the blocks, and their force be broken up and dispersed' (Kenworthy, 1985). Three centuries later, attention is shifted from wind comfort to air pollutant removal. Oribasius, suggests that winds should blow along the streets in order to promote removal of 'smoke, dust and all kinds of exhalations' (Kenworthy, 1985).

It is not before about 1960 that problems of wind environment and pedestrian comfort became an issue in scientific literature (Hutchinson, 1978). Uncomfortable wind conditions were experienced around several new high rise building developments. At the same time, new wind tunnel facilities became available which were able to simulate (the lower part of) the atmospheric boundary layer.

Two important facts became clear in this period:
-wind speed increases significantly with height
-high rise buildings tend to bring wind speeds at roof height down to pedestrian level

In the seventies and in the eighties, there was a rapid development in wind comfort research. Wind problems around typical (high rise and low rise) building configurations were identified (Gandemer, 1975), and parametric studies were carried out (e.g. Isyumov et al, 1975; Beranek, 1980; Maruta, 1984; Alberts, 1981). Research into wind effects on people (Hunt et al, 1976; Murakami et al, 1980) led to the development of several wind comfort criteria. Finally, there was important progress in boundary layer meteorology (see Panofsky, 1984) which allowed for linkage of local wind conditions to climate statistics on a meteorological station (Jensen et al, 1984).
In the last decade, computational fluid dynamics (Ferziger, 1990) became available as a tool for parametric studies. Knowledge based expert systems (Reed, 1990) came into the picture as well.

Incorporation of wind into the design process (figure 1.2) is an important issue. Until 1960, there were just a few very rough guidelines of good and bad practice, to be used in the early information stage. The development of wind tunnel techniques in the sixties brought a marked change. The growing awareness of wind problems resulted in a rapid growth in ad hoc wind tunnel testing, and this has become standard.
In the last decade, it has become clear that afterwards wind tunnel testing alone is not very effective. Wind comfort advice should be brought in at the early design stages, where most important design decisions are made (Arens, 1982). Such advice includes inventarization of suitable building geometries, and testing of selected building geometries. Glaumann and Westerberg (Glaumann et al, 1988; Westerberg et al, 1990) have tried to transfer the existing wind comfort knowledge to the architect and town planner in handbook form. Stathopoulos et al (1991) proposed an expert model which is also based on existing data. However, this model is merely a controlling device, and therefore more suitable for the sketch design stage than for the information stage.

The above mentioned expert model and handbook are both handicapped by the lack on reliable flow field data around buildings. Numerical simulation may be a tool to obtain a better understanding of wind flow around buildings, and to extend the flow field 'data base'.

1.3   Aim of the present work

By 1988, when the present study was started, the need for incorporation of wind comfort knowledge into the early design stages was recognized in the Netherlands. Rules of thumb (Beranek, 1982) did exist but they did not make clear whether wind climate was acceptable for certain human activities or not.

The initial aim of this study was to analyze and supplement existing knowledge of prediction of wind comfort, and to communicate the results to architects and town planners by means of either verbal or graphical design rules. This aim can be summarized with the words 'technology transfer'.

The proposed investigation methods were mainly literature study and analysis of existing experimental results, supplemented with own experiments and numerical simulations.

During research, several problems were encountered which raised a great number of questions. These questions were often very fundamental. For example, it turned out that results of comfort investigations (Jackson, 1978) were incorporated in none of the present comfort criteria (chapter 3). Other 'fundamental' issues are related to reliability of common measurement techniques (see Bottema et al, 1991) and to the interpretation and presentation of results. It does not make sense to state that a near zero wind speed has increased threefold after introduction of a high rise building. Yet, such kinds of statements are quite common in scientific literature.

The above problems called for some adjustment in the initial aim. The aims of the present study can now be formulated as:

1. *critical re-evaluation of the present wind comfort knowledge, and its presentation.*
2. *extension of the present knowledge of the prediction of wind comfort in order to allow for general guidelines*
3. *transfer of wind comfort knowledge to the architect. This knowledge should be applicable in the information stage and in the sketch design stage (figure 1.2).*

The importance of the above mentioned investigation methods has also changed during the present investigations.

In the present study, numerical simulation has become the main tool to extend knowledge of wind flow around buildings, despite its limitations and inaccuracies (see the end of chapter 2). An advantage of numerical simulation is a better understanding of mutual relations between flow properties (e.g. wind speed and wind pressure; wind speed, its gradients, and gustiness) and their spatial distributions.

Wind tunnel measurements are most suitable for validation of numerical results. Comparison of numerical and experimental results has increased knowledge and awareness of experimental errors (Bottema et al, 1991).

Literature study is mainly used to choose suitable wind comfort (and safety) criteria, and to choose a method to link wind conditions at the building site to wind conditions on a meteorological station. Literature results were also used to choose geometries of interest and, where possible, to supplement (and comment upon) numerical results.

5

1.4 Outline of the present thesis

Before discussing the contents of this thesis, we will introduce some important concepts.

Judgement of wind climate is the main issue of this thesis. Figure 1.3 shows components of such a judgement.
We start with a *discomfort threshold*: a wind speed at which wind starts to be experienced as unpleasant. If a gust speed is used as a threshold, the next step is to convert this speed into a local (hourly) mean wind speed.
Discomfort probability is defined as the percentage of hours for which wind conditions are unpleasant. Discomfort probability can be determined if we know how often a local wind speed occurs, i.e. if we know the long term statistics of mean local wind speed.
The final steps are judgement of wind climate (which discomfort probability is acceptable), and measures to improve the design.
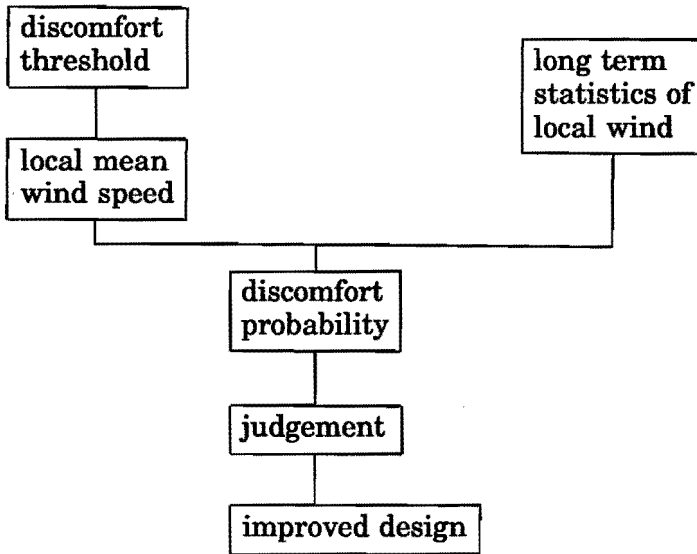
Figure 1.3: Scheme for judging acceptability of wind climate.

The scheme of figure 1.3 has a serious drawback: climate statistics are generally only available at a meteorological site, not at the location to be considered. This problem can be overcome by the definition of a *wind amplification factor* γ. Wind amplification factor is defined as the ratio of (hourly averaged) local wind speed U, and wind speed at 10 m height at an ideal meteorological site (the potential wind speed U_{pot}).

In formula, wind amplification factor γ is defined as:

$$\gamma = U / U_{pot} \qquad\qquad (1.1)$$

Figure 1.4 presents the relation between local wind speed and potential wind speed in a graphical way:
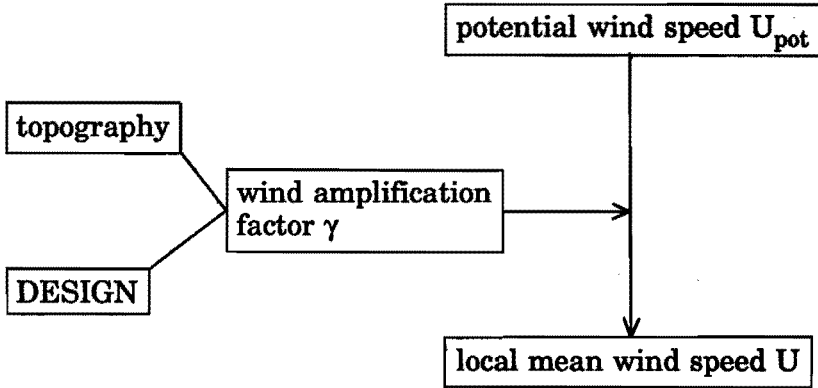
Figure 1.4: *Wind amplification factor γ is determined by design of building and site and by topography. Local mean wind speed U and potential wind speed U_{pot} are linked by $U = \gamma * U_{pot}$*

The structure of this thesis is as follows:

Chapter 2 discusses measuring and simulation techniques which are used in this study. Theory of flow in the atmospheric boundary layer (definition in chapter 2) is presented, as well as theory of flow around obstacles.

Chapter 3 discusses which thresholds should be used for discomfort and danger (i.e. risk of falling) due to wind. It is also discussed which maximum discomfort probability is acceptable, and how many shelter is needed in terms of wind amplification factor γ.

Wind amplification factor γ (*chapter 4*) is determined by processes on a hierarchy of scales:

-terrain (terrain roughness within 20 km, hills etc.)
-building (dimensions, orientation etc.)
-detail (architectural features of building and site: e.g. corner shape and wind screens)

In figure 1.4, building and detail are indicated as 'design'; terrain roughness, hills etc. are indicated as topography.

Chapter 5 gives estimates of discomfort probability as a function of terrain type and building geometry.

Chapter 6 is about applicability and accuracy of wind comfort forecasts. The first part discusses cooperation between the architect and the wind engineer. In the second part, accuracy of early wind comfort forecasts is judged by comparison with wind tunnel data.

The information of the chapters 2 through 6 is condensed into *chapter 7* which gives a number of 'design rules' for the architect. Chapter 7 gives simple tools for judging acceptability of wind climate, and it presents alternatives if a proposed building does not meet the requirements for a comfortable wind climate.

Now which chapters are meant for the specialist, and which for the architect?
Chapter 7 is the most important chapter for the architect. The interested architect may also read chapter 3, 5 and the first part of chapter 6. Most other chapters (chapter 2, 4 and the second part of chapter 6) require some knowledge on either meteorology, aerodynamics or computational fluid dynamics.
It is recommended to read the summary of each chapter first. Generally, this summary gives references to key figures, and to the contents of each section. Especially chapter 4 gives many details, and one should not read the whole text if one is only interested in the 'headlines'.

2   Theory

This wind comfort study is based on obstacle aerodynamics, boundary layer meteorology, computational physics, building science, and some psychology and physiology. Boundary layer meteorology (section 2.1) and obstacle aerodynamics (section 2.2) are used most frequently in this study. Section 2.3 discusses the wind tunnel techniques, measuring methods and numerical simulation methods, as used in this research.

2.1   Boundary layer meteorology

The atmospheric boundary layer (ABL) is the layer in which properties of the flow are directly influenced by the earth's surface. Moisture, heat, air pollution and momentum are mixed by turbulence in this layer. The ABL is also the layer where the flow is retarded by surface friction: wind speed increases with height.

The *ABL depth* δ is not constant with time but depends upon the strength of surface generated mixing. During daytime, the earth's surface is heated and strong thermal mixing (convection) yields an ABL depth of 1000 m or more. By night, the earth's surface is relatively cool. The result is a stable thermal stratification and suppression of turbulence. The ABL depth shrinks to about 100 m or less. In cloudy conditions and in strong winds ABL depth is of the order of 1000 m, both during day and during night. In that case mechanical production (by surface friction) of turbulence prevails, at least in the lowest 20% of the ABL. Terrain roughness becomes the dominant parameter in these (thermally) neutral conditions.

Classification of terrain types

Each terrain can be described by an *aerodynamic roughness length* z_0 and a (zero) *displacement length* z_d. The latter can be interpreted as the vertical displacement of the flow due to the presence of obstacles and obstacle wakes. The aerodynamic roughness length z_0 is not a real obstacle height. It can be interpreted as a measure of the size of eddies at the surface (Panofsky et al, 1984), or as a roughness height which is 'felt' by the flow. The roughness parameters z_0 and z_d are not only determined by obstacle height, but also by obstacle spacing, and by other factors. Therefore, a roughness classification is the most appropriate method.

Some typical z_0 values are 0.03 m for a grass covered open plain (airport), 0.4 m for London suburbs (Helliwell, 1971) and 0.8 m for central London. Table 2.1 gives a classification of z_0 for different landscapes and terrains (Wieringa, 1991, 1992). These estimates are valid for fetches $\geq$ 5 km. For shorter fetches, other z_0-values may be appropriate. Moreover, z_0 can be dependent on wind direction (e.g. due to orientation of obstacles).

9

No.	z_0 (m)		Landscape description
1.	0.0002	Sea	Open sea or lake (irrespective of wave size), tidal flat, snow covered flat plain, featureless desert, tarmac, concrete, all with a free fetch of several kilometres.
2.	0.005	Smooth	Featureless land surface without any noticeable obstacles; negligible vegetation: beaches, pack ice without large ridges, morass, snow-covered or fallow open country
3.	0.03	Open	Level country with low vegetation (grass) and isolated obstacles with separations of at least 50 obstacle heights (50H): grazing land without windbreaks, heather, moor, tundra, runway area of airports
4.	0.10	Roughly open	Cultivated area with regular cover of low crops, or moderately open country with occasional obstacles (low hedges, single rows of trees, isolated farms) at relative horizontal distances of at least 20H.
5.	0.25	Rough	Recently-developed 'young' landscape with high crops or crops of varying height and scattered obstacles (dense shelterbelts, vineyards) at relative distances of about 15H.
6.	0.50	Very rough	'Old' cultivated landscape with many rather large obstacle groups (large farms, clumps of forest) separated by open spaces of about 10H. Also vegetation like bush land, orchards, and young, densely planted forest (with small interspaces). Dense low buildings: suburb (Wieringa, 1992).
7.	1.0	Closed	Landscape totally and quite regularly covered with similar size large obstacles with open spaces comparable to the obstacle heights: mature regular forests, regularly built large town, villages.
8.	≥ 2.0	Chaotic	Centres of large towns with mixture of low-rise and high-rise buildings (definition?; at least 10 storeys?). Irregular forests with many clearings.

Table 2.1 *Classification for visual determination of roughness length z_0 (Wieringa, 1991). The estimate is valid for fetches ≥ 5 km. For shorter fetches, other z_0 values may be appropriate.*

Wieringa did not present values for the zero displacement length z_d. For central London, Helliwell found that $z_d/H \approx 0.8$. For dense vegetation, Oke (1987) suggested: $z_d/H \approx 0.7$. However, the uncertainties in such estimates are large.

Mean wind speed in the ABL

It is very important that we can link wind speed at the building site to wind speed at a meteorological station. First, two important definitions are given:

The *potential wind speed* U_{pot} is the wind speed over a grass covered plain (aerodynamic roughness length $z_0 = 0.03$ m) at a height of 10 m. This is the wind speed that would be measured on an 'ideal' meteorological station.
Wind amplification factor γ is the ratio between the local wind speed U and U_{pot} : $\gamma = U/U_{pot}$.

In this section, we concentrate on the *surface layer*: the lowest 10-20% of the ABL over uniform (fetch at least 10-20 km; Jensen, 1978) flat or gently rolling terrain. Equation 2.1 gives the mean wind speed as a function of height:

$$U(z) = \frac{U*}{\kappa}(\ln(\frac{z - z_d}{z_o}) - \psi(\frac{z}{z_L})) \qquad \text{for} \quad z > 20z_o + z_d \qquad (2.1)$$

where z_0 is the aerodynamic roughness length, z_d the zero displacement length, κ the Von Karman constant (0.4; Panofsky et al, 1984) and $U*$ the friction velocity. The thermal stability correction ψ will be discussed later in this section. The friction velocity $U*$ is defined by:

$$\tau_o = \rho U*^2 \qquad (2.2)$$

where τ_o is the surface shear stress (drag force / unit area), and ρ the air density (kg/m^3). For a fixed value of U_{pot}, both τ_0 and $U*$ increase with increasing surface roughness z_0.
Equation 2.1 can only be used if there is no influence of *individual* roughness elements. Hence the requirement $z > 20z_0 + z_d$. In the case of large, scattered obstacles, eq. 2.1 can only be used well away from the obstacles, i.e. more than 1.5-2.5 obstacle heights above the obstacles or more than 20 obstacle heights downstream of the obstacles. There is also an upper height limit to which eq. 2.1 can be used. Panofsky (1972) states that above land, eq. 2.1 can be used up to heights of 150 m without loss of accuracy.

Above the surface layer, wind speed and wind direction gradually approach the values at the ABL top. The height of the neutral ABL is (Tennekes, 1972):

$$\delta = 0.3 \frac{U*}{f} \qquad (2.3)$$

where f is the Coriolis parameter ($1.146*10^{-4}$/s for 52°NB). The wind speed at the top of the ABL is often referred to as the 'geostrophic' wind. The

geostrophic wind is the result of a stationary, frictionless balance between pressure gradient force and Coriolis force. An exact balance of forces is seldom achieved in practice. Therefore, we use the actual wind at the ABL top, the *macro wind speed* G. In stationary conditions (over at least one hour), macro wind speed is given by (Petersen et al, 1984):

$$G = \sqrt{U_s^2 + V_s^2} = \frac{U_*}{\kappa} \sqrt{(\ln(\frac{U_*}{f z_o}) - A)^2 + B^2} \qquad (2.4)$$

A and B are constants. In a neutral atmosphere they are 1.8 and 4.5. Other values apply in the presence of significant horizontal temperature gradients (Clarke et al, 1974), and for non neutral boundary layers (Petersen et al, 1984).

The angle between surface wind and macro wind is:

$$\alpha = -\arcsin(\frac{B \, U_*}{G \, \kappa}) \qquad (2.5)$$

The negative sign indicates that the macro wind is veered relative to the surface wind. For moderate winds (U_{pot} = 10 m/s), the angle α is 17° for open water, 23° for open terrain, and 32° for a large urban area. The required fetch to obtain these wind direction changes is at least 20 km.

open field   **large city**
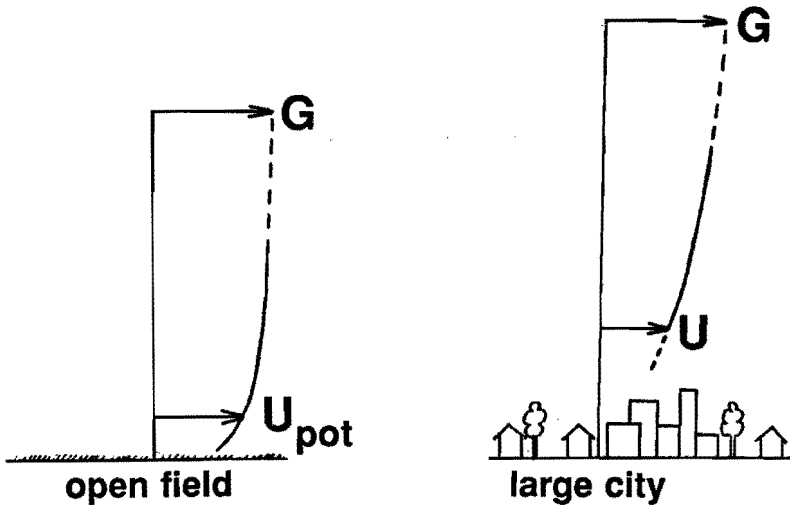
Figure 2.1: *Linkage of wind speed U above a large city and potential wind speed U_{pot} on a grass covered plain by assuming a constant macro wind speed G.*

Eq. 2.4 provides an implicit relation between $U*_1$ and $U*_2$ of two different terrains if we assume that G is constant (over distances of 10-100 km). Simiu et al (1986) propose a simpler relation with an accuracy better than 5%:

$$\frac{U*_1}{U*_2} = (\frac{z_{o1}}{z_{o2}})^{0.0706} \tag{2.6}$$

Figure 2.1 illustrates how wind profiles over different terrains are linked.

So far, we have not discussed any thermal effects. Local thermal circulations (sea breeze, urban heat island) are generally unimportant, as we are interested in rather strong winds ($U_{pot} > 5$ m/s). Moreover, their effects are 'smoothed out' as wind climate is considered, not daily weather.

At temperate latitudes, macro wind increases generally with height ('thermal wind'), at least in a climatological sense. This is caused by horizontal temperature gradients (McIlveen, 1992). Typical values horizontal temperature gradient and of U_{pot} are chosen as 0.008 K/km (1 K / 250 km) and 5 m/s. For this case, thermal wind effects result in 10% increase in G/U_{pot}. In the surface layer wind speed increase is less than 5%. The same applies to the ratio $U*_2/U*_1$, $U*_2$ being the larger of the two.

Effects of surface heat flux ('thermal stability') are much more important. In the surface layer, z/z_L is the relevant stability parameter, z_L being the *Monin Obukhov length*. The Obukhov length can be written (Petersen et al, 1984) as:

$$z_L = \frac{\rho c_p T U*^3}{g \kappa H_o} \tag{2.7}$$

where c_p is the specific heat of air (1004 J/K*kg), T the air temperature (K), g the gravitational acceleration (-9.81 m/s^2) and H_o (W/m^2) the sensible heat flux from the surface. The parameter z/z_L gives the ratio between thermal (buoyant) and mechanical influence on turbulence production. Mechanical production prevails if $|z/z_L| \ll 1|$. In that case, the boundary layer is approximately neutral.

In the non-neutral case, the stability correction ψ (eq. 2.1) becomes important. The constants A and B in eq. 2.4 and 2.5 must also be modified (Petersen et al, 1984). Holtslag (1987) and Petersen et al (1984) provide schemes to estimate z_L and ψ for unstable and stable conditions respectively. Kondo (1975) provides a scheme for estimating z_L over open water.

Table 2.2 shows the minimum U_{pot} for which the neutral estimate of γ (eq. 2.1 and 2.6) is within 10% or 20% of the 'real' γ (an estimate of γ which includes surface heat flux effects).

In the remainder of this study, we will neglect thermal effects on γ. This is because these effects can only be corrected for if U_{pot} is large (because of inconsistencies in the above schemes) and if the terrain is uniform. Errors in

this neutral estimate are acceptable if U_{pot} is not too small (table 2.2), and if marine weather stations are not used to predict γ over land (and vice versa).

	diff < 20%	diff < 10%
daytime	4.8 m/s	11.4 m/s
nighttime	7.6 m/s	10.8 m/s

Table 2.2: *Minimum U_{pot} for which difference between neutral estimate of γ (eq. 2.1 and 2.6) and real γ is less than 10% or 20%. The estimate is valid for extreme (clear sky) daytime and nighttime conditions. Considered heights: z < 100 m. Considered z_o: 0.01 - 1.0 m. Note: these estimates do not apply for surfaces with different stability conditions (warm sea / cool land).*

Turbulence in the ABL

Turbulence should be considered for wind comfort and for simulation of obstacle flow. There is no generally accepted definition of turbulence. We can describe turbulence as a superposition of several eddies which interact with each other and which are transported by other eddies and by the mean flow. This results in a chaotic and apparently random velocity variation in space and time (Panofsky et al, 1984). The size of the eddies varies between 500 m (and more) down to 1 mm and less. First let us consider the magnitude of fluctuations relative to the mean flow. This can be described by the *turbulence intensity* T_u:

$$T_u = \frac{(\overline{u'(t)^2})^{0.5}}{U} = \frac{\sigma_u}{U} \qquad (2.8)$$

where U is the time averaged streamwise velocity, and u'(t) is the fluctuating component (the deviation from the mean). The overbar denotes time averaging; σ_u is the *standard deviation* of u'(t). The total *turbulent kinetic energy* K (per unit mass) is given by:

$$K = 0.5*(\sigma_u^2 + \sigma_v^2 + \sigma_w^2) \qquad (2.9)$$

where v and w denote the lateral and vertical component. Turbulence can be generated by velocity gradients and by unstable thermal stratification (heating of earth's surface). On the other hand, turbulence is suppressed by stable stratification and by viscous dissipation (dissipation rate: ϵ). Budget equations for K are discussed in section 2.2.

Another important parameter is the *shear stress* u'w'. In the surface layer, u'w' is linked to the wind profile because $-u'w' = U^{*2}$.

14

Standard deviations σ_i, turbulent kinetic energy K, and shear stress u'w' are all approximately constant in the surface layer. Typical values for a wide range of z_0 are (Panofsky et al, 1984):

$$\sigma_u = 2.4\,U* \qquad\qquad K = 5.5\,U*^2$$
$$\sigma_v = 1.9\,U* \qquad\qquad \overline{u'w'} = 1.0\,U*^2 \qquad\qquad \textbf{(2.10)}$$
$$\sigma_w = 1.25\,U*$$

These values are dependent on thermal stability. Turbulence levels (σ_i and K) are increased in unstable conditions ($z/z_L < 0$). Low frequency variations with large amplitude (large eddies), may increase σ_u/U^* and σ_v/U^* up to 4. This increase can even be experienced for $|z/z_L| \ll 1$ because large eddies depend on $|\delta/z_L|$, not on $|z/z_L|$. In stable conditions ($z/z_L > 0$), turbulence levels (σ_i and K) decrease. The σ_i/U^* terms are roughly constant for $z/z_L < 1$. On complex (hilly) terrain, σ_u/U^* and σ_v/U^* can be increased by a factor 2, but there is no significant change in σ_w/U^*.

The structure of turbulence can be further clarified with spectra (dominant frequencies), probability distributions (peaks), and coherence (a measure for spatial correlation). Only probability distributions are discussed here.

In fully developed turbulence, turbulent fluctuations can approximately be described by a Gaussian probability distribution (Jensen and Busch, 1982):

$$p(u) = \frac{1}{\sqrt{2\pi}\,\sigma_u} \exp\left(-\frac{1}{2}\left(\frac{u'(t)}{\sigma_u}\right)^2 \right) \qquad\qquad \textbf{(2.11)}$$

where p(u) is the probability density function and u'(t) the fluctuating u-velocity. The probability on u'(t) > M (written as P(u'(t) > M)) can be calculated by integrating eq. 2.11 from M to ∞. Similar expressions apply for the v and w component.
Figure 2.2 shows an example of a near Gaussian probability distribution. The ratio $u'(t)/\sigma_u$ is an important parameter, and is called the peak factor k. It can be seen that eq. 2.11 performs well if k is 3 or less.

The peak factor k is used in the definition of the equivalent wind speed U_e (eq. 2.12) which is often used in chapter 3 and 5.

$$U_e = U + k\sigma_u = U(1 + kT_u) \qquad\qquad \textbf{(2.12)}$$

A high value of the peak factor k (say 3) corresponds with infrequently occurring gusts, e.g. an hourly peak gust of a few seconds duration. A low value of k (say 1) corresponds with gusts occurring more frequently and/or gusts of longer duration.
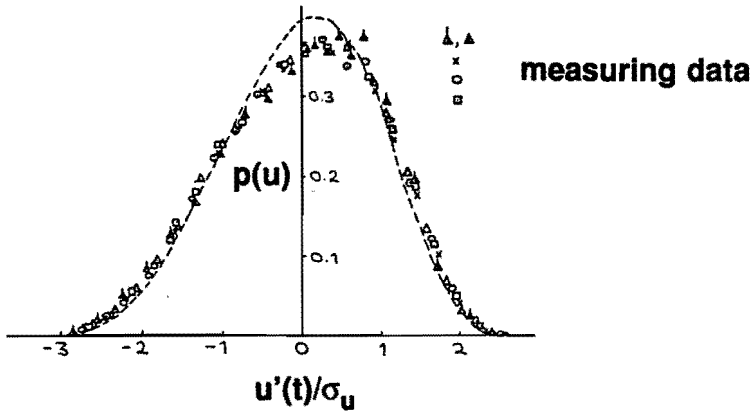
Figure 2.2: Sketch of probability distribution p(u) in the shear layer above an obstacle wake (Castro, 1980). Dots denote measuring results for different approach flows. Dashed line is for plane mixing layer and approximates Gaussian distribution (eq. 2.11).

In strongly disturbed flows (e.g. recirculation zones at windward and leeward sides of a building), eq. 2.11 is not generally valid (Isyumov et al, 1975; Bottema, 1990). Better alternatives are not available however.

Effects of inhomogeneous terrain and topography

Equation 2.3 through 2.6 can only be used for uniform terrain, e.g. if fetch over a terrain is at least 10-20 km (Jensen, 1978). On smaller scales, inhomogeneities in the ABL become important: changes in roughness, changes in surface temperature and humidity, hills etc. In the following, the effects of simple changes in surface properties will be discussed, as well as the effects of small topography (hills). Flow in mountainous regions will not be considered in this study.

The simplest case is normal flow over a two dimensional roughness change. In fact this is the only case for which a fair amount of theory and experiments is available. The roughness change is considered to be two dimensional if W/z_0^+ >> 100, and W/H >> 1. W is the width of the roughness change, H the obstacle height, and z_0^+ the larger of the two roughness lengths.

The *internal boundary layer* (IBL) is defined as the layer which is influenced by the new surface conditions. Outside (and upstream of) the IBL, the flow is only slightly modified. The *IBL height* h_{IBL} is primarily dependent on z_0^+: the larger of the two roughness lengths (Wood, 1982; Claussen, 1989). Jensen et al (1984) defined h_{IBL} from 'kinks' in the wind profile, and proposed:

16

$$\frac{h_{IBL}}{z_{o^*}} = 0.3(\frac{x}{z_{o^*}})^{0.8} \tag{2.13}$$

Above the IBL, wind profiles are effectively the same as upstream. For $z < h_{IBL}$, eq. 2.1 can be used as well, but with a location dependent U^* and with the downstream z_o. There may be some overshoot in z_o however (Vermeulen, 1986). Figure 2.3 gives an example of wind profiles in the IBL.
Data on turbulence in the IBL are almost absent. The available data (Mulhearn, 1978) suggest that, at least for a rough to smooth change, turbulence levels gradually approach to their new equilibrium values.

In practice, oblique flow, multiple roughness changes, lateral roughness changes, and roughness islands have to be considered as well. Some wind tunnel data are available (Vermeulen, 1986). The data, and their modelling, will be discussed in chapter 4.
However, even IBL models for simple two dimensional roughness changes have serious uncertainties and limitations.

internal boundary layer (IBL)
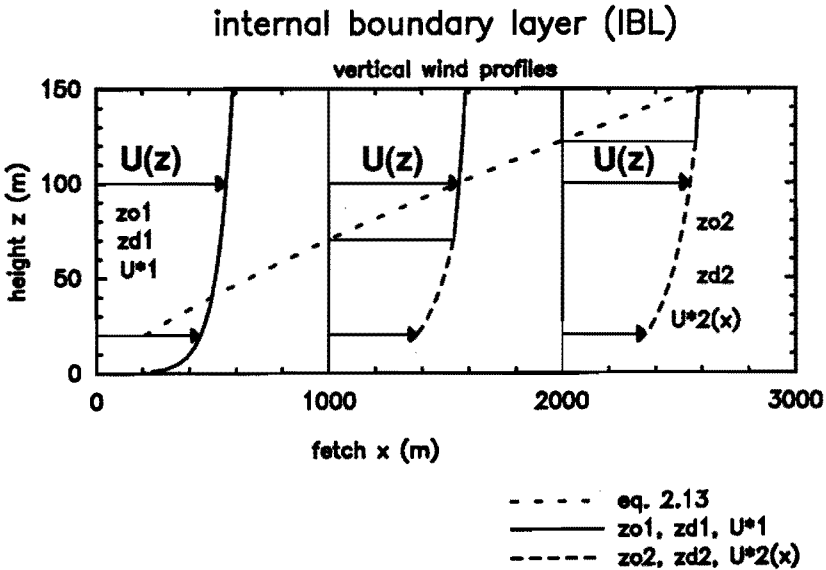
Figure 2.3: Modelled wind vertical wind profiles U(z) for a two dimensional roughness change (normal flow). Upstream z_o (z_{o1}) is 0.03 m, downstream z_o (z_{o2}) is 1.0 m, $z_d = 0$. Short dashed line represents IBL height. Long dashed line represents wind profile within the IBL, solid line represents wind profile above the IBL and upstream. Profiles are given for a fetch of 0 m (upstream profile), 1000 m and 2000 m.

A major limitation is that IBL theory is not valid outside the surface layer, i.e. for fetches greater than about 2.5 km. Extrapolation of IBL theory requires unrealistically large fetches (~10000 km) before equilibrium is attained, i.e. before eq. 2.6 is satisfied.

On very short fetches, IBL theory is only valid if individual roughness elements are not important, i.e. beyond 20 obstacle heights or about 200 z_0.

The small amount of experimental data, does not allow for accurate modelling, and this can be considered as a major error source.

Another important error source is the fact that thermal effects are neglected. If the *whole* boundary layer is strongly unstable, h_{IBL} grows as $x^{1.5}$. In strongly stable conditions h_{IBL} grows as $x^{0.5}$. This will also affect the range of fetch for which IBL theory is valid.

Errors (within the IBL; for neutral estimate of γ) due to thermal effects are the largest in unstable (daytime) conditions: stability effects may result in up to 15% underestimation of γ near a town edge (height z = 20 m). Above the IBL, errors may be much larger (up to 20%; table 2.2).

The error estimates have been carried out with U_{pot} values of table 2.2 and with a stability dependent formula for IBL height, as proposed by van Wijk et al (1990). The formula is not suitable for prediction of γ in all conditions as it is only valid for small disturbances, and for a single value of z_L.

The effects of wind flow over hills often outweigh the effects of roughness changes (Jensen et al, 1984). For wind flow over hills, the following speed up factor ΔS is often used:

$$\Delta S \equiv \frac{U(z) - U_o(z)}{U_o(z)} \qquad (2.14)$$

where z is the height above the *hill* surface. For the maximum ΔS above the crest of a gentle sloping hill (no separation) Jensen et al (1984) proposed:

$$\Delta S \approx a * \frac{H}{L} \qquad (2.15)$$

where H is the hill height, and L the length of a hill slope. The constant a increases slowly with decreasing roughness, and is about 4. The maximum speed up is reached at $z = 0.3\,z_0\,(L/z_0)^{0.67}$. Below this height, the logarithmic wind profile (eq. 2.1) applies.

For relatively steep slopes (upstream L/H < 2 or downstream L/H < 3.5), flow separation is likely to occur. Section 4.2 gives estimates of speed up factor ΔS for steep slopes, as well as for gentle slopes.

2.2 Aerodynamics of obstacles

By understanding the mechanisms of wind flow around buildings, we can identify the cause of high wind speeds around buildings, and we can judge which remedial measures are appropriate. This section provides some explanations of the flow around obstacles, and discusses the influence of geometry and approach flow parameters.

First, concepts and basic equations will be presented. Next, mechanisms of obstacle flow and the influence of building geometry and approach flow parameters will be discussed.

Concepts and basic equations

We will use the following notation:
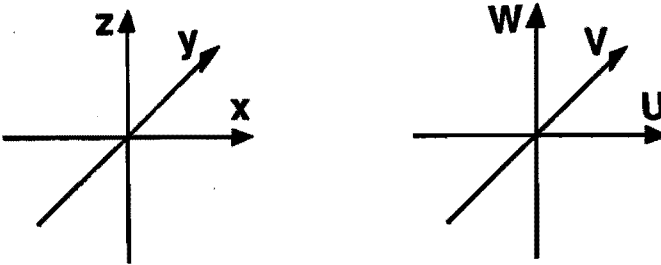
Figure 2.4:   *Coordinate system, and notation of velocity components.*

The instantaneous streamwise, lateral and vertical mean velocity components are often denoted as U, V, W; the coordinates are x, y, z. For economy, we will use the notation x_1, x_2, x_3 / U_1, U_2, U_3 in formulas, together with the *summation convention* (all repeated indices in a product are added), i.e.:

$$U_j \frac{\partial T}{\partial x_j} \equiv \sum_{j=1}^{j=3} U_j \frac{\partial T}{\partial x_j} = U \frac{\partial T}{\partial x} + V \frac{\partial T}{\partial y} + W \frac{\partial T}{\partial z} \tag{2.16}$$

where the sign '$\equiv$' means: 'by definition equal to'.

The momentum equations (per unit mass), or the Navier Stokes equations, can be written as:

$$\frac{D U_i}{D t} \equiv \frac{\partial U_i}{\partial t} + U_j \frac{\partial U_i}{\partial x_j} = g \delta_{i3} - \frac{1}{\rho} \frac{\partial p}{\partial x_i} + \frac{\partial}{\partial x_j} \nu \frac{\partial U_i}{\partial x_j} \tag{2.17}$$

together with a mass conservation equation for incompressible flow:

$$\frac{\partial U_i}{\partial x_i} = 0 \tag{2.18}$$

19

In eq. 2.17, D/Dt denotes the so called material derivative, the time derivative of a property of a particle moving with the flow. In the middle part of eq. 2.17, $\partial/\partial t$ denotes time derivative on a fixed location; $u_j*\partial u_i/\partial x_j$ represents change of U due to advection ('inertial force') on a fixed location.

On the right hand side, $g\delta_{i3}$ represents the gravitational acceleration (by definition, $\delta_{ij}=0$ for $i \neq j$, and $\delta_{ij}=1$ for $i=j$, so $g\delta_{i3}$ works only in vertical direction), $\partial p/\partial x_i$ and $\partial/\partial x_j*v*\partial u_i/\partial x_j$ represent accelerations due to pressure gradients and due to viscous friction respectively. Coriolis effects have been neglected.

If we multiply eq. 2.17 with U_i and use the summation convention for the i-indices, we obtain an equation for the kinetic energy (E) per unit mass, where $E = 0.5*(U_i U_i) = 0.5*(U^2 + V^2 + W^2)$. For stationary flow ($\partial/\partial t = 0$), combination this with eq. 2.18, and integration along a flow path, yields the extended equation of Bernoulli which is valid along a flow path:

$$\frac{p}{\rho} + \frac{1}{2}U_i U_i + gz + \delta W = \text{constant} \qquad (2.19)$$

The term δW represents work by the flow. A positive δW means energy loss of the flow, e.g. due to friction along a flow path.

Generally, the term 'gz' is not important as it is compensated by the (hydrostatic) decrease of pressure with height. In other words, our flow particle is 'floating' in the air. Wind pressures are often normalized by $0.5*\rho*U^2$ as this term is assumed to be dominant. This results in a *pressure coefficient* C_p:

$$C_p = \frac{p - p_o}{0.5*\rho U_i U_i} \qquad (2.20)$$

The significance of C_p is that the effects of wind speed and geometry (building and surroundings) on wind pressures are virtually separated by using C_p.

In eq. 2.16 through 2.20, we did not take into account that flow in the atmospheric boundary layer is turbulent. The *Reynolds number* is the ratio between inertial (turbulence generating) forces and viscous (turbulence dissipating) forces:

$$\text{Re} = \frac{\text{inertial force}}{\text{viscous force}} = \frac{U_j \dfrac{\partial U_i}{\partial x_j}}{\dfrac{\partial}{\partial x_j} v \dfrac{\partial U_i}{\partial x_j}} = \frac{UL}{v} \qquad (2.21)$$

L is a characteristic length; U is a characteristic wind speed. In the atmospheric boundary layer (and in a wind tunnel boundary layer) Re >> 10^4. At locations with velocity gradients, the flow will become unstable and *turbulent*: Velocities and pressures become highly variable in time and space, and eddies of several sizes develop.

If statistical properties such as the average do not change in time (statistically stationary flow), we can split each variable in *mean* (*uppercase*) and *fluctuating* (*lowercase*) parts:

$$U_t(x,y,z,t) = U + u(x,y,z,t) \qquad (2.22)$$

The notation convention is as follows: Time averaged velocities are given in uppercase (U_i), fluctuating parts are given in lowercase (u_i) or with a prime (T', p'; p is mean pressure), and instantaneous parts with a subscript t (U_t). Time averaging of eq. 2.22 results in:

$$\overline{u'(t)} = 0 \quad ; \quad \overline{U + u} = U \qquad (2.23)$$

If each variable (U_i, p) in eq. 2.17 and 2.18 is substituted by the sum of a mean and fluctuating part (as in eq. 2.22), and if we apply the averaging rules of eq. 2.23, we obtain the Reynolds (averaged) equations for the mean quantities:

$$\frac{DU_i}{Dt} = g\delta_{i3} - \frac{1}{\rho}\frac{\partial p}{\partial x_i} + \frac{\partial}{\partial x_j}v\frac{\partial U_i}{\partial x_j} - \frac{\partial}{\partial x_j}(\overline{u_i u_j}) \qquad (2.24)$$

together with:

$$\frac{\partial U_i}{\partial x_i} = 0 \qquad (2.25)$$

for mass conservation. The $u_i u_j$ terms are called *Reynolds stresses* and represent mixing by turbulence. Generally, these stresses are much more effective in mixing than their viscous counterparts.

In flows with some turbulence, Bernoulli's equation (eq. 2.19) can still be a fair approximation for particles following the mean flow. Eq. 2.19 is certainly not valid near or after separation.

Turbulent kinetic energy K is defined as $0.5*u_i u_i$ or $0.5*(\sigma_u^2 + \sigma_v^2 + \sigma_w^2)$. The K-budget can be described by:

$$\frac{DK}{Dt} = -\overline{u_i u_j}\frac{\partial U_i}{\partial x_j} - 0.5\frac{\partial}{\partial x_j}\overline{u_j u_i u_i} + \frac{1}{\rho_o}\frac{\partial}{\partial x_i}\overline{u_i p'} - g\delta_{i3}\overline{u_i T'} - \varepsilon \qquad (2.26)$$

The different terms on the right hand side represent production (1) (occasionally: dissipation) of K by turbulent shear stresses, redistribution of K by transport (2) and velocity-pressure correlation (3), buoyant production (or dissipation) (4) and viscous dissipation (5).

The latter term is given by:

$$\varepsilon = \nu \overline{(\frac{\partial u_i}{\partial x_j})^2} \qquad\qquad (2.27)$$

Viscous dissipation ε is almost isotropic. On the other hand, the shear stress production term in eq. 2.26 works mainly on the u-component, whereas the buoyancy term mainly works on the w-component. The ratio of buoyancy over shear stress production is equal to z/z_L (see eq. 2.7 for expression of z_L).

Explanation of flow around an obstacle

Turbulent flow around obstacles is very complicated: mean flow, turbulence, and pressure field are highly dependent on each other. Few data exist, because many properties are hard to measure. A brief description and -where possible- an explanation of the flow around obstacles follows.

First, we will make some bulk estimates which illustrate the relation between pressures and wind speeds.
Obstacles in the atmosphere experience a wind force. The drag force F_d on the fluid is the same, except for the sign. The work (per unit time t_o) on the fluid equals F_d*U_o. This energy is extracted (per unit time) from the mean flow along a length of $U_o t_o$. Hence, F_d equals the decrease of mean flow kinetic energy, and the increase of the kinetic energy of secondary flows and turbulence, per unit length.
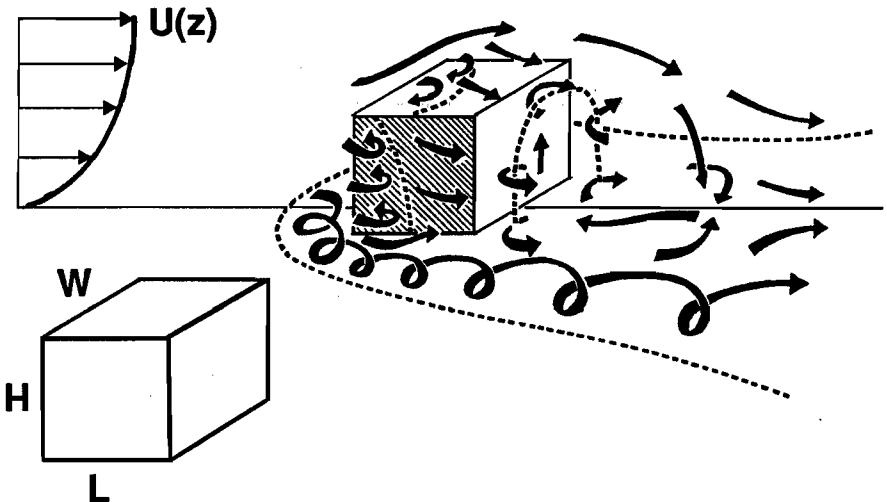
Figure 2.5: Flow field around an obstacle which is immersed in the atmospheric boundary layer, together with notation definition.

Wind speed in a passage between buildings can be estimated by Bernoulli's law, provided that the pressure field is known. If friction is neglected, pressure difference along the passage is related to wind speed by:

$$p_1 - p_2 = 0.5 * \rho * (U_1^2 - U_2^2) \qquad (2.28)$$

In many cases, this is a good first approximation.

In the following, properties of the different flow zones around an obstacle will be discussed. Figure 2.5 and 2.6 show the time averaged flow around an obstacle which is immersed in the atmospheric boundary layer. The instantaneous flow can be rather different from the time averaged flow field.

Frontal vortex (region A in fig. 2.6):
In the approach flow, wind speed increases with height. So do the wind pressures on the frontal building face (except near the top of the building). The resulting pressure gradient drives a downward flow near the building face (Melbourne et al, 1971). Depending on the width over height ratio of the building (W/H), a stagnant zone or a frontal vortex develops. Most turbulence production terms $-u_i u_j \partial u_i / \partial x_j$ are positive in the windward and upper parts of the frontal vortex. This results in increased turbulence in the frontal vortex.

Corner streams (region B in fig. 2.6):
Corner streams can be characterized by increased wind speeds (see section 4.3) and low turbulence intensity (σ_u/U). Melbourne et al (1971) state that corner streams are driven by the pressure difference over a building. However, corner streams can also exist without drag force (in potential flow). These increased wind speeds are caused by mass conservation. (eq. 2.25 integrated over y = 0 to y >> B).

Separation at building corners (see sketch):
A fluid particle can not follow abrupt changes in surface direction (Hosker, 1985) as an infinite force would be required for this. Therefore, the flow separates from the surface at the side corners and at the upstream roof edge. It should be noted that the location of separation (and hence the flow field) of obstacles with *rounded* corners is strongly dependent on approach flow properties. This is a marked difference with flow around sharp cornered obstacles, where the separation location is fixed to the corner.
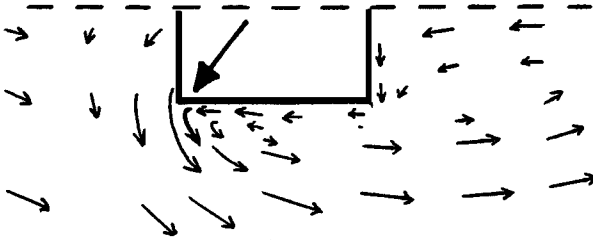
Negative wake pressures (see sketch on previous page):
Downstream of separation, part of the 'stagnant' air in the wake is entrained
into the shear layers which bound the wake. This results in a pressure decrease
in the wake. Turbulence in the approach flow tends to decrease wake pressures
further because of increased entrainment (Laneville et al, 1975).

The recirculation zone (region C in fig. 2.6):
The flow in the recirculation zone is turbulent and highly unsteady (Peterka et
al, 1985). On average, there is a return flow towards the pressure minima near
separation. Interaction with the shear layers results in a complex flow pattern
(fig. 2.5). The length of the recirculation zone tends to decrease with increasing
approach flow turbulence because of entrainment and shear layer curvature.
The recirculation zone can change drastically in shape once the flow reattaches
to the roof or the sides. This is approximately the case if L/H > 1.4 or L/W > 0.7
(Hosker, 1985).
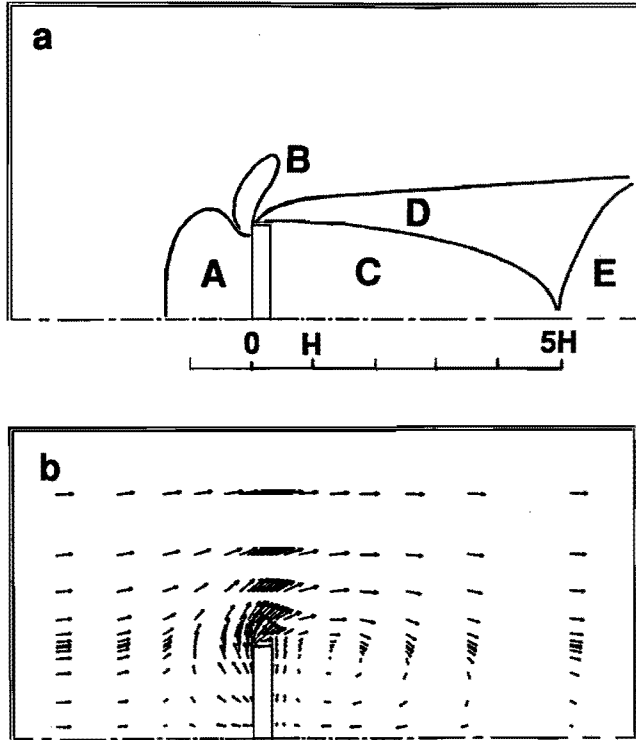
Figure 2.6:   Computed time averaged flow properties at pedestrian height (1.75m)
around an obstacle with L,W,H = 15, 150, 50m (normal flow); z_o = 0.03m.
Because of symmetry, half of the domain is given.
a)   Flow zones around the obstacle: frontal vortex (A), corner streams (B),
recirculation zone (C), shear layers (D) and far wake (E).
b)   Velocity vectors; vector length is proportional to wind speed
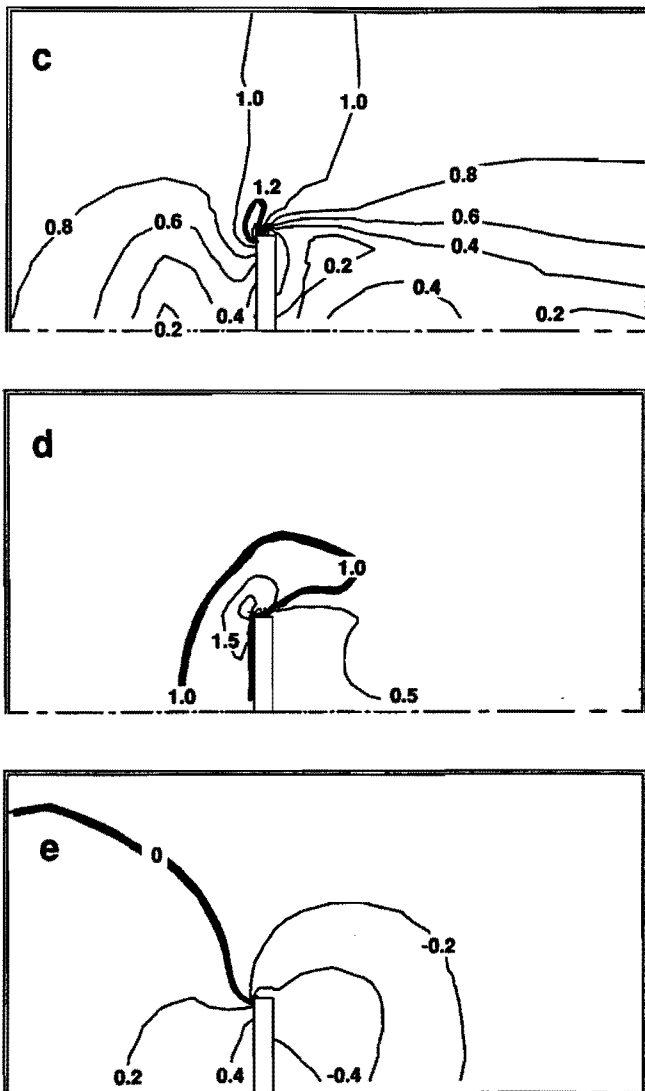
Figure 2.6: Continued, see previous page for captions.
c)   Normalized wind speed $U(z)/U_0(z) = 0.2, 0.4, ...,1.2$ (thick line), 1.4
d)   Normalized turbulent kinetic energy $K/K_0 = 0.5, 1.0$ (thick line), ..., 2.5
e)   Pressure coefficient $C_{pHo} = -0.6, -0.4, -0.2, 0$ (thick line), 0.2, 0.4

Shear layers bounding the wake (region D in fig. 2.6):
The shear layers are be characterized by high velocity gradients. Turbulence levels are high because of advection from the frontal vortex, and because of local generation. Part of this turbulence is advected and diffused into the far wake and into the recirculation zone.

The far wake (region E in fig. 2.6):
This zone is characterized by lower mean velocity, higher turbulence intensity and smaller turbulence scales (Peterka et al, 1985). Velocity defect ($U(z)-U_o(z)$) is slowly diffused upward and decreases roughly as $(x/H)^{-1.5}$. Velocity defect is reduced to ≈5% for x/H > 2-20, depending on W/H (Peterka et al, 1985).

The frontal vortex and the recirculation zone can clearly be recognized from figure 2.6b. Corner streams (wind speed maxima) and shear layers can best be recognized from figure 2.6c.
Figure 2.6d shows that, for this case, most turbulence is generated in the frontal vortex and is advected downstream. Both mean wind speeds and K are relatively low in the recirculation zone.
There is no simple relation between wind pressure and wind speed, i.e. eq. 2.19 (Bernoulli) can not be used for all flow zones. Pressures (fig. 2.6e) are lowest at the corners, as expected. Corner stream pressures are low as well (eq. 2.19). Near the leeward building face, a 'stagnation zone' develops, and pressures are slightly higher than elsewhere in the recirculation zone.
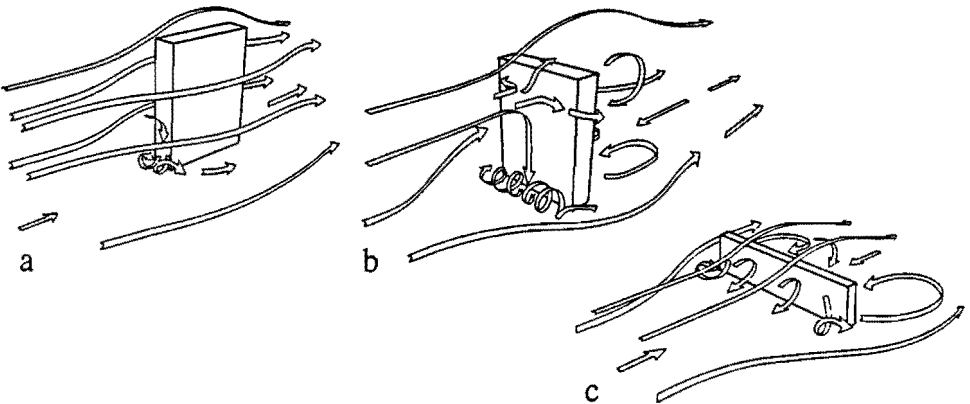
Figure 2.7:   Flow patterns around buildings (Beranek, 1984).
a)   tall building; flow mainly along the sides
b)   intermediate or transitional type
c)   wide building; flow mainly over the roof

26

Building geometry and flow parameters

Our primary concern is the influence of building geometry on the flow field. In the case of a rectangular building, Beranek (1980) recognized three different flow patterns (figure 2.7).

In the tall building case (a), most of the air flows along the building sides. Note that the large alongwind length of the building promotes flow reattachment. In case of a wide building (c), most of the air flows over the roof. In both cases, the recirculation zone is more or less two dimensional. The frontal vortex is only weakly developed. This is not the case for the transitional type (b). A complex, three dimensional flow pattern results, with a strong frontal vortex.

The *influence area* (for recirculation zone, corner stream etc.) is estimated with a length scale L_i. The two extremes of case (a) and (c) suggest that L_i is proportional to the lesser of W and 2H (Cook, 1990). Wilson (1989) proposed $L_i = L_1^{0.67} L_2^{0.33}$ for $L_2/L_1 < 8$, where L_1 is min(W,H) and L_2 is max(W,H). It appears that Cook's definition is preferable (chapter 4).

Flow *reattachment* on the roof or on the sides can change the flow pattern considerably. Flow reattachment is likely if L/H > 1.4 or L/W > 0.7 (Hosker, 1985). Although pressure difference over a building decreases with increasing building length L (Akins et al, 1980), corner stream speeds are hardly affected.

The basic patterns, as described above, can be modified by a number of approach flow parameters.

The *Reynolds number* U*L/v is of little importance for sharp edged obstacles: Flow patterns are observed to be Reynolds independent for Re > $\approx 10^5$. On the other hand, flow patterns around obstacles with rounded edges can be very sensitive to changes in Re (Simiu et al, 1986).

Approach flow turbulence is an important parameter. Laneville et al (1975) point out that in turbulent flow, wake pressures become more negative, unless the flow reattaches on the sides or roof of the building. If no reattachment occurs, wake pressure is decreased by turbulence, and the recirculation zone becomes shorter.

The flow field around obstacles can also be dependent on *thermal effects*, i.e. buoyant production (or suppression) of turbulence. It is to be expected that thermal effects are negligible for $|H/z_L| < c$, where c is a constant < 1. Using Holtslag's (1987) scheme for estimating z_L, it can be proved that for the worst case (solar altitude 60°, sunny) $|H/z_L| < c$ is roughly equivalent to the following empirical expression:

$$H < c|z_L| \approx 0.6 \, c \left(\frac{z_0}{0.03}\right)^{0.3} U_{pot}^{2.5} \tag{2.29}$$

In other conditions (low solar altitude, clouds), neutral flow is maintained for much larger building heights H. If we combine the present result with Murakami's (1983) measurements in a city, we can estimate c for a 10% difference in mean wind speed to be larger than 0.5. In the worst case, this results in maximum building heights of at least 17, 32 and 48 m for roughness class 3, 5, 7 (table 2.1).
In sheltered streets, the mean flow can be driven by temperature differences. Measurements by Nakamura and Oke (1988), and by DePaul and Sheih (1986) suggest that thermally driven flow can become dominant for U(local) < 1.5-2 m/s.

Pedestrian level wind speeds are extremely sensitive to the local *surface roughness* ($z_{0,loc}$). The flow pattern as a whole is merely sensitive to the surface roughness of the approach flow wind profile (H/z_0). If the upstream terrain is rough (say $H/z_0 < 100$), vertical gradients of wind speed increase. This results in a stronger frontal vortex. In the corner streams, $U(z)/U_0(z)$ increases because the frontal vortex increases the upstream pressures. Effects of H/z_0 on U/U_{Ho} are inconclusive.

A very important aspect is the *orientation* of a building. Normal flow (with respect to the building faces) has been discussed already. The most significant differences for oblique flow are the shape of the recirculation zone and the strength of the corner streams (see figure 2.8).
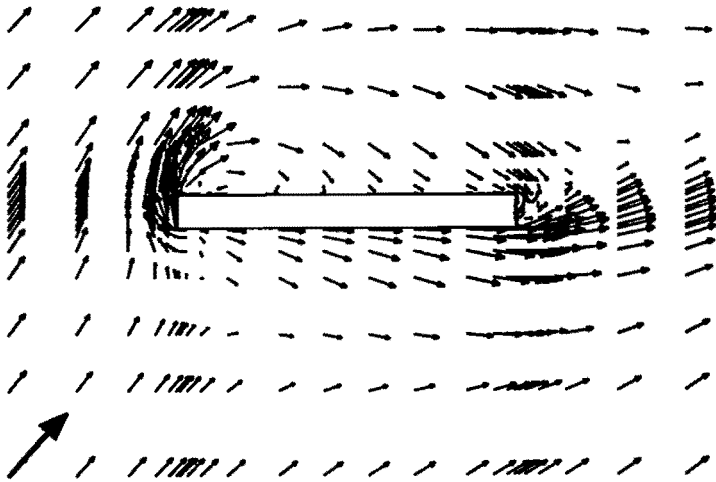
Figure 2.8: Computed velocity vectors for oblique flow (45°). See figure 2.6 for building dimensions and z_0.

Figure 2.8 shows that the upstream stagnation point is moved to the upstream building corner. Corner stream wind speeds are about 20% higher for oblique flow. This is mainly caused by the fact that the stagnation zone is decreased in width for oblique flow (stagnation not on whole building face, but only near corner). This promotes wind flow along the building sides (instead of over the roof). Wind speed increase may be affected by 'effective' building width (for 45°: $L/\sqrt{2} + W/\sqrt{2}$): less increase for $L/W < 0.3$ and a larger increase for $L/W > 0.3$.

The initial angle (at separation points) between corner streams and approach flow is only 45° (90° for normal flow of fig. 2.6). Therefore, the recirculation zone tends to be shorter. For wide obstacles, the wake is also narrowed and turned in the direction of the longer building face, as shown in figure 2.8.

Finally, *grouping* of buildings is very important. Three flow regimes can be distinguished (Hussain, 1978): 'isolated roughness flow', 'wake interference flow', and 'skimming flow'. Typical flows are shown in figure 2.9:
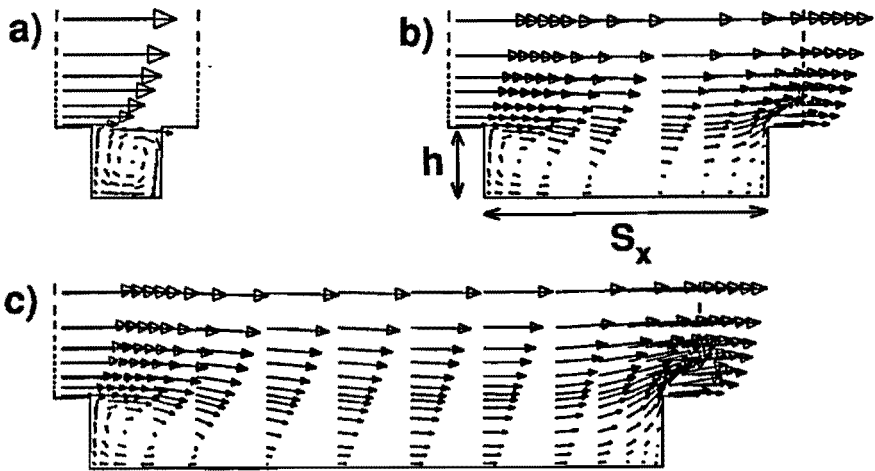
Figure 2.9: Computed flow patterns (2 dim.) typical of flow regimes in building groups.
a) $S_x/h = 1$ skimming flow
b) $S_x/h = 4$ wake interference flow
c) $S_x/h = 8$ isolated roughness flow

In the case of isolated roughness flow, flow patterns are more or less similar to those of isolated buildings (although L_R, the length of the recirculation zone, can be significantly shorter). In wake interference flow, the upstream wake and the downstream recirculation zone are about to merge into one vortex. In skimming flow, a stable vortex develops, which is well separated from the flow above the buildings.

2.3 Measuring and simulation techniques

A great number of flow fields around buildings has to be determined in this study. Numerical simulation has the advantage that both maximum wind speeds and flow fields can be determined rather easily. Furthermore, numerical simulation provides insight in relations between different flow properties (wind speed, pressure, turbulence). This section deals with theory and validation of the numerical model which is used for the present study. First, some measuring and wind tunnel techniques will be discussed.

Wind tunnel and measuring techniques

There are no computational methods without physical or numerical errors. Experimental results for validation are always needed. Full scale results are scarce and generally not suitable for validation (geometry too complex). Experiments on a scale model in a wind tunnel are much more suitable. An overview of (the present) wind tunnel and measuring techniques is given below.

Wind tunnel techniques

A good wind tunnel simulation can predict full scale mean wind speed with a standard relative error of 10-15% or better (Carpenter, 1989; Isyumov et al, 1975). Carpenter (1989) compared peak gusts of 3 sec. duration) with wind tunnel data as well. He found that the standard relative error in wind tunnel peak gusts was about 10%.

A first requirement for a good wind tunnel simulation is a correct simulation of the (neutral) atmospheric boundary layer. For the surface layer of the ABL, the *scaling requirement* is: $H_m/z_{0,m}$ (of the model) = $H_{fs}/z_{0,fs}$ (full scale). For the upper part of the boundary layer, additional scaling parameters (e.g. spectra) can be chosen (Plate, 1982a).

A long wind tunnel (required fetch: 30 boundary layer heights) yields the best ABL simulation (Simiu et al, 1986). With mixing devices (Cook, 1982; Plate, 1982a), the required fetch can be reduced to about 7.5 boundary layer height without too much loss of accuracy.

Generally, the requirement $Re_m = Re_{fs}$ can not be satisfied in a wind tunnel. For sharp edged obstacles, the requirement can be relaxed to: $Re > 10^5$ (Simiu et al, 1986). For a typical tunnel dimension of 1 m, this yields a minimum wind speed of 1.5 m/s. The *scale factor* λ_S (L_m/L_{fs}) is generally between 1:1000 and 1:100. If λ_S is too large, details (and pedestrian height!) can not be modelled. The upper limit of λ_S is generally determined by the tunnel dimensions (fetch, and δ_m). In both cases, Re must be larger than 10^5.

Some wind tunnels can simulate thermal stability effects. In unstable conditions, $(H/z_L)_m$ should be equal to $(H/z_L)_{fs}$. In stable conditions, $Fr_m=Fr_{fs}$ is taken, where the Froude number Fr is $U / (g*H*\Delta T/T)^{0.5}$ (Plate, 1982a). Often, the required wind *reduction* in the wind tunnel is not compatible with Re requirements. In that case, modelling in water tunnels can be an alternative.

Figure 2.10 shows the wind tunnel where the experiments of this study have been carried out.
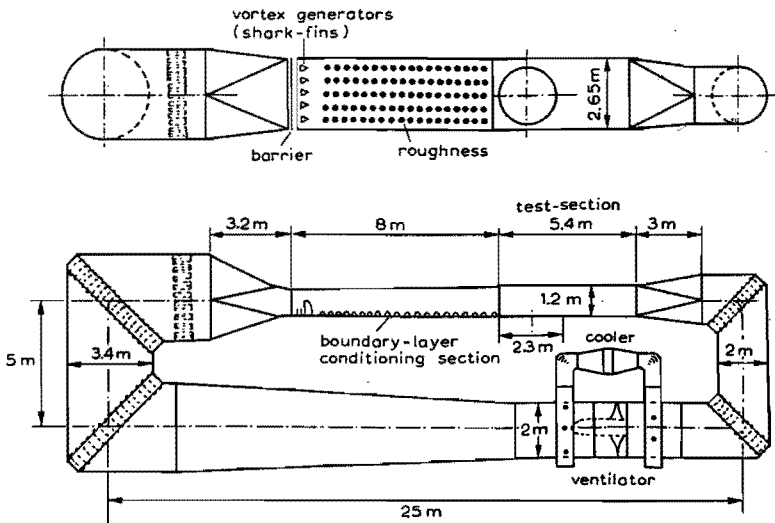
Figure 2.10: *Wind tunnel MIA at the Department of Fluid Dynamics of IMET-TNO where the present experiments have been carried out (Bottema et al, 1991b)*

Measuring techniques

A general description of measuring techniques and their errors will be given here. Most important experimental data (mainly with LDA: a Laser Doppler Anemometer) which are used for validation of numerical results are given later. Details of the experiments are given in (Bottema, 1990) and (Bottema, 1991a).

For (a first) wind comfort evaluation, a continuous measuring technique would be the most suitable, e.g. a sand erosion technique (Beranek, 1984). The accuracy of this technique is of the order of 30% (see Livesey et al, 1990) which is not good enough for validation of a numerical model.

Many measuring techniques are based on cooling by the velocity component perpendicular to one or more thin (5 μm), heated wires (see e.g. Logan, 1986). The conventional hot wire anemometer (HWA) has been widely used. Accuracy in HWA (for U, σ_u) is generally within 5-10%, except for $T_u > 30\%$. In the present study, X-wires have been used so that the u and w component can be measured simultaneously. The Reynolds stress u'w' can be determined as well. Sample duration and cut off frequency are chosen as 8 sec. and 500 Hz (Bottema, 1990), which corresponds with 0.5 h, and 0.5 sec. full scale.
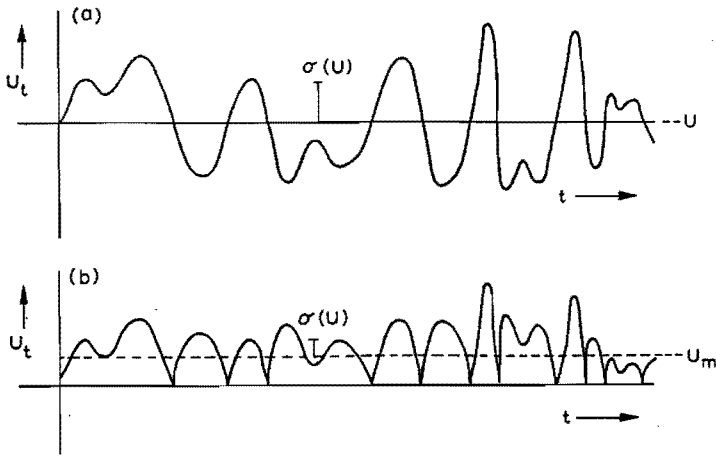
Figure 2.11:   Instantaneous streamwise velocities (a), compared with 'hot wire results' (b). Only absolute values of U(t) are measured in (b). U and σ_u denote real mean velocity and standard deviation, U_m and σ_{um} 'measured' values.
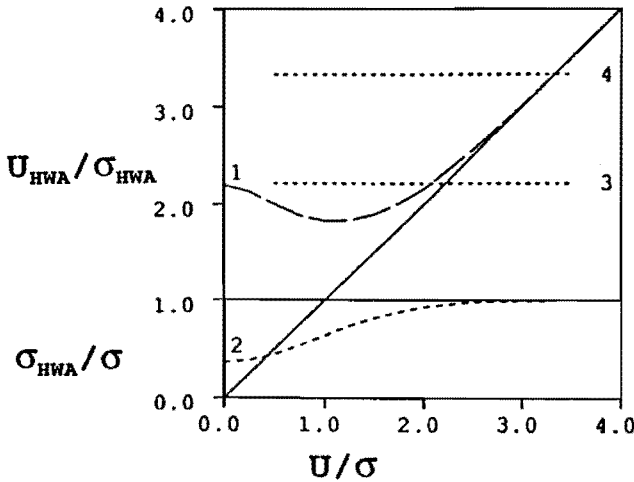
Figure 2.12:   Theoretical estimate (Gaussian; eq. 2.11) of hot wire errors in highly turbulent flow. U_{HWA}/σ_{HWA} (1) and σ/σ_{HWA} (2) are given as a function of real U/σ (1/T_u). Note the large errors for $1/T_u < 1.5$, and that T_u can be anywhere above 45% if $U_{HWA}/\sigma_{HWA} < 2.2$. Results are reliable if $U_{HWA}/\sigma_{HWA} > 3.3$ (4), i.e. if $T_{u, HWA} < 30\%$.

Hot wire errors are primarily caused by the fact that cooling of the wire is dependent on the wind *speed* perpendicular to the wire. Alternating positive (U_t) and negative ($-U_t$) velocities are measured as *only positive* (i.e. $|U_t|$). This is shown in figure 2.11. For high T_u, this results in overestimation of the mean (U) and underestimation of σ_u (figure 2.12).

Tutu et al (1975) show similar trends for X-wires and for σ_v, σ_w, u'w'. Errors in σ_u/U become larger than 10% for T_u > 30%. Both the change in sign of U_t and the component perpendicular to the plane of the X-wire are important.

For the case of oblique flow, Bottema (1990) recommends that T_u < 30% and that the flow angle is not more than about 20° from normal.

It is important to note that for T_u > 100%, measured T_u decreases again. Therefore, it is impossible to correct for these hot wire errors without additional information.

McGill probes (Lawson, 1980) are sometimes proposed as an alternative for HWA techniques. However, with a frequency response up to 100 Hz, McGill probes tend to underestimate turbulence. As conventional HWA, they are also sensitive to temperature fluctuations. Cimbala et al (1989) found that a 1°C temperature increase resulted in about 10% wind speed decrease.

Pulsed wire techniques and Laser Doppler techniques (LDA) are not sensitive to such temperature fluctuations. Pulsed wires are not suitable for comparison with numerical data as their frequency response is limited to only 35 Hz.

For this reason, LDA has been considered. LDA techniques of the present study are described in (Bottema, 1990). LDA is based on particles (oil drops) in the flow which reflect 'pulses' of light when they cross the interference pattern of two intersecting light beams. By using light beams of slightly different frequency, the interference pattern is made to move with a fixed velocity. This allows us to measure the *sign* of a velocity component, and not only the absolute value.

Possible error sources of LDA are discussed in (Bottema, 1990). It is important to know the minimum velocity (which determines the pattern velocity and the required frequency difference Δf) in *advance*. Large errors (see figure 2.12) may result if Δf is chosen wrong.

The (sensitive) optics of the LDA can be another error source. Slight misalignments can result in a dramatic decrease in light intensity and signal / noise ratio. The result is increased scatter and an increasing number of erroneous points. Reflections (obstacles; tunnel walls; windows) can cause erroneous results as well.

Errors due to the size of the measuring volume (2.4*0.16*0.16 mm) can be made negligible by a suitable orientation of the probe.

A limitation of LDA is the time needed for an LDA sample: 10-100 times larger than for a HWA sample of equal size. This is because scattering particles (LDA) must be seeded without disturbing the flow (i.e. at sufficient large distance from the measuring point). In the present study, sample size has been taken 100 for LDA and 4000 for HWA. Still, the accuracy is within 10% of U and σ_u.

Special probes are needed to measure the vertical component if the free path is less than 300 mm. Horizontal components can still be measured, although less accurately (because of vertical orientation of probe).

Numerical simulation

Essentially the problem of numerical simulation is to determine the mean and turbulent (fluctuating) flow properties with the Navier Stokes equations (eq. 2.17 and 2.18). Both direct solution of the Navier Stokes equations, and Large Eddy Simulation (LES; eq. 2.17 and 2.18 are only solved for large eddies) require too much computer time and storage for routine application.

The alternative is to consider time averaged velocities and to solve the Reynolds equations (eq. 2.24 and 2.25). Numerical methods which are based on solution of the Reynolds equations are less accurate, but they require only a fraction of LES computer time.

These models have in common that the Reynolds stress $u_i u_j$ must be estimated from other (time averaged) flow properties. Unfortunately, there is no single parametrization for all flow zones around an obstacle (fig. 2.6). Different approaches are needed for each flow zone, i.e. a 'zonal approach'. Ferziger (1990) states that the accuracy of models which solve eq. 2.24 and 2.25 can be good enough if such a zonal approach is used. The present model (FLUENT; Creare, 1990) does not allow for a zonal approach. Instead, the model is tuned to the flow zone which has most influence on the flow field around an obstacle: the dominant flow zone. The theory of the K-ε model (see Launder et al, 1974; Rodi, 1980) and the tuning procedure are discussed below. Applications of the *standard* K-ε model are described by Murakami et al (1988), Paterson et al (1989), Baskaran et al (1989), Häggkvist et al (1987) and Hoxey et al (1989), and several others.

The basic equations of the present model (FLUENT; Creare, 1990) are the time averaged Reynolds equations (eq. 2.24 and 2.25), and two budget equations for K and ε (Creare, 1990). The flow is assumed to be incompressible. Only isothermal flow is considered as buoyancy effects on turbulence are not incorporated in FLUENT. The turbulent (or eddy) viscosity v_t is computed from a turbulent velocity scale ($K^{0.5}$) and a turbulent length scale ($K^{1.5}/\varepsilon$):

$$v_t = C_\mu * K / \varepsilon \tag{2.30}$$

C_μ is a model constant (0.09 for the standard K-ε model). The turbulent fluxes $u_i u_j$ can be estimated as:

$$\overline{u_i u_j} = v_t \frac{\partial u_i}{\partial x_j} \tag{2.31}$$

Equation 2.24 can now be simplified by omitting the $u_i u_j$ terms and by replacing the viscosity v by the turbulent viscosity v_t ($v \ll v_t$). Note that v_t is assumed to be isotropic.

34

The next step is to tune the model to the approach flow. The present tuning procedure (Detering et al, 1985) is only possible for the K-ε model, not for more sophisticated (second order) models. The latter have too many constants which need to be tuned.

In the atmospheric surface layer, and in a wind tunnel boundary layer, the following expressions hold (Panofsky et al, 1984):

$$v_t = \kappa z U* \quad ; \quad \varepsilon = \frac{U*^3}{\kappa z} \tag{2.32}$$

With eq. 2.31, this leads to the following expression for the model constant C_μ:

$$C_\mu = (\frac{U*^2}{K})^2 \tag{2.33}$$

$C_\mu^{0.5}$ can be interpreted as the part of K which is effective in mixing. If the model is matched to U* and K of the approach flow (not the obstacle flow) C_μ equals 0.032. For the far wake (say x/H > 7), other C_μ values are appropriate (Launder and Spalding, 1974).

Other constants of the K-ε model are maintained because there is no experimental or physical evidence to modify them. Further improvements, as discussed in (Baskaran et al, 1989), could not be incorporated in FLUENT.

The model constant C_μ is especially important near the surface. As a wall function the model uses:

$$\frac{U}{U*} = \frac{1}{\kappa} \ln(\frac{E'U*z}{v}) \tag{2.34}$$

The constant E' is 9.8 for a smooth wall, and is smaller for a rough wall. Eq. 2.34 is the logarithmic law if E'=v/(z_0 U*).
The model calculates U* from the K-value at the first grid node near the wall, using eq. 2.33. When C_μ in the model is not equal to C_μ of the flow, a wrong value of U* and z_0 results.

The wall function is only valid when the distance from the surface is greater than $20z_0$. Below $20z_0$ the flow is determined by individual roughness elements. This has important consequences for grid resolution near rough surfaces. For example, wind speed at pedestrian level can only be computed if z_0 of the local ground surface roughness is less than 0.0875 m.
Near separation the wall function is not valid. Therefore, the wall function is not used at the upstream separation edge. Instead, free slip conditions are chosen. Elsewhere in the wake the wall function is maintained, as free slip conditions are unrealistic for a rough surface.

The solution procedure of FLUENT is given in (Creare, 1990). It can be summarized with the following key words: Control Volume Method, staggered grid, pressure solution with the 'SIMPLE' algorithm, Power Law interpolation

scheme. See Paterson (1986) and Patankar (1980) for background information and discussion of similar procedures.

Murakami (1990a) noted that the second order QUICK scheme is preferable over the (mainly first order) Power Law scheme. However, the QUICK scheme of the present model proved to work only on nearly uniform grids. This required much more grid storage than available.

All computations were carried out on an ALLIANT FX-28 computer. About 500 iterations are needed for convergence, and about 10 hours of CPU time. The total number of grid points is generally close to the allowed number of 25000 (storage ~ 3 MByte). Further details of the computations are given below.

Accuracy of the K-ε model; validation

The accuracy of the numerical simulation is determined by physical modelling and by numerical errors. We will make estimates of numerical errors, as well as overall error estimates. The overall errors can be determined by comparison with experiments.

Poor convergence is not a major error source. Generally, the flow variables (U, K, C_p) did not change more than 0.5% after 500 iterations. Only in one or two cases, the errors in K were larger (up to 5% in the recirculation zone).

Major errors can be caused by too coarse a computational grid. A typical simulation has to cover all length scales from 0.1*min(W,H) up to 5*max(W,H) or 20*min(W,H) (the largest). This requires strongly non uniform grids as the available number of grid points is only 25000.

	Frontal vortex	Corner streams	Recirc. zone
Normal flow:			
VM/U_{Ho}	0.05	-0.08	-0.05
K (rel. error)	-59%	-40%	-33%
C_{pHo}	-0.06	0.18*	0.06
Oblique flow:			
VM/U_{Ho}	0.05	-0.15	-0.02
K (rel. error)	-50%	-32%	+/-20%
C_{pHo}	-0.05	0.10?*	0.05?

Table 2.3: Estimate of maximum differences between a standard simulation (24x24x24 points; see text) and a coarse grid simulation (16x16x24 points). The difference is a fair but conservative estimate of truncation errors in the standard simulation. Corner stream pressures (*) are minimum pressures near separation. VM denotes wind speed $(U^2 + V^2 + W^2)^{0.5}$

Truncation errors were estimated for a standard simulation around a typical building (L,W,H = 15,15,100 m, z_0=0.03 m, normal and oblique flow). A 24x24x24 points grid was used, and a domain of 1200x1200x400 m. Grid

spacing varied between less than 1 m near walls up to about 100 m elsewhere. The standard simulation was compared with a simulation on a coarse grid (16x16x24) in order to estimate the truncation error in the *standard* simulation:

$$e_t = \frac{V_1 - V_2}{(\lambda_{max})^p - 1} \qquad (2.35)$$

V_1 and V_2 are variables on the coarse grid and on the fine grid, e_t is the truncation error, λ_{max} (2) is the maximum relative increment in spacing between neighbouring grid lines. The order of the interpolation scheme p is assumed to be 1.0. In this particular case, the estimated truncation error of the standard simulation is equal to the difference between the two simulations. However, it should be noted that the choice of a minimum p and a maximum λ_{max} leads to a conservative error estimate.

Table 2.3 shows that truncation errors in U/U_{Ho} and C_{pHo} are generally small or moderate. This is not true for errors in K (or in σ_u). However, Murakami et al (1990b) show that the K-ϵ model tends to overestimate production of turbulent kinetic energy in the frontal vortex (Murakami et al, 1990b). The latter effect, and the present truncation errors, tend to cancel each other.

numerical result   experiment
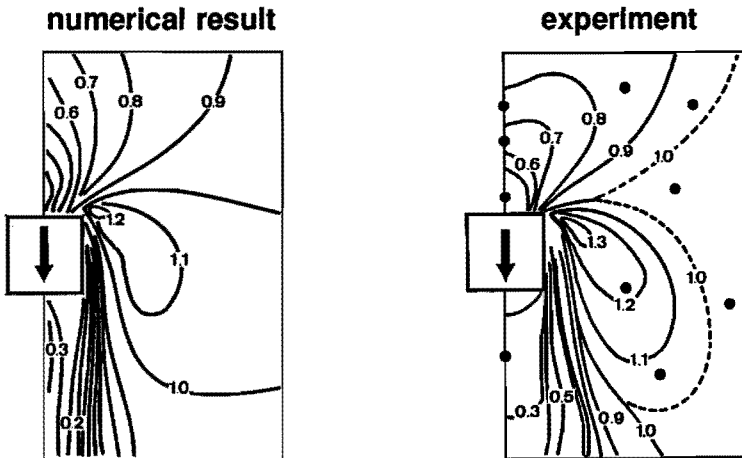
Figure 2.13:   *Normalized wind speeds U/U_o at $z/H = 0.05$ for a building with W/H = 0.3 and L/W = 1; U_o is the approach flow wind speed at $z/H = 0.05$.*
a)   *Numerical results: L, W, H, = 15x15x50 m, z_o = 0.03 m.*
b)   *Experimental results (Maruta, 1984): L, W, H, = 18x18x60 m, power law exponent α = 0.14, scale factor 1:300. Black dots are measuring points. Corner stream wind speeds are increased due to smooth floor between turntable roughness elements.*

In the following, numerical simulations will be compared with experiments. In this way, an estimate of the combined effects of numerical errors and errors in physical modelling can be made.

The most interesting flow zones for wind comfort are the high wind speed regions around building corners. Numerical predictions have been compared with hot wire results of Maruta (1984). Computed mean wind speeds are somewhat lower, but within about 10% of the measuring results (figure 2.13). Both numerical errors and experimental errors contribute to the observed difference. Turbulence data were not available. The position of shear layers could not be validated because the number of measuring points was too low.
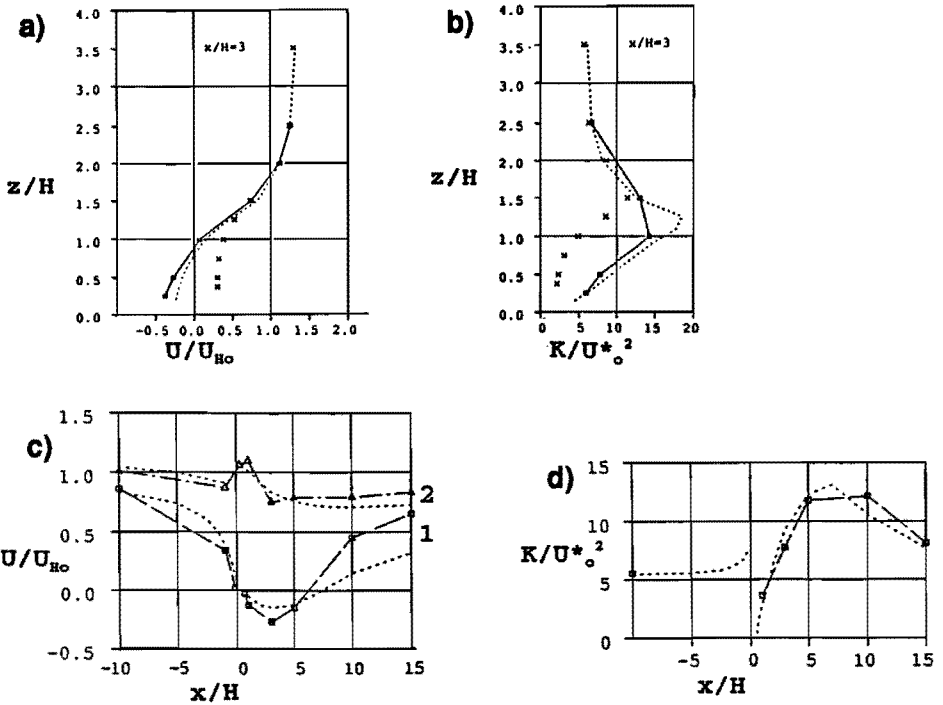
Figure 2.14: *Normalized mean velocity U/U_{Ho} and normalized turbulent kinetic energy $K/U*_o^2$ behind single wide block (normal flow: 0°). Cross points: hot wire results; square points / solid line: LDA results; dotted line: FLUENT results.*

a) *U/U_{Ho} as a function of z/H (centre plane, 0°; $x/H = 3$)*
b) *As fig. 2.14a, but for $K/U*_o^2$*
c) *U/U_{Ho} as a function of x/H for $z/H = 1.5$ (upper line) and $z/H = 0.5$ (lower line)*
d) *As figure 2.14c, but for $K/U*_o^2$ at $z/H = 0.5$*

38

Wind speeds in the wake and the position of shear layers are tested by comparison with Laser Doppler data (Bottema et al, 1991a). Numerical estimates of flow around a single wide block (data: L,W,H = 0.04, 2.0, 0.08 m, $z_0 = 2.6*10^{-4}$ m, 5% blockage) correspond well with LDA results (fig. 2.14).

Differences between computations and LDA results are of the order of 20% of K and 10-15% of U_{Ho} (relative errors in U can not be given as U=0 on some locations). Numerical errors in the far wake (x/H > 7) may be larger.
Conventional hot wire techniques may result in large errors. This applies both for the wake and for the shear layers of an obstacle. LDA data are more suitable for validation of a numerical model as they do not suffer from these errors.
Computations with the Algebraic Stress Model (ASM) or with the standard K-ε model ($C_\mu = 0.09$) resulted in a poor prediction of the near wake. ($L_R \approx 35\%$ too short, shear layer $K \approx 50\%$ too large). This was even the case when wall function constants E' and κ were modified, so that a local $C_\mu=0.032$ applied near walls. Therefore, it is of great importance to simulate the approach flow correctly by matching C_μ to the approach flow value.

Comparison for oblique flow (same geometry as above, but for 30°) is only made with a 2 dimensional simulation as incorporation of wind tunnel walls required too much grid. Differences (in the centre plane of the obstacle) between the numerical and experimental results were of the same order as for normal flow.
Corner stream wind speeds were tested by comparing the 45° (oblique flow) simulation of table 2.3 with HWA measurements of Maruta (1984, p 91) (data L,W,H = 30x30x180 m; power law exponent α = 0.25, z/H = 0.055). Numerical predictions of corner stream U/U_0 were up to 15% higher. Hence, the numerical data are conservative for this case.
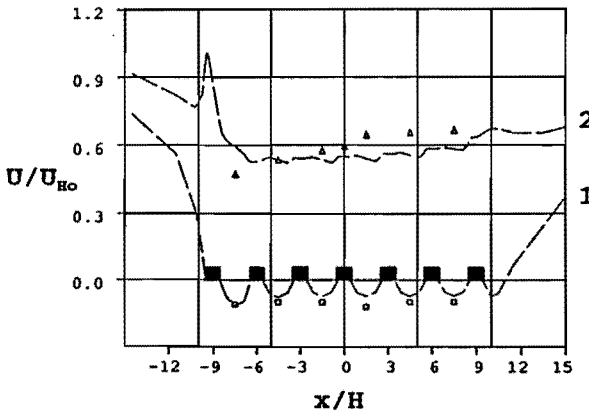
Figure 2.15: Normalized mean velocities (U/U_{Ho}) for a group of 7 obstacles (centre plane; 0°) as a function of x/H. Lower line is for z/H = 0.35 (1), lower line is for z/H = 1.25 (2). FLUENT results are given as long dashed lines.

Numerical performance for skimming flow over an obstacle group has been investigated as well. Seven (7) blocks with L,W,H = 0.04, 1.6, 0.4 m are placed behind each other (clear spacing S_x = 0.08 m). For practical reasons a smooth turntable is used. Approach flow z_0 and turntable z_0 are $5*10^{-6}$ m. The blockage factor is 5%.

Numerical simulations with an approach flow C_μ (0.034) underestimate wind speeds in the canyons. This is caused by the fact that turbulence generated by the obstacles dominates mixing into the canyons, not the approach flow turbulence. Canyon flow and canyon pressure fields are well predicted (within 5-10% of U_{Ho}) by the standard K-ε model where C_μ = 0.09 (figure 2.15).

In a building group, flow along (parallel to) streets is equally important as perpendicular flow. Simulations of normal flow entering a group of 50 mm cubes (data: clear spacing S: 100 mm, z_0 = $2.6*10^{-4}$ m, street surface and building z_0: $5*10^{-6}$ m) have been compared with some very limited hot wire data which are not reported in (Bottema, 1990). They show that U/U_0 on the streets (z = 10 mm) is underestimated by about 30% in the numerical simulations (measured $U/U_0 \approx 1.0$). These differences increase further if the approach flow C_μ is used. Therefore, the present model is not suitable to compute flow along streets. The model performs fairly well for wind flow across streets, as for the 'canyons'.

Finally, simulations with cyclic boundary conditions have been tested. No experimental results were available. However, the flow field in and above the streets turned out to be dependent on the initial wind profile. This was even the case after 1000 iterations, and convergence errors < 10%. Therefore, numerical results which are obtained with cyclic boundary conditions are not reliable without additional validation.

The results of the error estimates can be summarized as follows:

1. -comparison with various experiments has shown that in the case of normal flow (0°) U/U_{Ho}, K and C_{pHo} can all be predicted within 10%-20%.

2. -the (grid) errors for oblique flow (45°) are of the same order, or somewhat larger (in the corner streams).

3. -The main error sources are too coarse a grid and imperfections in K-ε modelling. These two errors tend to cancel each other in the present simulations. Significant improvement is only expected if better modelling techniques are combined with a finer grid (a factor 10 increase in grid points).

4. -the right choice of the model constant C_μ is essential for an accurate prediction: about 0.09 for skimming flow over an obstacle group; 0.034 (approach flow value) for other geometries.

Application of the K-ε model; limitations

The accuracy of the present K-ε model results has been discussed already. An accuracy of 10%-20% seems to be the best which can be achieved for not too complicated geometries. The accuracy can be even poorer if the computational grid is much coarser or finer than in the present simulations.

Geometry limitations can be dependent on the model which is used. The following limitation applies to almost all models:

1. *-The first grid node near a wall and the building height H must always be greater than $20z_0$.* In practice, H must be larger, depending on the allowed grid expansion factor, and the desired grid spacing at building walls.

Other geometry limitations do apply to the present model, but not always to other models:

2. -The $20z_0$ criterion has to be extended if pedestrian level is considered. In urban simulations, the urban canopy should be at least $20z_0$ above pedestrian level. In the present simulations, the urban canopy had to be omitted, or its z_0 had to be decreased to about 0.1 m.
3. -Only rectangular, right angled buildings can be considered with the prsent model. Oblique flow can (and must) be considered. In that case, the grid must be aligned with the building surfaces. Non rectangular geometries can be considered if models with body fitted coordinates (for rounded shapes; see Majumdar et al, 1989; Hoxey et al, 1989) or finite element models (e.g. for triangular shapes) are used.
4. -Building groups can be considered if the geometry is not too complex. Flow around two buildings can generally be considered on a 25000 points grid, unless none of the building faces is aligned with another. Some examples of allowed geometries are given below.
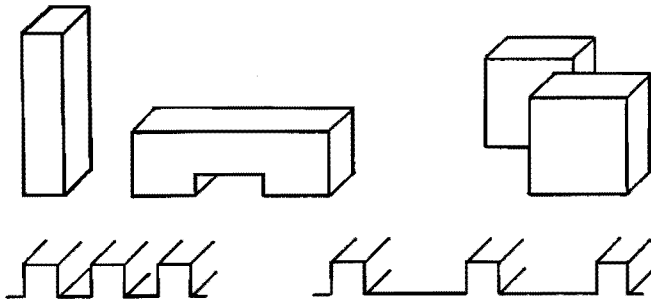
5. -Velocity and pressure peaks can not be determined with the K-ε model.
6. -Simulations with periodic (cyclic) boundary conditions are dependent on initial conditions. Such results are not reliable without additional validation.

41

Numerical simulations have been carried out for various rectangular buildings and building groups. Typical building dimensions are (L,W,H) 15 - 250 m. Typical approach flow z_0 values are 0.03 - 1.0 m, local surface z_0 is generally 0.03 m or less. The buildings are chosen to be 'featureless': z_0 of the building surface ≈ 1 mm.

The dimensions of the computational domain are 1200 x 1200 x 400 m. This is sufficient to make wall constraint effects insignificant, except maybe in the far wake (x/H > 7). Figure 2.16 gives a vertical section of a computational domain.

```
J   I=   2   4   6   8  10  12  14  16  18  20  22  24  26  28 =I  J
   22    S S S S S S S S S S S S S S S S S S S S S S S S S S S S   22
   21   IK . . . . . . . . . . . . . . . . . . . . . . . . . . O  21
   20   IJ . . . . . . . . . . . . . . . . . . . . . . . . . . O  20

   14   ID . . . . . . . . . . . . . . . . . . . . . . . . . . O  14
   13   IC . . . . . . . . . . . . . . . . . . . . . . . . . . O  13
   12   IB . . . . . . . . . .W3W2W2W2W2W2 . . . . . . . . . . O  12
   11   IA . . . . . . . . . .W2W2W2W2W2W2 . . . . . . . . . . O  11
   10   IO . . . . . . . . . .W2W2W2W2W2W2 . . . . . . . . . . O  10

    4   I4 . . . . . . . . . .W2W2W2W2W2W2 . . . . . . . . . . O   4
    3   I3 . . . . . . . . . .W2W2W2W2W2W2 . . . . . . . . . . O   3
    2   I2 . . . . . . . . . .W2W2W2W2W2W2 . . . . . . . . . . O   2
    1   WOWOWOWOWOWOWOWOWOWOWOWOWOWOWOWOWOWOWOWOWOWOWOWOWOWOWOWOWO  1
J   I=   2   4   6   8  10  12  14  16  18  20  22  24  26  28 =I  J
```

Figure 2.16: *Vertical section of computational domain showing grid cells. See text for explanation.*

At the upstream end(s) of the domain, inlet cells (I) are used. U, K and ε in these cells are equal to the approach flow values. Outlet cells (no streamwise gradient) have been placed at the downstream ends. Symmetry cells (S) are used for the upper boundary. For normal flow, symmetry cells are also used for the lateral boundaries. Different wall cells (W) are used for ground surface and building walls, depending on the roughness (z_0) of the considered surface. The wall function is not used near separation (W3).

The computational grid is staggered and non uniform, with grid intervals of 0.5 - 1 m near walls, and roughly 100 m far away from the obstacle. Grid expansion factors are generally 2 or less, except in complex geometries. Where possible (normal flow), symmetry planes are used to reduce the number of grid points.

The approach flow is chosen as an initial condition for each computation. This prevents dependence of the solution on a former computation.

For a well converged solution, 500 iterations are needed if the underrelaxation factors (see Patankar, 1980) are about 0.5, and if the number of sweeps (Patankar, 1980) for the pressure solution is about 25. The resulting normalized residuals are 10^{-3} or less, except for complex geometries. Convergence errors in the variables are always less than 5-10%, but in most cases less than 0.5%.

3 Wind comfort criteria

Local wind climate can only be judged if we know which conditions are uncomfortable, and how often they occur. This chapter discusses wind and different degrees of discomfort, and how local wind climate can be evaluated.
Section 3.1 discusses wind effects on people.
The minimum wind speed and turbulence level for uncomfortable conditions is given by a *discomfort threshold*. The reverse of a discomfort threshold is a *comfort requirement*: the maximum wind speed etc. for comfortable conditions. Comfort and safety requirements are discussed in section 3.2.
Section 3.3 gives the relation between shelter and local wind climate.
The acceptability of local wind climate can be judged with discomfort and danger *criteria*. Criteria consist of a threshold and an exceedance probability of the threshold. Criteria are discussed in section 3.4.

3.1 Wind effects on people

Wind effects on people can be the cause of uncomfortable or even dangerous conditions. Both thermal and mechanical wind effects will be discussed in this section.

Thermal effects of wind

Thermal comfort is determined by a large number of parameters such as air temperature, (short-wave and long-wave) radiation, metabolism (human activity), exposure time, clothing insulation, air humidity, mean wind speed, turbulence.

In equilibrium conditions, the thermal balance of the human body can be related to comfort. Thermal comfort models are proposed by Penwarden (1973), Fanger (1972), and others. These models are generally not suitable for outdoor use because equilibrium conditions (at least 1 hour with constant outdoor conditions and constant human activity) are rare.

For conditions with sufficient long exposure (e.g. outdoor restaurant), thermal comfort evaluation is possible with appropriate thermal comfort models. Fanger's (1972) model assumes that cooling by the wind is proportional to $U^{0.5}$. This proportionality is valid for laminar boundary layers (see Fanger, 1972; page 36), but not in turbulent flow. In the atmospheric boundary layer, cooling is expected to be roughly proportional to U.

Turbulence effects on comfort are not included in the present models for prediction of outdoor thermal comfort. Fanger's draught model (Fanger et al, 1988) clearly shows the importance of turbulence: the equivalent air velocity

(which includes turbulence effects on comfort) can be four (4) times the mean wind speed. The draught model is only valid for indoor conditions and for $U < 0.5$ m/s; $20^{\circ}C < T < 26^{\circ}C$. Still, Fanger's results show the importance of considering turbulence effects in the prediction of outdoor thermal comfort.

Mechanical wind effects; steady winds

The extended Beaufort scale (table 3.1) gives a summary of wind effects on people. It is not made explicit whether the wind effects in table 3.1 are caused by steady wind or by wind gusts. A first indication of steady wind effects can be obtained by converting (i.e. multiplying with 0.7) the wind speeds of table 3.1 to pedestrian level (1.75 m) wind speeds.
In the following, steady wind effects are discussed by a number of theoretical and experimental estimates.

Beaufort Number	Description	Wind speed in m/s	Wind effect
2	Light breeze	1.6 - 3.3	Wind felt on face
3	Gentle breeze	3.4 - 5.4	Hair disturbed; clothing flaps; newspaper difficult to read
4	Moderate breeze	5.5 - 7.9	Raises dust and loose paper; hair disarranged
5	Fresh breeze	8.0 - 10.7	Wind force felt on body; possible stumbling when entering a windy zone
6	Strong breeze	10.8 - 13.8	Umbrellas used with difficulty; hair blown straight; difficult to walk steadily, wind noise on ears unpleasant
7	Near gale	13.9 - 17.1	Inconvenience felt when walking
8	Gale	17.2 - 20.7	Generally impedes progress; great difficulty with balance in gusts
9	Strong gale	20.8 - 24.4	People blown over

Table 3.1   *Part of extended Beaufort scale (after Lawson et al, 1975), showing wind effects on people. The listed wind effects can be caused by gusts and by steady winds. Tabulated wind speeds U(10) are measured at 10 m height over open terrain ($z_o = 0.03$ m). They are averaged over 10 minutes (instead of one hour). Wind speed at 1.75 m height is 0.7*U(10). Maximum gust at 1.75 m height (3 sec. duration) within 10 minutes is about 1.1*U(10).*

Steady winds can interfere with people's activities by affecting people's balance (see fig. 3.1), by increasing the energy required for walking (Hunt et al, 1972, Penwarden, 1973), and by affecting performance (Hunt et al, 1976), walking, hair, clothes etc. (Murakami et al, 1980).

First, some theoretical estimates concerning people's balance and the energy required for walking and cycling are made.

The effect of wind force is to increase the effort of walking and to affect people's balance. The wind force on a human body is given by:

$$F = 0.5 \rho U^2 C_D A_p \qquad (3.1)$$

where A_p is the projected area normal to the wind (m^2), and C_D the drag coefficient. U is the pedestrian level (1.75 m) wind speed (m/s).
Penwarden (1978) gives values of A_f (area facing the wind) and A_s (side wind area) as a fraction of the total body area A_{Du} (DuBios area):

$$A_f / A_{Du} = 0.326 \pm 0.022 \quad (\pm 7\%)$$
$$A_s / A_{Du} = 0.219 \pm 0.016 \quad (\pm 7\%) \qquad (3.2)$$

The DuBois area, or the total body area is given by:

$$A_{Du} = 0.0769 \, (m \, g)^{0.425} \, h^{0.725} \qquad (3.3)$$

where m is the body weight in kg and h the body height in m. A typical value of A_{Du} is about 1.85 m^2, assuming that m = 70 kg and h = 1.75 m.

Typical drag coefficients are about 1.15 for head winds and about 1.0 for side winds (Penwarden, 1978). These drag coefficients are likely to be 10-20% too low as C_D is determined in a wind tunnel with wind speed decreasing above 1.40 m. Both projected area A_p and C_D can increase (open or flapping coat) or decrease (skirt) by about 10%. This results in a 20% variation in the total wind force.
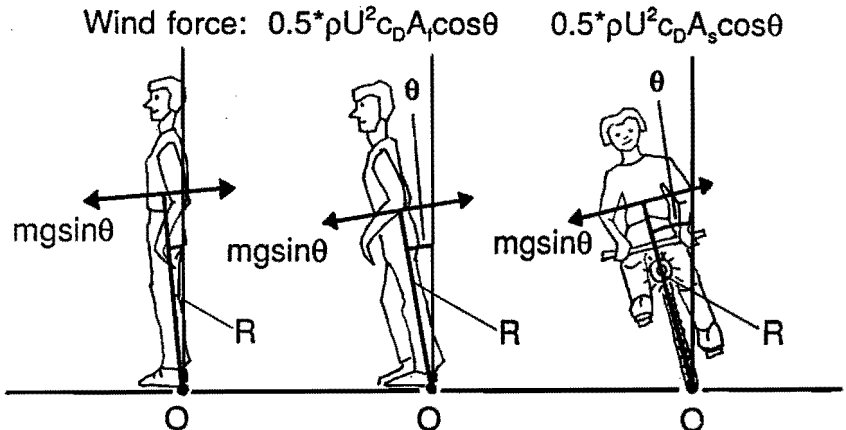
Figure 3.1: Force moments due to wind force and gravitational force on people standing right up, people leaning into the wind, and a cyclist leaning into the wind.

In strong winds, one has to lean forward or sideways in order to keep balance (see fig. 3.1). Assuming a constant drag coefficient C_D, the equilibrium angle is given by:

$$\theta = \arctan(0.5 \, \rho \, A_p \, C_D \, U^2 / (m \, g)) \qquad (3.4)$$

Eq. 3.4 is valid for pedestrians and for cyclists (side winds). If the ground surface is sufficiently rough, people (standing) can withstand constant wind speeds up to 30 m/s (Murakami, 1982). Penwarden (1973) gives an example of a man standing (hanging) in a steady 45 m/s wind. The equilibrium angles are 27° and 43° respectively. For pedestrians, an equilibrium angle $\theta > \approx 8^o$ ($U > 15$ m/s) is potentially unstable.

Walking against the wind requires extra energy. Table 3.2 (after Penwarden, 1973) gives some characteristic metabolic rates for different activities.

activity		metabolic rate (W/m^2) M/A_{Du}
sleeping, digesting		47
sitting quiet		59
standing		71
strolling	(0.7 m/s)	107
level walking	(0.9 m/s)	116
walking fast	(1.35 m/s)	150
marching	(1.8 m/s)	220
level running	(4.5 m/s)	590
sprinting	(10 m/s)	2400

Table 3.2: *Metabolic rate M/A_{Du} (W/m^2) for different activities (after Penwarden, 1973)*

The maximum metabolic rate which can be maintained by average untrained people is taken as 220 W/m^2 (Penwarden, 1973). Well trained people are expected to be able to maintain a metabolic rate of 600 W/m^2 for a few minutes. The rate of extra work when walking (with speed V) against the wind is:

$$EW = 0.5 \, \rho \, A_p \, C_D \, (U + V)^2 \, V \qquad (3.5)$$

Due to the extra work, metabolism (in W) increases with η_e*EW. The efficiency for extra work $\eta_e = 0.44$ (Penwarden, 1973). The total efficiency η_t (work / total metabolism) is never larger than 0.2 (Fanger, 1972). Therefore, the allowed extra work EW for untrained people is not more than about 80 W. Table 3.3 gives some values of maximum walking speed (uncertainty $\approx 20\%$) as a function of pedestrian level wind speed.

Progress into the wind is slightly slowed at 9 m/s. At 20 m/s, people can hardly make any progress into the wind.

Wind speed (m/s)	Max. walking speed (m/s)
0	1.8
9	1.35
14	0.9
20	0.45

Table 3.3:   Maximum walking speed for untrained people (maximum metabolic rate $220\ W/m^2$) for a number of wind speeds.

For cyclists, eq. 3.5 applies as well. Let us assume a 'base' metabolism of 70 W/m^2 (standing), and that all work is used to overcome the air resistance. Drag coefficient (1.15) and frontal area (0.60 m^2) are assumed the be the same as for pedestrians. Figure 3.2 shows which cycling speed (uncertainty $\approx$25%) can be reached for given head wind or tail wind speed and a given metabolic rate.

———————— high effort (600 W/m2)
— — — — — medium effort (220 W/m2)
- - - - low effort (107 W/m2)
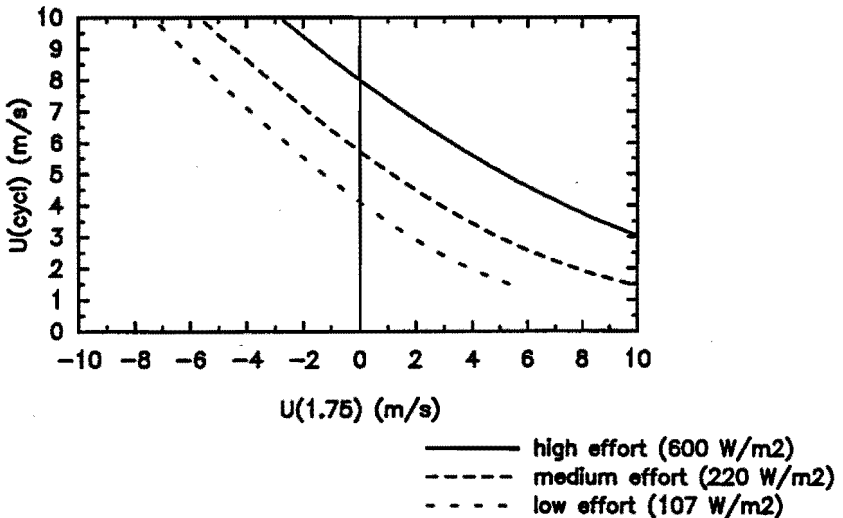
Figure 3.2:   Maximum cycling speed (uncertainty ≈25%) as a function of wind speed. Negative x-axis: tail winds; positive x-axis: head winds. Base metabolic rate 70 W/m^2. All work is used to overcome the air resistance.
Upper line: M/A_{Du} = 600 W/m^2: maximum for well trained people
Middle line: M/A_{Du} = 220 W/m^2: maximum for untrained people
Lower line: M/A_{Du} = 107 W/m^2: little effort required

Figure 3.2 shows that cycling at 4 m/s (U=0) requires little effort. In practice, 3 m/s appears to be the speed at which people can cycle with only little effort. In that case, 15-20 W is needed for moving the legs. Then, the lower curve of fig. 3.2 will be about 1 m/s lower. The other curves will hardly change.
It can be seen that average untrained people can cycle only slowly (3 m/s) in head winds of 5 m/s (4 Beaufort over open terrain). In 10 m/s (6/7 Beaufort), untrained people can not cycle any more and even well trained people have to cycle very slowly. These data should be considered if comfort criteria are applied to cycle-tracks.

Hunt et al (1976) and Murakami et al (1980, 1982) have investigated the effects of steady winds on people. Hunt et al (1976) found that increasing the mean wind speed from 4 to 8 m/s resulted in a more eye blinking and in a longer time needed for tasks like putting on a raincoat. Murakami et al (1980, 1982) have carried out an extensive research on wind effects on people. Table 3.4 shows some effects of steady winds.

As far as can be judged from these subjective assessments, wind effects on walking (effort; body posture) correspond well with table 3.3 and eq. 3.4. Wind effects of the extended Beaufort scale generally occur at lower wind speeds. This is an indication of the influence of wind gusts.

U (m/s)	wind effects:
5 m/s	-No effect on walking -Minor disturbance of hair and clothes -Wind felt on face
10 m/s	-Walking not easy (some subjects); footsteps irregular; posture/balance affected -hair disturbed; fluttering clothes; difficult to hold umbrella -wind noisy; frequent blinking
15 m/s	-walking difficult to control; upper body bends forward -clothes fluttering; hair violently disturbed; impossible to hold umbrella -impossible to open eyes continuously; tears falling
20 m/s	-walking very difficult; whole body bends windward -violent fluttering of clothes -impossible to face wind; earache, headache, breathing difficult
25-33 m/s	-impossible to stand in the wind; blown away (Murakami, 1982).

Table 3.4: Wind effects on people in uniform wind; effects on walking, hair/clothes, face. After Murakami et al (1980).

Mechanical wind effects; non uniform winds

Wind conditions near building corners can be dangerous because of very sudden changes in wind speed and wind direction. A sudden increase of wind speed to 15 m/s or more can be sufficient to bring people out of balance.

Murakami et al (1980) carried out some walking tests in a wind tunnel. Footstep irregularities were measured when people were walking through a 'jet' of strong side winds, caused by an opening in a fence. For female subjects, course deviations increased up to 0.3 m for a 'jet' wind speed (U_{max}) of 20 m/s. The observed wind effects (i.e. footstep irregularities) were roughly comparable with wind effects in uniform flow with a speed of $1.5*U_{max}$ or more. Wind effects were generally small for $U_{max} < 10$ m/s.

Mechanical wind effects; wind gusts

Wind force on the human body increases progressively with wind speed, as is shown by eq. 3.1. Therefore, most investigators have concentrated on the effect of peak gusts. First, effects on safety are discussed.

A sudden gust can be sufficient to blow someone over, depending on gust speed, gust dimensions and gust duration, and on reaction time and body posture. The required gust speed must be large enough to 'lift' or push someone over his feet (or heels). This corresponds with an equilibrium angle θ (eq. 3.4) of 8°, and a gust speed $U_g > 15$ m/s.
The minimum gust duration t_g (time that gust speed is approximately constant) to bring someone out of balance can be determined by $x = 0.5*(F/m)*t_g^2$, where x being a 'critical' displacement of the human body (at which the body begins to overbalance) and F/m the body acceleration due to wind. This results in:

$$U_g t_g > (\frac{4 \, x \, m}{\rho \, A_p \, C_D})^{0.5} \qquad (3.6)$$

x is the distance over which the centre of the body must move before it begins to overbalance. If $U_g = 15$ m/s and $x = 0.12$ m, a gust with $t_g \approx 0.4$ sec. is sufficient to bring someone out of balance. The length (or height) L_g over which the gust speed is constant can be estimated as $L_g = U_g t_g$. In the present case, $L_g = 6$ m, which is clearly large enough to cover the whole body.

Suitable publications on wind effects on bicycles have not been found. The dynamics of a bicycle is too complicated to allow for simple estimates of the effects of wind gusts. If the gust duration is more than a few seconds, the equilibrium angle for side winds can be approximated by eq. 3.4. The effect of a sudden wind speed decrease after some time of 'hanging into the wind' (fig. 3.1) is to leave the cyclist in an unstable position. The minimum 'dangerous' wind speed before the decrease will be of the order of 15 m/s (own experience). Clearly, more research is needed before side wind (and safety) thresholds for cyclists can be developed.

Clothes are also affected by wind gusts. Clothes can be blown up by friction effects or by pressure fluctuations in the flow. Hunt et al (1972) gave an expression for the 'friction effect'. It turned out that the friction effect required too large wind speeds and turbulence intensities to be effective. Therefore, the pressure effect is expected to be dominant.

Flapping of clothes is related to vortex shedding around (parts of) the human body. A typical streamwise length scale of the vortices is about St^{-1} times body width, where St is the Strouhal number (≈ 0.20). Vortex shedding is enhanced by 'approach flow' eddies of similar size (Hunt, 1975). For a body width of 0.2-0.6 m (depending on flow angle), the scale of the vortices is 1-3 m; an order of magnitude smaller than vortices which affect walking balance. Flapping of clothes probably requires a gust speed of 4 m/s, when wind can extend a light flag (table 3.1). The minimum gust duration is probably a few seconds or less.

It is not easy to correlate wind effects on people with measured wind speeds because wind speeds in small scale gusts are only constant within a few metres or less. Experimental work has been carried out by Hunt et al (1976), Jackson (1978), and Murakami et al (1980, 1982, 1986). Unfortunately, it is often not made explicit which gust speed, gust duration and gust dimension are needed for certain wind effects.

Murakami et al (1980) carried out several outdoor experiments; mainly walking tests. In his first set of outdoor experiments, wind effects on clothes, hair, and walking were observed from instantaneous gust speeds of about 7 m/s (gust duration not given). Figure 3.3 gives an example of observed footstep irregularities. Murakami chose to correlate wind effects on people with a mean wind speed averaged over 10 seconds (U_{10}). This results in a poor correlation between wind speeds and wind effects. Still, it can be concluded from his results that for $U_{10} < 10$ m/s the effect of head winds on walking is much larger than the effect of tail winds.
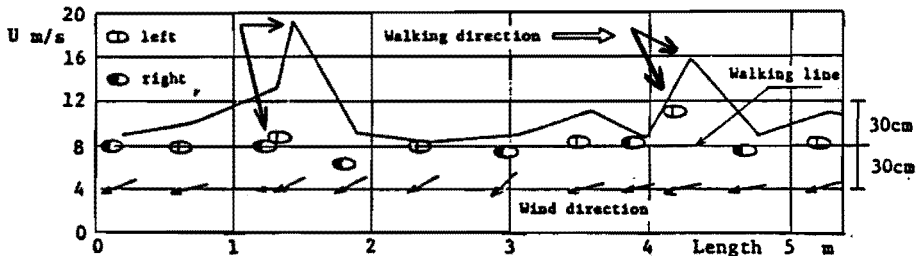
Figure 3.3:   Observed footstep irregularities and wind speed (1 m height) near a high rise building (Murakami, 1982)

In Murakami's second set of outdoor experiments, 2000 random pedestrians near a high rise building were filmed. Mean wind speed (10 min average at 1 m height) ranged between 4 and 11 m/s, peak gusts U_3 (3 sec. duration) between 9 and 19 m/s. Turbulence intensity T_u was about 30%. Wind effects on walking were assumed (but not verified) to correlate well with a peak gust of 3 sec. duration. The best correlation was found between footstep irregularities and U_3 (see table 3.5 for results). Still, differences between subjects were very large: If one subject hardly notices any wind ($U_3 = 9$ m/s), another subject can have serious difficulties with walking.

Inhabitants near a 14 storey high rise building in Tokyo have been involved in a long term investigation of wind effects (Murakami et al, 1986). It was assumed (not verified) that wind effects correlated with U_2; the maximum gust of 2 sec. duration within an hour. Unfortunately, the anemometers were protected by trees, and wind speeds were probably not representative of the actual (maximum) wind conditions.

u_g(m/s)	t_g (s)	author	wind effect
4	5	B/JA	clothing flaps
	5	B/JA	hair is disturbed
7	1-10?	B	dust and paper being raised
	5	B/JA	hair disarranged
10	3?	MU	irregular footsteps; walking difficult to control; eyes felt dry
	5	JA	violent flapping of clothes
	10	JA	progress into wind slightly slowed
14	2	JA	blown sideways
	10	JA	appreciably slowed into wind
15	2	eq. 3.4	people can be brought out of balance by gusts
	3?	MU	walking difficult
			dangerous for elderly person
16	10	JA	almost halted into wind
	10	JA	uncontrolled tottering walking downwind
20	3?	M	great difficulty with balance in gusts
21	2	JA	unbalanced; grabbing at supports
23	3?	M	people blown over by gusts

Table 3.5: *Wind effects on people as a function of gust speed U_g and estimated gust duration t_g. Data are from M (Melbourne et al, 1971) MU (Murakami et al, 1980), JA (Jackson, 1978) and B the extended Beaufort scale (Penwarden, 1973). The gusts are given for 1.0 (MU), 1.75 (B) and 2 m (JA) height.*

Jackson (1978) reported some wind effects in (very) strong winds. Gust speed was measured; gust duration was estimated.

Jackson also made a summary of wind effects as a function of standard mean wind speed. Table 3.5 gives a similar summary, but now as a function of gust speed and gust duration (if available: taken from Jackson, 1978). If gust velocity is not given explicitly, it is assumed to be equal to the maximum gust with a recurrence time of 1 h (using equation 2.11).

It is seen that wind gusts below 4 m/s have little effect. Serious wind effects (i.e on walking) occur for gust speeds > 8-10 m/s. Balance and walking path are affected from 15 m/s on. This may be dangerous for elderly people. Gust speeds in excess of 20 m/s can also be dangerous for young people.

Comparison with table 3.1 and 3.4 shows that the effects of peak gusts can be much larger than the effects of steady winds with the same speed. This is due to the surprising effects of gusts.

3.2   Requirements for comfort and safety

In the previous section, an overview is given of wind effects which can cause discomfort or danger. It has been shown that wind effects due to gusts are most severe. However, wind effects due to a rarely occurring gust do not always result in discomfort. This section discusses requirements for comfort and safety, and the investigations which led to requirements.

Wind comfort requirements

Good wind comfort requirements (i.e. the reverse of discomfort thresholds) are based on comfort investigations. These investigations are very scarce. Often, only wind effects have been considered, not wind comfort.

In many discomfort thresholds, a so called equivalent wind speed U_e is used:

$$U_e = U + k\sigma_u = U(1 + kT_u) \tag{3.7}$$

where k is the peak factor (see section 2.1). A high value of k (3 or 3.5) corresponds with an hourly peak gust of a few seconds duration. A lower value of k (say 1) corresponds with gusts occurring more frequently and/or gusts of longer duration (see also eq. 2.11).

The early discomfort thresholds, in which gust effects were not made explicit, (Isyumov et al, 1975; Lawson, 1978) were based on the Beaufort scale (k=0). Later, it was recognized that wind gusts were important. Melbourne (1978) used a 3 sec. peak gust $U + 3.5\sigma_u$ as a threshold for discomfort; Gandemer (1975) an equivalent wind speed $U + \sigma_u$.

Hunt et al (1976) investigated wind effects and wind comfort by wind tunnel experiments. He based his comfort requirements mainly on the observed wind

effects on performance and walking. Some verbal assessments of comfort were made (e.g. quiet-noisy; eyes dry-watery; pleasant-intolerable) but they were not condensed into a single comfort criterion.

Not only high wind (gust) speeds can lead to discomfort but also large spatial gradients (Hunt, 1976). Hunt gave separate thresholds for non uniform winds. They are mainly based on wind effects on walking and balance. Therefore, they are more suitable as a safety requirement.

Jackson (1978) investigated wind comfort by means of a street survey (questionnaire) in Wellington (NZ). The subjects were asked for verbal assessments of comfort and of outdoor conditions. Clusters were identified which related to personal comfort, perception of wind conditions and perception of thermal conditions. Jackson summarized the results of the first cluster in an overall comfort score. The percentage of people which felt comfortable was $92 - 8.2 * U_e$, where U_e is an equivalent wind speed (eq. 3.7). The peak factor k is equal to 1.1 ± 0.2.

ref	comfort requirement (m/s)		applicable for:
COMFORT:			
ISY75	U (Beauf.)	< 6B	tolerable for 'walking fast'
ISY75	U (Beauf.)	< 5B	id. 'strolling/skating'
ISY75	U (Beauf.)	< 4B	id. 'standing/sitting: short'
ISY75	U (Beauf.)	< 3B	id. 'standing/sitting: long'
LAW75	U	< 5 m/s	remedial action of shop owners
HUN76	$U + 3\sigma_u$	< 6 m/s	for activities very sensitive to wind
HUN76	$U + 3\sigma_u$	< 9 m/s	for most activities to be unaffected
GAN78	$U + \sigma_u$	< 6 m/s	applied to all activities
LAW78	U (Beauf.)	< 6B	tolerable for roads, car parks
LAW78	U (Beauf.)	< 5B	id 'walking'
LAW78	U (Beauf.)	< 4B	id. 'standing, entrances'
LAW78	U (Beauf.)	< 3B	id. 'covered areas'
VIS80	U	< 5 m/s	applied to all activities
MUR86	U_3 (daily max)	< 10 m/s	applied to all activities
MUR86	U_3 (daily max)	< 15 m/s	applied to all activities
WIL91	U_t	< 4.2 m/s	acceptable for 'sitting'
WIL91	U_t	< 6.1 m/s	id. 'standing'
WIL91	U_t	< 8.3 m/s	id. 'walking'
eq. 3.8	$U + \sigma_u$	< 6 m/s	walking / strolling
fig. 3.2	U	< 5 m/s	max. head wind for cyclists

Table 3.6: Requirements for comfort as proposed by Isyumov et al (1975); Lawson et al (1975); Hunt et al (1976), Gandemer (1978); Lawson (1978); Visser (1980); Murakami et al (1986), Williams et al (1991). Wind speeds are measured at 1.5 - 2 m height. For Beaufort thresholds: Use values of table 3.1 and multiply with 0.70 to obtain U(1.75 m).

Jackson (1978) reported a k-value of 3 because he compared his field data with results of Hunt. In Hunt's wind tunnel experiments however, turbulence conditions were rather different from outdoor conditions (Hunt, 1976). Jackson (1978) did not account for this. As the differences can not be fully corrected, we will use Jackson's field data only, which yield an equivalent wind speed with the peak factor $k = 1$:

$$U_e = U + \sigma_u > 6 \text{ m/s} \qquad (3.8)$$

The threshold of 6 m/s has been chosen in order to allow for comparison with existing criteria, and corresponds with 57% dissatisfied people.

Eq. 3.8 is only valid for walking/strolling. For other activities, other requirements (or thresholds) may be appropriate. Table 3.6 gives a number of existing comfort requirements. These comfort requirements are not based on extensive comfort investigations. It can be seen that Gandemer (1978) had a good intuition as he was the only one who chose the right peak factor k (k=1).

Recently, Durgin (1991) has tried to make discomfort thresholds more comprehensible by describing steady effects and gust effects by a single parameter. Williams et al (1991) recognize the fact that a single peak gust is not a good indicator of discomfort. They consider the total time that the instantaneous wind speed exceeds a certain threshold. Neither Durgin's nor Williams' proposals are based on comfort investigations.

ref	safety requirements (m/s)		based on:
CONTROL OF WALKING:			
HUN76	$U + 3\sigma_u$	< 15 m/s	experiments
MUR80	U_3	< 15 m/s	experiments
SAFETY:			
ISY75	U (Beauf.)	< 8B	Beaufort scale
HUN76	$U + 3\sigma_u$	< 20 m/s	observations of Melbourne et al (1971)
MEL78	$U + 3.5\sigma_u$	< 23 m/s	outdoor observations during storm
WIL91	U_t	< 26.4 m/s	calculations (assumptions?)

Table 3.7: Requirements for control of walking and for safety as proposed by Isyumov et al (1975); Hunt et al (1976), Melbourne (1978); Murakami et al (1980), Williams et al (1991). Wind speeds are measured at 1.5 - 2 m height. For Beaufort thresholds: Use values of table 3.1 and multiply with 0.70 to obtain U(z = 1.75 m)

Safety requirements

The number of proposed danger thresholds is much smaller than the number of comfort thresholds. This is due to a lack of experimental data. The results of Melbourne's (1971) observations during a storm are often used. Similar observations are made by Jackson (1978). The measured gust speeds, and the estimated gust durations are given in table 3.5.

54

Wind tunnel experiments have been carried out by Hunt (1976) and Murakami (1980). Murakami used results of outdoor experiments as well and found that walking became difficult for $U_3 > 15$ m/s (mainly young subjects). However, for gust speeds up to 20 m/s, no one was reported to fall.

Table 3.7 gives a summary of proposed safety requirements. They can be divided into two groups: Control of walking, and safety. The two 'control of walking' requirements are almost equivalent.
Most experiments and observations are based on young people. Downward revision is required for elderly people and probably also for cyclists. This can be done by using the first set of requirements (control of walking) as a safety limit. Hunt's (1976) thresholds for non uniform flow are not included in table 3.7: they are less restrictive than results for 'conventional' turbulent flow.

Regarding the observations of Melbourne et al (1971) and Jackson (1978), Williams' u(t) limit seems to be too high. Hunt's threshold seems to be most appropriate as there is considerable risk of loss of balance at gust speeds of 20 m/s (table 3.5). For young people, Melbourne's expression may be more appropriate as a safety threshold.
From 9 Beaufort on, safety is not only determined by pedestrian wind speed. Falling roof tiles, tree branches etc. may be dangerous for pedestrians as well.

3.3   Wind comfort climatology

In most climates, wind conditions on a location can not always be comfortable (except maybe indoors). We must accept uncomfortable wind conditions for a certain percentage of time. Local wind climate can be improved by providing shelter. This section discusses the relation between shelter and local wind climate, as well as the accuracy of predictions of local wind climate. The acceptability of wind climate, and the amount of required shelter will be discussed in section 3.4.

Definitions and assumptions

Wind comfort refers to local conditions. Long term wind statistics on the location of interest are generally not known. They must be derived from statistics at a meteorological station in open terrain (e.g. airport).

First, local mean wind speed must be linked to the airport mean wind speed. The airport wind speed is assumed to be fully exposure corrected (measuring height 10 m; roughness length z_0: 0.03 m), and is called the *potential wind speed* U_{pot} (see section 2.1). The *wind amplification factor* γ is defined as $U(local)/U_{pot}$. At an 'ideal' meteorological station, $\gamma = 0.7$ at 1.75 m height. In the next sections we will use a direction independent γ to compare different thresholds and criteria, i.e. a γ which is the same for all wind directions.

The next step is to relate U_e to the mean (hourly) wind speed U. This can be done by using eq. 3.7, if we know T_u or σ_u.

In previous research it was often assumed that T_u is roughly constant. This is caused by the use of hot wire anemometers which underestimate high T_u (section 2.3). Laser Doppler results and numerical simulations (Bottema et al, 1991) show that T_u is far from constant. In fact, pedestrian level σ_u is approximately constant, not T_u. It will be assumed that local σ_u is equal to σ_u measured at a meteorological site. The relative error in this estimate is about 25%. Estimates of T_u and σ_u will be discussed in more detail in chapter 4 (e.g. p. 92).

The last assumptions relate to the long term airport statistics.
First, it is assumed that the frequency distribution of hourly mean wind speeds can be described by a cumulative Weibull distribution:

$$P(U_{pot} > M) = exp(-(M/a)^k) \qquad (3.9)$$

$P(U_{pot} > M)$ is the probability that U_{pot} is larger than M. The parameter a is a velocity scale (m/s), k is a shape parameter. A small k results in a long tail of the distribution: the peaks are high compared to the mean yearly wind speed.
The Weibull distribution is well suitable if $4 < U_{pot} < 16$ m/s (Wieringa, 1983). This range in U_{pot} covers most wind speeds of interest for wind comfort.
We will use the Weibull distributions of Troen et al (1989). For practical applications, and for statistics of rarely occurring storms (<36 hours/year) Wieringa's data (Wieringa et al, 1983) are recommended. It should be noted that these data are only corrected for roughness within a few kilometres of the meteorological site, not for the large scale roughness.

The methods given above allow for estimates of *discomfort probability* and *danger probability*. Discomfort and danger probability are defined as the percentage of hours in which the comfort and safety requirements of table 3.6 and 3.7 are not met.

Local wind climate and shelter

In the following, the relation between shelter (or γ) and discomfort and danger probability (see also Wisse et al, 1991) will be presented. In this way, one can judge which shelter is needed to reduce discomfort probability to a given level.
The results of this section can also be used for a comparison between different comfort requirements. Figure 3.4 shows probability on different degrees of discomfort for the climate of Amsterdam airport (climate data from Troen et al, 1989). Discomfort probability is given as a function of γ for a number of thresholds (see table 3.6 and 3.7).

For each threshold, there is a γ_{min} for which discomfort or danger probability is negligible (say 1% and 0.1%). For $\gamma > \gamma_{min}$, discomfort (danger) probability increases progressively until a level of about 25% is reached. Above this level,

the rate of increase becomes smaller. The different thresholds can be compared by comparing their γ_{min}.

Figure 3.4a shows the results for discomfort thresholds. The value of γ_{min} is dependent on the effective wind speed U_e and on the peak factor k (eq. 3.7). For the proposed threshold (eq. 3.8), k = 1 and γ_{min} = 0.3. A too high k (3) may result in underestimation of γ_{min} (γ_{min} = 0.2), and in the creation of too much shelter. The reverse applies for too small a k (k = 0; γ_{min} = 0.4).
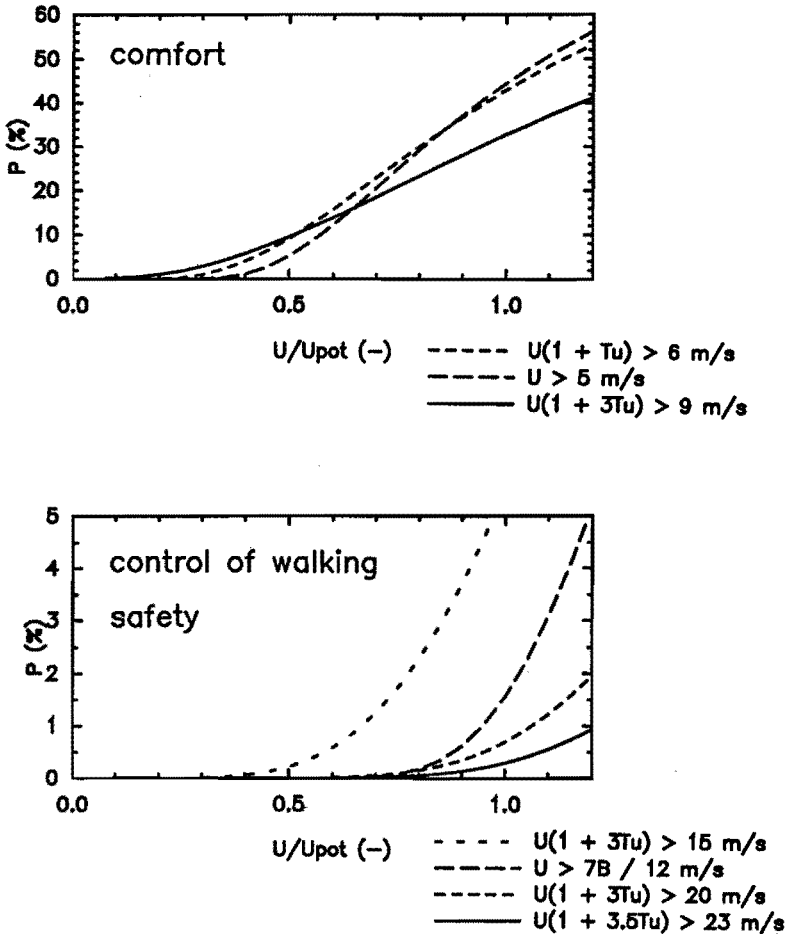

Figure 3.4: Percentage of time that comfort and safety requirements are not met as a function of direction independent wind amplification factor γ (U/U_{pot}). Climate statistics: Amsterdam airport (Troen et al, 1989).
a) comfort: standing/sitting and strolling/walking
b) control of walking and safety

For 'control of walking' and safety (fig 3.4b), γ_{min} depends mainly on U_e. For all thresholds, γ_{min} varies between 0.4-0.5 for 'control of walking' to about 0.7 for safety. The actual discomfort probability is strongly dependent on the threshold used.

Thresholds which are not based on comfort or safety investigations do not always lead to erroneous criteria. This is because the maximum acceptable discomfort probability can be adjusted to a level which results in the same required shelter. Of course, this can only be done if discomfort probability P varies significantly with γ, i.e. for $\gamma > \gamma_{min}$. In practice this approach does not work well because of spatial variations in wind climate.

A final point of interest is the accuracy which can be achieved in a prediction of discomfort probability. An uncertainty of 10% in γ must be considered as very small. Actually, thermal effects may result in over 20% error in γ if U_{pot} is less than 5 - 7.5 m/s (daytime; nighttime; see table 2.2). This corresponds with discomfort probabilities greater than 20-45%.
The relative errors in these high discomfort probabilities (P > 20%) are 30-45%. For smaller discomfort probabilities (and larger U_{pot}), these relative errors are larger, even though the accuracy in γ is better for large U_{pot}. The uncertainty in danger probability may be a factor 2, even if γ can be estimated within 10%.

In reality, the uncertainties may be somewhat smaller. This is because γ depends on wind direction so that some of the errors may be independent of each other (and compensate each other).

Wind comfort climatology for different locations

The notion of wind climate (not 'local wind climate') implies that it is constant over a rather large area. When both climate and terrain are comparable, the same amount of shelter, and the same design measures for control of local wind climate are needed. In practice, surrounding terrain has a large influence on γ and on wind climate. This issue will be discussed in section 4.2.
This section discusses only *climatic* differences within the Netherlands and within parts of Europe, and their consequences for design (see Wisse et al, 1991).

For all comparisons, two thresholds are used:
     -discomfort: $U + \sigma_u > 6$ m/s (eq. 3.8)
     -danger: $U + 3\sigma_u > 20$ m/s (Hunt et al, 1976)

Figure 3.5 shows such a comparison for a number of Dutch stations. It can be seen that climatic differences between coastal, inland and intermediate stations (i.e. Terschelling, Eindhoven, Amsterdam) are rather small. If Amsterdam is chosen as representative for all stations, the observed differences correspond to less than 10% variation in γ. For wind danger, observed regional differences are larger (greater frequency of storms along Dutch coast), but still within 15% variation in γ. Chapter 7 will discuss the consequences for design.

Further comparison was made for Ålborg (DK), Berlin (FRG) and Nantes (F), as is shown in figure 3.6. For $\gamma < 0.6$, wind climates correspond quite well. Differences with Amsterdam correspond with a 15-20% variation in γ. For larger γ, the observed differences decrease, except for Nantes. For danger, climatic differences increase up to a 15-25% variation in γ.

In Middle and Southern Europe, wind climate can be very different from the Dutch climate. The further South and East one goes, the smaller the influence of depressions, and the larger the local effects. This can result in both very calm (e.g. near Milano) and very windy regions (e.g. the Rhone valley).

Figure 3.5: *Discomfort and danger probability (%) as a function of direction independent γ (U/U_{pot}) for different parts of the Netherlands. Terschelling is a typical coastal station, Eindhoven a typical inland station, Amsterdam is an intermediate station.*

a) *Discomfort: $U + \sigma_u > 6$ m/s (eq. 3.8)*

b) *Danger: $U + 3\sigma_u > 20$ m/s (Hunt et al, 1976)*

59

If one considers danger, the implications for design are not very different for a roughly 100-200 km wide coastal zone from Northern France up to Denmark. In the case of comfort, people may get used to windy conditions. This will decrease the influence of wind climate on design. However, Lawson's (1975) results of complaints of shop owners did not show any habituation to (and acceptance of) windy conditions.
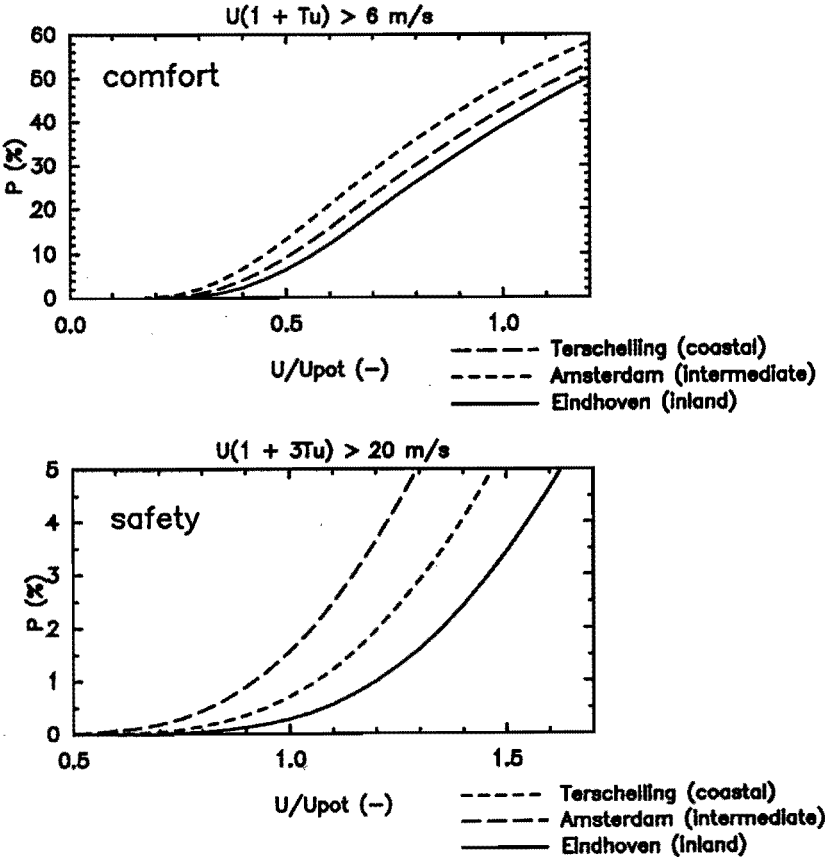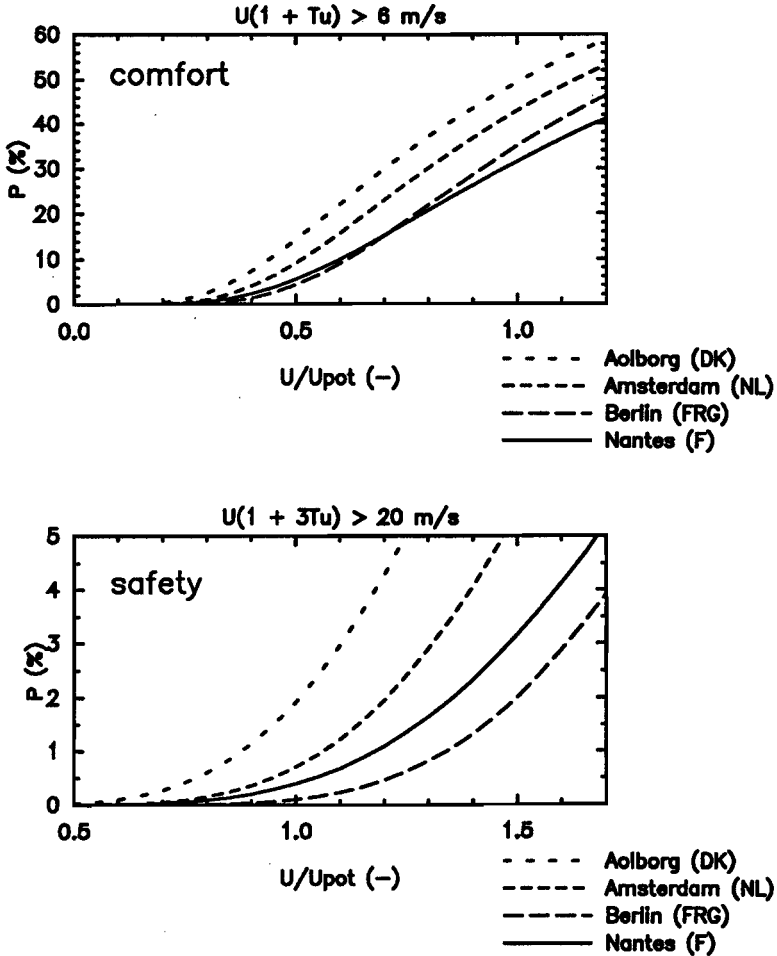

Figure 3.6: *Discomfort and danger probability (%) as a function of direction independent γ (U/U_{pot}) for some European stations: Amsterdam (NL), Ålborg (DK), Berlin (FRG) and Nantes (F).*
a)   *Discomfort: $U + \sigma_u > 6$ m/s (eq. 3.8)*
b)   *Danger: $U + 3\sigma_u > 20$ m/s (Hunt et al, 1976)*

3.4 Wind comfort criteria

Section 3.2 presented a number of thresholds for discomfort and danger. The relation between wind climate and shelter was discussed in section 3.3. For practical applications, it should be known which discomfort (or danger) probability is acceptable for a given human activity. In other words: discomfort and danger thresholds must be extended to discomfort and danger *criteria*.

Requirements for wind comfort criteria

A first requirement for comfort criteria is that there is experimental evidence for the choice of a maximum acceptable discomfort probability. Although rather trivial, this requirement is generally not satisfied. In fact, there is just one publication (Lawson et al, 1975) in which investigations on the maximum acceptable discomfort probability have been reported.

Lawson and Penwarden (1975; p. 609-611) analyzed complaints of shop owners. They reported that if $U > 5$ m/s for 10% of the time, remedial action (wind reducing measures) was contemplated. Generally, remedial action was taken if $U > 5$ m/s for 20% of the time or more. These percentages were estimated by using the concept of γ, not by long term measurements on the sites.
Furthermore, it was assumed that high (corner stream) wind speeds applied to all wind directions. In reality, wind speeds are reduced for at least 25% of the wind directions (2 out of 8). Therefore, Lawson's probabilities should be reduced from 10/20% to 8/15%.

A second requirement is that the threshold corresponds to the type of activity for which the criterion is used. It is useless to determine danger probability from a threshold for long term sitting, and vice versa.

For many criteria, the threshold does not correspond to the activity considered. Such criteria are called *indirect criteria*. They are only correct for a single wind climate.
The criteria of Melbourne (1978) and Beranek (1984) are indirect criteria. As a threshold, they use a yearly maximum gust ($U + 3.5\sigma_u$; $U + 3\sigma_u$). This may be correct for a fixed wind climate and a fixed relation between T_u and γ, but certainly not for all climates. In the USA, Ratcliff et al (1990) compared a number of comfort criteria, including those of Melbourne (1978). Melbourne's criteria were rather restrictive compared with other criteria which were developed before 1978, even though Melbourne based his criteria on comparison ('averaging') of the same 'early developed' criteria. This is a clear indication that such indirect criteria can only be used for a single wind climate.

There is another class of indirect criteria (e.g. Gandemer, 1978; Visser, 1980) which use a single threshold for all human activities. Generally, this does not give rise to major problems, except when safety is judged by comfort criteria instead of by safety criteria.

61

A final requirement for comfort criteria is flexibility (in using them). As discussed in section 3.3, and in chapter 2, the relative error in γ is of the order of 10-20%. This may result in considerable uncertainty in the estimation of discomfort and danger probability. Therefore, it may be wise to use criteria with a 'good-moderate-bad' classification instead of 'good-bad'. The 'moderate' classification should cover a range in discomfort probability which is representative for the uncertainty in γ.

Comparison of discomfort and danger criteria

In the following an overview of existing comfort and safety criteria will be given. It will also be discussed which criteria are too restrictive or too lenient for use in Western Europe.

Probably the best way to compare wind comfort criteria is to classify them according to human activity, and to determine the minimum required shelter for 'tolerable' or 'acceptable' conditions. As a measure of the required shelter, we use the maximum allowed γ (γ_{max}), where γ is again independent on wind direction (i.e. the same for all wind directions). For T_u and for σ_u we make the same assumptions as in section 3.3 (local σ_u is equal to σ_u at meteorological site). For peak gusts (U_3), U_e is estimated by using the reported T_u and eq. 2.11 (Gaussian probability distribution).

It is noted once again that there is just one criterion with an experimental basis: the (corrected) shop owners criterion of Lawson et al (1975). For strolling, the 8% limit can be considered as tolerable and the 15% limit as unacceptable. It is worth noting that the Dutch climate is considered as unpleasant because it rains so often: about 7% of time.

Many criteria (i.e. Melbourne, 1978; Visser, 1980; Beranek, 1984) are based on (comparison of) previously developed criteria. These previously developed criteria are generally based on the experience of the investigator, not on published results of investigations.

Melbourne (1978) and Visser (1980) state that most comfort criteria correspond quite well, despite the apparent differences. Table 3.8 shows that this is only partly true, even for the old T_u estimate ($T_u = 30\%$). For example, Lawson's (1978) criteria for 'unacceptable' conditions tend to be more lenient than other criteria, while Melbourne's (1978) criteria are rather restrictive for 'strolling' and 'walking'.

If we use the present estimate of T_u and σ_u, it is found that the differences between criteria are much larger. Within the class of 'strolling', Murakami's (1986) and Williams' (1991) criteria clearly yield a larger γ_{max} than Lawson's 'shop owners' criterion. These two criteria are too lenient. On the other hand, Melbourne's criteria are too restrictive. For the 'sitting/standing' classes, Beranek's (1984) criteria are too restrictive as well. Both criteria require $\gamma = 0$ for 'sitting/standing long'. This is due to the present assumption of constant σ_u.

REF.		THRESHOLD	P_{max}	γ_{max}(old)	γ_{max}(new)
Sitting/standing long:					
ISY75	U (Beauf.)	> 3B	0.14%	0.25	0.25
GAN78	$U + \sigma_u$	> 6 m/s	2%	0.40	0.35
LAW78	U (Beauf.)	> 3B	4%	0.36	0.36
MEL78	$U + 3.5\sigma_u$	> 10 m/s	1/yr	0.27	0
VIS80	U	> 5 m/s	0.03%	0.29	0.29
BER84	U_3	> 10 m/s	1/yr	0.28	0
Sitting/standing short:					
ISY75	U (beauf.)	> 4B	0.14%	0.36	0.36
GAN78	$U + \sigma_u$	> 6 m/s	10%	0.53	0.51
LAW78	U (Beauf.)	> 4B	4%	0.53	0.53
MEL78	$U + 3.5\sigma_u$	> 13 m/s	1/yr	0.35	0.11
VIS80	U	> 5 m/s	1.37%	0.41	0.41
BER84	U_3	> 15 m/s	1/yr	0.43	0.29
MUR86	U_3	> 9 m/s	10%	0.50	0.50
WIL91	U_t	> 4.2 m/s	20%	0.57	0.57
Strolling:					
ISY75	U (Beauf.)	> 5B	0.14%	0.56	0.56
LAW75	U	> 5 m/s	15%	0.63	0.63
HUN76	$U + 3\sigma_u$	> 9 m/s	10%	0.51	0.51
GAN78	$U + \sigma_u$	> 6 m/s	15%	0.59	0.59
LAW78	U (Beauf.)	> 5B	2%	0.65	0.65
MEL78	$U + 3.5\sigma_u$	> 16 m/s	1/yr	0.43	0.28
VIS80	U	> 5 m/s	9.6%	0.57	0.57
BER84	U_3	> 20 m/s	1/yr	0.57	0.57
MUR86	U_3	> 13.5 m/s	3.6%	0.66	0.74
WIL91	U_t	> 6.1 m/s	20%	0.83	0.83
Walking fast:					
ISY75	U (Beauf.)	> 6B	0.14%	0.66	0.66
LAW78	U (Beauf.)	> 6B	2%	0.84	0.84
VIS80	U	> 5 m/s	20.5%	0.70	0.70
BER84	U_3	> 25 m/s	1/yr	0.71	0.84
MUR86	U_3	> 13.5 m/s	7%	0.74	0.90
WIL91	U_t	> 8.3 m/s	20%	1.14	1.16
Danger:					
ISY75	U (Beauf.)	> 7 B	1/yr	0.66	0.66
MEL78	$U + 3.5\sigma_u$	> 23 m/s	1/yr	0.62	0.66
WIL91	U_t	> 26.4 m/s	0.1%	1.3	1.6

Table 3.8: *Maximum allowed γ for different discomfort and danger criteria. References (column 1) are Lawson (1978), Beranek (1984) and further as in table 3.7. Column 2 and 3 and 4 give threshold and discomfort probability. Column 5 gives γ_{max} ('unacceptable') with the old T_u estimate of 30%. Column 6 gives γ_{max} with the present estimate of T_u and σ_u. The γ_{max} data are exact for the wind climate of Amsterdam airport.*

For 'walking fast' and for 'danger', $\gamma_{max} > 0.8$ results in a considerable increase in danger probability (figure 3.5). From this viewpoint, Murakami's (1986) and Williams (1991) criteria are (much) too lenient.

Separate danger criteria for the elderly and for cyclists have not been developed. Hunt et al (1976) proposed: $U + 3\sigma_u > 15$ m/s as a threshold for the elderly. He did not state how often this threshold is allowed to be exceeded. It is fair to assume that $U + 3\sigma_u > 15$ m/s for 1 h / year is just acceptable, as for the other danger criteria.
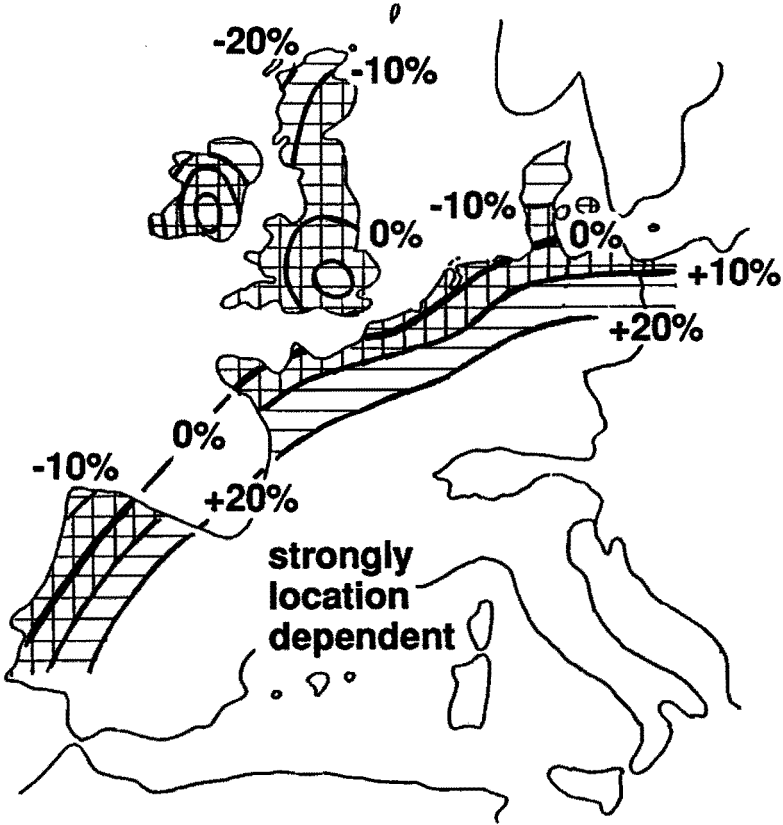
Figure 3.7: *Relative difference in required shelter or in γ_{max} for different locations in the EC. Hatched: difference < 10%; cross hatched: < 20%. The data apply to the shop owners criterion (Lawson et al, 1975) which is corrected to: $P(U > 5$ m/s) > 15%. γ_{max} is the (direction independent) γ for which conditions for strolling become unacceptable. The differences are referred to $\gamma_{max,0} = 0.63$ for Amsterdam airport.*

An important issue is the application of comfort criteria to other wind climates. Figure 3.7 shows the relative difference between a local γ_{max}, and γ_{max} of Amsterdam airport, for several locations in Europe. The corrected 'shop owners' criterion of Lawson et al (1975) is used: Wind conditions are not acceptable if $P(U > 5 \text{ m/s}) > 15\%$.

Within the hatched area of figure 3.7, we may estimate the required shelter from table 3.9, provided that the plotted percentages are used as a correction factor on γ_{max}. Table 3.9 should not be used outside the hatched area, and for very exposed or very sheltered regions. At such locations, habituation to wind may become important.

A final point of interest is the development of new, local, criteria. New thresholds, based on comfort investigations, require an estimate of maximum allowed discomfort probability (P_{max}) as well. P_{max} is preferably determined by experiment. Alternatively, P_{max} can be determined by considering the criteria (of table 3.8) which are in accordance with the corrected 'shop owners' criterion. The resulting γ_{max} of these 'good' criteria is shown in table 3.9.

Table 3.9 can also be used for existing (discomfort or danger) thresholds. In practice however, the use of incorrect thresholds (not based on comfort or safety investigations) may result in errors in γ_{max} of up to 5%.

activity	γ_{max}
sitting/standing; long time	0.3-0.4
sitting/standing; short time	0.4-0.5
strolling	0.6
walking fast	0.7
all activities: safety	0.7
id.; for elderly people	0.3?

Table 3.9:   *Estimate (±0.1) of maximum allowed wind amplification factor γ_{max} (direction independent) for different human activities. The γ_{max} values are valid for the present estimate of T_u and σ_u and for Amsterdam airport. For other locations, the plotted percentages in fig. 3.8 can be used as an approximate correction factor. 'Good' criteria should predict that wind conditions become unacceptable if γ_{max} is exceeded.*

3.5   Summary and conclusion

Wind effects on people can be the cause of uncomfortable or dangerous conditions. Probably the best known wind effect is the cooling action of wind. In steady conditions, thermal comfort models can relate cooling effect to the feeling of comfort. These models do not include any turbulence effects and are not suitable for outdoor use.

This chapter concentrates on mechanical wind effects and their consequences for comfort. Wind effects on people are mainly caused by peak gusts of 1-10

seconds duration (table 3.5). For some applications (effect of head winds on cyclists), steady winds are of importance as well.

Wind effects can not be translated directly into comfort indicators. This is because people do not consider every single gust to be uncomfortable. Jackson's (1978) street enquiry showed 57% 'dissatisfied' if $U + \sigma_u > 6$ m/s. Other comfort indicators are generally not based on comfort investigations.
Unlike comfort indicators, safety (or danger) indicators can be directly based on wind effects. Hunt et al (1976) propose: $U + 3\sigma_u < 15$ m/s for control of walking. This can be considered as a safety requirement for the elderly. For safety of average people, Hunt et al (1976) propose: $U + 3\sigma_u < 20$ m/s.

For cyclists, head winds of 5 m/s generally impede progress (fig. 3.2). Head winds in excess of 10 m/s make it impossible for most people to keep cycling. Safety requirements for side winds could not be developed.

In most climates, wind conditions can not be always comfortable. Section 3.3 presents the relation between shelter (alternatively: γ) and discomfort and danger probability. Uncertainties of 10-20% in γ can result in large errors in discomfort probability. Climatic differences within the Netherlands, and parts of neighbouring countries are smaller than resulting from the uncertainty in γ (fig. 3.5 and 3.6). Still, consequences for design may be significant (chapter 7).

Wind comfort criteria consist of a threshold and a maximum acceptable discomfort probability P_{max}. Generally, P_{max} is based on intuition, not on investigations. For many criteria, the threshold and P_{max} do not correspond with the activity considered. Application of such (comfort or safety) criteria to other wind climates can lead to false and misleading conclusions.
Even when the correct (discomfort or danger) threshold and P_{max} are used, one should realize that the uncertainty in γ may cause large errors in discomfort probability. Therefore, any criterion should be used with caution and flexibility.

As already noted, there is no firm (empirical) basis for the present criteria. This applies to the thresholds, and especially to P_{max}. Table 3.9 gives minimum requirements for criteria in terms of maximum γ. The following sets of criteria are in accordance with table 3.9 for strolling and sitting/standing: Gandemer (1978), Isyumov (1975), Lawson (1978) and Visser (1980; westerly part of Netherlands only). However, only Gandemer uses the type of threshold (eq. 3.8) that is in accordance with comfort investigations.
Thresholds for danger are given above. The maximum γ for safety is given in table 3.9.

A final issue is the presentation of criteria. For scientific literature, criteria should be given explicitly, i.e. as threshold and maximum acceptable discomfort (or danger) probability. For other applications criteria may also be given as a maximum allowed (direction independent) γ, γ_{max}. For mutual comparison, criteria should be presented in γ_{max} form, as in table 3.8.

66

4   Wind amplification factor

The previous chapter has made clear that local wind climate is strongly dependent on wind amplification factor γ. Table 3.9 gives an indication of which maximum value of γ is allowed for certain types of human activities.

The present chapter will quantify the relation between γ and properties (geometry) of building, site and surrounding terrain.
In section 4.1, three scale levels will be defined: terrain, building (including site) and detail. Contributions of these spatial scales to γ will be discussed in sections 4.2 (terrain), 4.3 (building) and 4.4 (detail). A summary of these data, together with a discussion of prediction methods of γ, is given in section 4.5.
In later chapters, we will use the estimates of γ for wind climate forecasts (chapter 5 and 6) and for rules of thumb for design (chapter 7).

4.1   Contributions of different spatial scales

Prediction of wind amplification factor γ is not easy as γ is determined by a large number of parameters. There are two ways to overcome this problem:
-by separately considering contributions to γ on different spatial scales.
-by making a suitable classification of the combined effects of building and terrain on γ.

The second approach (classification) is well suitable to determine integral effects: i.e. a judgement of wind climate in terms of (dis)comfort probability. This method will be discussed in chapter 5.

First however, we must analyze how processes on different scales contribute to γ. Generally, the processes on the larger scales are almost independent of the small scale processes. In that case, we can split γ into contributions on different spatial scales (Wisse, 1988).
For the present purpose, we can define three different scale levels (table 4.1). The subdivisions show which issues are going to be discussed in this chapter.

In practice, building and detail can not always be considered as separate scale levels. Equation 4.1 shows how γ can be split into a terrain related contribution (U_{pot}/U_{Ho}) and a design (building and detail) related contribution (U/U_{Ho}):

$$\gamma \;=\; \frac{U}{U_{pot}} \;=\; \frac{U_{Ho}}{U_{pot}} \frac{U}{U_{Ho}} \tag{4.1}$$

U_{Ho} is a reference speed (at roof height H) which governs the flow around the building.

Section	Scale level	Dimensions	Subdivision and issues
4.2	TERRAIN	0.1-200 km	
			4.2.1 Region: Homogeneous terrain
			4.2.2 City: Changes in terrain roughness
			4.2.3 District: Hills etc.
4.3	BUILDING	10-1000 m	
			4.3.1 Reference speed, reference location
			4.3.2 Single high rise building
			4.3.3 High rise building groups
			4.3.4 Streets and squares
			4.3.5 Urban environment
4.4	DETAIL	1-500 m	
			4.4.1 Building: architectural features
			4.4.2 Site: screens and trees

Table 4.1: *Contributions to γ by processes on different scale levels, and issues which are discussed in this chapter. The overlap in dimensions is due to the fact that physical processes determine the scale level, not the actual dimensions.*

The terrain related contribution to γ relates to boundary layer meteorology (section 2.1), whereas the design related contribution relates to obstacle aerodynamics (section 2.2). Generally, only the design related contribution is measured in a wind tunnel.

The architect may create shelter by reducing the design related contribution to γ (U/U_{Ho}). The terrain related contribution to γ can be considered as a precondition for design: it determines which shelter should be provided by the building.

4.2 Region, city, district

Large scale processes yield an important contribution to γ (fig. 4.1). These processes determine the reference speed of a building, e.g. U_{Ho}. In the following, we will discuss the effects on γ for uniform terrain, and for non uniform terrain (roughness changes). Local effects such as small hills will also be considered. Turbulence effects are discussed in chapter 2 (section 2.1).

4.2.1 The scale of the region

The region can be defined as a scale with uniform terrain and uniform wind climate. For the present purpose, wind climate is roughly constant over distances up to 50-200 km (section 3.3 and 3.4). Horizontal gradients in the flow are only negligible in a fully developed boundary layer. This requires uniform terrain over at least 10-20 km (Jensen, 1978), as the fetch must be much larger than the boundary layer height δ (δ is of the order of 1 km).
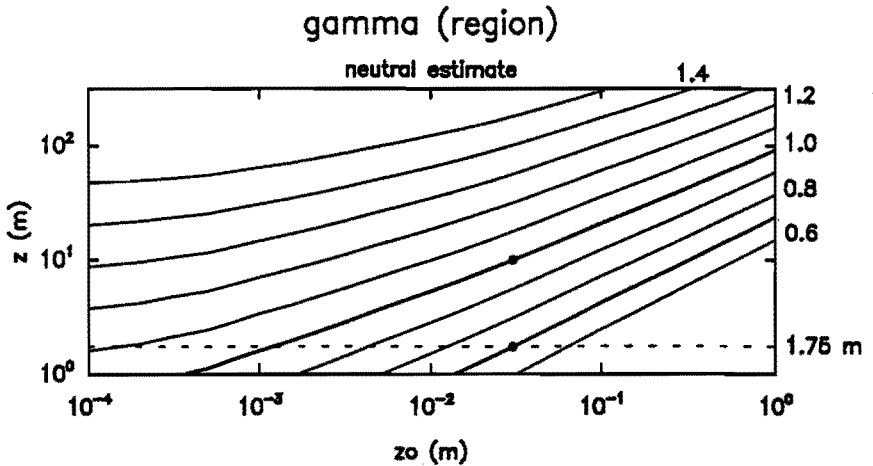
Figure 4.1: Wind amplification factor γ (U/U_{pot}) as a function of z_0 and z (logarithmic scale), as estimated by eq. 4.2 and 4.3. Dots denote γ values for $z_0 = 0.03$ m (airport), and for $z = 10$ m height and 1.75 m height.

Figure 4.1 gives an estimate of γ (or U/U_{pot}) over uniform terrain as a function of roughness length z_0 and height z.
The estimate is based on the logarithmic wind profile (eq. 4.2)

$$U(z) = \frac{U^*}{\kappa} \ln(\frac{z-z_d}{z_0}) \quad \text{if} \quad z > 20\,z_0 + z_d \quad (4.2)$$

As mentioned in section 2.1, we may link the U^* values of two different terrains (with roughness lengths z_{01} and z_{02}) by the following approximate expression (Simiu, 1986):

$$\frac{U_{*_1}}{U_{*_2}} = (\frac{z_{01}}{z_{02}})^{0.0706} \quad (4.3)$$

Limitations and accuracy of equation 4.2 and 4.3 (and figure 4.1) will be discussed below.

First of all, equation 4.2 and 4.3 are only valid for heights $z > 20\,z_0 + z_d$; i.e. well above the roughness elements. At the same time, z must be much smaller than the boundary layer height δ (say $\delta \approx 1$ km; eq. 2.3). If z_0 is very large, (2 m or more), these two requirements can not be met at the same time. In that case, there is no surface layer, and eq. 4.2 and eq. 4.3 are not valid (see also Tennekes, 1972).

69

The total error in γ is made up of uncertainties and systematic errors.

Systematic errors are due to the assumptions in eq. 4.2 and 4.3:
1. Horizontal gradients in macro wind G (eq. 2.4) are negligible.
2. Turning of wind in the surface layer is neglected.
3. The U^* values over different (uniform) terrains are linked by eq. 4.3 instead of eq. 2.4.
4. Local (see breeze or urban heat island) circulations are neglected.
5. Horizontal temperature gradients are neglected.
6. Effects of surface heat flux are neglected.

Assumption 1 and 2 are not a significant error source because of the definition of the region (1), and because turning of wind in the surface layer is never more than 15° (2). The third assumption may result in about 5% underestimation of U^* (and γ) over open water, and over large cities.
Assumption 4, 5 and 6 are already discussed in section 2.1. At temperate latitudes, neglect of horizontal temperature gradients (5) may result in a few percent underestimation of γ over large cities, especially for z > 100 m.
The main error source is neglect of surface heat flux (or thermal stability) effects (6). During daytime, eq. 4.2 and 4.3 overestimate γ for z > 10 m. The reverse applies for nighttime conditions. Over a large city however, eq. 4.2 and 4.3 may underestimate γ during daytime *and* during nighttime. Table 4.2 (see also table 2.2) gives the smallest U_{pot} for which the maximum error in γ is less than 10 or 20%.

	diff < 20%	diff < 10%
daytime; summer	4.8 m/s	11.4 m/s
nighttime or cloudy conditions in winter	7.6 m/s	10.8 m/s

Table 4.2:   *Minimum U_{pot} for which the error in γ due to thermal stability effects is less than 10% or 20%. γ is estimated by eq. 4.2 and 4.3. Considered heights: z < 100 m. Considered z_o: 0.01 - 1.0 m. Note: the estimates do not apply to surfaces with different stability regimes (warm sea / cool land).*

For wind comfort applications, we are interested in U_{pot} > 5 m/s (discomfort probability less than 50%). A maximum error of 20% (table 4.2) is about twice the desired error (see chapter 3). In practice however, this error is less important. This is because thermal effects are not only neglected in the present calculations of γ, but also in the calculation of maximum acceptable discomfort probability (p. 61) where the concept of γ has been used as well (Lawson et al, 1975).
Still, we should avoid the use of marine weather stations for prediction of γ over land, and vice versa.

The total relative error in γ can be 20% or even more, and consists of uncertainties:

  -due to z_0 estimate: up to +/- 15% (both positive and negative)
and systematic errors:

  -errors due to estimate of eq. 4.3: about 5% over cities
  -neglect of horizontal temperature gradients: about 5% over cities
  -neglect of surface heat flux: up to 10-20% over cities
All systematic errors result in underestimation of γ over cities. However, the effect of the latter two errors may be (partly) compensated because of similar errors in the computation of maximum discomfort probability (see discussion above).
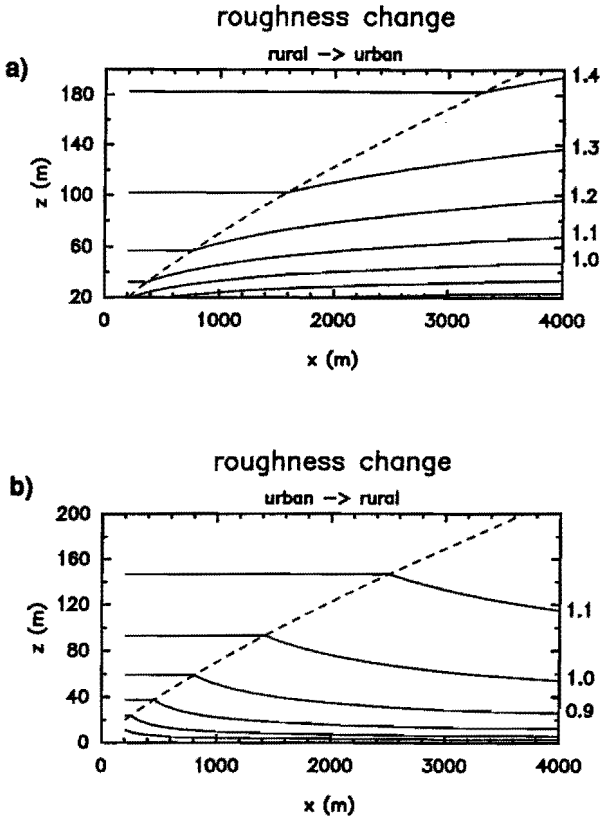
Figure 4.2: Lines with equal wind amplification factor γ as a function of fetch x and height z for two dimensional roughness changes (normal flow). The IBL interface (eq. 4.4) is given as a dashed line.

a) Rural -> Urban: $z_{o1} = 0.03\ m$, $z_{o2} = 1\ m$, $z_{d1} = z_{d2} = 0\ m$.
b) Urban -> Rural: $z_{o1} = 1\ m$, $z_{o2} = 0.03\ m$, $z_{d1} = z_{d2} = 0\ m$.

4.2.2 The scale of the city

The scale of the city can be defined as the scale where terrain inhomogeneities become important. Typical dimensions for the scale of the city are 0.2 - 20 km. Yearly mean wind speeds over the Hague (Vermeulen, 1986b) may serve as an example: At 30 m height, yearly mean wind speed decreases from 6.5 m/s at the coast to 5 m/s in the city centre.

An important concept in this section is the internal boundary layer (IBL). The IBL can be defined as the layer which, after a change in surface conditions (e.g. z_0), is influenced by the new surface conditions. See figure 2.2 and figure 4.2.

First some results are presented for the case of normal flow (0°) over a two dimensional roughness change. The IBL height is defined by 'kinks' in the vertical wind profile (fig. 2.2), and is given by (Jensen et al, 1984):

$$\frac{h_{IBL}}{z_0^+} = 0.3 \left(\frac{x}{z_0^+}\right)^{0.8} \tag{4.4}$$

where x is the fetch and z_0^+ the largest of the two roughness lengths.

Above the IBL, wind profiles are effectively the same as upstream. Within the IBL, wind profiles can be described with eq. 4.2 if the downstream z_0 is used. U* and γ can be determined by matching the upstream and downstream wind profiles (eq. 4.2) at $z = h_{IBL}$, not by using eq. 4.3.
Figure 4.2 shows γ as a function of fetch and height as obtained with this 'IBL model'. Two cases are considered: a smooth to rough change (fig. 4.2a) and a rough to smooth change (fig. 4.2b). For both cases, changes in γ are of the order of 20% or less.

In practice we have to consider lateral roughness changes, multiple roughness changes and roughness islands, both for normal flow and for oblique flow.

Figure 4.3 shows γ at 20 m height for a lateral roughness change. The major changes in γ occur in the first downstream kilometre. Further downstream, γ changes rather slowly. The lateral influence zones increase at a rate of approximately 1:13. Gradients of γ in these influence zones are the largest over the rougher terrain.
Figure 4.3 is based on wind tunnel data and modelling proposals of Vermeulen (1986a). He suggested that the extent of the lateral influence area is almost equal to h_{IBL} over the 'new' roughness (a linear increase of y_{IBL} with x would be better in agreement with surface layer theory; Panofsky et al, 1984). Wind profiles (U(y)) in the lateral influence zone can be divided into two linear segments. At the roughness change, $U = U_{min} + 0.65*\Delta U$. Outside the lateral influence zone, the flow develops as for a conventional two dimensional roughness change.

72

Vermeulen (1986a) presented some wind tunnel data for oblique flow and for roughness islands as well.

For oblique flow, and for *small* perturbations, it is expected that γ can be found by superposition of flow components normal and parallel to the roughness change. There are not sufficient experimental data to confirm this assumption.

a)

lateral roughness change

x > 0 and y > 0: urban

b)

lateral roughness change

x > 0 and y > 0: rural
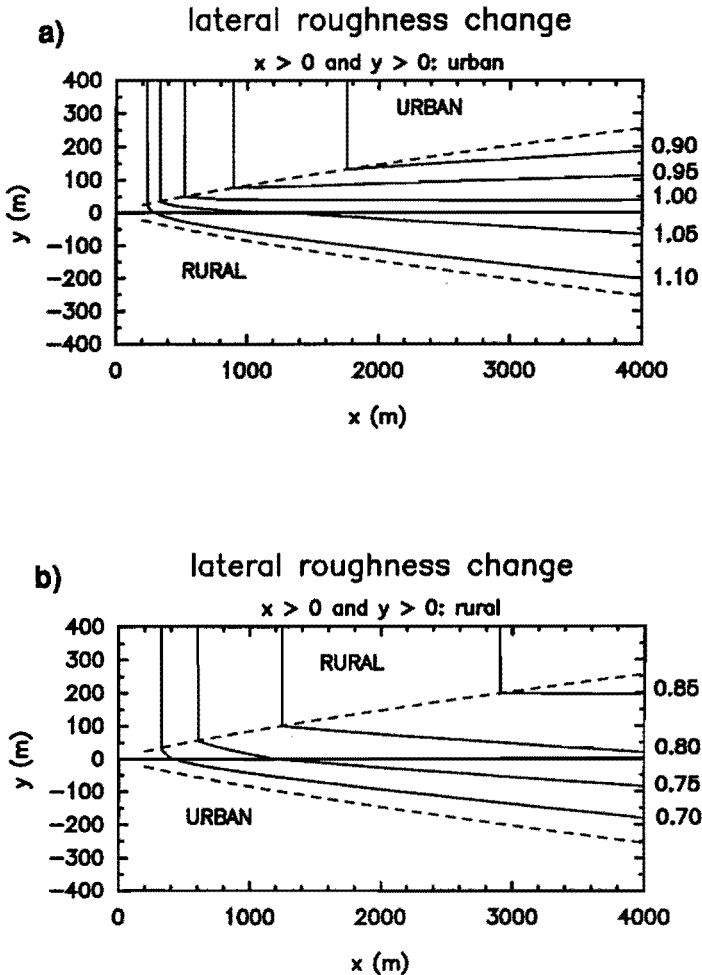
Figure 4.3: *Modelled lines of equal wind amplification factor γ at 20 m height for a lateral roughness change. γ is given as a function of fetch x and lateral distance y. The extent of the influence area (y_{IBL}) is given as a dashed line.*

a) $z_o = 1$ m and $z_d = 0$ (urban) for x > 0 and y > 0; elsewhere, $z_o = 0.03$ m (rural).

b) $z_o = 0.03$ m (rural) for x > 0 and y > 0; elsewhere, $z_o = 1$ m and $z_d = 0$ (urban).

Roughness islands are defined as roughness changes with lateral dimensions $W/z_0^+ < 500$ (or $W/H < 10$), where W is the width of the change, and H the obstacle height.

A significant part of the flow around roughness islands can be deflected sideways. This can result in a factor 2 increase in apparent z_0 over the roughness island (Vermeulen, 1986a), as compared with the z_0 for a two dimensional roughness change. Another feature of long roughness islands is mutual interaction of lateral influence zones. Vermeulen suggests that in this interaction zone, U is independent on the lateral coordinate.

For multiple roughness changes, IBL principles are probably valid as well. Deviations from IBL theory are to be expected if $L/z_0^+ < 300$ (Claussen, 1989), where L is the streamwise length of the roughness strip. For such small strips (≈ 30 obstacle heights), the influence of individual buildings is important.

Limitations

Internal boundary layer theories, and its extensions, are only valid for a limited range of fetch.
For very short fetches, the effects of individual buildings become important. Therefore, IBL theory can only be used for fetches greater than 30 building heights. In most practical cases, we may use a minimum fetch of about 300 z_0 or 300 m.
The maximum fetch is determined by the fact that IBL theory (including wind profiles of eq. 4.2) is only valid in the atmospheric surface layer. This yields a maximum height of the order of 100 m, and a maximum fetch of 2-3 km. Further extrapolation yields rather large errors: even after several (say 20) kilometres, there remains a 20% difference with predictions for uniform terrain (eq. 4.2 and 4.3). Therefore, it is to be expected that for fetches greater than 2-3 km, adaptation to new surface conditions proceeds at a faster rate than is indicated by IBL theory.

The effects of surface elevations and slopes (even < 5%) can be much larger than the effects of a simultaneous roughness change (Jensen et al, 1984).
Regular building arrays yield a surface elevation (i.e. z_d) as well. This elevation is generally not important for wind profiles in the IBL as the influence of individual buildings has become small for $x/H > 30$ or $x/z_0 > 300$. However, a downstream change in surface elevation of the order of the IBL height can have significant influence on the flow (Vermeulen, 1986a).

Accuracy

The small amount of experimental data (Garratt, 1989), does not allow for accurate modelling, and this can be considered as a major error source. Data for urban roughness changes are almost absent.
An important error source is the fact that thermal effects are neglected. If the *whole* boundary layer is strongly unstable, h_{IBL} grows as $x^{1.5}$. In strongly stable

conditions h_{IBL} grows as $x^{0.5}$. This will also affect the range of fetch for which IBL theory is valid.

Some estimates of systematic errors in γ are already given in chapter 2 (section 2.1): neglect of thermal effects may result in 15% underestimation of γ near a town edge (at 20 m height). Above the IBL, errors may be somewhat larger (up to 20%; see table 4.2). In practice, the effect of these errors is less important, as for uniform terrain (p. 70). However, it is still recommended to avoid the use of marine weather stations for prediction of γ over land, and vice versa.

Due to lack of data there are also many uncertainties in IBL theory. Therefore, it seems quite realistic to assume that within the internal boundary layer, errors in γ of up to 10-15% (both positive and negative) are possible. This uncertainty includes the effects of errors in the estimation of urban z_0.

In future, IBL theory has to be extended to urban z_0 and to fetches up to 10-20 km. Issues such as oblique flow, roughness islands, and lateral flow have to be considered as well. As there are often considerable difficulties in theoretical treatment, the creation of a suitable experimental (or numerical) database seems to be the only way to solve the problem.

Inclusion of thermal (stability) effects yields further improvement in prediction of γ on uniform and on non uniform terrain. By now, there are no theories which can cope with simultaneous changes in roughness and stability conditions. The creation of an experimental or numerical database is rather difficult as a great number of data is needed.

4.2.3 The scale of the district

The scale of the district includes all effects on a building reference speed which can not be described by theories of the former sections:
-effects of terrain elevations
-effects of distant upstream buildings
-effects of building lay out on flow over regular building arrays.

This section will be mainly about the effects of terrain elevations. Effects of distant upstream building will be discussed in section 4.3.2, which is about flow around single high rise buildings. Effects of building lay out are difficult to model, and are only discussed briefly.

Wind flow over hills

According to Jensen et al (1984), orographic effects are generally much stronger than the effects of roughness changes. Therefore, effects of terrain elevations are worth to be considered, even in the Netherlands.

Theory and experimental data of flow over hills are given in Hunt and Simpson (1982), Bowen (1977), Lemelin et al (1988), Goliger et al (1989), and Jensen et al (1984). In the following, only a brief description of orographic effects will be given.

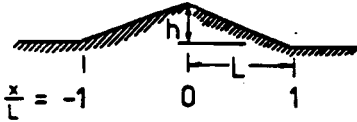Wind flow over hills is often described by the fractional speed up factor ΔS (Hunt et al, 1982):

$$\Delta S = \frac{U(z) - U_o(z)}{U_o(z)} \qquad (4.5)$$

where z is the height above the *local* surface. ΔS is primarily dependent on the effective slope H/L, where H is the hill height, and L the streamwise length of one (upstream) side of the hill (fig. 4.4). The following approximate expression can be derived for ΔS (Jensen et al, 1984):

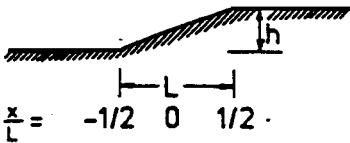$$\Delta S \approx 2\,\sigma(x,z)\,\frac{H}{L} \qquad (4.6)$$

where $\sigma(x,z)$ is a shape factor. This solution is only valid in the so called outer layer. Close to the surface, i.e. for heights $z < 0.3\,z_0\,(L/z_0)^{0.67}$, the speed up factor ΔS remains constant. In this 'inner layer', the wind profile must be matched to the outer layer profile by eq. 4.2. Other requirements are a moderate slope with H/L << 1 (Hunt et al, 1982) and hill dimensions which are much larger than the surface roughness, i.e. $L/z_0 > 500$.

Triangular Ridge

$$\sigma(x,z) = \frac{1}{2\pi}\ln\frac{\left[\left(\frac{x}{L}-1\right)^2+\left(\frac{z}{L}\right)^2\right]\left[\left(\frac{x}{L}+1\right)^2+\left(\frac{z}{L}\right)^2\right]}{\left[\left(\frac{x}{L}\right)^2+\left(\frac{z}{L}\right)^2\right]^2}$$

$$\frac{x}{L} = -1 \qquad 0 \qquad 1$$

Triangular Ramp

$$\sigma(x,z) = \frac{1}{2\pi}\ln\frac{\left(\frac{x}{L}+\frac{1}{2}\right)^2+\left(\frac{z}{L}\right)^2}{\left(\frac{x}{L}-\frac{1}{2}\right)^2+\left(\frac{z}{L}\right)^2}$$

$$\frac{x}{L} = -1/2 \qquad 0 \qquad 1/2$$

Figure 4.4: *Notation definition for flow over two dimensional hills, and solutions of $\sigma(x,z)$ for two typical hill shapes. The solutions are valid for slopes $H/L < 0.3$, and for $z > 0.3\,z_0\,(x/z_0)^{0.67}$; z is the height above local surface.*

The dependence of ΔS on location and on hill shape (not H/L) is given by σ(x,z) (Jensen et al, 1984). Figure 4.4 gives some solutions of σ(x,z) for two typical hill shapes. For both cases σ(x,z), and therefore ΔS, is (anti)symmetric in x = 0.
Table 4.3 gives some estimates of ΔS for the geometries of figure 4.4. The estimates are also valid for oblique flow, provided that the perpendicular component is taken (Jensen et al, 1984).
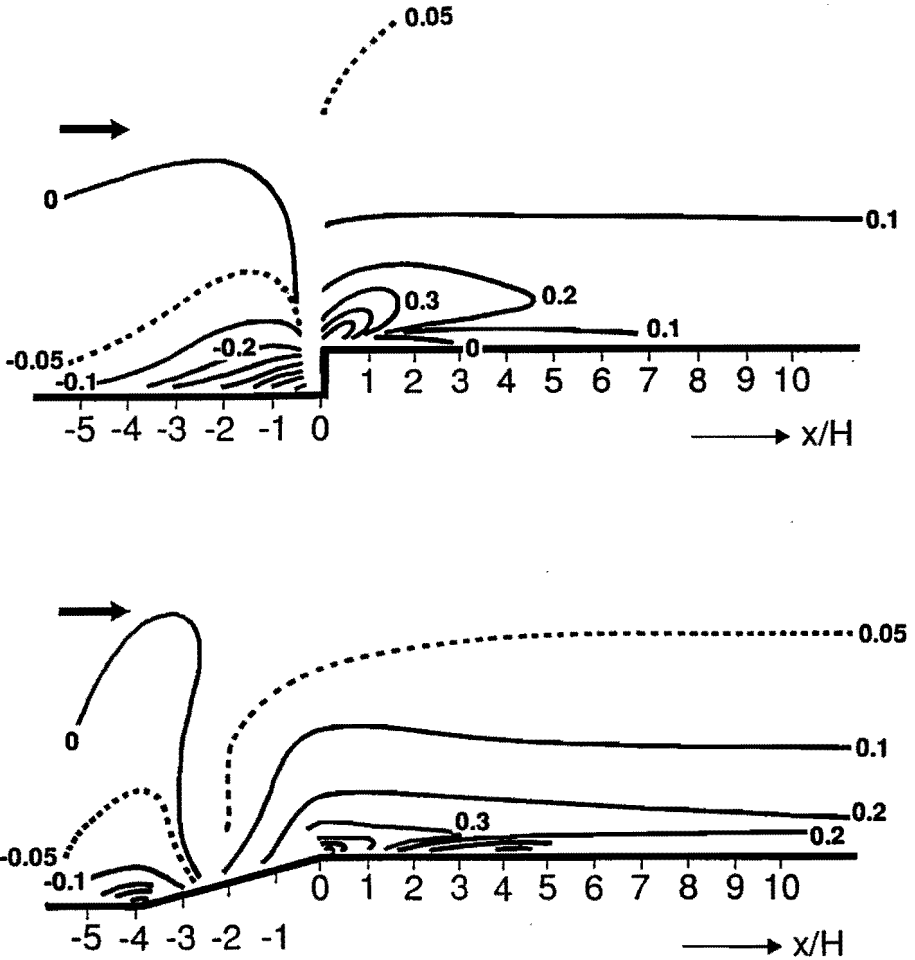

Figure 4.5:   *Fractional speed up factor ΔS as a function of x/H and z/H over a cliff escarpment and over a gentle sloping ramp (after Bowen, 1977).*

77

	foot	crest
ridge	-3 H/L	5.4 H/L
ramp / escarpment	-2.7 H/L	2.7 H/L

Table 4.3: *Estimates of fractional speed up factors ∆S by the method of Jensen et al (1984) over typical two dimensional topography (figure 4.4). The estimates are valid for $L/z_0 > 500$, $H/L \ll 1$, and for $z \ll L$.*

Table 4.3 shows that the foot of a hill is well sheltered, but that the summit is very windy. This is especially true for the summit of a ridge. Even for small H/L (say 0.1), the speed up factor can be as high as 0.5, a 50% increase in γ.

In the case of separated flow (H/L > 0.3), the speed up (almost) ceases to depend on H/L (Jensen et al, 1984), and there is some analogy with the flow over buildings. Distributions of ∆S around escarpments with and without flow separation are given in figure 4.5. Maximum fractional speed up factors ∆S are of the order of 0.7.

Jensen et al (1984) show that the above mentioned estimates are not always very accurate; a typical relative error in ∆S can be of the order of 25%.
Lemelin et al (1988) made predictions of ∆S over three dimensional hills (only hill tops) and compared the predictions with various experimental data. The predictions compare well with Jensen's (1984) estimates. Typical differences between experimental data and Lemelin's (1988) predictions varied between 0.05 and 0.3.

A disadvantage of Lemelin's approach is that only regions with accelerated flow are considered. Figure 4.5 gives an overall picture of flow over two escarpment shapes which allows to estimate ∆S at the foot of hills as well.

Thermal stability effects can be important in cases with stable stratification (Hunt et al, 1982). As we are interested in $U_{pot} > 5$ m/s, where $z_L > 80$ m (over land), it is expected that thermal stability effects are mainly important for rather large hills (from Dutch viewpoint), and at the sea coast. ·

Roughness parameters as a function of building lay out

Often, high rise buildings are surrounded by (sub)urban areas, consisting of low rise buildings. In regular groups, it is to be expected that z_0 and z_d can be described as a function of building lay out. Figure 4.6 gives a notation definition for such a regular building array.

Hussain (1978) investigated flow over groups rectangular buildings in a 'normal' array (fig. 4.6). Only normal flow was considered (0°). The roughness of

ground surface and of the buildings were neglected. Hussain correlated his data with the frontal area density λ_f, where $\lambda_f = (w\ h)\ /\ (d_x\ d_y)$. In Hussain's (1978) experiments λ_f was chosen such that $\lambda_f = (d_x/h)^2$.

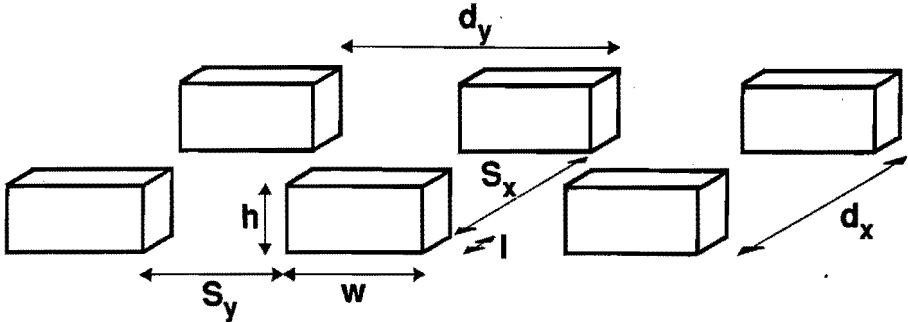*Figure 4.6:* *Notation of building dimensions and building arrangement for regular building arrays. The frontal area density λ_f is (w h) / ($d_x d_y$)*

First, let us consider zero displacement height z_d. We may assume that z_d/h is a function of λ_f if z_d is determined by the volume of buildings and their recirculation zones (where U < 0), and if the buildings are thin (l/h << 1) and wide (w/h >> 1).

In that case (using Hussain's data) z_d may be approximated by:

$$z_d/h = (1.5\pm0.5)\,\lambda_f \qquad \text{if} \quad \lambda_f < 1 \qquad\qquad (4.7)$$

Next, the ratio z_0/h is considered. This ratio can not be quantified well as it is not clear which are the key parameters. Hussain (1978) suggests a maximum ($z_0/h = 0.2\pm0.1$) for $\lambda_f = 0.15\pm0.10$. This corresponds with the wake interference flow regime (figure 2.9b).

The uncertainties in the above z_0 estimate are not smaller than in the roughness classification of table 2.1. The latter is still recommended for estimation of z_0.

For estimation of z_d however, equation 4.7 is recommended.

4.3 Buildings and building groups

This section deals with the effects of buildings and building groups on wind amplification factor γ. Most data of this section are based on the present numerical simulations (see section 2.3 for details). The following issues will be discussed:
- reference speed and reference location (section 4.3.1)
- flow around a single high rise building (4.3.2)
- high rise building groups (4.3.3)
- low rise building groups; streets and squares (4.3.4)
- influence of urban surroundings (4.3.5)

4.3.1 Reference speed and reference location

First, we should choose the right variables to describe mean and turbulent flow properties. These variables must satisfy the following two requirements:
- they must allow for an easy link to the conditions on larger scales
- their dependence on geometrical and (approach) flow parameters must be as small as possible

For the mean flow field, either U_{Ho} or $U_0(z)$ are generally chosen as reference speed. U_{Ho} is the approach flow wind speed at roof height H; $U_0(z)$ is the approach flow wind speed at the measuring height z; in our case pedestrian height (1.75 m).

Numerical simulations indicate that building influence extends to $5L_g$ upstream, where the geometrical length scale L_g is the lesser of W and 2H. This is assumed to be a good estimate of the minimum distance for an upstream reference location for U_{Ho} and, in complex geometries, probably the most suitable distance.

The best reference speed for flow around high rise buildings is U/U_{Ho}. This is because the mean flow field is closely related to the pressure field which, in turn, can best be normalized by U_{Ho} (Meroney, 1988).
Only Lawson et al (1975) use U_{Ho} to normalize pedestrian wind speeds. In virtually all publications (e.g. Gandemer, 1975; Beranek, 1980, 1984a, 1984b; Maruta, 1984, Stathopoulos et al, 1985, 1986, 1991), mean pedestrian level wind speeds U (or equivalent wind speeds U_e; eq. 3.7) are normalized by $U_0(z)$ (or $U_{e,o}(z)$) at about 1.75 m height.

It is beyond doubt that U_0 is a convenient parameter, which allows us to identify areas with increased wind speed. However, U_0 is strongly dependent on upstream (roughness) conditions, and U/U_0 may be more representative of the upstream conditions than of the conditions near the building of interest. Sometimes, U_0 is taken at the building location in the absence of the building, instead of in the approach flow. Still, this does not allow for an easy link to wind speeds on larger scales (and to U_{pot} at a meteorological station).

80

Turbulent properties are seldom given explicitly. Stathopoulos et al (1985, 1986) present amplification factors of turbulence intensity (T_u), but generally only mean wind speeds or equivalent wind speeds are given (Beranek, 1980, 1984a, 1984b; Gandemer, 1975).

By its definition, turbulence intensity T_u is strongly dependent on mean wind speed U. If one is interested in absolute turbulence levels, K/K_0 (or its square root) is a much better variable; K is kinetic energy of turbulence per unit mass.

The above discussion can be summarized as follows:
U_{Ho} and K_0 are preferred as reference parameters as they allow for an easy link to larger scales. For groups of low rise buildings, reference conditions above the building group should be chosen.

However, U_0 should be used as an additional reference speed if the areas of increased wind speed must be identified. Turbulence intensity T_u can be a useful parameter if the reliability of measuring devices (fig. 2.12) is considered.

Finally, it is noted that in the remainder of this chapter, (local) K and U represent *pedestrian level* (1.75 m) conditions, unless stated otherwise.

4.3.2 Flow around a single high rise building

Wind flow in the built environment is determined by a large number of parameters. Wind flow around a single building can be considered as a reference case. The effects of building arrangement (section 4.3.3) can be judged by comparing flow in building groups with the isolated building case.

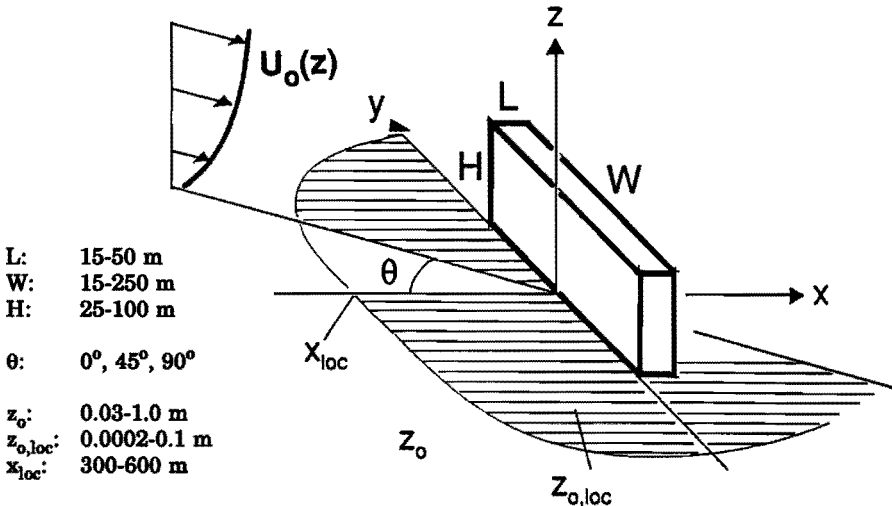|	
L:	15-50 m
W:	15-250 m
H:	25-100 m
θ:	0°, 45°, 90°
z_0:	0.03-1.0 m
$z_{0,loc}$:	0.0002-0.1 m
x_{loc}:	300-600 m

Figure 4.7:   *Notation definition and range of parameters for flow around single high rise building. Roughness parameters z_0 (approach flow) and $z_{0,loc}$ (local surface roughness) are also indicated.*

81

First, we will introduce the relevant flow parameters and flow zones. For each flow zone, flow properties, are discussed. At the end of this section, an overview is given of exposed and sheltered locations. An overall estimate of turbulence intensity T_u will be given as well.

Flow zones and flow parameters

Even for a single rectangular buildings, there is a large number of flow parameters:

-building length, width and height L, W, H;
-approach flow angle θ
-roughness parameters: z_0 and $z_{0,loc}$ for the approach flow and the local ground surface (fetch x_{loc}).
-'thermal' parameters such as z_L, which are not considered in this study.
A notation definition sketch is given in figure 4.7 (previous page).

In this section, we will only consider 'ideal' geometries, where $z_0 = z_{0,loc}$. In most simulations, we assume: $z_{0,loc} = 0.03$ m. This seems to be a fair choice, but there are no measuring data available to confirm this. Non ideal cases (urban flow), where $z_0 > z_{0,loc}$, will be discussed in section 4.3.5. In all cases however, $z_{0,loc}$ should be less than 0.09 m, so that $20z_{0,loc}$ remains below pedestrian height.

Dimensionless parameters, such as W/H (relative width), L/H (thickness), z_0/H (relative upstream roughness) etc., lead to further parameter reduction. In wind comfort applications however, a fixed height ($z = 1.75$ m) is considered, not a fraction of a building dimension. Therefore, only part of the flow field properties can be described by the above given dimensionless parameters.

Many of the parameters are interrelated. Therefore, it is almost impossible to discuss the influence on wind flow (and comfort) of each separate parameter. An alternative approach is analysis for each separate flow zone, as will be done below. This allows for the elimination of parameters that are not important for a given flow zone.

In section 2.2 the concept of flow zones has been introduced. Figure 4.8 shows the influence area and flow zones around a building. The influence area is defined as the area where U is changed by 10% or more. Estimates of flow zone dimensions are given as a multiple of the geometrical influence scale L_g. Cook (1985) defines L_g as the lesser of W and 2H. Alternatively, the following interpolation formula can be used:

$$L_g / H = \frac{(W/H)}{1 + 0.5\,(W/H)} \qquad (4.8)$$

In the following, we will extensively discuss the flow properties of each flow zone. First, the reader is advised to reconsider fig. 2.6-2.8 (section 2.2) which give a visual impression of flow properties around buildings.
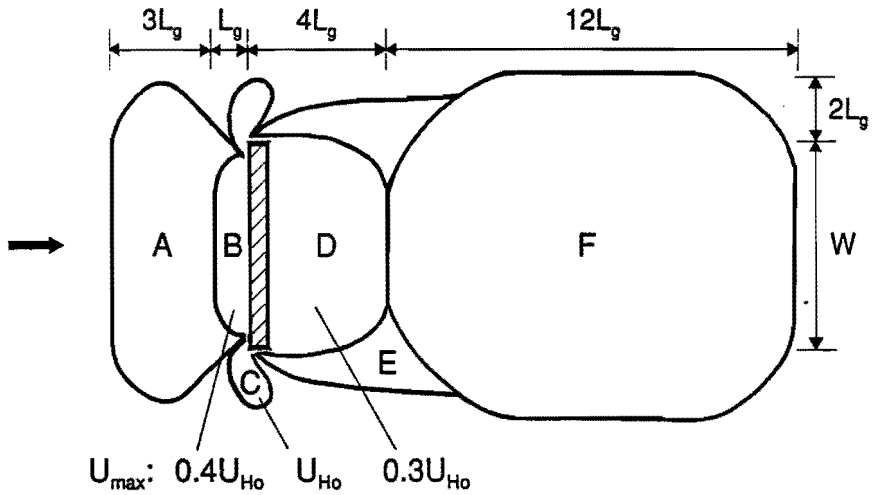
$3L_g$ | L_g | $4L_g$ | $12L_g$

$2L_g$

A B D F W

C E

U_{max}: $0.4U_{Ho}$ U_{Ho} $0.3U_{Ho}$

Figure 4.8: *Influence area and flow zones around a building (normal flow; 0o). Dimensions (mainly from numerical data discussed later) are given as a multiple of the geometrical influence scale L_g (eq. 4.8). Maximum wind speeds are given as well. Flow zones given are: upstream retarded zone (A), frontal vortex (B), Corner streams (C), recirculation zone (D), shear layers (E), far wake (F).*

Upstream flow; frontal vortex

In front of a building, wind speeds are decreased because of the positive wind pressure gradient. Modelling of these wind speeds was not feasible because the influence of building shape (W/H) and approach flow angle (θ) could not be accounted for in a simple way.

The frontal vortex is defined as the region with recirculating flow in front of the building. The lateral boundaries (fig. 4.8 and 2.6) are the corner streams. The frontal vortex dimensions are determined by W/H, H/z_0, $H/z_{0,loc}$ and x_{loc}/H. For wind speeds, H (or L_g) should be considered as an additional parameter.

The length of the frontal vortex L_F is of the order of L_g. Figure 4.9 shows the dependence of L_F on W/H. For small W/H, the FLUENT data tend to be too low, or the frontal vortex is not present at all. This may be caused by increased mixing due to imperfections in the K-ε model (section 2.3). For very wide obstacles (W/H >> 3), the frontal vortex becomes much weaker and smaller (L_F/H < 1). This feature is generally overlooked in literature.
The influence of the H/z_0 ratio is not clear at once, because Beranek considered only one terrain. Additional numerical simulations suggest that both small (say 100) and very large H/z_0 (10^5) can reduce L_F by 40%.

83

Maximum wind speeds (numerical estimate) in the frontal vortex are about $0.3*U_{Ho}$ for $1 < W/H < 4$, and for H/z_0 of the order of 10^3. Literature data for the same range of W/H are not found. For a slender building (W/H = 0.6), Britter et al (1978) find that both L_F (0.4*H) and U/U_{Ho} (0.4) are larger than numerical estimates. This is not surprising, given the imperfections in the K-ε model discussed in section 2.3. For oblique flow (45°), a rough estimate of the perpendicular component is sufficient as flow parallel to the upstream building walls is much stronger.
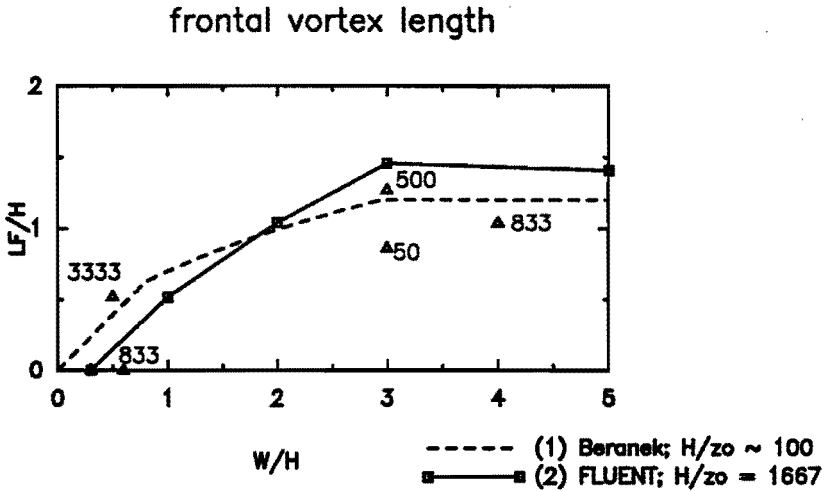
frontal vortex length

Figure 4.9: *Frontal vortex length L_F as a function of W/H. Dashed line (1): flow visualisation data for urban approach flow, followed by about 500 m open terrain (Beranek, 1984). Solid line (2): numerical data for open terrain ($H/z_0 = 1667$). Triangle points represent additional numerical data (H/z_0 given in plot).*

Corner streams

Corner streams of high rise buildings are often considered to be the most important flow features. In the present study, corner streams are defined as the areas near building corners where U/U_{Ho} or U/U_0 exceeds a certain value. Before giving precise definitions, some general flow features are discussed.

Figure 4.10 gives wind speeds U/U_0 for a building of 15x150x50 m (L,W,H) and $z_0 = 0.03$ m. Corner streams for oblique flow are stronger (U/U_{Ho} up to 1) than corner streams for normal flow (see section 2.2). This feature is often overlooked in literature, or attributed to interaction effects (Gandemer, 1975) in building groups. Flow direction is determined by the wall the flow was attached to (fig. 4.10a), not by the approach flow direction. This may cause dangerous surprising effects. However, for small W/H, the flow turns rapidly towards the wake (fig 4.10c).

84

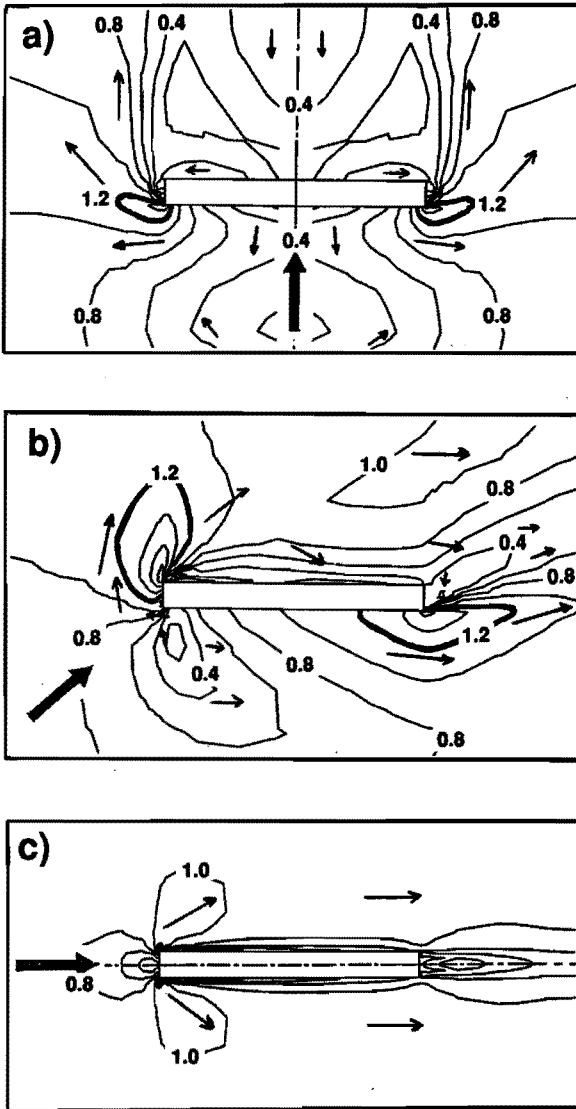Figure 4.10: *Normalized wind speed U/U_o around building with L, W, H =*
15x150x50 m and $z_o = z_{o,loc} = 0.03$ m, showing location, dimensions and
shape of corner streams. $U_o/U_{Ho} = 0.55$. Contour intervals: 0.2; thick line:
$U/U_o = 1.2$. See fig. 2.6-2.8 for vector plots and flow patterns.
a)   *normal flow (0°)*
b)   *oblique flow (45°)*
c)   *parallel flow (90°)*

85

A great number of parameters is needed for a complete description of corner streams. Suffice to say here that oblique flow and a large W/H ratio (compare fig. 4.10a and 4.10c) yield the largest corner stream areas, and that both the upstream extent and lateral dimensions of corner streams are relatively small.

In the remainder of this chapter, we will use the parameter R, where R is the radius of a corner stream circle where $U/U_o > 1.2$ for at least one wind direction. The 20% wind speed increase covers all building dimensions of interest, and is large enough to exclude errors due to eventual gradients in the undisturbed flow. Figure 4.11 gives R as a function of building width W and building height H.
For wide buildings, corner stream radius R is about 1.4*H. For slender buildings, R increases up to 2.3*W (note that L_g can not be used here). For given frontal area W*H, wide buildings yield the best wind conditions as maximum corner stream speeds are reduced because of smaller H. Moreover, corner stream radius R is smaller, and the sheltered area in the wake is larger.
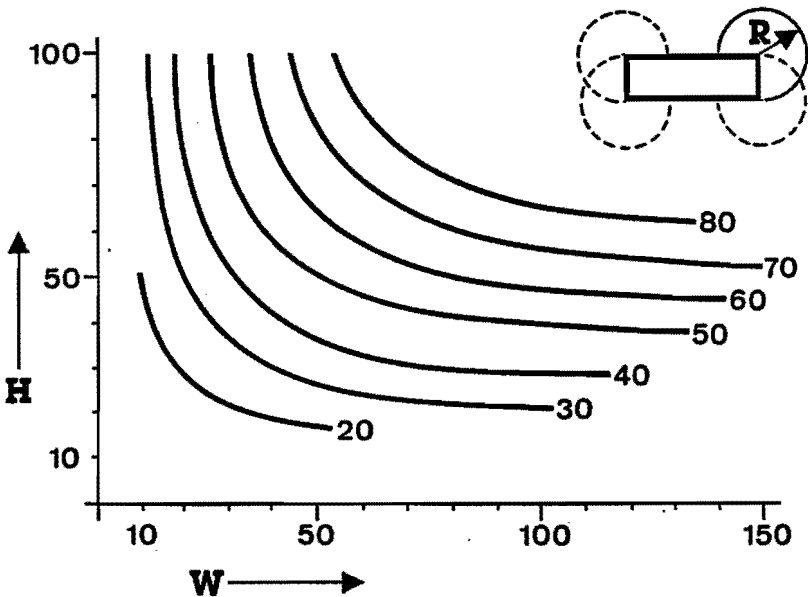

Figure 4.11: Corner stream radius R as a function of building width W and building height H. Within the 'corner stream circle', $U/U_o > 1.2$ for at least one wind direction. This graph is 'exact' of $z_o = z_{o,loc} = 0.03$ m, and if L = 15 m. For application in complex urban geometry use $U/U_{Ho} > 0.66$.

Figure 4.11 is 'exact' for $z_0 = z_{0,loc} = 0.03$ m, and $L = 15$ m. For other L and for other z_0 (and/or $z_{0,loc}$), we can use fig. 4.11 to estimate R within 25%, provided that in the latter case U_0 is taken as the wind speed at the building location in the absence of the building ($U_{0,loc}$).

In complex urban geometries (nearby low rise buildings), corner streams should be defined as areas where $U/U_{Ho} > 0.66$ as U_0 can not be defined here. With this definition, R can still be estimated with the same accuracy, except when $W/H < 1$, or $H/h < 5$ (h is low rise building height).

Maruta (1984) has developed a similar corner stream radius which is valid if $W/L < 4$ and $W/H < 2$. Maruta's results are up to 25% lower (for small W/H) than the present R. This is a fairly good agreement as R is rather sensitive to the U/U_0 ratio: a 10% change in U/U_0 results in about 35% change in R, and even more if U/U_0 is near its maximum value.

max corner stream speeds

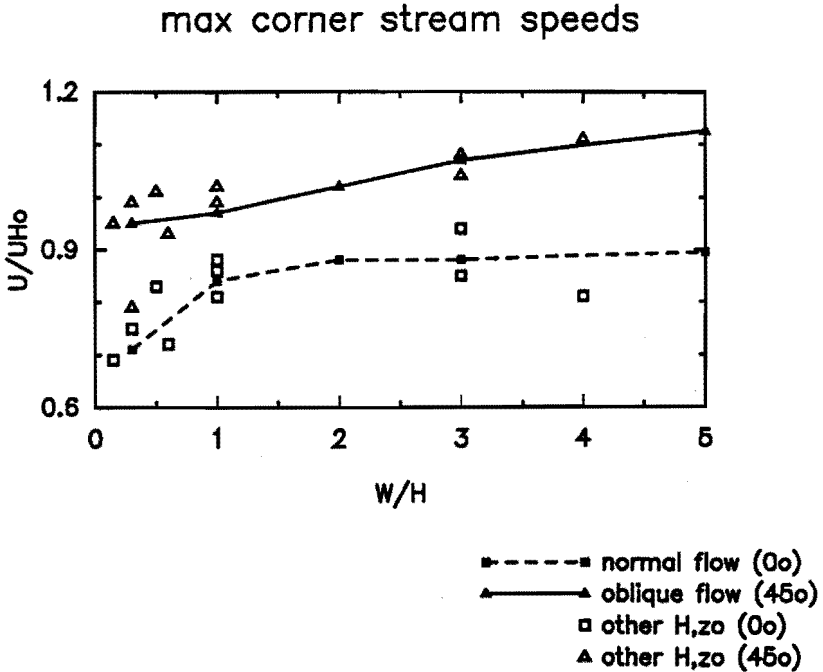*Figure 4.12: Maximum corner stream wind speeds U/U_{Ho} as a function of W/H for two approach flow angles: $0°$ (lower curve) and $45°$ (upper curve). Further data: $H = 50$ m; $L = 15$ m; $z_0 = 0.03$ m. For large W/H, blockage effects (up to 2.5%) result in slight overestimation of U/U_{Ho}.*

Another important issue is the estimation of maximum corner stream speeds.
Lawson et al (1975) stated that the maximum U/U_{Ho} in corner streams is about
0.95. Leene (1991) found a maximum U/U_{Ho} of 0.99±0.10 for a large number of
routine wind tunnel investigations (urban flow). In their wind tunnel
experiments, a smooth turntable is used ($z_{0,loc} \ll z_0$).

The present numerical data (U/U_{Ho}) range between 0.6 and 1.1. Clearly, corner
stream wind speeds are dependent on building and approach flow parameters
such as: θ, W/H, H, L/H or L/W, and z_0.
Figure 4.12 shows maximum corner stream speeds as a function of W/H for two
wind directions. For normal flow (0^0), U/U_{Ho} increases up to about 0.9 for
W/H > 2. For oblique flow (45^0), U/U_{Ho} is about 20% larger, and U/U_{Ho} reaches
its maximum (1.12) at W/H ≈ 5.
The influence of L/W and H/z_0 is generally of secondary importance.

Urban approach flow ($z_0 = 1$ m; $z_{0,loc} = 0.03$ m) results in up to 7% increase in
U/U_{Ho} provided that the fetch $x_{loc} > 12H$. Nearby low rise buildings result in
5% reduction in U/U_{Ho} (compared to fig. 4.12) for W/H ≈ 1 and 15% reduction
for W/H < 0.5. Maximum U/U_{Ho} is also dependent on $z_{0,loc}$. For W/H < 1, a $z_{0,loc}$
of $2*10^{-4}$ m (instead of 0.03 m) may result in 5-10% increase in U/U_{Ho}. Such
small $z_{0,loc}$ values are used in almost all published wind tunnel data.

The effect of $z_{0,loc}$ is very significant in areas with slight wind speed increase.
This effect can partly be 'corrected' by using $U_{o,loc}$ as a reference speed where
$U_{o,loc}$ is the speed that would be measured in the absence (not upstream) of the
building.

Recirculation zone and shear layers

Wind speeds in the recirculation zone behind an obstacle are reduced
considerably. The dimensions of the recirculation zone are much larger than of
the frontal vortex, and in this way a large sheltered area is obtained.

For normal flow (0^0) the length L_R (measured from frontal building side) of the
area with recirculating flow is about $4L_g$. The sheltered area is even larger. A
small H/z_0 (urban approach flow) results in up to 10-20% reduction in L_R. For
large L/H or L/W (greater than 1), the flow reattaches at building sides and
roof, and L_R should be measured from the leeward building side.
Maximum wind speeds (U/U_{Ho}) vary from 0.2 for small W/H to about 0.3 for
W/H > 1. A small $z_{0,loc}$ (0.0005 m), as in many wind tunnel experiments, results
in 20% increase in U/U_{Ho}.

For oblique flow, L_R (measured as for 0^0) is reduced by a factor 2, and much of
the shelter disappears (fig. 4.10). Wind speeds are close to those in the
undisturbed flow, except very close to the building. If W/H > 2, downward flow
near the reattachment line ($x ≈ L_R$) may even result in increased wind speeds
($U/U_{Ho} ≈ 0.6$; U/U_0 up to 1.3). This has been observed by Gandemer (1975) as
well. An explanation is given by Jacobs (1983).

The recirculation zone is bounded by zones with sharp wind speed gradients, the shear layers. These layers originate at the separation points. Figure 4.10 gives an impression of the shear layer position, and the associated wind speed gradients. Note that for oblique flow (45°), wake and shear layers are turned by about 20° (compared with approach flow). This is due to flow conduction along the longer building faces.

The far wake

Upstream buildings can significantly alter the wind speed on a location, even when the distance of the upstream buildings is 30 obstacle heights.

In the following, empirical estimates of wind speed reduction in obstacle wakes are given. The estimates are based on literature survey and experiments (Leene et al, 1990; Leene, 1991). Numerical estimates are not given as the present model is not suitable for the far wake (section 2.3).

Figure 4.13 shows the basic graph (Leene et al, 1990) for a building with W/H = 8, $H/z_o > 30$, and for normal flow (0°). The upstream face (or downstream face if L/H > 1.4 and/or L/W > 0.7) is at x = 0. For non standard conditions, the wake length L_o (or x/H) of figure 4.13 must be converted to the actual wake length L_a by a number of correction graphs (fig. 4.14).
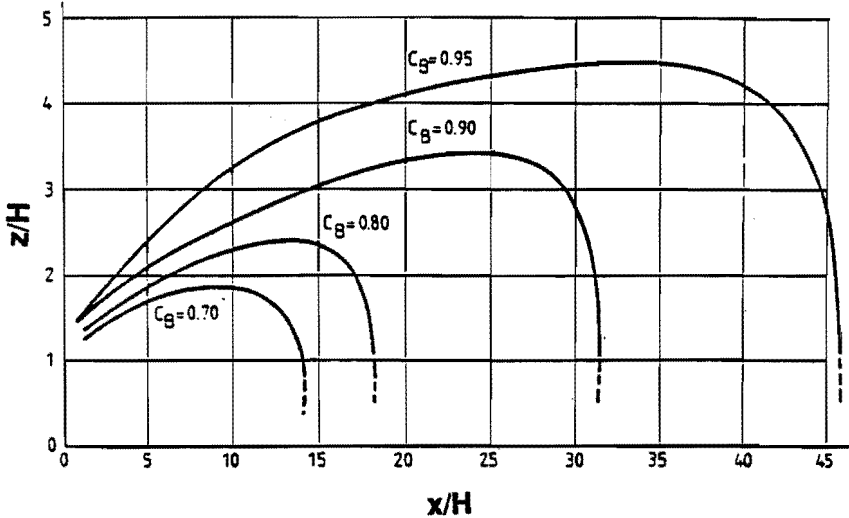
Figure 4.13: Wind speed reduction factor $C_B = U(z)/U_o(z)$ in the far wake of a building (Leene et al, 1990). The graph is valid for normal flow (0°), W/H = 8, $H/z_o > 30$, $C_B > 0.7$, and x/H > 10. See figure 4.14 for correction graphs for non standard conditions.

89

The formula for the actual wake length in non standard conditions reads:

$$L_a = L_o \, \lambda_W \, \lambda_\beta \, \lambda_e \, \lambda_r \qquad (4.7)$$

where λ_W, λ_β, λ_e and λ_r are correction factors for relative building width (W/H), approach flow angle, end effects, and the ratio of building height over terrain roughness (H/z_0). The correction factors can be taken from figure 4.14.

The accuracy of the basic graph (fig. 4.13) is estimated by comparison with data of Raine et al (1977), and of Jacobs (1983). The relative error in C_B ($U(z)/U_0(z)$) is 6%, which is quite good.

Figure 4.14: *Correction graphs for wake length of figure 4.13 (after Leene et al, 1990).*
a) *Effect of relative obstacle width*
b) *Effect of approach flow angle*
c) *Effect of obstacle ends*
d) *Effect of ratio of building height and terrain roughness H/z_0 (use of graph not recommended for $H/z_0 < 20$)*

For non standard conditions, the model is less reliable. For oblique flow, the errors can be extremely large because of turning and narrowing of the wake (fig. 4.10b). This 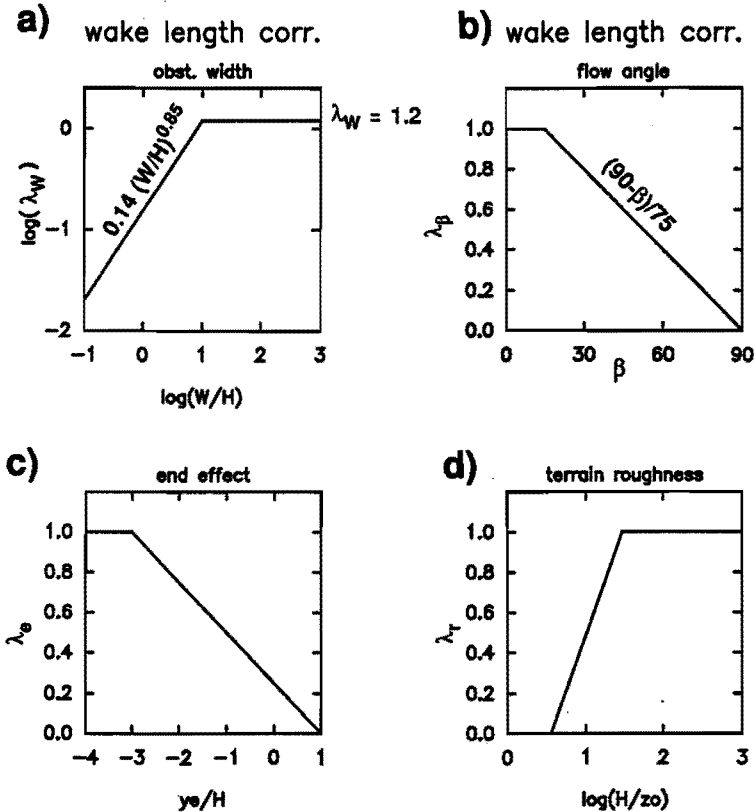is especially the case if W/H > 2 and W/L > 5. It is recommended to apply no wind speed reduction at all (U/U_o ≈ 1) for these geometries.
Streamlined bodies have hardly any wake. For this case, wind speed reduction is also strongly overestimated by the present wake model. The same applies to gentle sloping hills.

Other issues relevant to the application of fig. 4.13 and 4.14 are:
1. -The wake method is only valid for isolated obstacles and, eventually, for very small obstacle groups (2 or 3 buildings). The wake method can not be used the predict wind speed reduction downstream of a town edge.
2. -In an urban environment, where z_o ≠ $z_{0,loc}$, $U_o(z)$ can often not be defined well. A way to overcome this problem is to wind speed reduction factors on a local $U_o(z)$, measured in the absence of the building.
3. -The graphs can not be used for porous obstacles, and for obstacles with sloping surfaces (dikes). Alternative graphs are given in (Leene et al, 1990).

Estimates of turbulence properties

Turbulence data are very scarce in literature. Common (hot wire) measuring techniques become unreliable if turbulence intensity T_u > 30% (section 2.3). However, most flow zones around an obstacle have typical turbulence intensities far above 30%. Reliable measurements are only possible in the far wake and in corner streams, unless Laser Doppler techniques are used. In the following, estimates of T_u are given, which can be used if no reliable measuring technique is available.

Section 2.3 and Bottema et al (1991) show that the present numerical estimates of K (kinetic energy of turbulence) compare well with Laser Doppler results. These LDA results (Bottema, 1990) suggest that turbulence variations (σ_u) around an obstacle are much smaller than variations in mean wind speed. Hence, we can take, as a first approximation, σ_u to be constant.

In the present numerical simulations, σ_u can not be evaluated directly. The square root of K ($K^{0.5}$), is a convenient turbulence parameter, which can also be used in zones where the flow direction is indefinite. In the remainder of this chapter, we will use $K^{0.5}$ as a numerical estimate of σ_u. Near obstacles, this may result in some small errors, as the ratio $K^{0.5}/\sigma_u$ is not exactly 1 (typical error ≈ 10%). Upper and lower limits of the $K^{0.5}/\sigma_u$ ratio are:

$$0.82 < K^{0.5}/\sigma_u < 1.41 \qquad (4.10)$$

where 0.82 is representative of isotropic conditions ($\sigma_u = \sigma_v = \sigma_w$), and 1.41 of extremely sheared flow ($\sigma_v = \sigma_w = 0$).

Figure 4.15 gives an overall estimate of turbulence intensity $K^{0.5}/U$ as a function of γ. Similar graphs can be obtained with Laser Doppler techniques (Bottema, 1990), but not with conventional measuring techniques (hot wires) which are unreliable if T_u is larger than 30% (say if $\gamma < 0.6$). The present data allow for a fairly accurate T_u estimate by simply putting σ_u equal to the approach flow value $\sigma_{u,o}$. We can estimate $\sigma_{u,o}$ by combining eq. 2.1, 2.8 and 2.10: $\sigma_{u,o} \approx 0.96\ U_{Ho}\ /\ \ln(H/z_o)$.

Figure 4.15 is based on numerical data of flow around isolated buildings on rural terrain ($z_o = z_{o,loc} = 0.03$ m) and three different wind directions (0°, 45°, 90°). Building height H ranges from 25 to 100 m; building width W from 15 to 250 m. The relative error in the estimate is 15%, and increases to 20% for high rise building groups.
If $z_o \neq z_{o,loc}$, the error in the σ_u (and T_u) estimate may increase to 35%. In that case it is better to set σ_u equal to the airport σ_u (30% error) instead of the approach flow σ_u. A suitable *local* reference σ_u, if available, may decrease the standard relative error to 20-25% or less, except when $z_{o,loc} \ll 0.03$. In the latter case, building induced turbulence becomes too large compared with local turbulence levels in the undisturbed flow.

turbulence intensity
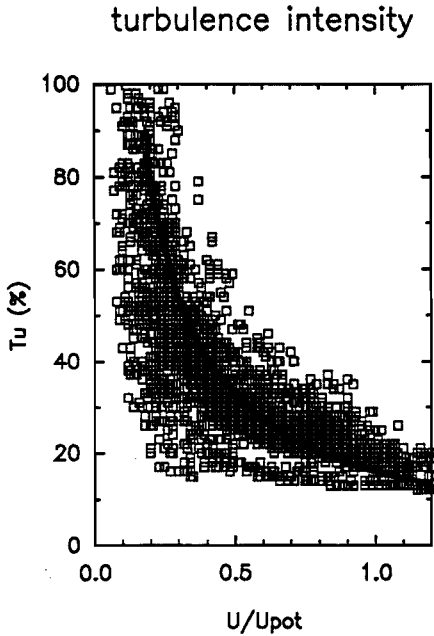
Figure 4.15: *Numerical estimate of turbulence intensity T_u (about 20000 data points) as a function of wind amplification factor γ. The estimate is made for isolated buildings and for $z_o = 0.03$ m. The standard relative error in a constant σ_u approximation is 15%.*

The above given estimate does make explicit which flow zones have increased turbulence levels (σ_u). A short characteristic of each flow zone (see also figure 4.16) will be given below.
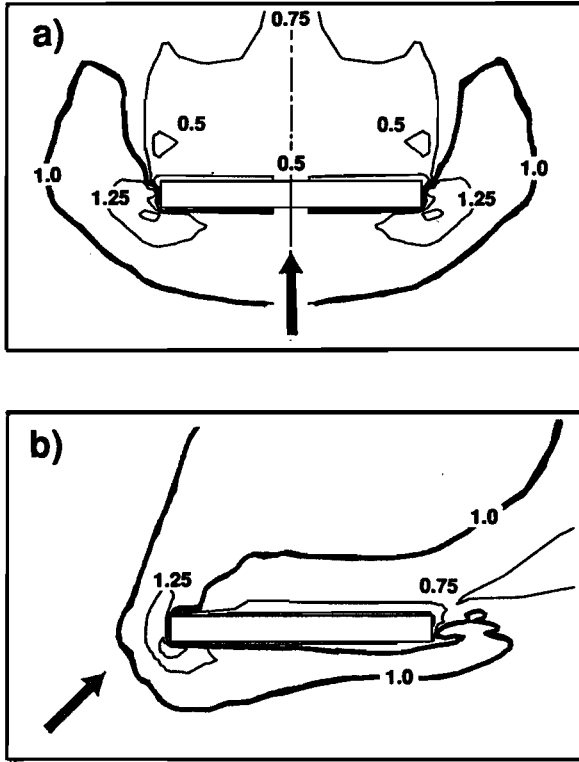
Figure 4.16: Lines with equal turbulence levels $(K/K_o)^{0.5}$ around a building with $L,W,H = 15x150x50$ m; $H/z_o = 1667$. Contour intervals: 0.25, thick line: $(K/K_o)^{0.5} = 1$
a) Normal flow $(0°)$
b) Oblique flow $(45°)$

The largest turbulence levels are found in the frontal vortex and in the corner streams (for normal flow $(K/K_o)^{0.5}$ is up to 2). Turbulence intensity T_u in corner streams is rather low: about 25%.
Corner stream estimates of T_u do not need to be very accurate. For danger evaluation, a 20% uncertainty in $(K/K_o)^{0.5}$ yields a 9% uncertainty in U_{pot}. For comfort, the uncertainty in U_{pot} is only 3%.
For oblique flow (45°), $(K/K_o)^{0.5}$ in the frontal vortex and in the corner streams is 1.5 or less. Corner stream T_u is between 15% and 20%.

In the recirculation zone, turbulence levels are generally reduced. $(K/K_o)^{0.5}$ varies from about 0.5 near the leeward building faces to about 1.0 near reattachment $(x = L_R)$. Thus, buildings provide less shelter against turbulence than against mean flow. For oblique flow (45°), the reduction in turbulence levels has virtually disappeared, and there may be even a slight turbulence increase (near reattachment).

In literature, shear layers are often associated with high turbulence levels. Numerical data show that local generation dominates only if $z_{0,loc} << 0.03$ m. In other cases, turbulence of the approach flow and of the frontal vortex is dominant. Near reattachment $(x=L_R)$, most of the turbulence increase (of frontal vortex and corner streams) has disappeared.
The same applies for oblique flow (45°). However, downstream of the longer building face $(W/L > 1)$ some local turbulence generation can be seen.

According to Leene et al (1990), turbulence levels in the far wake are not very different from the upstream values. Data of Peterka et al (1975), and of Raine et al (1977) confirm this near the ground only (i.e. if $z/H << 1$). At $z/H \approx 1$, there is generally a peak (50% increase in σ_u if $H/z_0 >> 20$) in turbulence levels. Downstream of the maximum (at $x \approx L_R$, and $z \approx H$), the increase in turbulence levels is roughly proportional to x^{-1}.

The above estimates may also be used for other z_0 and $z_{0,loc}$, provided that a suitable $K_{0,loc}$ is chosen. However, if $z_{0,loc} << 0.03$, $K^{0.5}/U_{Ho}$ remains roughly constant because of building generated turbulence.
Uncertainties in the overall estimate of σ_u have already been discussed. The relative uncertainty is up to about:
-35% if σ_u is assumed to be equal to the approach flow value
-30% if σ_u is assumed to be equal to the airport value
-20% if σ_u is equal to a suitable $\sigma_{u,loc}$ measured in the absence of the building.

Exposed and sheltered locations around buildings

Wind speeds near (corners of) high rise buildings, are often increased. On the other hand, the same locations may be very sheltered if the wind direction changes. A first 'integration' of flow fields for different wind directions will be presented below. This allows us to identify exposed and sheltered areas. Discomfort probabilities for these areas will be discussed in chapter 5.

Corner streams are the main areas with increased wind speeds. Maximum wind speeds are found in the proximity of building corners where the flow separates (fig. 4.10). Oblique flow (45°) yields the largest wind speeds; $U_{max}/U_{Ho} \approx 1$. For wide buildings and for oblique flow (45°), another area with increased wind speeds is found at about 2H behind the longer building face.

The main area with reduced wind speeds is the leeward recirculation zone with a typical dimension of $4L_g$ (eq. 4.8). For oblique flow (45°), the sheltered area is

generally much smaller. Another sheltered zone is found at the upwind side of the building. This zone has a typical size of the order of L_g.

Figure 4.17 gives an indication of sheltered and windy locations if all wind directions are considered. It is clear that wind conditions near the centre of the longer building face are much better than near the ends.

Most shelter can be obtained by orienting the longer building face at a right angle to the wind, provided that there is a prevailing wind direction. The worst conditions will then be found at the upstream building corners. If the purpose is only to reduce the size (and strength) of the windy areas, then an orientation parallel to the prevailing wind direction may be beneficial.
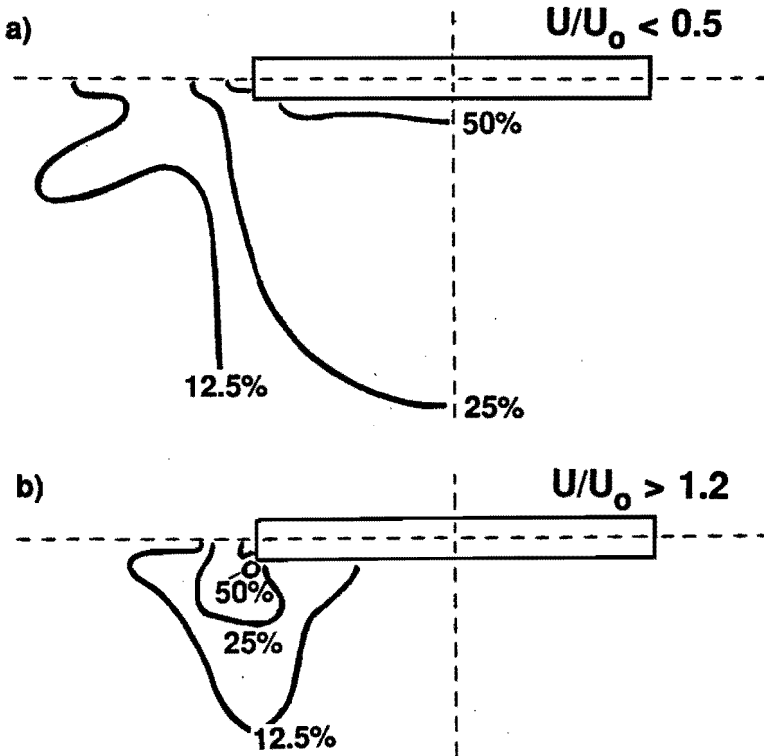
Figure 4.17: Indication of zones where sheltered and windy conditions prevail for a given percentage of wind directions (all wind directions have equal probability). Building dimensions L, W, H: 15, 150, 50 m; z_o = $z_{o,loc}$ = 0.03 m; θ = 0°; 45°; 90°.

a)   Sheltered conditions: U/U_o < 0.5
b)   Windy conditions: U/U_o > 1.2
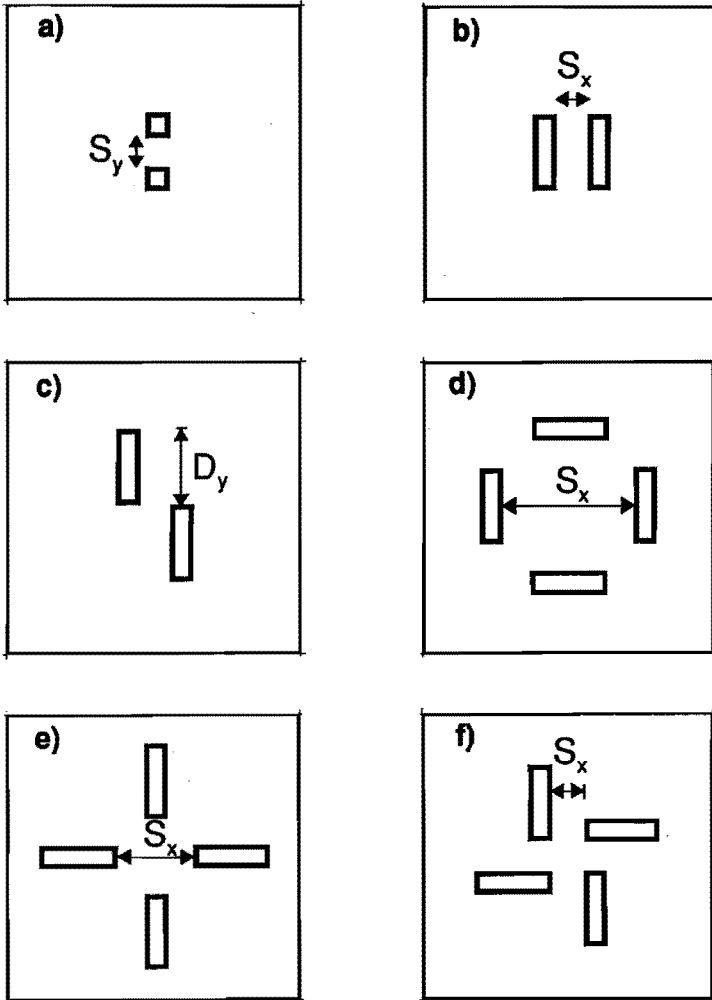
Figure 4.18: Arrangements of high rise building groups, and notation. In all cases z_o = 0.03 m, approach flow angle $\theta = 0^o$, 45°, 90°; building dimensions (L,W,H) are either 15x15x50 m (A) or 50x50x15 m (B).

a)	Aligned buildings: $S_y = 20$ m (A,B), and 50 m (B)
b)	Buildings behind each other: $S_x = 20$ m (A,B), 50 m (B) and 100 m (B)
c)	Shifted buildings: $S_x = 20$ m; $D_y = 25$ m and 50 m (B)
d)	Square: $S_x = S_y = 85$ m (B)
e)	Cross: $S_x = S_y = 50$ m (B)
f)	Shifted cross: $S_x = S_y = 20$ m (B)

96

4.3.3 Groups of high rise buildings; interaction

In this section, some characteristic building arrangements are selected, and their flow features are discussed. The degree of interaction (wind modification or amplification due to building arrangement) can be estimated by comparison with flow properties around isolated buildings. Figure 4.18 gives a plan view of different building arrangements in this study. It will be clear that there are so many parameters that we can not discuss all geometries. Therefore, only typical examples will be given.

Groups of parallel buildings

We can define two types of parallel building arrangements:
-aligned buildings and buildings right behind each other (fig. 4.18a or fig. 4.18b; depending on wind direction)
-shifted buildings (fig 4.18c)

Figure 4.19a shows wind speed around two aligned buildings. Maximum wind speed at the passage centre line is governed by S_y/H, with U/U_0 decreasing from 1.3 for $S_y/H \approx 0.4$ down to 1 for $S_y/H \approx 2.3$. Amplification due to 'interaction' effects is small: up to about 10% for $S_y/H < 1$.
Outside of the passage, the general flow pattern behaves as for a single wide building with gap if $S_y/W < 1$. Isolated building behaviour is to be expected if $S_y/W > 7$ and / or $S_y/H > 2$.

If buildings are put right behind each other, a sheltered area is created (for normal flow; $0°$). Wind speed between the buildings is lower than in the wake of an isolated building if $(L_R-L)/S_x < 1$. Corner streams of the downstream building are absent because the wake of the upstream building is slightly wider than W.
Most shelter disappears for oblique flow ($45°$; fig. 4.19b), as for isolated buildings. Due to corner streams, wind speeds are increased in the passage. However, corner streams are rather displaced than intensified. Interaction effects (mainly corner stream displacement) decrease rapidly if S_x increases; almost no interaction is left if $S_x/H > 1$.
Results for aligned buildings (oblique flow; $45°$) are broadly similar.

An arrangement of shifted buildings (fig 4.19c) is particularly unfavourable because of strong transverse air currents. This is caused by short circuiting of positive wind pressures on the downstream building face and negative wind pressures behind the upstream building. Gandemer (1975) states that $D_x/H < 1$ (where $D_x = S_x + L$) is most unfavourable. Beranek's data (1982) suggest that, for given D_x/H, $D_y/W \approx 1$ yields the worst conditions.

Figure 4.19c shows wind speeds for the near worst case ($\theta = -45°$). Wind speeds are greater than $0.9*U_{Ho}$ over most of the passage, about 20% higher than in the isolated building case. Lateral gradients of the 'jet' are very sharp: over 5 m, wind speed changes as much as U_{Ho}.
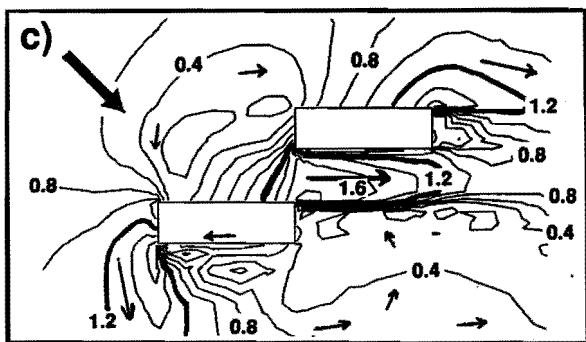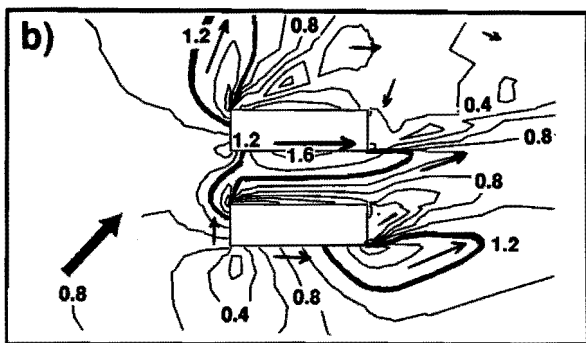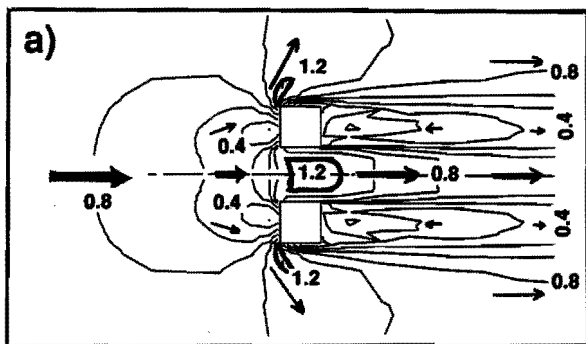
Figure 4.19: Normalized wind speed U/U_0 for different arrangements of parallel buildings. Roughness length $z_0 = z_{o,loc} = 0.03$ m; $U_0/U_{Ho} = 0.55$. Contour intervals: 0.2; thick line: $U/U_0 = 1.2$.

a) Buildings on line; normal flow ($0°$). L,W,H = 15x15x50 m, S_y = 20 m.
b) Buildings behind each other; oblique flow (45°). L,W,H = 15x50x50 m, S_x = 20 m.
c) Shifted buildings; oblique flow (-45°). L,W,H = 15x50x50 m; S_x = 20 m, D_y = 50 m.

98

For normal flow (0°) wind speeds in the passage are about $0.75 * U_{Ho}$, 30% higher than for an isolated building. Both for $\theta = 0^{\circ}$ and $\theta = -45^{\circ}$, pressure difference (i.e. ΔC_{pHo}) is a good estimate of $(U/U_{Ho})^2$ in the passage, indicating that U/U_{Ho} is the appropriate wind speed variable, not U/U_o.

Wind speeds in the passage are considerably reduced if D_y/W is reduced to 0.5. Similar reductions are expected if $D_y/W = 1.5$ (shifted cross arrangement, fig. 4.18f), and for very slender buildings (W/H << 1). Table 4.4 shows wind speeds and turbulence levels at the centre point of the passage (symmetry point in fig. 4.18c).

wind direction:	-45°	0°	45°	90°
pressure connection:	strong	moderate	none	weak
$D_y/W = 0.5$				
U/U_{Ho}	0.73	0.59	0.18	0.66
$(K/K_o)^{0.5}$	1.32	1.41	0.70	1.10
$D_y/W = 1$				
U/U_{Ho}	0.88	0.75	0.43	0.59
$(K/K_o)^{0.5}$	1.37	1.62	1.06	1.11

Table 4.4:   *Normalized wind speeds and turbulence levels in passage (centre point) between two shifted buildings (fig. 4.18c and fig. 4.19c) with L, W, H = 15x50x50 m; S_x = 20 m; $z_o = z_{0,loc}$ = 0.03 m; and U_o/U_{Ho} = 0.55. Note the 'critical' lateral displacement $D_y/W \approx 1$ in the second case.*

Turbulence levels may still be estimated by assuming that σ_u is assumed to be equal to the approach flow value. For shifted buildings, the uncertainty of this estimate is slightly larger than for isolated buildings, but generally below 20%.

Turbulence levels $(K/K_o)^{0.5}$ in passages (centre line; 0°) increase from 1.1 for $S_y/W = 1$ to about 1.5 for $S_y/W \approx 0.4$. Near the end of the high wind speed 'jet' (fig 4.19a), $(K/K_o)^{0.5} \approx 1.3$. For buildings behind each other, turbulence levels (normal flow) near the downstream building may be increased (by about 15%) if $(L_R-L)/S_x > 1$.
Turbulence properties for oblique flow (45°) behave largely as for isolated buildings. This suggests that interaction effects on mean flow properties are stronger than on turbulence.

In the case of shifted buildings, most turbulence is produced near the downstream building. In front of the downstream building and in the passage $(K/K_o)^{0.5}$ is about 1.5, both for normal (0°) and for oblique (-45°) flow. For $\theta = -45^{\circ}$, some very sharp wind speed gradients were observed (fig 4.19c) which result in very localized but strong turbulence increase (70%).
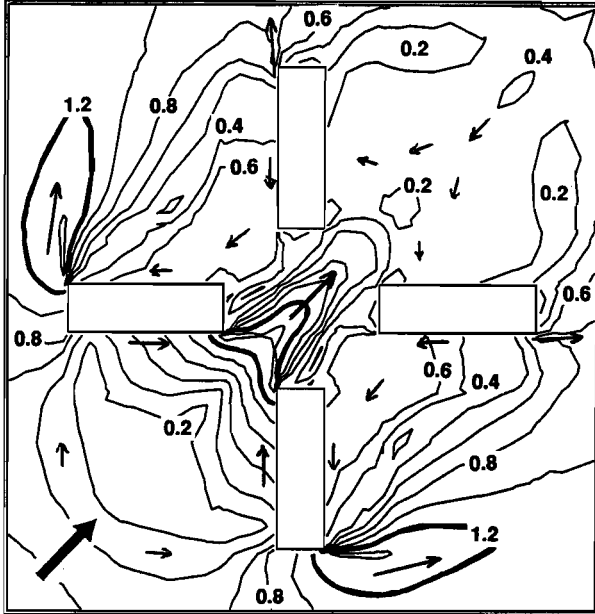
Figure 4.20: *Normalized wind speed U/U_o for a cross ('+') shaped building arrangement (oblique flow; 45°). Building dimensions are 15x50x50 m (L, W, H); $S_x = S_y = 50$ m; roughness length $z_o = z_{o,loc} = 0.03$ m; $U_o/U_{Ho} = 0.55$. Contour intervals: 0.2; thick line: $U/U_o = 1.2$.*

Parallel and perpendicular buildings

Figure 4.18 (d,e,f) gives examples of 'mixed' groups with parallel and perpendicular buildings. These building arrangements are quite complex. Some errors due to a too coarse computational grid can be expected: Both U/U_{Ho} and $(K/K_o)^{0.5}$ may be underestimated by about 10%.

The sheltering properties of the square arrangement (see fig. 4.18d for geometry) are not surprising. In this particular case, even the standing vortex between the two buildings is almost absent so that $U/U_{Ho} < 0.2$ and $(K/K_o)^{0.5} \approx 0.5$ in the centre of the square.

These sheltering properties depend critically on W/H (of order 1), L/W (much less than 1 to avoid pressure short circuiting), and the spacing S_i ($(S_i+L) < L_R$ and $S_i \cdot W < 2L$, where i is either x or y).

For oblique flow (45°), the upstream flow pattern is almost the same as for isolated buildings, resulting in a wind speed of $0.8 * U_{Ho}$ in the upstream passage. In other passages $U/U_{Ho} \approx 0.3$. Turbulence levels are hardly changed (i.e. $K/K_o \approx 1$), except in the wake of the group where $(K/K_o)^{0.5} \approx 0.7$.

100

The cross ('+') shape (fig 4.18e) should yield the adverse Venturi-effect (Gandemer, 1975). Due to mass continuity (eq. 2.25), wind speed in a closed channel increases if the channel cross section decreases. In practice, this Venturi effect is weakened by upward flow and by flow around the group. Beranek's (1984) results and the present data (fig. 4.20) show that there is hardly any interaction in the passage. Often, *the Venturi-effect is nothing more than a wrong interpretation of maximum corner stream wind speeds for oblique flow*. Real interaction is to be expected when pressure short circuiting effects become important, as in fig. 4.19c. The short circuiting effects have a sharp maximum if $D_y/W = 1$. Short circuiting effects are rather weak in the 'shifted cross' arrangement, where $D_y/W = 1.4$ (table 4.5).

wind direction:	0°	45°
cross / '+'		
U/U_{Ho}	0.47	0.69
$(K/K_o)^{0.5}$	1.11	1.03
shifted cross		
U/U_{Ho}	0.54	0.53
$(K/K_o)^{0.5}$	1.20	1.03

Table 4.5: *Normalized wind speeds and turbulence levels in centre point of cross arrangement (fig. 4.18e) and shifted cross arrangement (fig. 4.18f). Building dimensions (L, W, H) are 15x50x50 m; $z_o = z_{o,loc} = 0.03$ m; $U_o/U_{Ho} = 0.55$.*

Figure 4.10 and 4.12 show that oblique flow yields the highest corner stream speeds. Oblique flow conditions are not alternated with normal flow conditions if buildings are arranged in a '_' or 'Y' shape. These arrangements are expected to be more unfavourable than a '+' arrangement (as in fig. 4.20). Unfortunately, the present numerical model can not handle '_' and 'Y' arrangements.

High rise building groups; summary

Flow in groups of high rise buildings has a high degree of complexity. Still, many flow features can be described with the key words *dominance* and *interaction*.

In the case of dominance (called 'weak interaction' or 'superposition' by Beranek, 1984), the closest building determines flow properties at a given location or, alternatively, the building which causes the highest wind speeds at that location. This is very similar to isolated building behaviour.

Interaction effects (called strong interaction by Beranek, 1984) may increase or decrease wind speeds. The most important effects are mutual sheltering and pressure short circuiting.

101

In many cases, interaction effects are weak, as for aligned buildings (fig. 4.18a) or buildings right behind each other (fig. 4.18b). For some wind directions mutual sheltering works beneficial.

If the downstream building is shifted sideways (fig. 4.18c), pressure short circuiting often results in considerable wind speed increase. The effect is most pronounced for $D_x/H < 1$, $D_y/W \approx 1$, where D_x and D_y denote streamwise and lateral displacement of the downstream building.

Dominance effects prevail if buildings are placed perpendicular to each other. Cross ('+'), '_' and 'Y' arrangements cause deterioration of wind climate as corner streams dominate for many wind directions. These corner stream effects are largest for *oblique* flow (45°) and for large W/H.

A suitable building arrangement can also create very sheltered conditions. A closed square ($\square$) protects from any corner stream influence, and if S_x (or S_y) < $0.5*L_R$ ($2L_g$), wind speed and turbulence levels are strongly reduced. Wind conditions appear to be most favourable if $S_x \approx S_y$ (Smith et al, 1977).

The centre of an open square may provide much shelter as well. Optimum dimensions are given above.

4.3.4 Low rise building groups; streets and squares

The predominant flow feature in low rise building groups is mutual sheltering. This improves wind conditions for pedestrians, but not for the wind engineer. The latter has to deal with considerable problems (systematic errors) in measuring techniques and in numerical simulation techniques. Therefore, data of this section should only be considered as approximate.

Again, the flow is determined by a great number of parameters. The main parameters which will discussed are relative street length (S_x/h), relative street width (S_y/h) and building arrangement.

Street length

Street length influence on wind speeds in very wide streets can simply be described by an internal boundary layer (IBL) model (section 4.2.2). Table 4.6 shows how wind amplification factor γ varies with fetch x (behind last buildings), local ground surface roughness $z_{0,loc}$ and approach flow roughness z_0. The most rapid wind speed increase occurs for x < 600 m. Note that x must be increased by 5-10 building heights to obtain the minimum (building face to face) street length S_x.

The main parameters are the fetch x (or street length S_x) and the local ground surface roughness $z_{0,loc}$. The combined effect on γ of large S_x and small $z_{0,loc}$ (compared with 0.03 m) can be as large as 40%. The effect of approach flow z_0 (as long as representative for built up conditions) on γ, is small: about 10%.

Limitations of this approach are the minimum required fetch of about 300 m or 30h (no influence of wakes of 'individual' buildings), and the neglect of street width. Therefore, it is better to consider the few available experimental data.

102

fetch x:	z_o:	A	B	C	D
		1.0 m	1.0	1.0	0.5
	$z_{o,loc}$:	0.0002 m	0.03	0.1	0.03
300 m		0.56	0.43	0.37	0.49
500		0.61	0.46	0.39	0.51
1000		0.67	0.49	0.41	0.54
2000		0.72	0.52	0.43	0.56
∞		1.10	0.70	0.54	0.70

Table 4.6: *Estimate of wind amplification factor γ as a function of fetch x (m) based on internal boundary layer theory. The estimate is valid for very wide streets without friction of side walls. The effects of different approach flow z_o ($z_d = 0$) and ground surface roughness $z_{o,loc}$ are shown.*

Wind speeds in low rise building groups should be scaled (normalized) by a wind speed above the group. As downward mixing of momentum is dominant, the friction velocity U^* is a good choice. The present numerical and experimental (Alberts, 1981) results do not allow for accurate estimates of U^*. Therefore, a reference speed at 2.5 building heights ($U_{2.5h}$) is chosen, the height at which the influence of individual buildings has become small.
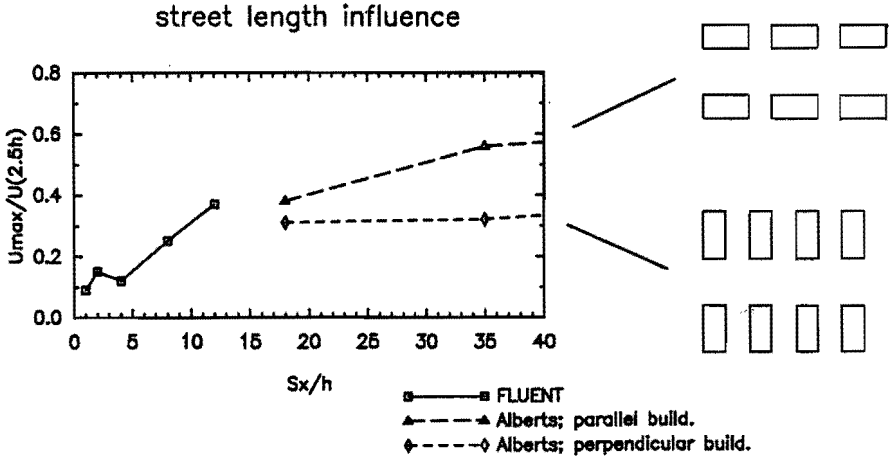
Figure 4.21: *Maximum normalized wind speeds $U_{max}/U_{2.5h}$ at street centre line as a function of street length S_x/h. Solid line: FLUENT data for $S_y/h \gg 1$, $h = 10m$, and $z_{o,loc} = 0.03$ m. Long dashed line: data of various arrangements (Alberts, 1981) with $S_y/h \approx 2$, $h \approx 9$ m and $z_{o,loc} = 0.0005$ m and buildings parallel to street. Short dashed line: as for long dashed line, but with buildings perpendicular to street.*

Figure 4.21 gives $U_{max}/U_{2.5h}$ as a function of relative street length S_x/h. U_{max} is the maximum wind speed in the street. Results of two dimensional numerical simulations ($S_y/h \gg 1$; $h = 10$ m; building group of 'infinite' size) are shown, as well as wind tunnel data (Alberts, 1981) for different building arrangements with $h = 9$ m, $S_y/h \approx 2$, $z_{0,loc} \approx 0.0005$ m. This $z_{0,loc}$ is very small, and typical of water surfaces or smooth, featureless tarmac. Group radius is about 32h. $U_{max}/U_{2.5h}$ is effectively independent on fetch, because $h_{IBL} > 2.5h$.

A street length S_x of less than h yields small wind speeds, as well as a S_x of about 4h. Wind speed increases considerably if S_x/h increases from 4 to 12. The increase may be even more pronounced for (too) small $z_{0,loc}$, as in the experiments. Maximum turbulence levels $(K/K_{2.5h})^{0.5}$ (FLUENT estimate) increase from 0.3 for $S_x/h = 1$ to about 0.7 for $S_x/h > 2$. Note that $K_{2.5h}$ is generally over 70% larger than the airport value (K_{pot}).

The difference between the dashed curves in figure 4.21 shows that street width is important as well. Another indication of street width influence is the fact that FLUENT data extrapolate to higher wind speeds than the experimental data, even though $z_{0,loc}$ in the experiments is much smaller.

Street width

Wind flow parallel to (along) streets yields generally the highest wind speeds.

Alberts (1981) shows that the influence street width (S_y/h) is rather small if buildings are parallel to the street: $U/U_{2.5h}$ at the street centre line increases from 0.53 for $S_y/h = 1.7$ to 0.60 for $S_y/h > 7$. Dimensions of the building blocks (l,w,h) are 60x60x12 m; clear spacing between the blocks ($S_x = S_y$) ranges from 20 to 100 m; street length is 'infinite'; group radius is 24h. The ground surface roughness length ($z_{0,loc}$) is 0.0005 m.
However, wind speeds are considerably reduced (fig. 4.21) if buildings are placed perpendicular to streets. This is especially true if $S_y/h < 2.2$.

In the case of perpendicular buildings, wind speeds at crossings are up to 15% larger than centre street values. The reverse applies for parallel buildings, but with smaller differences.
Side walk wind speeds are typically 5-10% lower than centre street values.

Data for oblique flow are scarce and often unreliable. Alberts' (1981) data suggest that superposition of flow components across and along the street yields a relative error in estimated $U/U_{2.5h}$ of about 10%. However, superposition can only be applied to the centres of sufficiently long streets ($S_x/h \gg 1$), not to crossings and to sidewalks.

The present data are derived from highly idealized geometries. Alberts (1981) noted that the presence of court yards in building blocks did not make much difference for wind speeds in streets. This is an indication that local street dimensions are dominant.

4.3.5 Influence of urban surroundings

In the following, it will be discussed whether estimates of the previous sections can be extended to high rise buildings in an urban 'context', i.e. with urban approach flow and nearby low rise buildings.

Urban approach flow

First, the influence of urban z_0 will be investigated, without considering z_d and the influence (wakes) of nearby low rise buildings. So we are considering a large open space (e.g. car park, lake, field) within a town, like in many wind tunnel investigations (where $z_{o,loc} \approx 0.0005$ m). In the present numerical simulations, $z_0 = 1$ m, $z_{o,loc} = 0.03$ m (this allows for comparison with data in section 4.3.2, and the fetch x_{loc} is 600 m. Two buildings have been considered with dimensions (L, W, H) of 15x15x50 m and 15x150x50 m.

Maximum corner stream wind speeds are up to 7% larger than for the rural case (fig. 4.12). Corner stream radius for the wider building (defined with $U/U_{o,loc} > 1.2$) is 25% larger than in fig. 4.12. Note that $U_{o,loc}$ is the 'real' $U_{o,loc}$ in the absence of the building. The 'real' $U_{o,loc}$ is about 10% higher than estimated by the (IBL) models of section 4.2.2 because of overshoot effects.
Dimensions and wind speeds of the frontal vortex, and of the recirculation zone, are 20-40% lower than for rural approach flow.

Turbulence levels $(K/K_{o,loc})^{0.5}$ are within 10% of the rural values of section 4.3.2. The main difficulty is to estimate $K_{o,loc}$ accurately. The effect of building induced turbulence is rather small, which decreases relative errors (to 20% or less) in estimates where σ_u $(K^{0.5})$ is taken as constant.
In the present case, $K_{o,loc}^{0.5}$ shows about half the undershoot (about 20%) which is expected for $U^*_{o,loc}$ (by matching wind profiles within and above the internal boundary layer). This applies only if z_0 is larger than $z_{o,loc}$. An overshoot in $U^*_{o,loc}$ and also in $K_{o,loc}^{0.5}$ is expected if z_0 is less than $z_{o,loc}$.

Flow in idealized urban geometry

The urban 'context' is not only characterized by urban z_0, but also by urban z_d and by nearby low rise buildings. These low rise surroundings may change wind flow around high rise buildings significantly. Other issues which will be discussed are:
-minimum building height for high rise building behaviour
-interaction effects between high rise building and low rise surroundings

Figure 4.22 shows wind speeds around a 50 m high cube, surrounded by low rise buildings. Immediately upstream of the high rise building, flow is similar to the isolated case ($z_0 = z_{o,loc} = 0.03$ m). Corner stream wind speeds are up to about 10% lower than for an isolated building ($z_0 = 0.03$ m), both for normal flow and for oblique flow. Corner stream maxima for oblique flow are least

affected. In the upstream side streets, the influence of the high rise building ($U/U_{Ho} \approx 0.4$) is noticeable for a few building heights H.

Other features worth noting are the flow conduction and high wind speeds (U/U_{Ho} up to 0.8) near the downstream building sides (for oblique flow; 45°), and very low wind speeds in streets in the wake of the building.
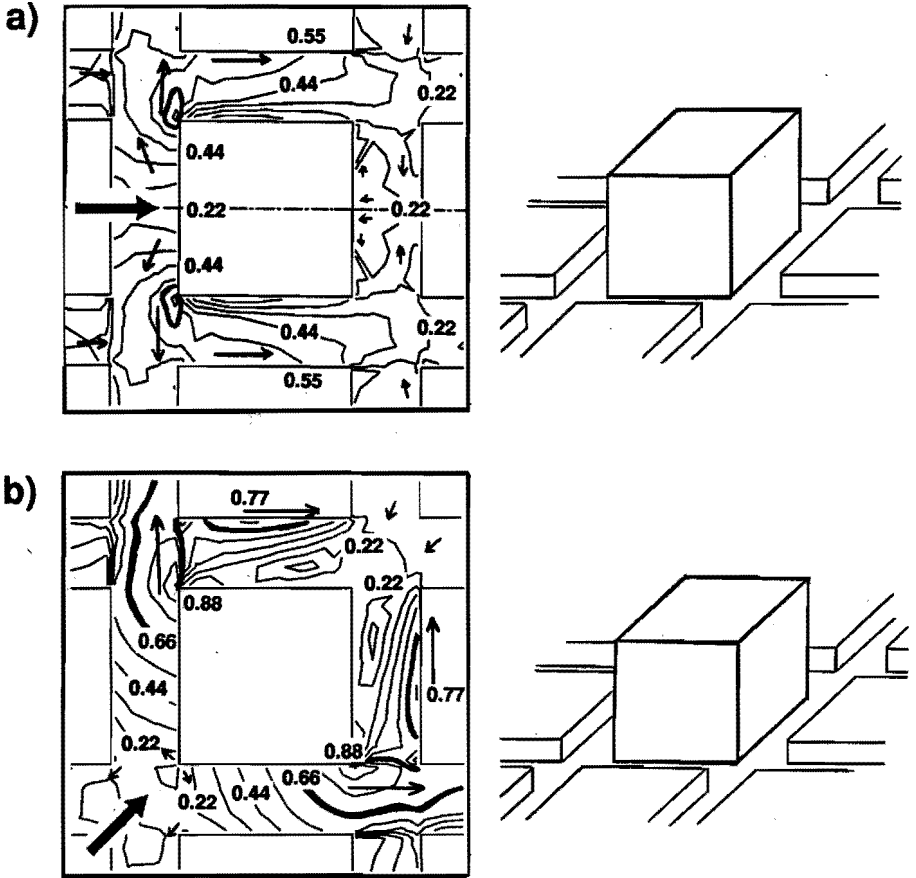
Figure 4.22: Lines of equal U/U_{Ho} around cube with H = 50 m. Further data: z_o = 1 m, z_d = 10 m, $z_{o,loc}$ = 0.03 m, x_{loc} = 600 m (skimming flow over buildings with h = 10 m over last 600 m), street width S = 20 m. Contour intervals: 0.11; thick line: U/U_{Ho} = 0.66.

a)   normal flow (0°)
b)   oblique flow (45°)

106

Turbulence levels are referred to K_0 as $K_{0,loc}$ can not be defined in complex geometries. In the frontal vortex $(K/K_0)^{0.5} \approx 1$ for normal and for oblique flow. After about one building height (50 m), turbulence levels are decreased by about 50%.

Narrowing the streets of fig. 4.22 (S/h = 1 instead of 2) yields almost the same results but with 10-20% lower turbulence levels. In these narrow streets, flow channelling may become important. Initial conditions, which are generated by the high rise building, may be maintained for several (over 10) street widths.

Wind speeds around slender buildings are much lower. Maximum corner stream wind speeds U/U_{Ho} around a 15x15x50 m tower vary between 0.6 for normal flow (0^0) and 0.8 for oblique flow (45^0). Both figures are 15% lower than in the isolated building case (z_0 = 0.03 m). Corner stream radius R (where U/U_{Ho} > 0.66) is strongly reduced (63%) as well: R is only 10 m. The influence of the building can be recognized within 15-30 m (2W) of the tower. Turbulence levels are comparable with those of the 50 m cube.

Nearby low rise buildings (as in fig. 4.22) may mitigate the effects of high rise buildings. The effects may be summarized as follows:
-less than 5% decrease in U_{max}/U_{Ho} if L_g/h > 3
-more than 15-20% decrease in U_{max}/U_{Ho} if L_g/h < 1.5

Corner stream radius R (with U/U_{Ho} > 0.66) can still be estimated with fig. 4.11, provided that H/h > 3 and W/H > 0.5. In other cases, corner stream radius R is much smaller, or wind speed maxima are found in the streets instead of near the corners.

Britter et al (1978) investigated interaction effects between a high rise building and its low rise 'surroundings' (one upstream building). Wind speed between the buildings is dependent on H/z_0, W/H, H/h and separation distance S_x/H (or S_x/L_g).
Britter et al (1978) propose a simple estimate by assuming that maximum wind speed between the buildings (frontal vortex) is the *sum* of the 'undisturbed' frontal vortex wind speed (maximum) of the downstream building, and the wind speed maximum of the low rise building's recirculation zone. We verified this assumption with a numerical prediction for a 15x150x50 m building (L, W, H), placed 50 m behind a 10x150x10 m low rise building. Britter's estimate is 20% too high for this case, probably because of high $z_{0,loc}$ (0.03 m) in the present numerical simulation.
Corner stream properties are hardly affected in the above mentioned numerical results. However, oblique flow with an *upstream* high rise building (θ =135^0) yields increased wind speeds between the two buildings, with U/U_{Ho} up to 0.8. Figure 4.19b shows a very similar flow pattern. No significant amplification effects were observed for other wind directions.
Finally, Britter's (1978) turbulence levels do not appear to be larger than for the isolated high rise building. This is confirmed by the present numerical result.

4.4   Building shape; details of the site

The previous section discussed wind flow around (groups of) simple rectangular buildings. Properties of the site have only been included by a $z_{0,loc}$ of local terrain.
In the following, we will discuss the effects of a number of building features and site properties which are of interest for wind climate.

4.4.1 Building shape

Architectural features may both improve and deteriorate wind climate. This section discusses the effect on wind of common building features, without pretending to be complete. An extensive study by Jamieson (1991) will be published by the end of 1992.
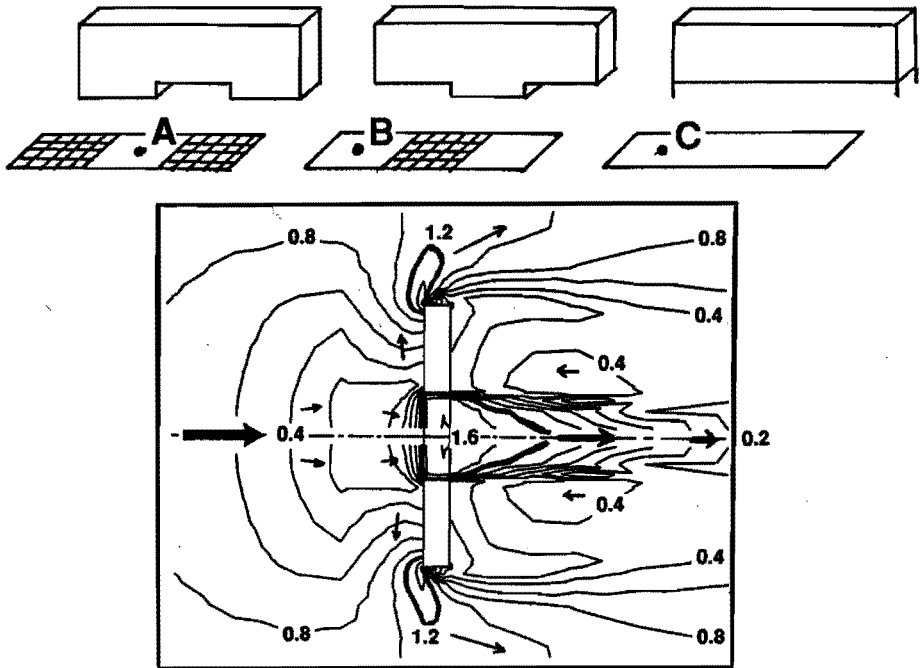
Figure 4.23:   Building with ground level gap(s): classification and flow field
      a)   Examples of buildings with ground level gaps; wind speeds for points A, B, C are given in table 4.7
      b)   Normalized wind speed U/U_0 around building with L,W,H = 15x150x50 m. Further data: normal flow (0°); gap width $W_{gap} = 50$ m; gap height $H_{gap} = 10$ m; $z_0 = z_{0,loc} = 0.03$ m; $U_0/U_{Ho} = 0.55$. Contour intervals: 0.2; thick line: $U/U_0 = 1.2$.

Buildings with gaps

Buildings with ground level connections between windward and leeward face were soon (Melbourne, 1971) recognized as particularly unfavourable. These high wind speeds are caused by pressure short circuiting between two building faces. Figure 4.23 shows some geometries, and a typical distribution of wind speeds. Table 4.7 gives typical wind speeds for the three passage types:

type; dimensions W_{gap}, H_{gap}	wind dir.:	N	NE	E	SE	S	SW	W	NW
A:									
centre gap	U/U_{Ho}	0.12	0.86	0.87	0.86	0.12	0.86	0.87	0.86
50x10	$(K/K_o)^{0.5}$	0.48	1.62	1.82	1.62	0.48	1.62	1.82	1.62
B:									
corner gap	U/U_{Ho}	0.58	0.99	0.87	0.86	0.10	0.86	0.87	0.99
50x10 (2x)	$(K/K_o)^{0.5}$	1.13	1.80	1.92	1.39	0.51	1.39	1.92	1.80
C:									
full gap	U/U_{Ho}	0.77	1.07	0.90	0.92	0.47	0.92	0.90	1.07
150x10	$(K/K_o)^{0.5}$	1.15	1.82	1.86	1.65	0.75	1.65	1.86	1.82

Table 4.7: *Normalized wind speeds U/U_{Ho} and turbulence parameter $(K/K_o)^{0.5}$ for gaps in building with $L,W,H = 15x150x50$ m, $z_o = z_{o,loc} = 0.03$ m for different wind directions. Building orientation is N-S, as in fig. 4.23.*

For all gaps, wind speeds for normal flow and oblique flow (NE, E, SE, SW, W, NW) are very large ($0.86 < U/U_{Ho} < 1.07$). Oblique flow yields the highest wind speeds, as for rectangular buildings, and normal flow (E, W) the highest turbulence levels. Near the gap, the estimate $K = K_o$ is not appropriate and it is advised to use the values of table 4.7, or a turbulence intensity T_u of about 25%. Only for parallel flow (northerly or southerly wind), wind speed in (some of) the gaps is not increased.
In figure 4.23, wind speeds in the gap are about 35% larger than in a similar passage between two buildings. This is because wind speeds in the gap are determined by pressure short circuiting effects. Only the shifted building arrangement of fig. 4.19 (table 4.4) yields comparable wind speeds, again because of strong pressure short circuiting effects.

The effects of gap dimensions on wind speeds are expected to be small, as pressure short circuiting is dominant. However, the length L_j of the 'jet' with increased wind speeds, is strongly dependent on gap dimensions and also on gap location. For centre gaps (fig. 4.23) and for full gaps ($W_{gap} = W$), Beranek's (1982) data and the present data lead to $L_j / min(W_{gap}, H_{gap}) = 10.7 \pm 2.4$ (normal

flow). For corner gaps, L_j is generally (much) smaller. In all cases, jet height
and jet width are roughly equal to H_{gap} and W_{gap}.
Building shape (W/H; L/H) and approach flow roughness (H/z_0) may influence
pressure distribution and gap flow properties as well. The effects of these
parameters have not been investigated.

Corner stream properties are hardly affected by small ($W_{gap}/W < 0.33$) centre
line gaps. For full gaps and for corner gaps, corner streams are part of the gap
flow. Generally, the zone with increased wind speeds ($U/U_{0,loc} > 1.2$ for at least
one wind direction) is within a distance R of each building face.

A final issue is the remedial action that can be taken to reduce gap wind
speeds and jet dimensions. Jet dimensions scale with $\min(W_{gap}, 2H_{gap})$, so L_j
becomes small if either L_{gap} or W_{gap} is kept small.
Gap wind speeds are very difficult to reduce without closing the gap. Gap wind
speeds may be reduced by making a long 'tunnel' with openings at sufficiently
large distance from the building (fig. 4.24). However, the required distance to
the building is so large that such an approach is often not feasible.
The effects of gap resistance are generally small. In the present numerical
simulations, L = 15 m, $H_{gap}/z_{0,loc}$ = 333, and with small z_{ob}, gap wind speeds
(at obstacle centre line) are about 5% smaller than is indicated by ground level
pressure difference. Obstacles in the gap (as in Grand Arche, Paris) are more
effective in reducing wind speeds near the gap. Beranek (1982) found
appreciable wind reduction when (alternating) wind screens of about the gap
size were placed in the gap.
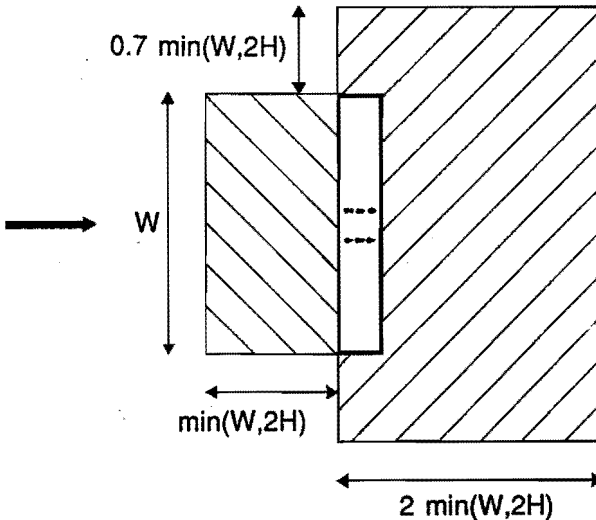
*Figure 4.24: Indication of distance of gap openings, required for appreciable reduction
in pressure difference and wind speeds (normal flow). Gap openings should
be outside hatched area.*

Podium shaped extensions; canopies; balconies

Podium shaped extensions of building are often considered as effective means for improving wind climate around high rise buildings. However, the introduction of a podium does not always improve wind climate at all locations (Jamieson, 1991). This is because high wind speed regions are often rather displaced than removed.

Figure 4.25 shows wind speeds around a 15x15x50 m building (L, W, H), with a podium 'length' (thickness) L_P of 17.5 m. Corner streams at the upstream podium corner are much weaker, but new wind speed maxima have developed near the downstream corners. Corner stream properties (U_{max}/U_{Ho} and R) and turbulence levels correspond well to the values which are expected for the podium only. The same applies to oblique flow.
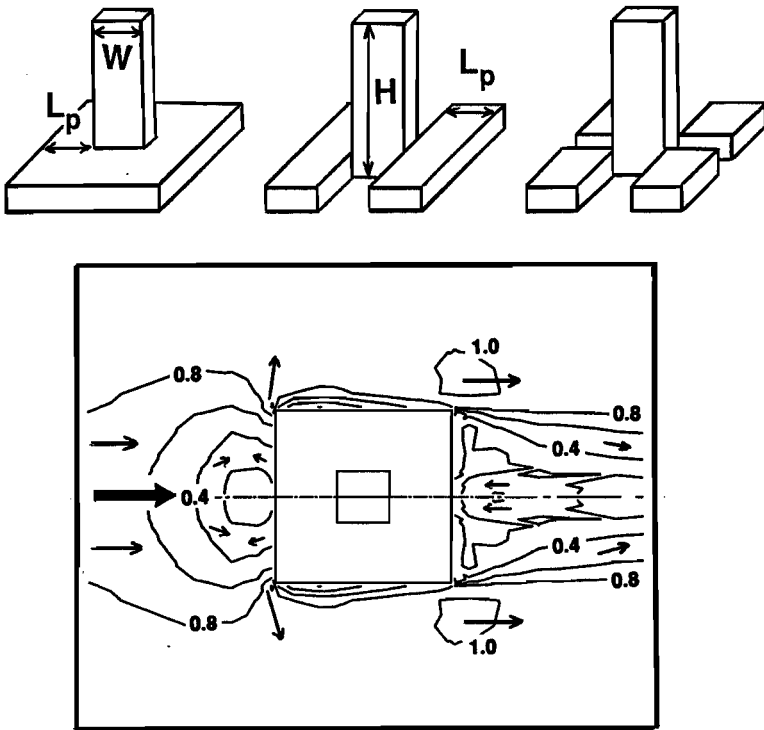
Figure 4.25: *Building with podium shaped extensions: geometry and flow field*
  a)   *Examples of podium shaped extensions*
  b)   *Normalized wind speed U/U_o around building with L,W,H = 15x15x50 m.*
          Podium length L_P is 17.5 m, podium height is 10 m. Further data: normal
          flow (0°); $z_o = z_{o,loc} = 0.03$ m; $U_o/U_{Ho} = 0.55$. Contour intervals: 0.2;
          $U/U_o = 1$ for closed contours at downstream building corners.

Beranek (1982) investigated wind flow near podia, mainly around slender buildings (W/H < 1). Podia with length $L_P > L_g$ will certainly have improved wind conditions. Wind conditions for podia with $L_P < L_g$ may be not so good. Beranek showed that it is sufficient to have a podium around or against the building corners (fig. 4.25a). Podium height does not appear to be very important.

Numerical data, and Beranek's data, show that podia can be very effective in reducing (removing) 'jet' speeds in passages between buildings, provided that podium height H_P is large enough (H_P/H larger than 0.2?).
However, podia are generally not very effective if pressure short circuiting is important (gap, narrow passage, shifted buildings; see Beranek, 1982).

In urban surroundings, podia can perform very well. If the building of fig. 4.25 is put in an 'urban grid' like in fig. 4.22, U_{max}/U_{Ho} (oblique flow) is as small as 0.65 (0.9 for open terrain). This is caused by the influence of low rise surroundings. The best conditions are expected for small street width (say 2h or $2H_P$ or less) and comparable heights of podium and surroundings ($H_P/h \approx 1$).

Canopies and enlarged stories are sometimes proposed as an alternative for podia. The influence of these devices on the pressure field, and therefore on corner stream speeds, may be small (Jamieson, 1991).
The effect of balconies is often accounted for by increasing effective building width and length slightly. Surface roughness of the building should be increased as well. The present model can handle z_{ob} (roughness length of building surface) up to 0.03 m. The main effects of this z_{ob} (up to 7% wind speed decrease and 50% turbulence increase) are observed in a thin boundary layer near the building. Boundary layer thickness is roughly 10% of the fetch along the considered building surface.
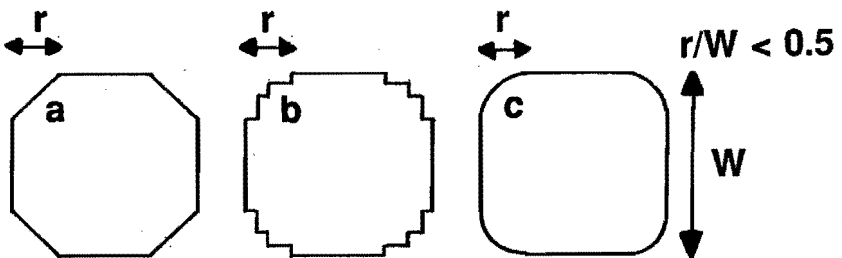
Figure 4.26: Basic shapes of building corners: chamfered (a), stepped (b), and rounded (c), together with notation definition

Corner shape

Rounded building corners are often considered to be beneficial for wind climate. However, the effects of rounded corners are difficult to investigate, both in wind tunnel experiments (dependence on Reynolds number) and in numerical simulations. There are many geometrical parameters, and only few data (Stathopoulos, 1985; Uematsu et al, 1991). Figure 4.26 shows four typical corner shapes. All investigations (the present one included) are limited to square sectioned buildings, i.e. L = W and, for the present numerical simulations, to stepped corners.

If W/L = 1, chamfering of all corners yields a building which is turned by 45° while building width is reduced by a factor √2. For normal flow (0°), chamfering will lead to increased corner stream speeds. This is because oblique flow yields higher wind speeds than normal flow, even for reduced W/H (fig. 4.12). For oblique flow chamfering leads to wind speed reduction in the corner streams. Corner stream radius (fig. 4.11) will be reduced as well, as W becomes a factor √2 smaller.
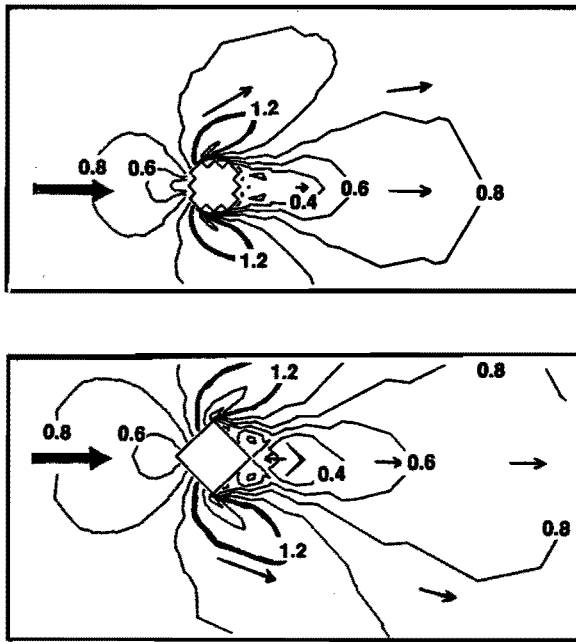
Figure 4.27: *Relative wind speed U/U_o around 15x15x50 m (L, W, H) building for oblique flow (45°); $z_o = z_{o,loc} = 0.03$ m; $U_o/U_{Ho} = 0.55$. Contour intervals: 0.2; thick line: $U/U_o = 1.2$. Upper plot: with stepped corners; lower plot: without stepped corners. Note reduction in 'effective' (lateral) building width and in corner stream and wake dimensions in upper plot.*

Numerical simulations around buildings with varying width (W/H = 0.3 and 1.0; H = 50 m; z_0 = 0.03 m) and a chamfered length r of about 0.7*(W/2) show that the above arguments do not fully apply for buildings with stepped corners. In both cases, the flow patterns do not shift from a 'normal' (0°) regime to an oblique (45°) regime, and vice versa.

For oblique flow (45°), maximum corner stream speeds, and corner stream dimensions are reduced, as expected (fig. 4.26). However, wind speed reductions in corner streams are not always as large as expected, especially for the wider building (cube). The wake has decreased in size as well.
For normal flow, the results are rather indefinite: a 10% increase in corner stream speed increase for the slender building (W/H = 0.3), and a 20% decrease for corner stream maxima (not elsewhere) of the cube. The latter decrease may be caused by resistance of the 'steps'.
Differences with theoretical considerations, as discussed above, are probably caused by a 'partial' chamfering (r/W $\approx$ 0.35 instead of 0.5), and by the effects of stepped geometry.

Measurements of Stathopoulos (1985) and Uematsu et al (1991) (slender buildings with W/H < 0.5; smooth turntable) indicate corner stream wind speed reduction for normal flow, as opposed to the present results and the above theoretical considerations. The reason of these discrepancies is not known.

The effects of a roof 'chamfer' (steps over upper 10% of building) are very small, even for the wider building. For a 'real' roof chamfer Stathopoulos (1985) finds 10% decrease in corner stream speed even though W/H is only 0.15. The effect of roof chamfering should have been small for such a small W/H as flow is mainly around the building; not over the building. Again, it is not clear why these measuring results differ so much from theory.

4.4.2 The effects of screens and trees

In many cases modification of the buildings themselves is not feasible. In that case, it is the site which must be adapted. Screens and trees may sometimes be the solution to existing uncomfortable situations.

Wind screens

Wind screens can be an effective tool to provide local shelter. They can be considered as thin and very wide (W/H >> 1), obstacles. An important property of wind screens is their *porosity* ϕ. In the following, porosity is defined as the ratio between the volume of openings (connections) in a screen, and the total volume of a screen. Rows of trees (not scattered trees or tree canopies) will be treated as porous 'screens'. Leene et al (1990) give some examples which allow for visual estimation of porosity of tree rows. The optimum porosity (for wind reduction) is between 10% and 25% (Pereira, 1980; Gandemer, 1981; Raine et al, 1978). For a hedge, ϕ is close to the optimum porosity (Leene et al, 1990).

114

Wind speed reduction behind a wind screen can be estimated with the wake method of Leene et al (1990) which is discussed in section 4.3.2 (p. 89-91). The basic graph and the wake length correction graph for terrain roughness have to be adjusted for porous obstacles (figure 4.28). End effects decrease with increasing porosity, and with downstream distance. No single correction graph could be made (see Leene et al, 1990).

The wake model estimates are not always reliable for non standard conditions. In oblique flow, the wake is often very small, and wind speed reduction may be strongly overestimated by Leene's wake model (see section 4.3.2).

Turbulence is generally underestimated by the wake model. Better estimates are given at the end of section 4.3.2 (p. 94). Porosity can easily be accounted for: Raine's (1978) data show that the increase in $(K/K_o)^{0.5}$ is roughly proportional to 'solidity' $(1 - \phi)$.

For urban flow, wind tunnel results of Gandemer (1981) suggest that wake length of obstacles with large porosity ($\phi = 50\%$) may be reduced by 30%. However, $z_{0,loc}$ and x_{loc} of the experiments are not known.

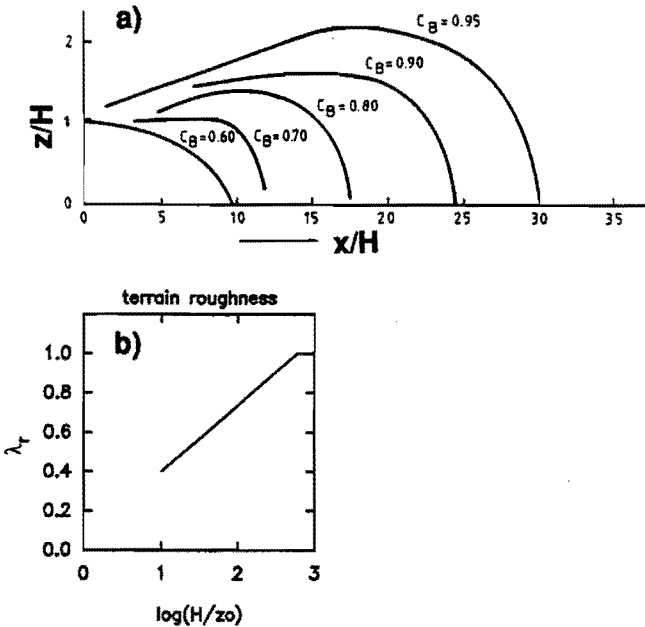
Figure 4.28: Wind speed reduction factor $C_B = U(z)/U_o(z)$ in the far wake of a porous obstacle (after Leene et al, 1990).
a)   Basic graph for normal flow (0°), $W/H = 8$, $H/z_o > 700$ and $C_B > 0.7$.
b)   Correction factor for wake length; effect of terrain roughness

Experiments in complex urban surroundings, yield roughly 35% further wake length reduction. The largest wake length reductions (up to 60%) are found in the wakes of buildings (Gandemer, 1981). It is not clear which reduction is to be expected in regions of strongly accelerated flow.

Screen details on the windward side have little influence on wake dimensions, provided that screen width and height are not changed. Downstream extensions like a ramp shape may reduce wake length somewhat (Gandemer, 1981). Wake length is also reduced if porosity increases with height. On the other hand, porous obstacle ends may increase wake length by 25%, probably because of a decrease in wake suctions.
Wind speeds in the near wake can be reduced by using small circular holes (say 10-100 mm) instead of slats (Pereira, 1980; Gandemer, 1981).

The effects of trees

Trees are often recommended as wind shelter, both in agricultural applications and in building applications. Still, there are very few published data about wind reduction due to trees in urban environment.

Single trees may cause local wind speed increase (Gross, 1987) because of pressure short circuiting and corner stream effects. Short circuiting effects under the tree can be reduced by making stem height small (say 3 m).
The choice of tree shape depends on the flow region to be sheltered: cone shaped crowns increase shelter under the tree; ellipsoid crowns increase shelter behind the tree.

Groups of trees (small 'canopies') can be effective shelter devices. Beranek's semi quantitative sand erosion data (1982) suggest that if groups of trees are placed against corners in the same way as the 'podium elements' of fig. 4.25, wind speed in the remainder of the corner streams is decreased by 10-20%. These wind reductions can even be obtained if tree rows are placed along or across a passage between shifted buildings (geometry in fig. 4.18). Large numbers of scattered trees in the passage yield similar wind reductions.

In streets, trees are often the only wind reducing devices which do not hamper traffic. Again, data are very scarce.

Visser (1987) made an indirect estimate of sheltering effects of tree rows. He compared estimates based on (Alberts, 1981) with wind tunnel data for simplified urban districts. Visser's wind tunnel model (with smooth turntable: $z_{0,loc} \approx 0.0005$ m) included streets with tree rows, which were not considered in Alberts' (1981) report.
In Visser's 3rd configuration (uniform building height), estimated wind reduction due to trees was:
        - 25±5% for wind along (parallel to) streets
        - 20±20% for wind across streets

The latter figure is highly dependent on location and building arrangement. Street characteristics (see also fig. 4.29) were not reported, but they were estimated to be: 8H for street width, 'infinite' for street length, 3H for the width of a centre street 'path' without trees.

Some very limited -unpublished- Laser Doppler data for a cube arrangement (fig. 4.29b) with smooth turntable ($z_{o,loc} \approx 0.0005$ m) yield 75% wind speed reduction for flow along a street, together with almost unchanged turbulence levels ($T_u \approx 200\%$). Street width was 2H, street length 'infinite', and the width of the 'path' without trees was about 0.36*H.

The above data make clear that data on wind reduction due to tree rows can not be generalized without knowing the dependence on parameters such as the width of the free path between tree rows and the street width. Moreover, the above estimates themselves are inaccurate because of the indirect method in the first example, and because of the very small amount of data in the second example.
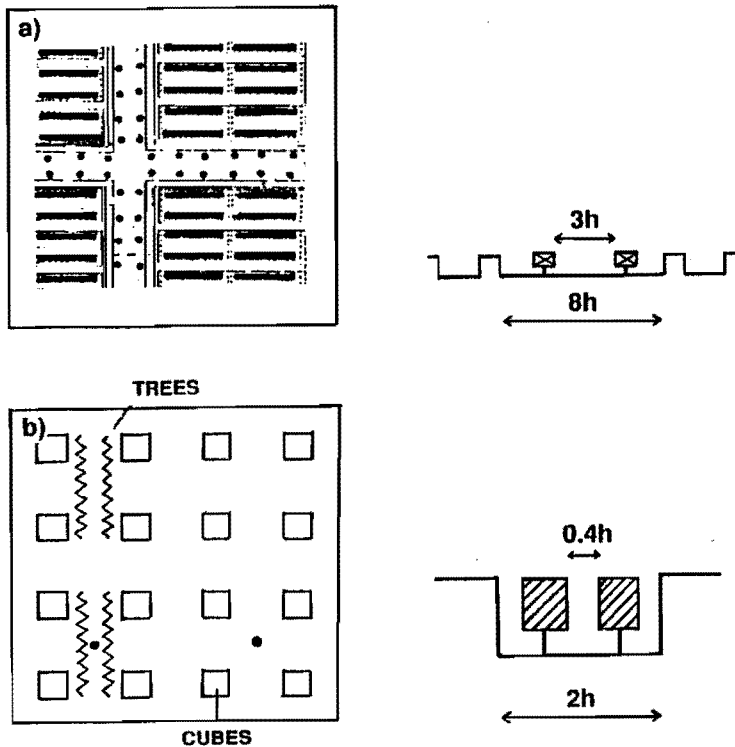
Figure 4.29: Geometries used to estimate the effects of trees in streets.
a)   Part of Visser's (1987) wind tunnel model
b)   Geometry for present Laser Doppler measurements

4.5 Summary; towards forecasting of wind amplification factor

Wind amplification factor γ is determined by processes on several spatial scales.

Figure 4.30 shows that we may calculate γ from a terrain related contribution U_{Ho}/U_{pot} and a building related contribution U/U_{Ho}. It is not always clear which should come first. The building contribution to γ may come first as building height determines which U_{Ho} should be taken. On the other hand, upstream terrain (roughness) influences flow patterns around buildings, and then U_{Ho}/U_{pot} should be taken first.
In the next chapters, we will work downwards in figure 4.30. In chapter 6, for example, we will first consider the terrain related contribution to γ. Then it will be judged which shelter the buildings and the site details should offer. Finally, a building geometry (shape, dimensions, arrangement) can be selected which satisfies the shelter requirements.
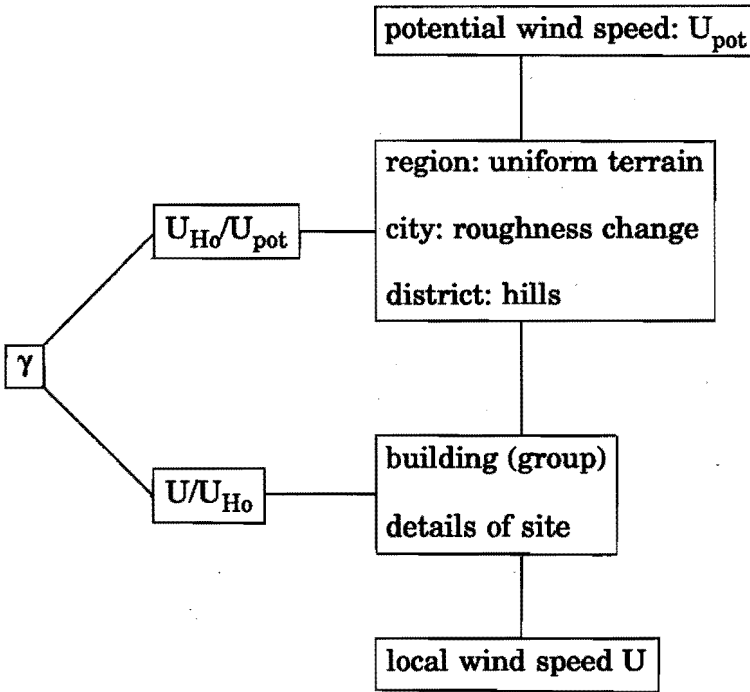
Figure 4.30: Scheme for estimating wind amplification factor by accounting for contributions on different scale levels.

4.5.1 Region, city, district

Large scale processes determine the reference speed of a building (group). Their contribution can be almost as important as the influence of the building itself. For high rise buildings, the reference speed (U_{Ho}) is taken at roof height. For low rise buildings, the reference speed ($U_{2.5h}$) is taken at 2.5 building heights.

Wind amplification factor over *uniform terrain* (at least 10-20 km fetch) can be estimated by figure 4.1. Errors in the γ estimate of figure 4.1 are caused by:
1. uncertainties in z_0 estimate: up to +/- 15% error (positive and negative)
2. errors in estimate of eq. 4.3: about 5% error over cities
3. neglect of horizontal temperature gradients: about 5% error over cities
4. neglect of surface heat flux: up to 10-20% error over cities

The latter three effects result in underestimation of γ over cities. However, the effect of horizontal temperature gradients (3) and surface heat flux (4) may be (partly) compensated because of similar errors in the computation of maximum discomfort probability (see p. 70-71).

For *non uniform terrain*, internal boundary layer (IBL) models can be used. Models are available for two dimensional roughness changes (fig. 4.2) and for lateral roughness changes (fig. 4.3). Approximate models are available for oblique flow, roughness islands, and multiple roughness changes.
It is important to note that IBL models are only valid for fetches of 0.3 - 2.5 km. For smaller fetches, the influence of individual buildings becomes important. For fetches of 2.5 - 20 km, there remains a large difference (10-25%) between IBL estimates and estimates for uniform terrain.

Errors in estimates of γ over non uniform terrain are caused by:
5. uncertainties in IBL models and z_0 estimate: up to +/- 10-15% error (positive and negative)
6. extrapolation of IBL theory to fetches of 2.5-20 km is inconsistent with theories for uniform terrain: up to +/- 25% error
7. neglect of surface heat flux: up to about 10-15% error within the IBL
Note that the effects of surface heat flux should only be accounted for once: either for uniform (4) or non uniform terrain (4 or 7).

On *smaller scales* (sometimes up to 1 km), effects of hills may be dominant. Even gentle sloping hills may cause considerable wind speed increase. Section 4.2.3 gives estimates of wind speed increase at hill tops.
Other small scale effects, such as the relation between roughness parameters and building lay out, are briefly discussed at the end of section 4.2.3.

Estimates of the terrain related contribution to γ suffer from several errors, and the total error in γ may exceed 20%. These errors will also affect routine wind tunnel predictions of wind comfort as well, unless the terrain contribution to γ is measured explicitly.

The accuracy can be improved considerably if methods are found which can estimate γ at larger distances (2.5 - 20 km) from roughness changes, and if thermal effects can be accounted for.

4.5.2 Buildings and site

Wind amplification factor γ depends on a great number of parameters, even if only the scale level of the building (group) is considered. Therefore, most methods to predict wind climate in advance (before wind tunnel experiments are carried out) are highly simplified. In the following, an overview is given of existing methods for estimation of the building contribution to γ, together with possible improvements.

Prediction of γ; existing methods

Most of the existing methods concentrate on prediction of (the building contribution to) γ in corner streams around high rise buildings.

The earliest estimates are from Lawson et al (1975). He assumes that for the wind speed maximum near building corners $U_{max} \approx U_{Ho}$ for all wind directions. The present numerical data show that in the worst case, wind speeds are increased for 50-75% of all wind directions.

Several other methods (Maruta, 1984; Beranek, 1984; Stathopoulos et al, 1991), use $U_o(z)$ (U_o or $U_o(z)$ is wind speed of undisturbed flow at height z) as a reference speed, not U_{Ho}. For example, Maruta (1984) provides a rather complex mapping method of U/U_o around mainly slender buildings (W/H < 2). Beranek gives estimates of the area with strongly increased wind speeds (U/U_o > 1.6), based on semi-quantitative sand erosion data. Stathopoulos et al (1991) have developed an expert model, based on literature and on experimental data. These methods can only be used if the building is surrounded by sufficient fetch of open terrain (say a few building dimensions). The methods can not be used in complex urban geometry where U_o can not be defined at all.

Leene (1991) found that, in routine wind tunnel investigations, maximum U/U_{Ho} (of all wind directions) near building corners is 0.99±0.10. For other wind directions, Leene assumes a $\cos^2$-dependence, which for $\cos^2(\theta) > 0.5$ corresponds reasonably well with his experimental data.

$$U(\theta) = U(\theta_{max}) * \cos^2(\theta - \theta_{max}) \qquad (4.11)$$

θ_{max} is the angle with the largest U/U_{Ho} (assumed for wind perpendicular to longer building face). Eq. 4.11 underestimates γ in sheltered areas (where $\theta - \theta_{max} \approx \pm 90°$). This yields minor errors in discomfort probability, provided that discomfort thresholds without turbulence are used (k = 0 in eq. 3.7). It is expected that the difference between measured and real maxima is small because of (too) small local ground surface roughness: $z_{0,loc} \approx 0.0005$ m.
Estimates of turbulence levels are not given, as in the other methods.

120

Wind speeds (γ) for other flow zones are modelled by Maruta (1984) and by Leene et al (1990). The latter model (section 4.3.2) can be used to estimate wind speed reduction in the far wake of obstacles. This wake model can also be used to estimate the total influence area of a building.

Improvements in prediction of γ

The above given methods are often limited in their application. Moreover, their predictions are not always correct. In the following, it will be discussed where the above methods need to be modified or extended.

First, corner stream properties will be discussed. Next, estimation of γ is considered for other flow zones, and for building groups, and details of the site. Finally a method for estimation of turbulence levels is proposed.

For corner streams, one should know maximum wind speeds, location of maxima, and corner stream dimensions.

Maruta (1984) assumed that corner stream maxima were in the very near proximity of building corners with flow separation. For simple rectangular buildings, this is confirmed by the present numerical data. Figure 4.10 shows locations of wind speed maxima for different wind directions.

Lawson et al (1975) and Leene (1991) found that U_{Ho} is a fair approximation for maximum corner stream wind speeds. This estimate can be improved by accounting for relative building width (W/H) and for the approach flow angle θ (figure 4.12).
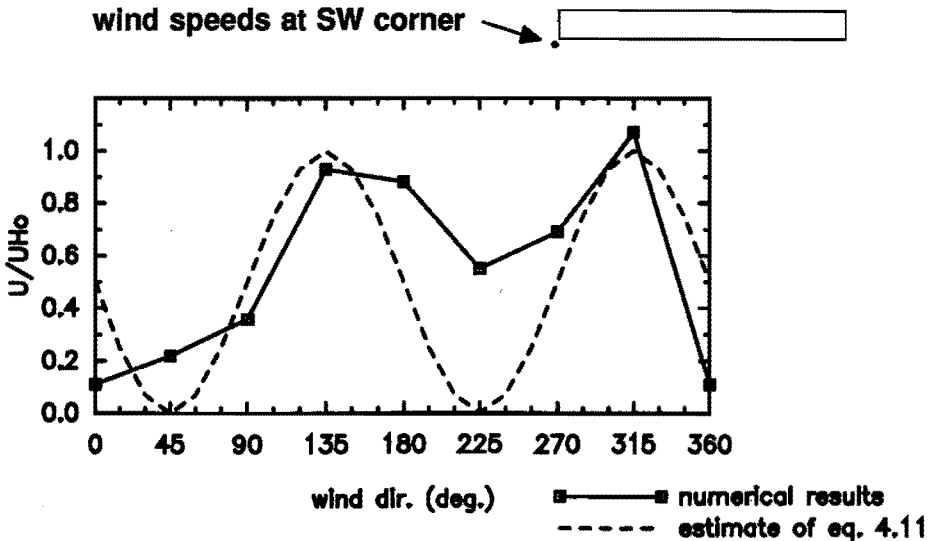

Figure 4.31: Wind conditions at SW corner of E-W oriented building (L,W,H = 15x150x50 m; $z_o = z_{o,loc}$ = 0.03 m): U/U_{Ho} as a function of θ. Solid line: present numerical data. Dashed line: estimate of eq. 4.11.

For a SW corner of a E-W oriented building (fig. 4.31), corner stream wind speeds apply for wind directions SE, S, W, NW. The highest corner stream wind speeds are associated with *oblique* flow (fig. 4.12).

Leene's (1991) $\cos^2$-function does not fit the numerical results very well, even though the location of the maxima is 'tuned'. In fact, only peaks in U/U_{Ho} are predicted well, not intermediate and low values. For wind directions SE, S, W and NW, better estimates can be obtained from fig. 4.12.

Corner stream dimensions are not given by Leene (1991). Existing prediction methods are either inaccurate (Beranek, 1980) or too complicated (Maruta, 1984). Figure 4.11 gives the radius R of the corner stream circle, within which $U/U_{o,loc} > 1.2$ ($U_{o,loc}$ is similar to U_o, but measured at building location in absence of building) for at least one wind direction. For complex urban geometry one should use $U/U_{Ho} > 0.66$ instead of $U/U_{o,loc} = 1.2$. U_{Ho} should be taken from a location $5L_g$ upstream, where L_g (eq. 4.8) roughly equals W or 2H.

Wind speeds within the corner stream circle can only be estimated with rather complicated methods, such as Maruta's empirical method (Maruta, 1984).

The influence of parameters such as L, approach flow z_0 and local surface roughness ($z_{0,loc}$) yields less than 5-10% and 25% variation in U_{max}/U_{Ho} and in corner stream radius R respectively, except in complex urban geometry if $L_g/h < 1.5$. *Building details* such as podia, gaps, and corner shape modifications may need separate treatment (see section 4.4.1).
Uncertainties in U/U_{Ho} due to numerical errors can be 10% or slightly more.

Wind speeds in other flow zones are generally much lower. Leene et al (1990) propose a model to estimate wind speed reduction in the far wake of an obstacle ($x/L_g > 5$). For oblique flow, wind speed behind the building may be *increased* if $W/H > 2$ (fig. 4.10b). Leene's model does not account for this effect. An overview of wind speeds and flow zone dimensions is given in figure 4.8.

At the end of section 4.3.2, and overview of *sheltered and windy locations* is given (fig. 4.17), integrating the effect of all wind directions and all flow zones. The windiest (and least sheltered) locations are near the building corners. Most shelter is found close to the (centre of the) longer building face.

In *high rise building groups*, the number of (geometrical) parameters becomes too large for a 'simple' description of flow field. In many cases, the closest building (or the building which causes the highest wind speeds) determines local wind speeds ('dominance'). As for isolated buildings, oblique flow yields the highest wind speeds. Equation 4.11 is not generally valid.
Wind speed 'within' the group can be estimated with tables 4.4 and 4.5, and with figure 4.19. Generally, wind climate improves with increasing enclosure (best case: '�口'; worst case: '+'; 'Y'). Pressure short circuiting effects are disadvantageous, an arrangement with two shifted buildings ('ᵢ|ᵢ; fig 4.19c) may create a hostile wind climate.

122

Flow properties 'outside' the group are sometimes hard to estimate. Corner stream properties for configurations of two buildings are still within accuracy limits for U_{max}/U_{Ho} and R, but deviations are possible for larger (more complex) obstacle groups.

For *low rise building groups*, the main parameters are relative street length (S_x/h), building arrangement (parallel/perpendicular to street) and relative street width (S_y/h). Short streets ($S_x/h < 4$) yield sheltered conditions. In long streets, shelter can be provided by buildings perpendicular to street if $S_y/h < 2$ (figure 4.21).

Site details (section 4.4.2) such as *screens and trees* can accomplish considerable wind reduction. Optimum screen porosity is about 20%. Wind speed reduction can be estimated with fig. 4.28 (see also Leene et al, 1990). However, wake length is often reduced (say 30%) in complex urban surroundings.
The effects of trees depend much on tree and building configuration. Tree 'canopies' against building corners may result in 10-20% wind reduction. In low rise building groups, the effects are strongly dependent on the width of the free path between tree rows, and on relative street width (S_y/H).

Turbulence levels ($K^{0.5}$) around high rise buildings can generally be estimated (standard relative error within 20%) by putting $K = K_{o,loc}$, where $K_{o,loc}$ is measured at the building location in absence of building. Corresponding turbulence intensity T_u is given in figure 4.15. Exceptions are buildings with gaps (see table 4.7 for typical gap values) and buildings in complex urban geometries. In low rise building groups and in complex urban geometry, we may put $K \approx K_{pot}$. The standard relative error in the estimate is about 30%. K_{pot} is the K value over uniform terrain with $z_0 = 0.03$ m.
Turbulence estimates for each separate flow zone are given at the end of section 4.3.2 (p. 91-94), and throughout section 4.3.3, 4.3.4 and 4.3.5. The highest turbulence levels are found in the frontal vortex, in corner streams, and, if present, in gaps (up to 100% increase). The lowest levels are generally found in the downstream recirculation zone (up to 50% decrease).

4.5.3 Future research

There is certainly a need for future research. By now, the errors in estimates of γ which may well exceed 20% (twice the desired error level).
At the larger scales (p. 119), this is caused by errors in the z_0 estimate, by errors and limits in application of internal boundary layer (IBL) models, and by thermal effects.
At the scale of the building, numerical errors (mainly in obstacle wakes: up to 10-20%; see section 2.3 for extensive discussion) are the main error source. These errors will be certainly larger if building geometry (or group arrangement) is more complex than the examples given in the present chapter.
At the scale of building and site details, there remain large uncertainties, both because of numerical errors, and because of the great number of parameters which could not all be accounted for.

Accurate estimates of γ on the *larger scales* are needed for both wind climate prediction for early design stages and for routine wind tunnel investigations.

The accuracy can be improved considerably if the effects of roughness changes in the fetch range between 2 and 20 km become known. Accuracy can be further improved if thermal stability effects can be accounted for. Both cases are difficult to treat theoretically. Numerical simulations and experiments may be the basis for empirical models.

An important problem on the *scale of the building* is the large number of parameters. Many issues have not been considered yet.

One of these issues is at which upstream distance the reference speed U_{Ho} should be taken. This distance is assumed to be $5L_g$ but this could not be verified experimentally.

Another issue is estimation of γ for non rectangular buildings. General guidelines of how to treat buildings of complex geometry are not known. Generally, the building envelope is taken, or the building is divided into 'independent' segments.

For tower buildings in urban surroundings, it should be further investigated for which L_g/h and W/H high rise building influence is still perceivable, and when (and which) 'special urban methods' are needed to estimate γ.

For building groups, several geometries remain to be investigated, such as 'Y' and '_' shaped building arrangements, and groups with buildings of different size.

Little is known about γ in streets and squares. Influence of street width, building arrangement, and especially of oblique flow are not clear. Measurements of turbulence in streets are virtually absent.

When *details of building and site* are considered, the number of parameters increases even further

In the case of building details, the effects of corner shape could not predicted well because of discrepancies between different data sets. Further investigations are desirable here.

In the case of site details, sheltering properties will be modified in the presence of strong pressure gradients. This issue deserves further consideration, as well as sheltering performance in other flow regions of nearby high rise buildings.

5   Wind climate forecasts

In the previous chapter, wind amplification factor γ has been quantified, the ratio between local wind speed (U) and potential wind speed at a meteorological site (U_{pot}). Figure 4.30 shows contributions to γ of different scale levels such as region, city, district, building, detail.

Knowledge of γ alone is not sufficient to judge wind climate. Wind climate should be judged by comparing discomfort (or danger) probability with comfort (or safety) criteria. Discomfort probability can only be determined if contributions of all scale levels to γ are 'integrated'.

The effects of building and terrain can be summarized by means of a combined building and terrain classification. A first classification will be discussed in section 5.1. In the next sections, the relation between urban geometry and wind climate will be considered in more detail. Wind climate patterns around (groups of) high rise buildings will be considered (section 5.2), as well as wind climate of streets and squares (section 5.3) and wind climate near high rise buildings in urban surroundings (section 5.4). The data will be summarized in section 5.5, which gives an improved building and terrain classification. This classification, and the other data of this chapter, are the basis of design rules which are presented in chapter 7.

5.1   Introduction

This section discusses the relation between wind amplification factor γ and wind climate. A first classification of building and terrain will be given as well.

Discomfort probability

We speak of discomfort (see section 3.2) when during an hour, a threshold wind speed of 6 m/s is exceeded for about 16% of time. In formula:

$$U + \sigma_u > 6 \text{ m/s} \tag{5.1}$$

Wind conditions are dangerous (see section 3.2) if, during an hour, a gust of a few seconds duration exceeds 20 m/s. In formula:

$$U + 3\sigma_u > 20 \text{ m/s} \tag{5.2}$$

Discomfort and danger probability (in the following often abbreviated as 'discomfort' and 'danger') are defined as the percentage of hours (during a year) in which the thresholds are exceeded.

Figure 5.1 shows the relation between wind amplification factor γ (or U/U_{pot}) and discomfort and danger for locations near Amsterdam. Figure 3.5 and 3.6 give graphs for other climates.

Discomfort probability (fig. 5.1a) is small for $\gamma < 0.3$ but increases progressively to about 22% for $\gamma = 0.7$ (typical for grass plain; 1.75 m height). For larger γ, the curve levels off. Southwesterly wind directions yield an important contribution to discomfort, but the influence of other wind directions can not be neglected.

Danger probability is small (a few hours per year or less) for $\gamma < 0.7$, but increases progressively for larger γ. Southwesterly winds yield the main contribution.

discomfort

$$U(1 + Tu) > 6 \text{ m/s}$$

a)

— all wind dir.
----- only 165o − 285o

P (%)

U/Upot (−)

danger

$$U(1 + 3Tu) > 20 \text{ m/s}$$

b)

— all wind dir.
----- only 165o − 285o

P (%)
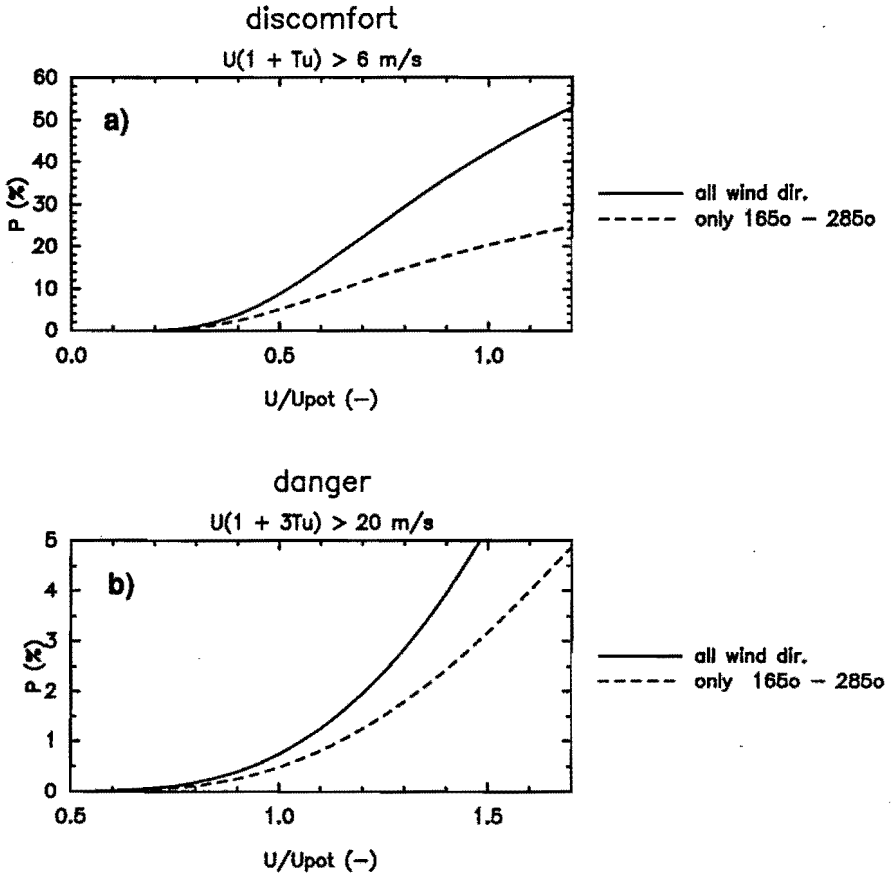
U/Upot (−)

Figure 5.1: *Discomfort and danger probability as a function of direction independent wind amplification factor γ (U/U_{pot}). Solid line: total probability. Dashed line: contribution of southwesterly wind directions (θ between 165° and 285°). Climate statistics: Amsterdam airport (Troen et al, 1989). Standard deviation σ_u is equal to airport value.*

a) *Discomfort probability: percentage of time that $U + \sigma_u > 6$ m/s.*

b) *Danger probability: percentage of time that $U + 3\sigma_u > 20$ m/s.*

Often, it is practical to discuss wind climate in terms of required shelter, or maximum γ. In practice, γ is not the same for each wind direction. Therefore, we define an *'effective γ'* (γ_e): a direction independent γ which yields the same discomfort or danger as in reality. For given discomfort probability P, we may estimate the corresponding γ_e with the solid line of fig. 5.1a. For example, a P of 22% yields a γ_e of about 0.7.

It should be noted that γ_e for discomfort is generally not equal to γ_e for danger. The latter is often close the actual maximum γ, because of the progressive increase of danger with γ (fig. 5.1b).

Table 5.1 shows maximum discomfort, and the maximum γ_e (or minimum shelter) for a number of human activities. Maximum danger probability should be a few hours per year or less. This is the case if γ is less than 0.7. These figures should not be taken too strictly as both thresholds and allowed discomfort probability are rather uncertain (see chapter 3).

	P_{max}	γ_e
sitting/standing long:	2%	0.35
sitting/ standing short:	10%	0.51
strolling:	15%	0.59
safety:		0.70*

Table 5.1:   *Maximum allowed discomfort probabilities and γ_e for different human activities as given by Gandemer (1978) (see also table 3.8). The relation between P_{max} and γ_e can be read from fig. 5.1a (solid line), except for safety where fig 5.1b should be used.*

Classification of building and terrain

Both building and terrain have strong influence on γ and therefore on discomfort. One of the simplest classifications can be made by considering two building types (low rise buildings and high rise buildings) and three typical terrain types (large water surface, grass plain, very large city).

Figure 5.2 shows which range in γ can be expected for each of the classes. The acceptability of wind climate is indicated as well. Discomfort and danger probability can be estimated by using fig. 5.1.

High rise buildings often yield too large wind amplification factor ($\gamma > 0.7$), especially if building height is greater than 50 m. Building height may be larger in the case of mutual sheltering (large Manhattan). In low rise building groups, γ may be too large as well. The influence of terrain is significant, both for low rise buildings and for high rise buildings.

building/terrain classification
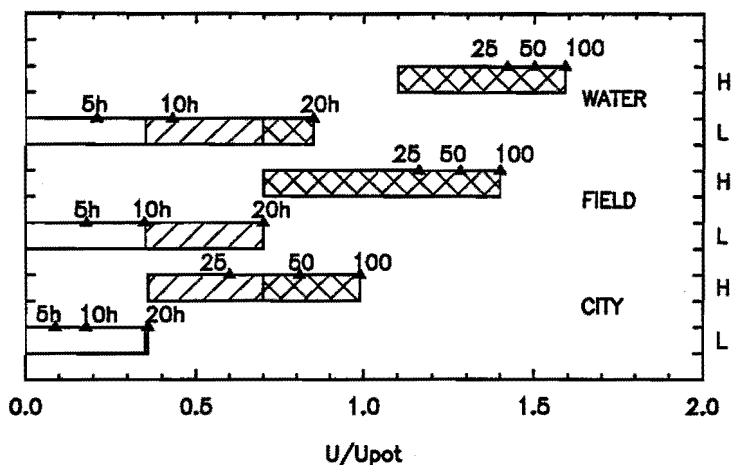
Figure 5.2: *Classification of building and terrain in terms of typical wind amplification factor* γ *(U/U$_{pot}$). Terrain type and building type are indicated in graph. Building height is indicated for high rise buildings, street length (in multiples of building height h for low rise buildings. Hatched area: probably uncomfortable for some human activities. Cross hatched area: probably uncomfortable for all activities.*

The next sections will discuss improvements in the estimates of figure 5.1 and 5.2. It will be shown that fig. 5.2 is slightly too conservative for estimates of danger and much too conservative for estimates of discomfort.

Assumptions

The following assumptions are made for the classification of figure 5.2:

1. Uniform terrain (fetch at least 10 - 20 km) has been assumed for all terrain classes. Aerodynamic roughness length z_0 is 0.0002 m, 0.03 m and 1.0 m (water, grass, city). For the city, a zero displacement height z_d of 10 m has been assumed.
2. For high rise buildings, γ is computed with eq. 4.2 and eq. 4.3, assuming that the approach flow wind speed at roof height (U_{Ho}) is 'brought down' to pedestrian level (all wind directions).
3. For low rise building groups, wind speed above the buildings ($U_{2.5h}$) is computed with eq. 4.2 and 4.3 as well. Pedestrian level wind speeds are estimated from FLUENT data in fig. 4.21. This approach is valid if the considered location is at least at a distance of about 250 m from the upwind group edge.

128

In the next sections, discomfort probability will be determined from numerical results (γ) of section 4.3 and 4.4. In these numerical results, approach flow z_0 has 0.03 (grass plain) to 1.0 m (city). The local surface roughness ($z_{0,loc}$) within 600 m of the considered building has been fixed at 0.03 m.

Numerical data have been linked to an ideal meteorological site ('infinite' grass plain with z_0 = 0.03 m; measuring height 10 m) with the methods of section 4.2.1. Wind direction intervals of 45° are taken as smaller intervals (15°) yield hardly any change in discomfort probability. Climate statistics (Amsterdam Airport) are fully exposure corrected (Troen et al, 1989). Building orientation is such that the long building axis is perpendicular to the southwest (θ = 225°).

Accuracy

Possible error sources are the criteria, the climatic data, and the estimation of wind amplification factor γ. Generally, only errors in γ_e are presented. Errors in discomfort and danger probability can be estimated by using figure 5.1.

Chapter 3 discussed the uncertainty in thresholds and criteria. The allowed effective γ (i.e. γ_e) for discomfort may vary by about ±10% (table 3.9).
The present judgements of wind climate are valid for locations near Amsterdam. For some other locations in Northwestern Europe, we may replace figure 5.1 by figure 3.5 or 3.6. Elsewhere, figure 3.7 allows for an estimate of the difference in maximum γ_e (see table 5.1) between the considered location and Amsterdam.
Errors in γ are due to numerical errors, and to errors in methods used to link numerical results to wind speed at a meteorological site.

Neglect of thermal effects on γ is an important error source. Neglect of surface heat flux effects results in up to 10% underestimation of γ over cities if U_{pot} < 11 m/s (table 4.2), and up to 20% if U_{pot} < 6 m/s. The corresponding discomfort or danger probabilities are greater than 3% and 32% respectively. Neglect of horizontal temperature gradients may result in another 5% underestimation of γ over cities. The effect of these errors is (partly) compensated because similar errors have been made in the estimation of P_{max} (p. 61 and 70). Thermal effects may also influence wind flow around buildings (see eq. 2.29) if

$$H > 0.3(\frac{z_0}{0.03})^{0.3} U_{pot}^{2.5} \tag{5.3}$$

H being the building height. Estimates of danger probability are not affected, except over open water. Estimates of discomfort near high rise buildings may be affected if H > 17-50 m (for open terrain and large city respectively).

By now, it is not possible to correct for any of these thermal effects. Luckily, the concept of a γ 'without thermal effects' has also been used in the estimation of P_{max} (p. 61). Therefore, we may expect that errors due to neglect of thermal effects are compensated (partly).

Further errors in γ are caused by errors in the U^* estimate, by errors in the z_0 estimate, and by numerical errors. The U^* estimate of eq. 4.3 results in about 5% underestimation of γ over cities. For small z/z_0, errors in the z_0 estimate may result in relative errors in γ of up to 15% (both positive and negative). Numerical errors are discussed in section 2.3. Generally, numerical errors are less than +/- 10-20% (largest errors in obstacle wake).

It should be noted that the estimates of this chapter are based on uniform terrain up to the edge of the computational domain. In practice, effects for terrain inhomogeneities (section 4.2.2 and 4.2.3) have to be accounted for as well. This results in additional uncertainties as estimation methods for non-uniform terrain are generally not very accurate.

A last important issue is the effect of errors in γ on discomfort or danger probability. Figure 5.1 shows that a 10% error in the effective γ (γ_e) results in about 30% relative error in discomfort probability, and in 50% relative error in danger probability. Hence, it is desirable to reduce errors in γ_e to 10% or less.

The main errors discussed above were:
1. -neglect of thermal effects: up to 15-25% underestimation of γ over cities
2. -errors in z_0 estimate: up to 15% (positive and negative)
3. -numerical errors: up to 10-20% (positive and negative)
and in practice also:
4. -errors in IBL models: up to 10-15% (positive and negative)
Errors due to thermal effects are (partly) compensated, as discussed above. Numerical errors and errors in the z_0 estimate may still be too high for the present wind climate forecasts. Even routine wind tunnel predictions of wind comfort are affected by most of the above errors.

5.2 High rise buildings

Wind climate near high rise buildings may be unacceptable, even in large cities. This section discusses how discomfort depends on building dimensions and on building arrangement. First single buildings are considered. Next, the effects of building arrangement (groups), of building and site details, and of building orientation are discussed. Throughout this section, the influence of surrounding terrain will be considered as well. Preliminary estimates are made for urban approach flow. These urban estimates will be further worked out in section 5.4.

Wind climate near a single high rise building

Two issues are of importance when considering wind climate near high rise buildings.

First, maximum discomfort and danger probability near a high rise building should be known. Some first estimates were given in the previous section. These estimates will be further worked out here.

Second, spatial distribution of discomfort probability should be considered, i.e. areas with increased and decreased discomfort probability. Figure 4.17 showed exposed and sheltered locations near a building. Figure 5.3 shows discomfort probability for the same building. Areas with increased discomfort probability are found near the corners, sheltered areas are found near the longer building face. The influence of southwesterly winds can clearly be seen (compare fig. 4.10a) but other wind directions are important as well.
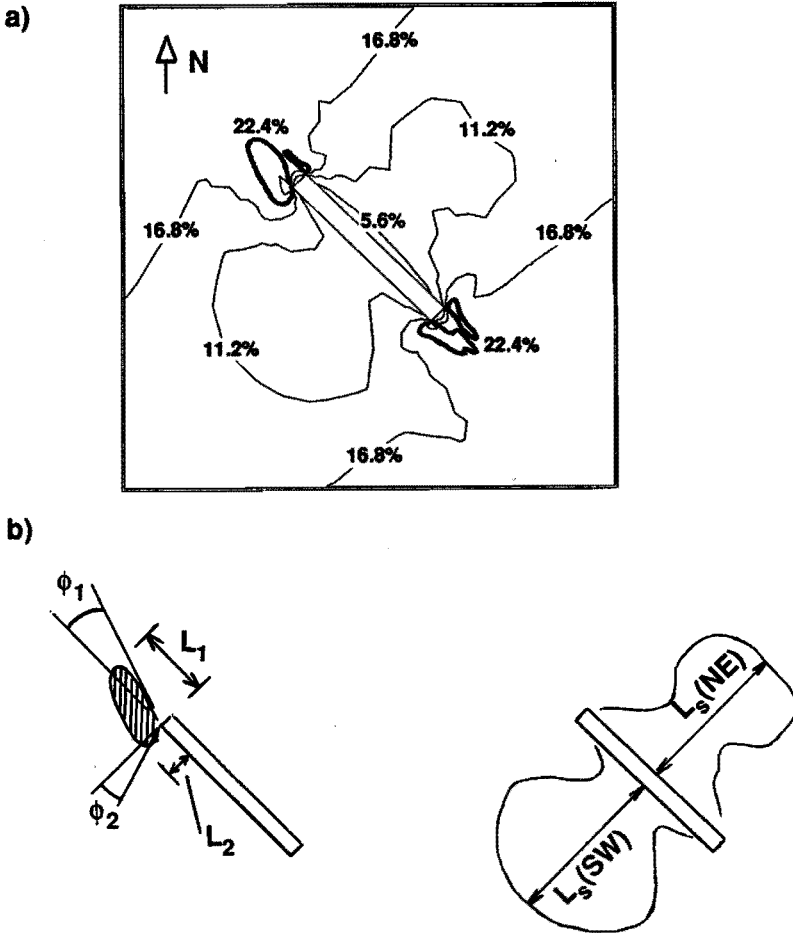

Figure 5.3: Lines of equal discomfort probability (a) around NW-SE oriented building with L, W, H = 15x150x50 m; $z_o = z_{o,loc} = 0.03$ m, together with notation definition (b). Contour intervals: $0.25*P_o$, where P_o (thick line) is discomfort probability without building (22.4%).

In the following, discomfort probability distributions near high rise buildings in the open field (z_0 = 0.03 m) are described. It will be shown that such distributions are highly dependent on building arrangement, orientation, surrounding terrain etc., and that generalization is very difficult.

The extent of sheltered areas, where discomfort probability P is half the approach flow value P_0 or less (P < 0.5*P_0), can be described with a length parameter L_s for each building face (i.e. L_s(NE), L_s(SE), etc.). The length parameters L_s(SE)/L and L_s(NW)/L have typical values of about 0.25±0.10, where L is the length of the shorter building face.

Sheltered areas of the longer building faces are given by:

$$L_s(NE) \approx \min(1.8\,W\,,\,3\,H)$$
$$L_s(SW) \approx \min(1.2\,W\,,\,2.7\,H) \tag{5.4}$$

For wide buildings with W/H > 2, the length of the downstream sheltered area (L_s(NE)) becomes very small (less than 2L; figure 5.3). For slender buildings (W/H < 0.6), both L_s(NE) and L_s(SW) are much smaller. The width of sheltered areas is of the order of the building width (NE,SW) or building length (SE,NW).

Areas with increased discomfort probability can be described with a discomfort circle, analogue to the corner stream circle with increased wind speeds of figure 4.11. Figure 5.4 gives an estimate of discomfort radius R_D for the worst affected (westerly) corner.

discomfort radius RD
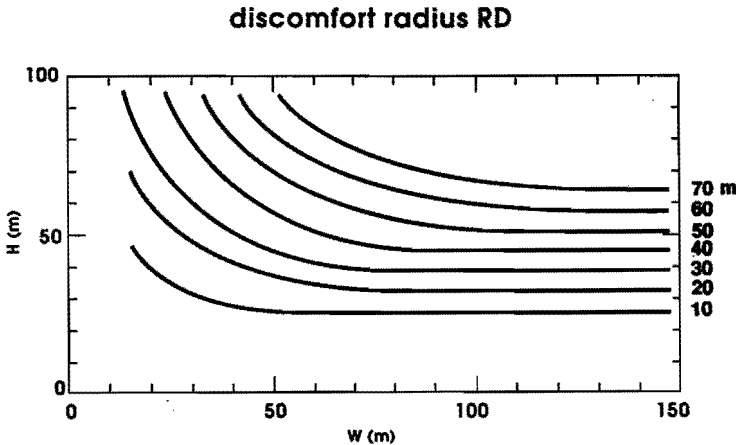
Figure 5.4: Radius R_D of area where discomfort probability is increased for worst affected (westerly) corner. The graph is valid for buildings with L = 15 m which are oriented perpendicular to the southwest, and for $z_0 = z_{o,loc} = $ 0.03 m. For larger L, 'real' R_D can be up to 40% lower if R_D < L.

Discomfort radius for the other corners is given by:

$$R_D(N) / R_D(W) \approx 0.54 - 0.13*L/W$$
$$R_D(E) / R_D(W) \approx 0.82 \pm 0.08 \qquad (5.5)$$
$$R_D(S) / R_D(W) \approx 0.88 - 0.18*L/W$$

The least affected corner is the northerly corner. For other orientations, the north(east)erly corner is generally least affected, while the (north)westerly corner is generally most affected.
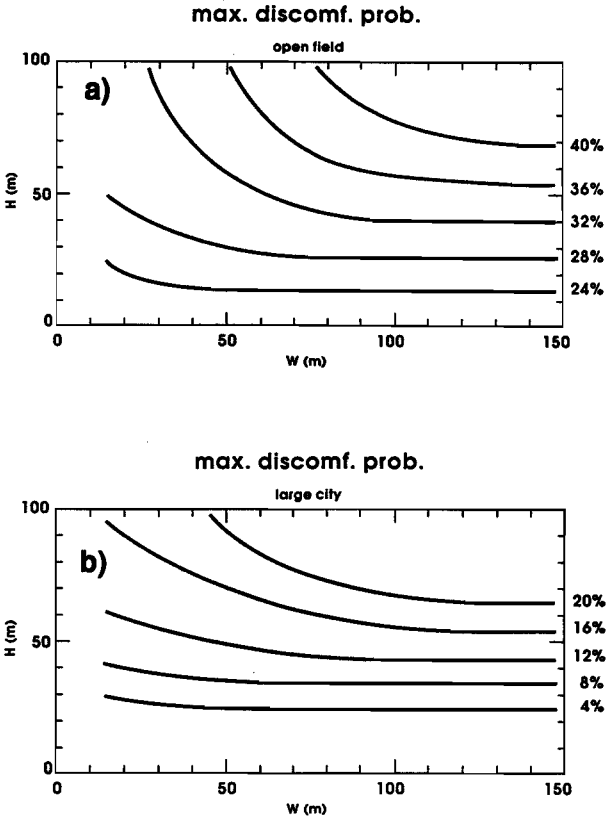
Figure 5.5:   *Maximum discomfort probability near (westerly corner of) high rise buildings for different terrains. Near a town edge, terrain classification is determined by terrain at a distance greater than 12 building heights. Building orientation is perpendicular to southwest.*

a)   *Data for open field based on present numerical simulations; $z_o = z_{o,loc} = 0.03$ m.*

b)   *Urban terrain; estimated data for $z_o = 1$ m; $z_d = 10$ m. Main assumption: U_{Ho} governs the flow at building corners.*

The shape of the discomfort area is approximately a triangle or quarter ellipse (long axis L_1, short axis L_2; fig. 5.3), together with two extensions (angles ϕ_1 and ϕ_2). The angle ϕ_2 (longer building faces) is generally less than 10°. The angle ϕ_1 (shorter building faces) can be 30°-45°, resulting in a typical 'V' pattern (fig. 5.3). This 'V' pattern is likely to develop if $R_D > L$, where R_D can be taken from fig. 5.4. For the present NW-SE orientation, discomfort areas are elongated in NW-SE direction (figure 5.3). The degree of elongation varies between a factor 2 for $L/W \approx 1$ to a factor 4 for small L/W.

Areas with increased danger can be described in a similar way. A typical dimension ('radius') of these areas is the lesser of 1.8*W and 3H.

Figure 5.5 shows maximum discomfort probability P_{max} near high rise buildings. The maximum is generally close to the (north)westerly building corner. Maximum probability is unacceptable near open water ($z_0 = 0.0002$ m; $P_{max} = 34$-42%), and in the open field ($z_0 = 0.03$ m; $P_{max} = 24$-36%). This applies to all building heights. In very large cities (fetch > 10-20 km), P_{max} is acceptable for strolling (table 5.1) if H < 50 m. For 'short stay' activities, building height should be less than 35 m.
Maximum danger probability $P_{max,d}$ can be estimated with fig. 5.1 and fig. 5.2. $P_{max,d}$ is acceptable (i.e. less than in open field) if building height (in a large city) is less than about 40 m. This safety requirement overrules the above comfort requirement.

The 'urban' data of figure 5.5 are estimated by assuming that -close to the building corners- all flow properties scale with the undisturbed roof height wind speed U_{Ho}. Errors in γ_e are expected to be within 10%. This approach is only valid in the near proximity of the corners; corner stream dimensions can not be determined. This will be done in section 5.4. Errors in the present estimates of maximum discomfort will be discussed in section 5.4 as well.

Wind climate for high rise building groups

By now, it is not feasible to develop methods for accurate description of distributions of discomfort probability for groups of buildings. This is because of the too large number of (geometrical) parameters, and because of lack of data.

An alternative approach is to classify building groups and to assign typical values of discomfort probability to corners and passages. Figure 5.6 shows maximum discomfort at the worst affected corners (C), and in passages between buildings (P). The following building arrangements are considered:

	type:	code in fig. 5.6:	definition sketch in:
1.	buildings on a line	P1/C1	fig. 4.18a
2.	buildings behind each other	P2/C2	fig. 4.18b
3.	shifted buildings	P3/C3	fig. 4.18c
4.	groups of four buildings	P4/C4	fig. 4.18d/e

134

All building groups are oriented perpendicular to the SW (i.e NW-SE).

Figure 5.6 shows that corner stream discomfort probability P is generally less for groups than for isolated buildings. In passages, P is larger for shifted buildings and much smaller for buildings behind each other. All data for groups of four buildings (C4, P4) are likely to be too low (30% relative error in P?) because of insufficient grid resolution in the numerical simulations.
In a large city, all data (i.e. P) are about a factor $(127 \pm 10)/H$ smaller (2.5 if H = 50 m). Some additional wind climate data for building groups are discussed below.

Figure 5.6 suggests that maximum discomfort probabilities near building corners are lower than values for corners of isolated buildings (P ~ 31%). This is especially true for shifted buildings (C3). Reduced discomfort for cross (+) and square (□) arrangements may be due to insufficient grid resolution.

The size of discomfort areas near building corners may be reduced by 50-75%, compared to the isolated building case (fig. 5.4). This is partly due to reduced maxima. However, similar reductions are found for buildings behind each other (C2), even though maxima are not affected. Discomfort areas are not reduced in size for aligned buildings (C1).

group classification
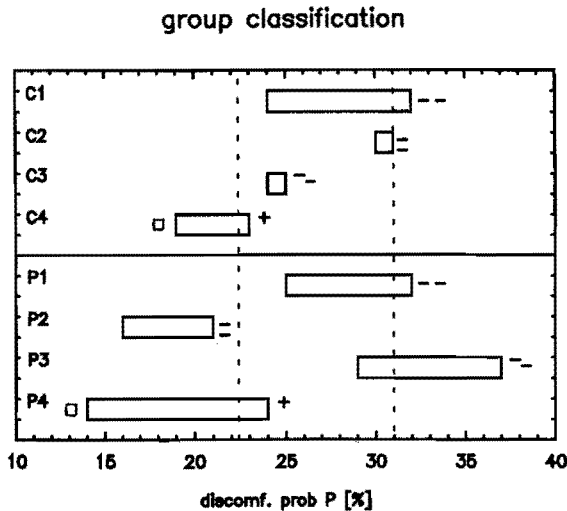
Figure 5.6: *Classification of building groups and discomfort probability. Building arrangements are indicated in graph and in figure 4.18a (P1/C1), 4.18b (P2/C2), 4.18c (P3/C3) and 4.18d/e (P4/C4). P denotes passage; C corner. In all cases $z_0 = z_{0,loc} = 0.03$ m, and building orientation is perpendicular to southwest (i.e. NW-SE). Dashed lines indicate approach flow discomfort probability (22.4%) and P_{max} for isolated buildings (31%).*

135

Variations of discomfort probability in passages are rather large, as is shown in figure 5.6. This indicates significant dependence of P_{max} on geometrical parameters.

For aligned buildings (P1), the main parameter is S_y/H. P_{max} increases from 25% to 31% as S_y/H decreases from 1 to 0.4.
For buildings behind each other (P2), the main parameter is S_x/H. P_{max} decreases as S_x/H increases from 0.4 to 2. This is because interaction effects (wind speed increase) for oblique flow become weaker for increasing S_x/H.
In the case of shifted buildings, both S_x/H and D_y/H (see fig. 4.18c for notation) are important. The worst case (and the strongest pressure short circuiting) is expected if S_x/H and D_y/H are close to 1 (D_y/H within 10-20%).
For groups of four buildings (P4), much depends on the degree of enclosure. The highest probabilities are found for the cross (+) arrangement, the lowest for the square (□) arrangement.

The area of increased discomfort does not extend far out of the passage. The danger 'influence area' is often larger, but its dimensions do not exceed the lesser of one building height and two passage widths, i.e. $\min(2S_y, H)$.

Building shape; details of the site

Building shape may have considerable impact on wind climate. The number of parameters is too large to allow for detailed parametrizations and generalizations. Some typical examples (based on the present numerical simulations) are given below. They may give an impression of possible effects.

Numerical simulations including details of the site are not available and discomfort could not be evaluated. As a rough guideline, it can be stated that:
-scattered trees or trees against building corners may accomplish about 10% reduction in γ_e.
-a properly placed wind screen (see sketch below) may accomplish considerable wind reduction for the two worst wind directions.
-multiple wind screens in □ arrangement yield considerable local wind reduction for all wind directions.
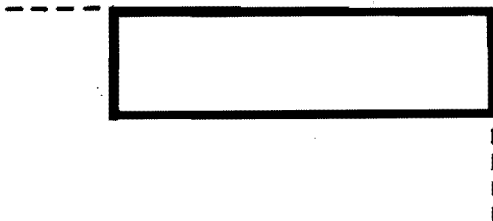

Figure 5.7: *Optimum location and orientation of wind screens near building corners. Note that screens (dashed line) should be attached to the building.*

In the following, effects of building shape will be discussed. The considered building types can be divided in three classes:
-buildings with podium shaped extensions (fig. 4.25)
-building with gaps (fig. 4.23)
-buildings with modified (stepped) corner shape (fig. 4.26)

Buildings with sufficient large podia (podium dimension L_p large than geometrical length scale L_g of eq. 4.8) yield a relatively good wind climate: the podium dominates the flow and discomfort probability is not larger than in the approach flow. Guidelines for the design of podia are given in section 4.4.1 and in chapter 7.
Some improvement in wind climate is also found near buildings with stepped corners. The reduction in γ_e is about 7% for discomfort and about 12% for danger. The radius of the discomfort area is reduced by 20-40% with no clear trend with W/H. The radius of the danger area is reduced by 10-20%.

Gaps yield considerable deterioration of wind climate. The increase in γ_e (both for discomfort and danger) is about 25%. Gaps adjacent to building corners yield significant increase in discomfort (and danger) radius as well: up to 50%. The 'length' of the affected area (perpendicular to longer building face; in SW-NE direction in figure 5.8) can be as large as $7\min(H_{gap}, W_{gap})$ for discomfort and $12\min(H_{gap}, W_{gap})$ for danger. Suggestions for wind mitigation near gaps are given in section 4.4.1 and in chapter 7.
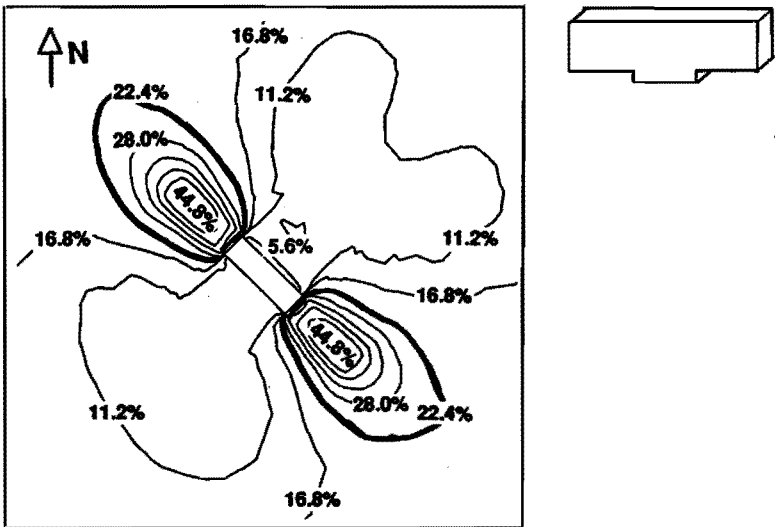

Figure 5.8:   Lines of equal discomfort probability around NW-SE oriented building with L, W, H = 15x150x50 m and two corner gaps with H_{gap} = 10 m, W_{gap} = 50 m, and $z_o = z_{o,loc}$ = 0.03 m. Contour intervals: $0.25*P_o$ where P_o (thick line) is discomfort probability without building (22.4%).

137

Table 5.2 gives discomfort probability for the building geometries discussed above. Podia yield the best wind climate, (corner) gaps the worst wind climate.

	open field	very large city
buildings with gaps	45-54% (35%)	20-25% (14%)
buildings with podium	22%* (28%)	7%* (10%)
modified corner shape	24% (28%)	7%* (10%)

Table 5.2: Estimated maximum discomfort probability for non rectangular buildings, together with data for similar rectangular buildings (in brackets). Building orientation is NW-SE. Building height is 50 m. Percentages with a * indicate maximum in approach flow instead of near building corner. Estimation method for urban terrain is the same as in figure 5.5.

The effects of building orientation

Building orientation parallel to the prevailing wind direction is often recommended as a measure to improve wind climate. Figure 5.9 shows the distribution of discomfort around a SW-NE oriented building. The following differences with the 'wind climate pattern' of fig. 5.3 can be observed:

-sheltered areas at the longer building faces are much weaker and smaller if prevailing wind is parallel to the building
-windy areas at the building corners are decreased in size (mainly length) as well, but maximum discomfort probability changes little.

These features will be discussed in the next.

Maximum discomfort and danger probability are only slightly dependent on orientation. The range of probabilities corresponds generally with less than 5% variation in γ_e. It is worth noting that these differences do not increase for urban flow. Discomfort probability is largest for building orientation perpendicular to the west (for square building plan; L/W ≈ 1) or southwest (other L/W). There is no clear trend for danger probability.

The relation between orientation and discomfort radius R_D (of fig. 5.4) is much more interesting. Discomfort radius is very sensitive to orientation if L/W is small. For the SW-NE oriented building of figure 5.9, R_D is 21 m, only 42% of the value for NW-SE orientation. For other orientations, and for L/W ≈ 1, the change in R_D is 30% or less. The effects of orientation on 'danger radius' are less than 30% (all orientations).

The next issue is discomfort radius for the other building corners. For NW-SE orientation, westerly corners are most windy. Discomfort radius for the other corners can be determined by eq. 5.5.

For N-S orientation, northwesterly corners are generally most windy. For other corners, we can use eq. 5.6:

$$R_D(NE) / R_D(NW) \approx 0$$
$$R_D(SE) / R_D(NW) \approx 0.74 + 0.42*L/W \qquad (5.6)$$
$$R_D(SW) / R_D(NW) \approx 0.50 - 0.25*L/W$$

Note that for L/W $\approx$ 1, the southeasterly corner is most windy. The northeasterly corner is very sheltered.
For other building orientations (SW-NE and W-E) equation 5.5 and 5.6 are a good approximation. Differences are generally less than 0.15.

The shape of the discomfort area is also dependent on orientation. For NW-SE orientation, the area is elongated by a factor 2-4 (figure 5.3), for other orientations only by a factor 1.5 ± 0.4.

Not only the areas of increased discomfort probability are highly dependent on orientation. The extent of sheltered areas is very sensitive to orientation as well. If W/H > 2 and if L/W is small as well, a NW-SE orientation is the only building orientation which creates large sheltered areas (see eq. 5.4). Otherwise, the width of the sheltered area is only of the order of L.

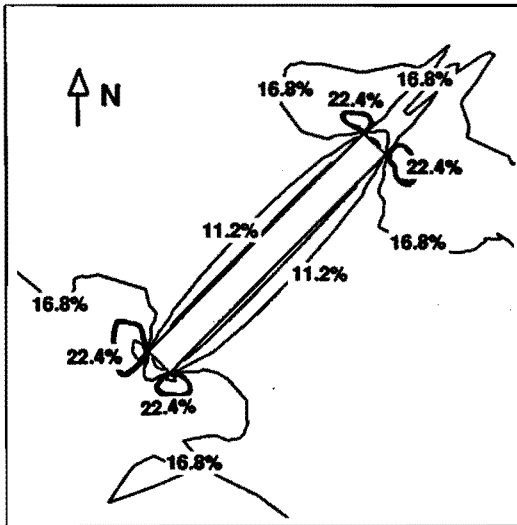Figure 5.9:   Lines of equal discomfort probability around SW-NE oriented building with L, W, H = 15x150x50 m, and $z_o = z_{o,loc} = 0.03$ m. Contour intervals: $0.25*P_o$, where P_o (thick line) is discomfort probability without building (22.4%).

In building groups, orientation has significant effect on discomfort probability in passages. Figure 5.10 shows the worst orientation for shifted buildings, resulting in a maximum discomfort probability of 39% (31% for single building). A '₁¹' arrangement (instead of '¹₁') arrangement results in a P_{max} of 34%, which corresponds with about 10% reduction in γ_e.

For aligned buildings (- -), and buildings behind each other (I I), orientation effects can be still larger (figure 5.6). Note that buildings on a line (P1) with NW-SE orientation are similar to buildings behind each other (P2) with a SW-NE orientation and vice versa. The relative difference in γ_e is about 15%, corresponding with a factor 1.4 in discomfort probability. In all cases, increased discomfort probability is limited to the passage and its near proximity.

In the case of non rectangular buildings, orientation is certainly significant if just one side of a building is equipped with a rounded corner or a podium. Such cases have not been investigated in the present study.

For symmetrical geometries, orientation effects are expected to be the largest for buildings with gaps. Orientation effects for buildings with centre line gaps are expected to be similar to but stronger than the effects for passages of the same size. Orientation effects for buildings with corner gaps are not larger than for buildings without those gaps.
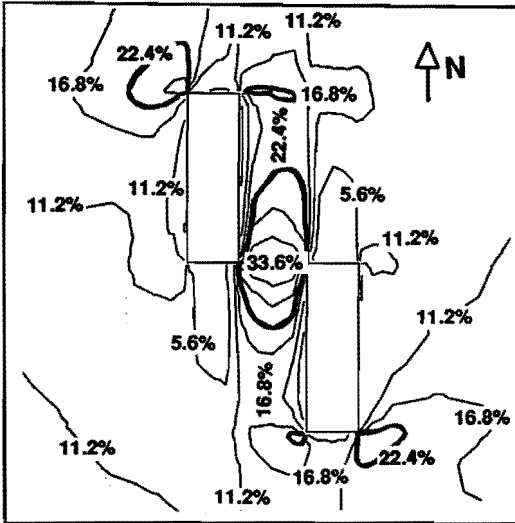

Figure 5.10: Lines of equal discomfort probability around N-S oriented group of shifted buildings with L, W, H = 15x50x50 m, S_x = 20 m, D_y = -50 m, and z_o = $z_{o,loc}$ = 0.03 m. Contour intervals: $0.25*P_o$, where P_o (thick line) is discomfort probability without building (22.4%).

5.3 Streets and squares

Many streets in newly developed parts of Dutch towns are considered as very windy, even without nearby high rise buildings. This section discusses the relation between dimensions and design of streets and squares and discomfort. If discomfort probability is known, the allowed activities can be judged from table 5.1.

Assumptions

Estimation of γ (and of maximum discomfort probability P_{max}) in streets requires a great number of assumptions. The main assumptions are:

1. The present estimates are based on numerical data for two dimensional geometries (fig. 4.21). The influence of street width is not accounted for, i.e. the influence of side walls is neglected.
2. Maximum γ is assumed to apply to the centre point of the street.
3. Reliable numerical data for oblique flow (45°) are not available. Alberts (1981) data suggest that superposition of flow components along and across the street yields a fair estimate of γ (standard error 10%) at centres of long streets ($S_x/h \gg 1$). This approach is not generally valid.
4. Turbulence levels (σ_u) are assumed to be equal to the airport values.
5. Local ground surface roughness ($z_{0,loc}$) is assumed to be 0.03 m (p. 82).
6. Building height is assumed to be uniform.

Assumption 1 leads to conservative (γ_e up to 50% too high) estimates of discomfort probability P because of neglect of side wall 'roughness'. This 'roughness' can only be accounted for in a few special cases (fig. 4.21).
The second assumption is conservative as well. In the worst case, γ_e may be 10% too high.
Assumption 3 may lead to underestimation of P_{max} if superposition is not valid (γ_e up to 30% too low?). There are no sufficient data to judge under which conditions superposition holds.
The influence of assumptions 4, 5 and 6 is not clear and depends on surrounding terrain, street design, and the distribution of building heights.
Finally, numerical simulations are assumed to be free of large errors.

In the remainder of this section, estimates of maximum discomfort probability (P_{max}) in streets and squares are given. These estimates are still highly inaccurate (see above discussion) due to lack of data.

Application

Figure 5.11 shows maximum discomfort probability as a function of relative street length S_x/h and relative street width S_y/h. The street has a SW-NE orientation, and is close to the town edge. It is important to note that there are no direct connections with the surrounding terrain, i.e. the street is completely within the built-up area (see sketch fig. 5.11).

Discomfort probability is very small if S_x/h and $S_y/h < 10$. For larger street dimensions, discomfort probability increases rapidly, until its maximum level is reached for $S_x/h > 20$ (or S_y/h). The allowed activities (long stay, short stay etc.) in the street are indicated by A, B, C, D.

Discomfort probability in streets with NW-SE orientation can be estimated by interchanging S_x and S_y. At crossings, maximum discomfort probability can be estimated if street width S_y is substituted by the length of the crossing street (with NW-SE orientation). For squares ($S_x \approx S_y$), substituting S_x and S_y by $(S_x{}^2 + S_y{}^2)^{0.5}$ yields an estimate which may be expected to be conservative.

Danger probability is generally less than in the open field ($z_0 = 0.03$ m), so that streets are at least suitable as 'walking fast' area. The only exception is the case of extremely smooth surroundings (e.g. open water).
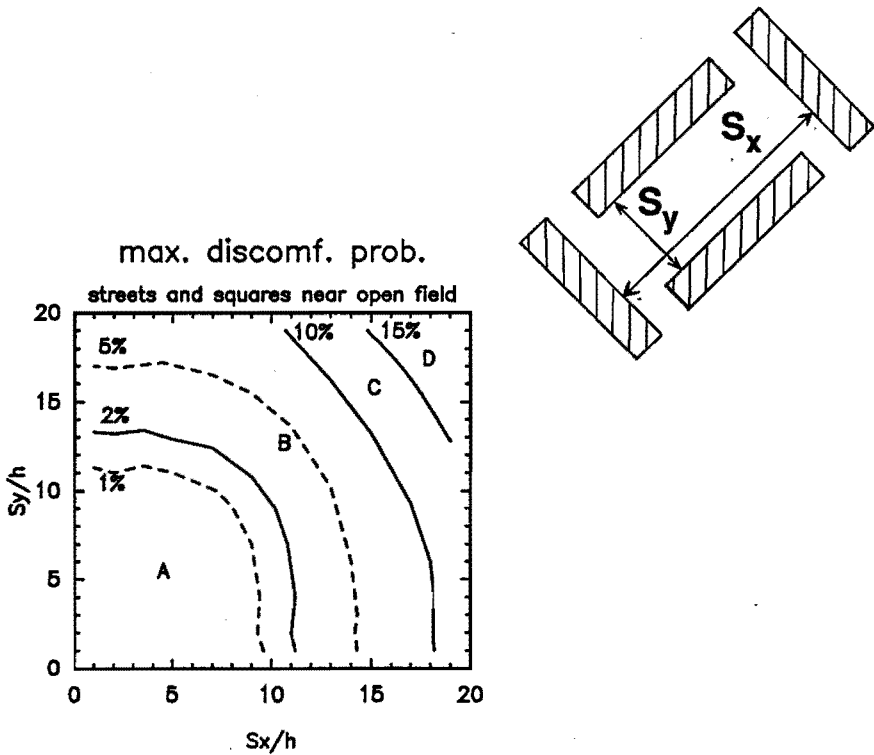
Figure 5.11: Estimated maximum discomfort probability as a function of relative street length S_x/h and relative street width S_y/h. Street orientation is SW-NE. Building height is 10 m. Surrounding terrain (beyond a distance of 30h) is open field ($z_0 = 0.03$ m). In all cases, streets are enclosed by buildings (see sketch). The symbols A, B, C, D (together with solid lines) indicate the allowed activities: long stay, short stay, strolling and walking fast.

Wind climate in streets is strongly dependent on surrounding terrain. Figure 5.11 can only be generalized if correction factors are applied to γ_e and to P_{max}. Table 5.3 gives correction factors for surrounding terrain, which can be applied on figure 5.11.

	for γ_e:	for P_{max}:
large city	0.52	~0.10
large suburb	0.67	~0.25
small city	0.70	~0.3
small suburb	0.84	~0.7

Table 5.3: *Influence of surrounding terrain on maximum discomfort probability P_{max} in streets and squares. Approximate correction factors for γ_e and for P_{max} to be applied to figure 5.11. For a city $z_o = 1$ m, and $z_d = 10$ m, for a suburb $z_o = 0.5$ m and $z_d = 5$ m. A small city/suburb has a radius of about 2 km, a large city/suburb at least 10-20 km.*

Table 5.3 and figure 5.11 contain much information on discomfort probability in streets. The designer however, is merely interested in the relation between street dimensions and allowed activities.

surroundings: (beyond about 30h)	allowed activities: long stay	short stay	strolling	walking fast
open water (radius > 10-20 km)	< 7h	< 9h	< 9h	< 9h
rural terrain	< 9h	< 14h	< 17h	-
small suburb (radius ~ 2 km)	< 10h	< 17h	-	-
large suburb (radius > 10-20 km)	< 15h	-	-	-
small city (radius ~ 2 km)	< 15h	-	-	-
large city (radius > 10-20 km)	< 19h	-	-	-

Table 5.4: *Estimate of maximum street length S_x (building face to face) in terms of building height h, for a given class of activities, and for given surrounding terrain. A '-' means that allowed street length S_x is greater than 20h. Street orientation is SW-NE.*

Table 5.4 gives an overview of maximum street length for given activity and given terrain. On all terrains, street length must be limited for 'long stay' activities. 'Short stay' and 'strolling' activities do only require street length reduction if streets are near rural terrain (or in small suburb). If the built-up site is surrounded by large water surfaces, safety requirements are not satisfied for long streets, and street length must be limited to about 9h. It is noted once again that streets must be within the built up area: there may be no direct connections with the surrounding terrain.

The above data can also be applied to crossings. The above 'design rules' may be too lenient for squares ($S_x \approx S_y$), but they will certainly be conservative if allowed street length is reduced by a factor $\sqrt{2}$.

A final issue is improvement of wind climate. Wind climate can be improved by orientation, by narrowing streets, and by trees. There are no general guidelines, but the following may give an indication of possible improvements:

A NW-SE street orientation (instead of SW-NE) allows for about $25\pm10\%$ increase in the maximum street lengths of figure 5.11.

Narrow streets ($S_y/h < 2$), combined with irregular building faces or side streets (fig. 4.21), yields the same wind climate as a wide street with $S_x/h \approx 10$. This yields sufficient wind reduction, except near open water.

Trees may accomplish considerable wind reduction in long streets. Wind reduction (and approximate reduction in γ_e) increases from 20% for $S_y = 8h$ (from tree to tree: 3h) to over 50% for $S_y/h = 2$ (from tree to tree: 0.4*h). These reductions should not be combined with wind reduction due to narrow streets.

5.4 Effect of urban surroundings

Figure 5.5b gave some first estimates of discomfort probability near high rise buildings in urban terrain. These estimates will be validated in the present section.

Influence of urban approach flow

The influence of urban approach flow on discomfort can be judged in two ways:
  -Is there any change in dimensions of the areas with increased or decreased discomfort (i.e. in fig. 5.4, eq. 5.4 and eq. 5.5)?
  -Is maximum discomfort probability P_{max} predicted well by figure 5.5b?

Two buildings have been considered: a 15x15x50 m (L, W, H) tower building, and a wide building of 15x150x50 m. Approach flow z_0 and z_d are 1 m and 4.5 m, local ground surface roughness $z_{0,loc}$ is 0.03 m with a fetch x_{loc} of 600 m. The default orientation of both buildings is NW-SE.

Maximum discomfort probabilities P_{max} for the tower building and the wide building are 14.1% (11.6%) and 17.8% (15.6%) respectively. The values in brackets denote estimates as for fig. 5.5b. Differences in P_{max} correspond with

144

5% difference in γ_e. For danger, a γ_e difference of about 10% applies. There is no increased sensitivity of P_{max} to building orientation.

Shape and dimensions of areas with increased or decreased discomfort probability are difficult to predict.
For example, discomfort radius R_D for the slender (15x15x50 m) building is increased from 10 (rural flow) to 26 m (urban flow). This is probably due to the fact that the 'rural' discomfort probabilities were just too small for a V-shaped (fig. 5.3) discomfort area which is much larger. For the wider building, R_D increases only by 20%. Further tendencies are an increase in size of other discomfort areas (their 'radius' approaches R_D, except for NE corner), and a change in shape: discomfort areas become more elongated.

For wide buildings, sheltered areas may increase markedly in size. This is because downwash (and increased wind speeds), which can be observed in the wake of wide buildings (W/H > 2) in the case of oblique flow (fig. 2.8 and fig. 4.10b), is reduced.
A NW-SE orientation is still most favourable. $L_s(NE)$ and $L_s(SW)$ are of the order of 3.3*H (2.5*H for rural flow). For a SW-NE orientation, $L_s(NW)$ and $L_s(SE)$ are about 0.8*H, not very large, but three times larger than for rural flow.

It is noted that even small changes in z_0 (from 0.03 m to 0.1 m) may result in considerable changes in the parameters (as given above) describing 'wind climate patterns' around buildings. Generalization seems hardly feasible.

Wind climate in idealized urban geometry

The urban 'context' is not only determined by urban z_0 but also by nearby low rise buildings. In the following, the estimates of section 5.2 (high rise buildings) and 5.3 (streets and squares) will be 'validated' for an urban context.

Three geometries have been used to validate the estimates of section 5.2 and 5.3. Building dimensions are 25x15x15 m, 50x15x15 m, and 50x50x50 m. Street width S_y is 20 m, low rise building height h is 10 m. Figure 4.22 shows the building arrangement. Approach flow z_0 and z_d are 1 m and 10 m, $z_{0,loc}$ = 0.03 m (skimming flow over low rise buildings). Fetch x_{loc} = 600 m (300 m for lower building). The orientation of all buildings is NW-SE. Table 5.5 gives discomfort probability, together with estimates from figure 5.5 (in brackets).

Maximum discomfort probability for the first two buildings is much smaller than estimated (in brackets). Differences for larger W/H are only small.

The influence of low rise buildings can be described with the parameter L_g/h, where L_g is given by eq. 4.8. The influence of low rise buildings on discomfort probability and on γ_e can be summarized in the following way:
-less than 5-10% decrease in γ_e if L_g/h > 3
-over 10-15% decrease in γ_e if L_g/h < 1.5

Building dim. L, W, H:	P_{max}	γ_e
25x15x15 m	1.52% (2.70%)	0.34 (0.38)
50x15x15 m	6.61% (10.4%)	0.46 (0.53)
50x50x50 m	13.3% (13.7%)	0.57 (0.58)

Table 5.5: *Maximum discomfort probability P_{max} and effective γ (γ_e) near high rise buildings in urban context ($z_o = 1$ m, $z_d = 10$ m, nearby low rise buildings). Estimates of figure 5.5 are given in brackets.*

A typical discomfort probability in streets (without high rise building influence) is 0.5% ($\gamma_e = 0.28$). Figure 5.11 and table 5.5 yield P = 1.2% ($\gamma_e = 0.32$), so section 5.3 gives a fair but conservative estimate of P in narrow streets.

The areas of increased discomfort probability are hard to define because their dimensions are strongly dependent on the ambient P in streets. The area of increased discomfort probability is at least 0.3*H.

building/terrain classification

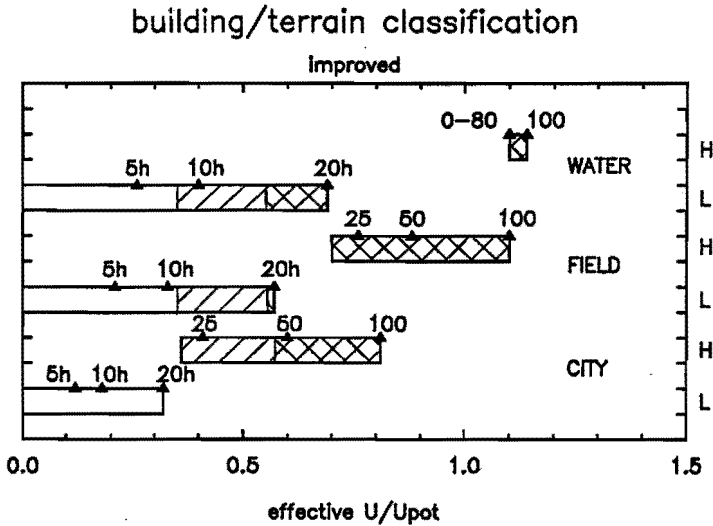*Figure 5.12:* *Improved classification of building and terrain in terms of γ_e (effective U/U_{pot}). Terrain type and building type are indicated in graph. Building height is indicated for high rise buildings, street length (in multiples of building height h for low rise buildings).*
Hatched area: uncomfortable for some human activities.
Cross hatched area: increased danger probability.

For comparison, the ambient P of a large field within the city ($z_{0,loc} = 600$ m; fetch $x_{loc} = 600$ m, with correction for z_d) is taken as well. In that case the areas of increased discomfort probability are almost vanished for $L_g/h < 1.5$. Even for $L_g/h \approx 3$, discomfort radius R_D is only half of its 'rural' value.

5.5   An improved classification of building and terrain

A first building and terrain classification has been given in section 5.1. Predictions of discomfort are much too conservative (γ_e up to 35% too high). Danger can be predicted well with figure 5.1b and 5.2.

Figure 5.12 presents an improved building and site classification in terms of γ_e. Discomfort probability P (not danger) can then be estimated from figure 5.1a. The acceptability of wind climate can be judged by comparing P with comfort criteria (table 5.1).

In very large cities, maximum discomfort probability near high rise buildings is only acceptable, if building height is less than 50 m. It should be noted that safety requires some (20%) additional reduction in building height. The requirements can be relaxed for large groups with mutual sheltering (interior of 'Manhattan').
In low rise building groups (uniform height), street length reduction may be required if the location is near open terrain. Near open water, street length reduction is required for safety. Additional reduction may be required for squares ($S_x \approx S_y$).

For other terrain types than indicated in figure 5.12, and for smaller fetches (say 2 km), one should consider the reference speeds U_r (U_{H_0} for high rise building; $U_{2.5h}$ for low rise groups). The ratio of U_r at the considered site and U_r for a building height and terrain type of figure 5.12 may serve as a correction factor for γ_e. This ratio can be determined with the methods of section 4.2. Some worked out results are given in chapter 7.

In many cases, further corrections must be applied to the γ_e's of figure 5.12. Correction factors are given in table 5.6. Figure 5.12 and table 5.6 allow for a fair estimate of maximum discomfort probability for a given geometry and for given surroundings.

A judgement of wind climate near high rise buildings is not complete if the areas of improved and deteriorated wind climate are not specified. However, these areas are highly dependent on building orientation, building arrangement (in groups), and surrounding terrain. A complete description is not feasible. Figure 5.4 allows for estimation of the 'discomfort radius' near building corners within about a factor 2. In almost all building groups, discomfort radius is (much) smaller than indicated by figure 5.4. The same is true for other building orientations (especially SW-NE), and for thick buildings ($L > 15$ m $> R_D$ of fig.

5.4). There are two important exceptions: buildings with corner gaps, and slender buildings (W/H < 1) in large open spaces within cities.

Discomfort areas of passages between buildings are generally limited to the passage and to adjacent building faces (for shifted buildings). The area of increased danger extends to a distance of about $\min(2S_y,H)$ from the passage opening.

	passage/gap:	corners:
single high rise building:		
orientation:		0.95-1.05
building width:		see fig. 5.5
high rise building groups:		
aligned building (- -)	0.9-1.0	0.9-1.0
buildings behind each other (I I)	≈0.8	1.0
shifted buildings ($^I{}_I$)	1.0-1.1	0.9
square (□) and cross (+) groups	0.7/0.9	0.8/0.7
urban surroundings:		
large open area		1.05-1.1
nearby low rise buildings; $L_g/h \approx 3$		≈0.95
nearby low rise buildings; $L_g/h \approx 1.5$		≈0.9
building shape:		
buildings with gaps:	1.25 in gap	1.0 (no corner gap)
rounded corners:		≈0.90
buildings with podia:		effective height reduced to podium height if $L_p > L_g$
details of site:		
trees against corners or scattered trees		≈0.90
streets and squares:		
NW-SE orientation instead of SW-NE:		≈0.8
trees; width of 'unoccupied' area 3h; 0.4*h		0.8/0.5
narrow streets (S_y < 2h):		'effective' street length < 10H
building height 20 m instead of 10 m		1.2

Table 5.6: *Approximate correction factors (± 0.05-0.1) for discomfort γ_e of figure 5.12 and danger γ_e of figure 5.1. By default, a NW-SE building orientation is assumed.*

5.6   Summary and conclusions

A first step into the prediction of wind climate is made in section 5.1. This section offers a combined building and terrain classification in terms of a maximum wind amplification factor γ. However, wind climate should be judged in terms of discomfort probability. The relation between γ and discomfort and

148

danger probability is shown in figure 5.1. Table 5.1 gives maximum discomfort probability for a number of human activities.

Extensive estimates of discomfort probability have been made in sections 5.2 through 5.4. These results are summarized in section 5.5 which gives an improved building and terrain classification (fig. 5.12).
In order to get better estimates of discomfort probability, one can apply a number of corrections relating to building shape, orientation and building arrangement. These corrections are given in table 5.6. Section 5.5 gives also suggestions (p. 147) for corrections relating to the effects of surrounding terrain and fetch.

Judgement of wind climate near high rise buildings should include a description of areas with improved and deteriorated wind climate. Figure 5.4 gives a rough estimate of the radius R_D of the discomfort area near building corners. Other parameters, describing distributions of discomfort and danger probability around buildings, are presented in section 5.2.
However, distributions of discomfort and danger probability are extremely sensitive to orientation, building arrangement, and surrounding terrain. Therefore, it is not possible to make suitable generalizations. Direct measurement (wind tunnel) or computation of γ may allow for a better estimate of discomfort areas.

A final point of interest is the accuracy of the present estimates. The accuracy of estimates of γ and of discomfort probability can be seriously affected by (see section 5.1; p. 129-130 for discussion):
-numerical errors
-neglect of thermal effects on γ
-errors in z_0 estimate
-errors in internal boundary layer (IBL) models.
In the worst case, each of these errors can be up to about 15-20% (in γ). Routine wind tunnel predictions of wind comfort can be affected by the latter three error sources ('thermal', 'z_0', 'IBL') as well.

6 Wind comfort evaluation in practice

Decisions made in the early design stages generally have the largest impact on wind comfort. These decisions include the choice of a site, the lay out of streets, the distribution and orientation of buildings, and the planned use of outdoor space (Arens, 1982). The present day practice is to test a design in a wind tunnel when it is nearly finished. Too often, this practice allows only for marginal improvements in wind climate.

Wind comfort advice in early design stages may allow the architect to optimize his design with respect to wind comfort. Wind tunnel tests are generally not suitable for early design stages as they require a scale model of the new development. Instead, design rules, desk estimates and expert models can be used.

In this chapter, it will be discussed how early cooperation between architect and consultant may lead to an improved wind climate. Later in this chapter, the accuracy of early advice will be discussed.

6.1 Early wind comfort advice; development of the IJ-plan

Recently, the council of Amsterdam has invited three architects to make a town plan for the so called 'Java-island' in the river IJ, a windy location. One of the involved architects (prof. R. Uytenhaak) gave high priority to the issue of wind comfort, and sought cooperation with the author.

The following issues will be considered in this section, and in section 6.2:

1. -which human activities are foreseen or planned
2. -which shelter is required for these activities
3. -which shelter is offered by the surrounding terrain (city)
4. -which shelter should be provided by the buildings
5. -development of sketch design with required shelter
6. -evaluation and finishing touches

Table 6.1:   *Issues which are considered during cooperation between architect and wind expert.*

Introduction; description of the site

The site is part of a long island which is oriented in WNW-ESE direction. It is situated in the easterly docklands of the IJ in Amsterdam (figure 6.1). Plans are being developed for the westerly part and the centre part of the island; called 'Java-island'. The remainder of the island is called 'KNSM-island'.

At the centre part of the island, about 1300 houses are planned, together with a park, some shops etc. and a 'main' road. An extensive overview of the plan is given by Uytenhaak (1991).

From a wind comfort viewpoint, fetch over open water and the small width (132 m) of the island are important. Fetch over open water is about 200 m for southerly wind directions and 250-800 m for northerly wind directions. Fetch is still larger along the IJ, i.e. in E-W direction. At larger distances, the site is surrounded by several kilometres of urban area, except for easterly directions. These urban surroundings will compensate part of the wind speed up over open water.
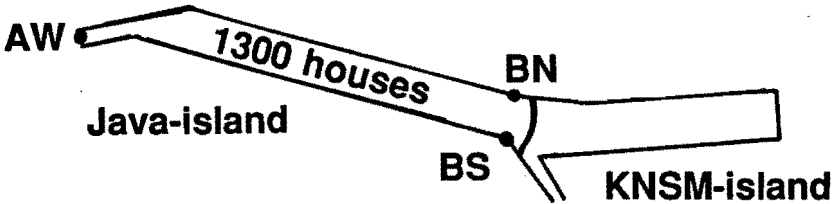
Figure 6.1: Location of Java-island with respect to centre of Amsterdam (from Uytenhaak, 1991). AW, BN and BS denote locations for which wind climate at the undeveloped site has been evaluated.
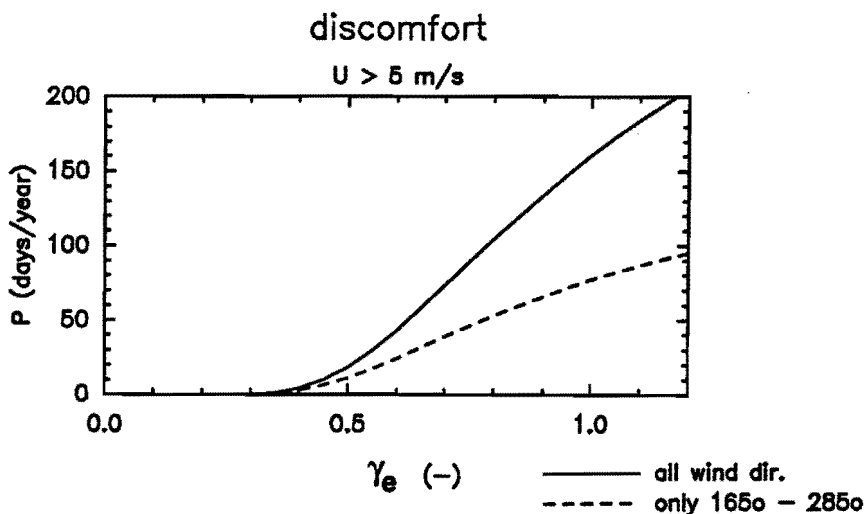
Figure 6.2: *Discomfort probability in terms of days (24 h) per year as a function of direction independent wind amplification factor γ (γ_e). Solid line: total probability. Dashed line: contribution of southwesterly wind directions (θ between 165° and 285°). Climate statistics: Amsterdam airport (Troen et al, 1989).*

Judgement of wind climate

In this chapter we will use TNO comfort criteria (Visser, 1980). This allows for comparison with results of routine wind tunnel investigations. Wind speeds greater than 5 m/s will be considered as uncomfortable. The fraction of time that the threshold is exceeded is called discomfort probability (P). Maximum discomfort probabilities for some typical human activities are given in table 6.2.

Figure 6.2 shows discomfort probability as a function of wind amplification factor γ, where γ is the ratio between local wind speed at 1.75 m height (U) and the potential wind speed (U_{pot}) at 10 m height at an 'ideal' meteorological site (airport) at a very large grass plain. Discomfort increases rapidly for $\gamma > 0.4$, and is 75 days per year for $\gamma = 0.7$ (at 1.75 m height at airport). Southwesterly winds yield an important, but not a dominant contribution to discomfort.

Often, it is practical to discuss (differences in) wind climate in terms of a γ. In practice, γ is strongly dependent on wind direction. Therefore, we define an 'effective' γ (γ_e), where γ_e is a direction independent γ which yields the same discomfort or danger as in reality. For example, a discomfort probability of 163 days per year yields a γ_e of about 1.0 (solid line in fig. 6.2).

153

	acc.	unpl.	intol.
walking fast: car-park, sidewalk, road, cycle-track	< 35	35-75	> 75
strolling: park, shop centre, footpath building entrance, bus station	< 5	5-35	> 35
sitting/standing short: shop centre, square, playground	< 0.1	0.1-5	> 5
sitting/standing long: terrace, swimming pool, open air theatre	0	0-0.1	> 0.1

Table 6.2: *TNO wind comfort criteria as proposed by Visser (1980). Column 1, 2 and 3 give acceptable, unpleasant and intolerable discomfort probability in terms of days (24 h) per year. Covered areas require more shelter and should be rated one class lower.*

The above discomfort probabilities may be converted to a maximum wind amplification factor (or a minimum shelter):

activity:	max. tolerable γ_e
walking fast	0.70
strolling	0.57
sitting/standing short	0.41
sitting/standing long	0.29

where γ_e is an 'effective' or direction independent γ as defined above. At the Java-island, most locations should at least be suitable for 'strolling' activities, i.e. γ_e should be less than 0.57.

Finally, it is noted that other, better, criteria are used in chapter 5. The results of chapter 5 and 6 should be compared by means of γ_e, not by means of discomfort probability (which is dependent on the applied discomfort threshold).

Wind climate of the undeveloped site

In the former, the planned human activities and the required shelter ($\gamma_e < 0.57$) are mentioned briefly. The next step (see table 6.1) is to judge wind climate of the undeveloped site. This allows for an estimate of the amount of shelter which the planned buildings should provide.

154

Table 6.3 gives wind amplification factor γ and discomfort probability P for three locations at the undeveloped site. Exposure corrected climate statistics of Amsterdam airport have been used (Troen et al, 1989). Wind amplification factor γ has been estimated with the methods of section 4.2.

wind dir.		γ_{AW}	γ_{BN}	γ_{BS}	P_{AW}	P_{BN}	P_{BS} (days/year)
N	0°	0.65	**0.78**	0.66	2.0	4.0	2.1
	30°	0.68	**0.80**	0.68	5.0	8.1	5.0
	60°	**0.78**	**0.89**	0.74	8.7	11.9	7.5
E	90°	**0.75**	0.71	0.71	4.5	3.8	3.8
	120°	**0.83**	0.70	**0.85**	3.4	1.6	3.8
	150°	0.63	0.57	0.67	1.9	0.9	2.5
S	180°	0.60	0.53	0.61	3.9	2.3	4.2
	210°	0.64	0.53	0.63	**6.8**	5.3	**6.5**
	240°	0.61	0.55	0.66	**9.4**	**6.5**	**11.8**
W	270°	**0.79**	0.60	**0.76**	**12.8**	6.1	**11.8**
	300°	**0.72**	**0.81**	0.64	**6.5**	**8.3**	4.9
	330°	0.62	**0.75**	0.63	3.7	**6.6**	4.0
γ_e and total P:		0.68	0.67	0.68	69	65	68

Table 6.3: *Wind amplification factor γ and discomfort probability P for three locations (AW, BN, BS) at the undeveloped Java-island (fig. 6.1). Climate statistics (fully exposure corrected) are from Troen et al (1989); wind comfort criteria (table 6.2) are from Visser (1980).*

Exposed wind directions ($\gamma > 0.7$; greater than on grass plain) are mainly easterly and between west and northwest, corresponding with the length axis of the IJ.

Discomfort probability is 65-70 days/year ($\approx$19%). According to table 6.2, wind climate at the undeveloped site is unpleasant, even for a 'walking fast' area. Activities like sitting and standing require about 50% further wind speed reduction (γ_e down to 0.3-0.4). Critical wind directions are NE (45°), and SW, W, and NW (225°-315°). For these wind directions, buildings should provide most shelter.
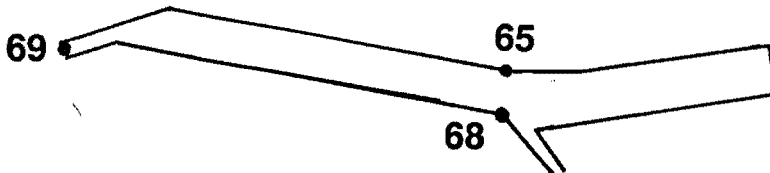

Figure 6.3: *Discomfort probability at the undeveloped site (days/year).*

Creating the required shelter

Wind climate at the undeveloped site is uncomfortable. Therefore, the planned buildings should provide much shelter. In the following, it will be discussed how this shelter can be created.

The first issue is the choice between a high rise building development or a low rise building development.
Because of the small width of the island, it is almost impossible to make a 'Manhattan'; i.e. a high rise building district with mutual sheltering. Short circuiting effects through passages (fig. 6.4) and corner effects (fig. 6.6a) will be dominant. At these locations, further deterioration of wind climate is to be expected.
Low rise buildings do not yield increase of discomfort. The required shelter can be created by sufficient reduction of street length and street width.
In the present case, a low rise development was chosen for various reasons including wind comfort.

Next, we may divide the island into an inner (enclosed) area and an outer area. For the inner area, sufficient enclosure is essential, so that the increased wind speeds over open water can not penetrate into the streets. Figure 6.4 shows how these penetration and short circuiting effects can be mitigated by zigzag streets.

Reduction of street length is essential in the inner area. A street length (face to face) of less than 8 building heights (8H) provides sufficient shelter. It should be noted that the ratio of street length and building height is most important, not the actual dimensions. However, shelter may be affected if *variations* in building height become too large (say more than about 50%).
For longer streets, shelter can be provided by sufficient reduction of street width (say 2 building heights), with tree rows, side streets and/or irregular building faces (figure 6.5).
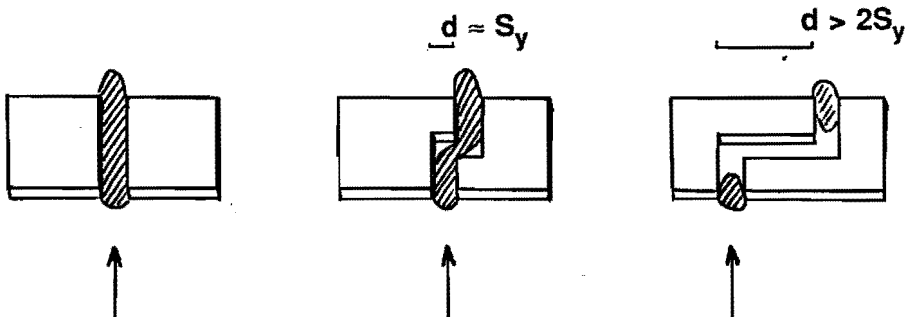

$$d \approx S_y \qquad d > 2S_y$$

Figure 6.4: Short circuiting effects across the island can be mitigated by zigzag streets. Street width: S_y; lateral displacement: d.
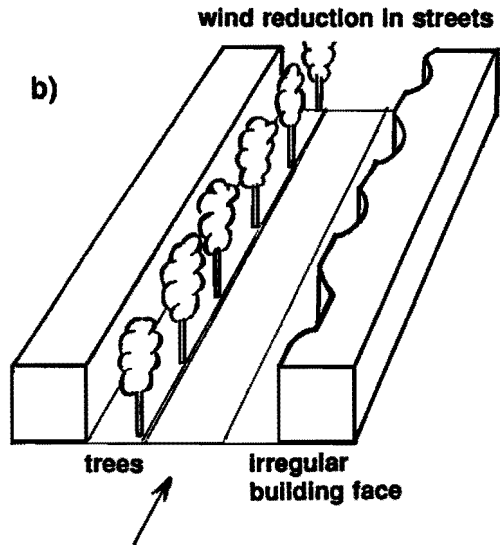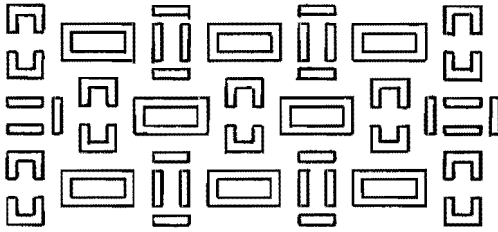
156

a) short streets

wind reduction in streets

b)

trees   irregular
         building face

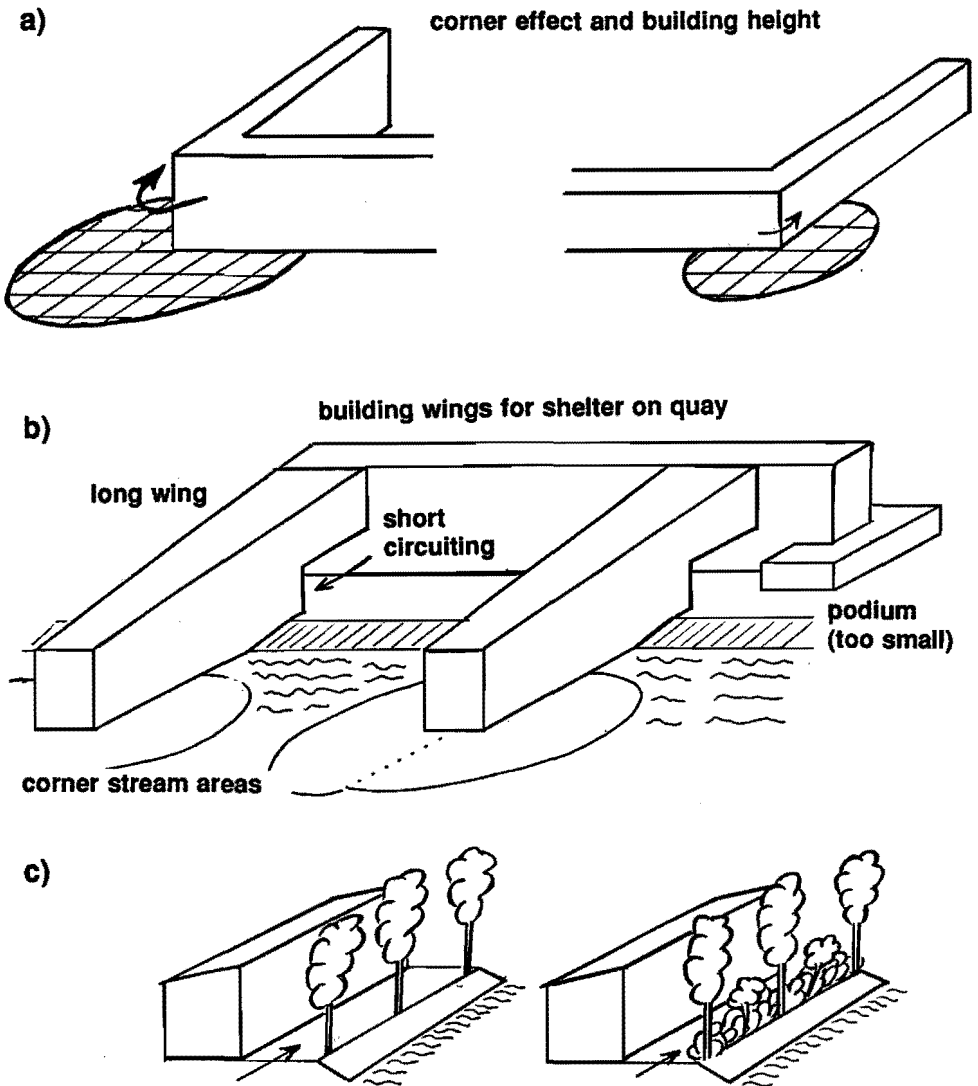*Figure 6.5:* *Means of reducing wind speeds in streets*
a) *Plan view of building arrangement with short streets.*
b) *Design of long streets. Small street width (less than 2-3 building heights), trees and irregular building faces reduce wind along the street.*

A different approach is needed for the outer areas. Wind speeds near building corners are generally increased. The extent of these corner streams is strongly dependent on building height (fig. 6.6a; see also fig. 4.11). Corner stream wind speeds increase with building height as well.
Outside the corner stream areas, there is almost no shelter if wind is parallel to the quay. At all these locations, wind climate may still be far from comfortable.

The quay can be sheltered if buildings along the quay are equipped with wings (fig. 6.6b). Wings should be sufficiently long (length greater than 2 wing heights) so that the corner stream area of the wings does not reach the quay. Corners of 'main' buildings on the quay should be equipped with wings (length greater than 2 building heights) or podia as well.

a)   corner effect and building height

b)   building wings for shelter on quay

long wing

short
circuiting

podium
(too small)

corner stream areas

c)

Figure 6.6:   Building along the quay; concepts and recommended design.
a)   *Near building corners, both corner stream wind speeds and corner stream*
        dimensions increase with building height.
b)   *Building wings may shelter the quay when wind is along the quay. Gaps in the*
        wings (for through traffic), will cause adverse short circuiting effects.
c)   *Trees and shrubs can provide shelter as well (for wind along the quay).*

158

There is no fully satisfactory solution if the quay is used for through traffic. The wings can be equipped with gaps, but these gaps yield adverse short circuiting effects.

Trees (combined with shrubs) may be a better solution for quays with through traffic. However, they may be a less effective sheltering device if placed near building corners or near passages between buildings.

Finally, connections across the island may result in dangerous surprising effects (cross winds) at the quay. Zigzag streets (fig. 6.3) can reduce these adverse short circuiting effects.

The above principles have been incorporated in the design of the Java-island, where possible (and practical). The next section will discuss the final design, and its wind climate.

6.2   The final IJ-plan; evaluation of wind climate

Wind climate for the final IJ-plan has been evaluated with desk estimates of γ (Bottema, 1992), and with wind tunnel measurements (Harst, 1992). First, the final design of the IJ-plan will be evaluated. Thereafter, both the expected wind climate and the evaluation methods will be discussed.

The final IJ-plan

Figure 6.7 shows the final IJ-plan. The interior of the island (from W to E) consists of a plaza, a district with closely spaced low rise buildings (2-3 storeys), and a park. At the northerly quay, buildings are 5-8 storeys high. Four towers of 14 storeys are placed at the western end of the island.

The final plan has a number of features which yield an improved wind climate. First of all, low rise buildings are planned on the major part of the island. Buildings at the northerly quay are somewhat higher, but high rise buildings (14 storeys) are only found at the westerly end of the island.

The outer areas (i.e. the quays) are used as traffic routes. In this way, the inner area remains 'compact' and sheltered (except near the bridges). The main traffic route is the northerly quay. Pedestrians and cyclists can also use the (sunny) southerly quay. The major part of the quays is sheltered by trees.

The inner area is 'protected' by rows of buildings at both of the quays. Most passages between these buildings are small, so that wind can not penetrate far into the inner area. However, buildings at the northerly quay are relatively high and between these buildings, discomfort may be increased.

The park is rather compact, so that large open areas at the inner area of the island are avoided. Dense tree rows and enclosure by buildings provide shelter against winds across the island (and from the water).

159

The plaza near the western bridge is sheltered in a similar way.

Finally, in the low rise building groups at the centre of the island, streets were kept short when across the island. However, streets along the island are longer than recommended.

a)

view from south
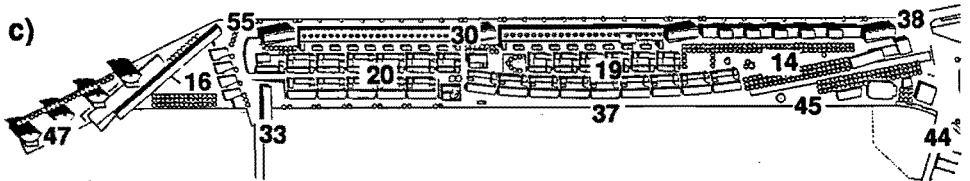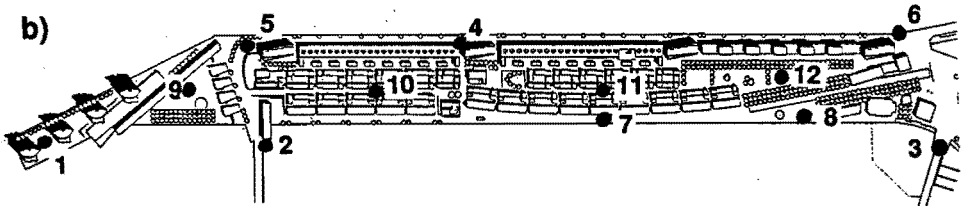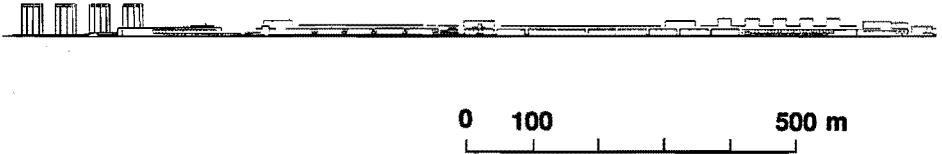

b)

c)

Figure 6.7:   *Final design of Java-island, and estimated discomfort probability as (Bottema, 1992). Shading (b/c) indicates building height.*
a)   *Side view of Java-island*
b)   *Locations for which discomfort probability is estimated (exact locations are given in Bottema, 1992)*
c)   *Discomfort probability (days/year); see table 6.2 for criteria*

160

Wind climate evaluation; desk estimates

The last issues in cooperation between wind expert and architect (see table 6.1) are evaluation of wind climate (see also Bottema, 1992) and 'finishing touches'. In the following, results of a desk evaluation of wind climate of the final IJ-plan will be discussed. The design rules of chapter 7 and the suggestions of the previous section can be used for further improvement of wind climate, i.e. the 'finishing touches'.

The desk estimates are made in the following way:

The effect of surrounding terrain (lake, river, city etc.) on wind amplification factor γ is accounted for by the methods described in section 4.2. Estimates of building influence are *not* based on data of chapter 4, as these data were not analyzed by the time the advice was asked for (1991). Instead, existing literature models (and data) have been used. Improved (new) estimates of building influence will be discussed in section 6.3.
Wind speeds in corner streams are estimated with Leene's (1991) method (see section 4.5.2; eq. 4.11). This method can be used for the worst affected locations. Ground surface is assumed to be very smooth (as in most routine wind tunnel investigations), so wind speeds in a corner stream area (fig. 4.11) are probably close to the maximum wind speeds.
Wind speed reduction in obstacle wakes is estimated by Leene's (1990, 1991) wake model (section 4.3.1). Estimates of the effects of downstream buildings, low rise building groups, and nearby tree rows are based on the present numerical data and on literature data (Visser, 1987; Oke, 1987). Climate statistics (Amsterdam airport) are taken from Troen et al (1989) and are fully exposure corrected.

Figure 6.7 shows the estimated discomfort probability for 12 typical locations.
Discomfort probability along the quays and near high rise buildings is between 30 and 55 days per year. In the interior of the island, estimated discomfort probability is 15-20 days per year. Critical wind directions are along the quays, and along the streets. Near high rise buildings, critical wind direction is location dependent.
All areas can be used as 'walking fast' area (see table 6.2). In the interior, wind climate is generally not suitable for sitting/standing activities.
Thus, wind climate does not meet comfort requirements, even though the issue of wind has been considered during design. This is partly caused by the fact that the width of the island was only 132 m, so that it was not easy to provide shelter. Another reason is the fact that (east-west) streets in the interior of the island are too long from a wind comfort viewpoint. Shorter streets require a complicated street lay out and will affect accessibility (local traffic) and social control (through sight). The latter was given high priority by the town council of Amsterdam.
Wind climate at the quays may be improved by additional trees and by shrubs, but this will affect the view.

161

Wind climate evaluation; wind tunnel test

A routine wind tunnel investigation (Harst, 1992) on a 1:750 scale model of the Java-island and surroundings has been carried out by IMET-TNO in Apeldoorn (NL).

The resulting discomfort probabilities are shown in figure 6.7. The 'wind tunnel' discomfort probability is generally much smaller than the desk estimates. Several factors, both in the desk method and in the TNO methods, contribute to these differences. This issue will be discussed in detail in the next section.

In the following, wind climate will be further evaluated. Corrections will *not* be applied here. This allows for comparison with Dutch wind comfort criteria which are partly based on consultants' experience (Visser, 1980) (and therefore 'tuned' to the TNO methods to determine γ and discomfort probability) and with results for other projects in the Netherlands.

The Java-island can be divided in a number of areas with similar wind climate. The interior of the island (the plaza in the W, the low rise building quarter, and the park in the E) has a sheltered wind climate which is suitable for 'short stay' activities and -mainly in and near the eastern park- even for 'long stay' activities.
Near (corners of) high rise buildings, discomfort probability ranges between 15 and 48 days per year. Wind climate is acceptable or tolerable for 'walking fast' activities.
Wind conditions are acceptable for 'strolling' activities at the quays, and in streets which are directly connected with the quays.

At most locations, (south)westerly winds yield the largest and sometimes dominant contribution to discomfort probability. However, northeasterly wind dominates at the northerly quay. Other wind directions dominate only at a few measuring points. These points are either near high rise buildings (NE corner) or in very sheltered areas.

Possible dangerous locations are mainly expected near the tower buildings at the westerly end. Near these buildings, dangerous conditions may exist for up to 36 hours per year. For other locations (passages between flats along the northerly quay), dangerous conditions exist for 8 hours per year or less. Dangerous surprising effects (sudden 'offshore' winds) are not expected on either of the quays.

Finally, it may be interesting to compare the present data with those of the neighbouring KNSM island (Harst, 1990). The KNSM island has a more 'open' structure (fig. 6.9) with a long main street, and a number of side streets connecting northerly and southerly quays. Typical building heights are between about 15 and 30 m; comparable with building heights along the northerly quay of the Java-island.

162

Discomfort probabilities along the quays are strongly dependent on location and are generally between 5 and 40 days per year. The main street and side streets have somewhat more shelter, the easterly 'bastion' somewhat less. Discomfort probabilities in parks and (partial) enclosures are generally less than 5 days per year.

Wind climate of both islands is largely similar. Quays of the KNSM island (except SW corner) are slightly more windy, but wind climate in adjacent streets is slightly better. The main difference is found in the interior of the islands. The easterly park of the Java-island and streets of the neighbouring building group (if not connected with one of the quays) are very sheltered. Their wind climate is comparable with that of the enclosed areas at the KNSM island.
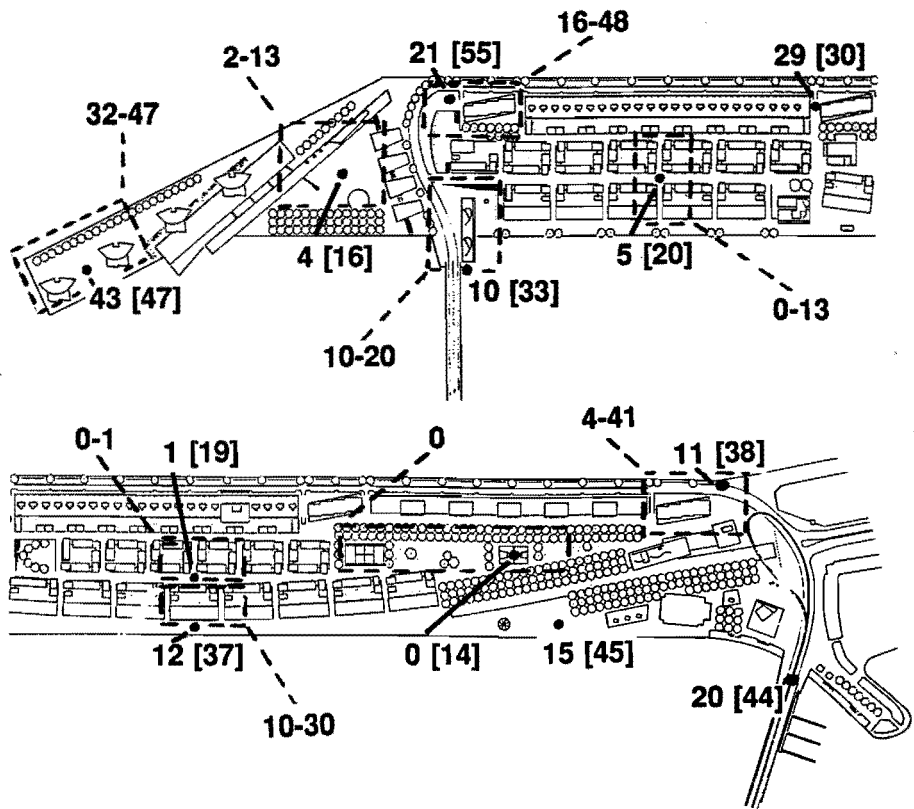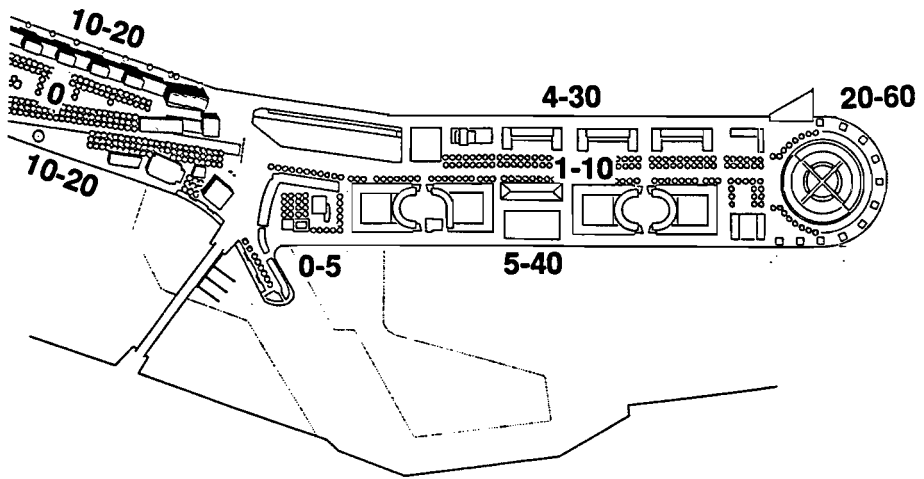

Figure 6.8: Discomfort probability (in days per year) for the 12 points of figure 6.7b and for some areas ('dashed boxes') as determined by IMET-TNO (Harst, 1992). See table 6.2 for criteria. Desk estimates are given in square brackets.

Figure 6.9:   *Easterly part of Java-island (with shading) and neighbouring KNSM island (without shading). Some typical discomfort probabilities (days/year) for the KNSM-island are shown. See table 6.2 for criteria.*

It can be concluded that a dense building structure, as for the Java-island, yields significant improvement in wind climate. However, wind climate on the quays appears to be rather insensitive to building structure on the island, except for a very open building structure or for buildings which are much higher than 20 m.

6.3 Discussion of evaluation methods

In this section, we will consider differences between wind tunnel predictions and the present desk estimates in more detail. The total accuracy of each method, and of wind climate forecasts in general, is discussed in section 4.5 and 5.1, not in the present section.

After some necessary corrections on wind tunnel data, it can (and will) be judged whether building influence on γ is estimated well with the present desk estimates. Finally, accuracy and prospects of wind comfort evaluation for early design stages are discussed.

Corrections on wind tunnel and desk estimates

A number of corrections must be applied before wind tunnel data are comparable with the present literature estimates. Factors which have to be accounted for are the applied climate statistics, methods used to link local wind speeds to 'airport' wind speeds, and wind tunnel techniques.

164

First of all, climate statistics are considered. In the present desk estimates, wind speeds on the meteorological station are fully exposure corrected (i.e. to uniform terrain with $z_0 = 0.03$ m; Troen et al, 1989). On the other hand, TNO uses data which are only partially corrected for terrain roughness.
Table 6.4 shows discomfort probability for the 12 locations of fig. 6.7b.

loc.	1	2	3	4	5	6	7	8	9	10	11	12
WT1	43	10	20	29	21	11	12	15	4.2	4.9	0.6	0.2
WT2	34	4.0	9.3	26	17	7.5	4.5	5.4	4.5	3.1	0.2	0.1
EST	47	33	44	30	55	38	37	45	16	20	19	14

Table 6.4: *Discomfort probability (days/year) for 12 locations of fig. 6.7b. 'WT1' is based on 'standard' TNO climate data (partially exposure corrected). 'WT2' is based on wind tunnel γ and on fully exposure corrected climate data (Troen et al, 1989). The desk estimate ('EST') is based on fully exposure corrected data as well.*

It can be seen that the use of different climate statistics has masked a significant part of the actual difference in wind climate. It will be clear that a good choice of climate data is of great importance.
The 'real' differences in γ_e are up to 0.2. In the following, these differences in γ will be considered in more detail.

A first cause of differences in γ is the linkage of local wind conditions to wind speed on the meteorological site ('airport'). Differences are caused by the linkage method (called *'far field linkage method'*), and by the estimation of the roughness (z_0) of the surrounding terrain.

The linkage method of TNO (Vermeulen et al, 1980) assumes that the so called internal boundary layer (IBL) which is influenced by new terrain grows at a rate of 1/10 (h_{IBL}/x). The flow is assumed to be in equilibrium with the new terrain if the IBL has reached a height of 500 m (fetch x = 5000 m).

Jensen (1978) noted that equilibrium is not reached before 10-20 km. In the present desk estimates, equilibrium is not assumed for flow over roughness changes within 15 km of the site. Instead, internal boundary layer (IBL) theory has been used. This approach is not correct either because IBL theory should only be used within the first 2-3 km over new terrain (section 4.2.2). However, there is no better alternative available.

Figure 6.10 shows the ratio between the present reference wind speed at the turntable edge and TNO data. Most of the observed differences (i.e. a ratio ≠ 1) are caused by the far field linkage methods. Differing z_0 estimates may

contribute to the observed difference in fig. 6.10 for a number of wind directions ($\theta < 135°$ and $\theta > 255°$; mainly northerly and easterly winds).

Compared with the present estimates, TNO overestimates shelter of the city by 10-20% for all southerly wind directions. For most other wind directions, the effect is small. For the 12 points considered here, differences in discomfort probability are generally not large, as γ is often small for southerly wind directions.
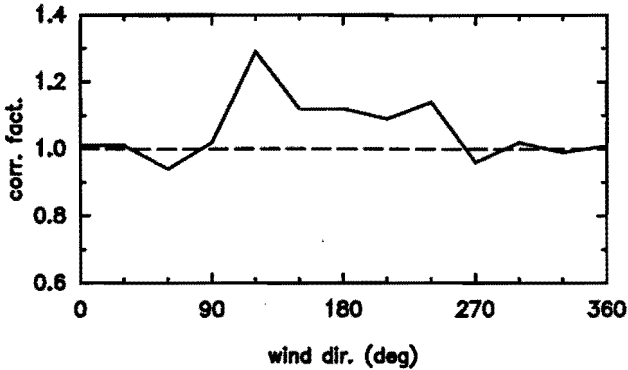
far field correction factor

Figure 6.10: *Ratio of present reference wind speed and TNO data as a function of wind direction θ. Reference speed is given at turntable edge (863 m from centre of island) and at 26 m height. The ratio can be considered as correction factor for TNO data.*

Experimental errors in wind tunnel data are a second cause of the differences in γ. Wind speeds have been measured with so called 'thermistors' which tend to overestimate wind speeds if wind amplification factor γ smaller than 0.4. However, the contribution of these γ's to discomfort happens to be small for the discomfort thresholds used by TNO.

The most important error source is the turntable roughness. For open water, a roughness length $z_0 = 0.0002$ m applies (table 2.1). However, even a perfectly smooth turntable (see eq. 2.34 for wall function) yields a full scale z_0 of 0.002 m (pedestrian wind speeds $\approx$10 m/s; scale factor 1:750). In the present case, turntable z_0 is estimated to be slightly larger than 10^{-5} m, which results in $z_0 \approx$ 0.01 m in full scale.
Wind tunnel results can not be corrected for this z_0, so the literature estimates are adapted to an 'open water' z_0 of 0.01 m. Because of this modification, the data of table 6.5 are only suitable for mutual comparison, not for wind climate evaluation.

166

loc.	1	2	3	4	5	6	7	8	9	10	11	12
WT	44	5.2	11	28	17	8.7	5.0	7.0	4.9	2.4	0.3	0.3
EST	47	28	24	27	50	37	20	25	11	8.5	8.5	11

Table 6.5:   *Discomfort probability (days/year) for 12 locations of fig. 6.7b. Wind tunnel data (WT) have been corrected for climate statistics (table 6.4) and for the 'far field' influence (fig. 6.10). Desk estimates (EST) have been corrected for the turntable roughness in the wind tunnel (see text). Climate statistics (Amsterdam airport) are from Troen et al (1989).*

Comparison with table 6.4 ('WT2' versus 'EST') shows that the difference between wind tunnel estimates and desk estimates has become smaller.
This is mainly caused by the correction for turntable roughness. Still, the differences in discomfort are large: they correspond with a difference of up to 0.15 in γ_e (0.20 without corrections).

It can be concluded that the main errors are made in the desk estimates of the building influence. Still, differences due to climate statistics, 'far field' methods (fig. 6.10) and turntable roughness (in wind tunnel) are very significant.

Building influence

It is already concluded that significant errors are made in desk estimates of building influence.
In the following, this issue will be considered in more detail. Both the present desk estimates (based on literature data) and improved estimates will be considered. The improved estimates (see table 6.6) are based on FLUENT data, and on data of chapter 4. It is to be expected that the accuracy of the improved estimates is comparable with the accuracy which can be achieved with expert models.

locations	Proposed modification(s):
1,2,4,5,6	Use flow field of similar FLUENT geometries (use U_{Ho} as reference speed).
7	Take lateral roughness change (section 4.2.2) into account
10,11	Use reference speed above building group (i.e. $U_{2.5h}$) instead of pedestrian level reference speed U_o (section 4.3.3)
3,8,9	No modifications.

Table 6.6:   *Proposed modifications in order to improve present (literature) desk estimates of γ. Locations are indicated in figure 6.7.*

167

The 12 considered locations on the Java-island for which discomfort probability is estimated may be classified as follows:

class:	locations:
high rise build.:	1, 2, 4
quay:	3, 7, 8
high rise build. / quay:	5, 6
low rise build. group:	10, 11
complex geometry:	9, 12

Table 6.7: *Classification of locations (fig. 6.7) for which discomfort probability is estimated.*

Figure 6.11 shows examples of γ as a function of wind direction θ for some typical locations (of each of the above classes) on the Java-island. Wind tunnel results, desk estimates, and improved estimates are shown. The results will be discussed below.

For location 1, the desk estimate predicts the location of peaks and minima in γ fairly well. The magnitude of γ is somewhat overestimated (15%). Minima in γ are much too low. However, it is convenient to use a $\cos^2$-function (eq. 4.11), and the contribution of 'real' (wind tunnel) minima to discomfort is small.
The improved estimates are 10-15% lower than wind tunnel γ for the majority of wind directions. This is probably due to too large a surface roughness in the FLUENT simulations ($z_0 = 0.03$ m instead of 0.01 m). Larger differences can be observed for θ = 255° (near westerly wind) due to 'unexpected' pressure short circuiting, and for θ = 300° due to the sheltering effects of trees.

For location 4, the position of maxima and minima is again predicted fairly well with the desk estimate. However, the magnitude of γ is incorrect for southerly winds.
The improved estimates correspond well with the wind tunnel data for θ ≈ 90° (easterly winds) and for θ ≈ 300°. Significant differences exist for other wind directions. For southerly winds, this is due to the fact that trees are placed close to the upwind building corners, so that the trees act as a podium (section 4.4.1). For northerly winds, the non rectangular building arrangement yields (again) some unexpected pressure short circuiting effects.

For location 5, the desk estimate (eq. 4.11) is tuned to the anticipated extremes of γ. The dependence of γ on wind direction is predicted well. Estimated wind speeds are generally too high.
The improved estimates are close to the wind tunnel data, except for northerly winds. Only half of the difference for northerly winds can be explained by too high a z_0 in the FLUENT results; the remainder of the difference can not be explained. For southerly and westerly winds (150° < θ < 300°), wind tunnel γ is lower than the FLUENT estimate. This is probably due to trees (25% wind speed reduction).
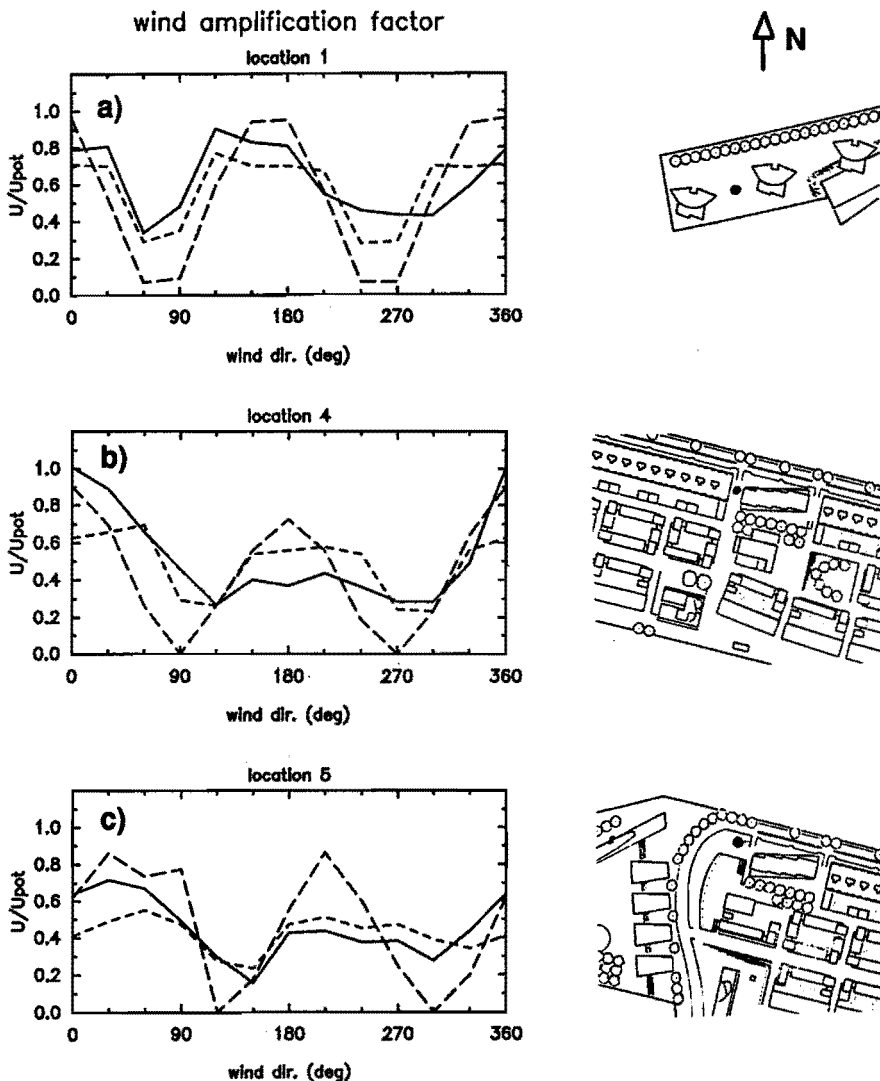
Figure 6.11: Wind amplification factor γ as function of wind direction θ (0° = North; 30° intervals). See text for applied corrections and fig 6.7 for locations of measuring points. Solid line: wind tunnel results (Harst, 1992). Long dashed line: present desk estimate. Short dashed line: improved estimate.

a) Location 1: between WSW-ENE oriented tower buildings
b) Location 4: on northerly quay; passage between approx. E-W oriented buildings
c) Location 5: on northerly quay; near NW corner of high rise building

wind amplification factor

location 7

d)

location 10

e)

location 9

f)
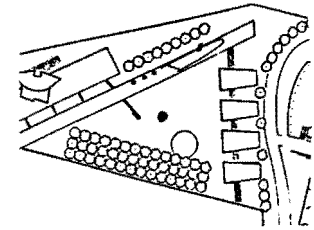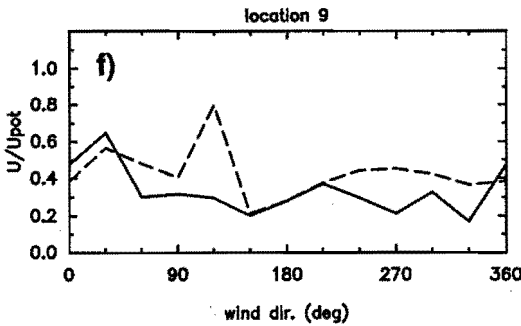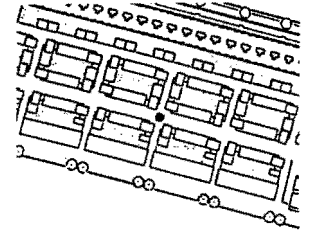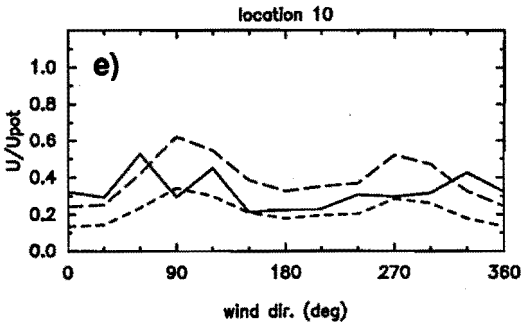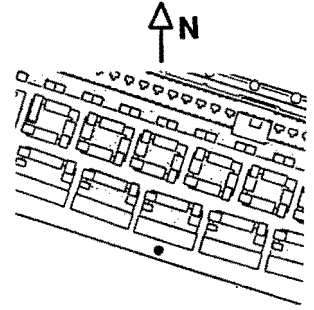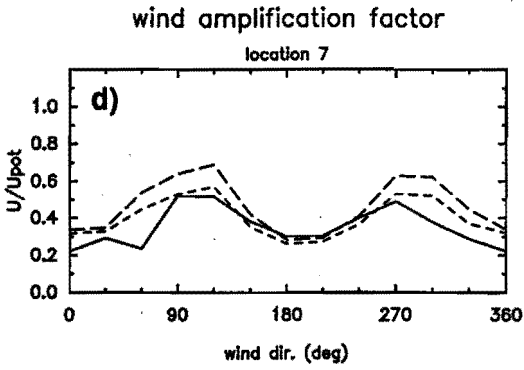
Figure 6.11: Continued.
d)   Location 7: at southerly quay
e)   Location 10: street crossing; interior of island
f)   Location 9: plaza at western part of island

170

For location 7, there are no complicated building geometries, trees, and other features which can make prediction of γ difficult. Desk estimates give a fair but conservative estimate of γ.

For many wind directions, there is excellent agreement between the improved estimate and the wind tunnel data. For northerly winds however, wind speed reduction in the wake of the buildings has been underestimated.

Location 10 is placed within a regular building group. Still, desk estimates prove to be inaccurate and overconservative. This is because data were taken rather straightforward from Visser (1987).

The improved estimates use a reference speed above the building group, e.g. $U_{2.5h}$. Still, the measured peaks are not predicted by the improved method. Furthermore, it is worth noting that at (the similar) location 11, only the peak at 330° is observed, not both peaks around 90°. The behaviour, and the cause, of these peaks can not be explained yet.

Location 9 is typical for rather complex geometry around a plaza. The estimates are too high for $\gamma \approx 120^\circ$ and for westerly winds. In the first case, it was wrongly assumed that the wind could just pass around the trees, without any wind speed reduction. In the second case, shelter of the nearby plaza building is underestimated.

No improved results are available because of the complexity of the site.

The position (in terms of wind direction θ) of peaks in γ is generally predicted well (see fig. 6.11). Half of the predicted peaks is within 45° of a measured (wind tunnel) peak. Near high rise buildings, 80% of the peaks is within 45° of a measured peak.

Up till now, we have discussed differences between wind tunnel data and estimated data in a rather qualitative way. In the following, the errors will be quantified. The differences between desk estimates and wind tunnel estimates may be judged in two ways.

First, we may consider the difference in the 'effective' wind amplification factor γ_e (the difference is written as $\Delta\gamma_e$). In this way, we can judge the resulting wind climate (discomfort).

Alternatively, we may consider the difference between wind tunnel γ and estimated (desk) γ for each location (fig. 6.7), and for each wind direction. These differences may be combined in a 'standard difference' σ_Δ which is defined in the same way as a conventional standard deviation σ:

$$\sigma_\Delta^2 = \overline{(\gamma_{EST} - \gamma_{WT})^2} \qquad (6.1)$$

This squared difference between wind tunnel γ and estimated γ is averaged for all (12) wind directions.

We may interpret σ_Δ and $\Delta\gamma_e$ in the following way:

A small σ_Δ with large $\Delta\gamma_e$ indicates errors in magnitude of (peaks in) estimated γ. On the other hand, a large σ_Δ with small $\Delta\gamma_e$ indicates errors in prediction of wind direction with maximum γ.

loc.	1	2	3	4	5	6	7	8	9	10	11	12

STANDARD DIFFERENCE σ_Δ (estimate minus wind tunnel):

	1	2	3	4	5	6	7	8	9	10	11	12
EST	0.27	0.19	0.16	0.25	0.22	0.25	0.15	0.14	0.19	0.15	0.19	0.24
IMP	0.14	0.19	0.16	0.17	0.12	0.11	0.14	0.14	0.19	0.14	0.10	0.20

EFFECTIVE DIFFERENCE in γ : $\Delta\gamma_e$ (estimate minus wind tunnel):

	1	2	3	4	5	6	7	8	9	10	11	12
EST	0.01	0.13	0.06	0	0.13	0.13	0.09	0.10	0.05	0.06	0.13	0.15
IMP	-0.02	0	0.06	0	-0.02	0.01	0.03	0.10	0.05	-0.11	-0.03	0.11

DISCOMFORT PROBABILITY (days/year):

	1	2	3	4	5	6	7	8	9	10	11	12
EST	47	28	24	27	50	37	20	25	11	8.5	8.5	11
IMP	40	5.2	24	29	12	10	8.6	25	11	0.0	0.1	6.6
WT	44	5.2	11	28	17	8.7	5.0	7.0	4.9	2.4	0.3	0.3

Table 6.8:   *Standard difference σ_Δ, effective difference $\Delta\gamma_e$, and discomfort probability (in days/year) for 12 locations of fig. 6.7b. Note that average γ is if the order of 0.5. WT denotes corrected wind tunnel data, EST present desk estimate, IMP improved estimate. Climate statistics (Amsterdam airport) are from Troen et al (1989).*

Table 6.8 gives the results for all locations, i.e. σ_Δ, $\Delta\gamma_e$ and discomfort probability.

Differences in γ (σ_Δ) decrease from 0.20 for the original desk estimate to 0.15 for the improved estimate. It appears that much of this difference is caused by inaccurate prediction of small γ, and by errors in the prediction of peaks in γ (50% of the peaks is predicted within 45° of a measured peak in γ).

Differences in wind climate (discomfort) are much smaller than suggested by σ_Δ. Typical values of $\Delta\gamma_e$ (difference in the 'effective' γ) are 0.10 and 0.06.
However, even an effective difference in γ ($\Delta\gamma_e$) of 0.06 (12%), results in a discomfort probability which is wrong by a factor 2-3.

For the original desk estimate, large errors are made for almost all locations. Typically, discomfort probability is a factor 3 too high, except in passages between buildings. Clearly, some of the convenience and simplicity must be

sacrificed in order to improve the estimation method. Some suggestions for prediction of γ near high rise buildings are made in section 4.5.

For the improved estimate, the errors are still on the large side. The main errors are:

1. -effects of scattered trees, and trees near building corners, could not be accounted for yet. Both yield typically about 20% reduction in γ.
2. -the assumed z_0 in the improved (FLUENT) estimates was not equal to the wind tunnel (turntable) z_0, which may result in up to 15-20% underestimation of γ near high rise buildings.
3. -non rectangular building geometries (including non rectangular building arrangements) may yield unexpected pressure short circuiting effects which can not be accounted for yet.
4. -too little is known of flow behaviour in low rise building groups, especially in the case of oblique flow.

In the present case, the first two errors will compensate each other (partly). Therefore, further improvements in prediction of γ are only feasible if both the effects of trees, and the effect of turntable z_0, are accounted for.

However, the complexity of the built environment can always be an important error source, as is shown by differences of the locations 3, 8, 9, 10 and 12.

Wind climate evaluation; accuracy and prospects

In the following, we will discuss two issues:
-which is the (feasible) accuracy of a 'simple' desk estimate
-which is the accuracy which can be obtained by an expert model

The accuracy of both estimates is judged by comparison with wind tunnel data. Other factors (e.g. far field linkage methods) will affect the accuracy of estimates as well. This issue is discussed in sections 4.5 and 5.1, not in the present section.

Both desk estimates and expert models should predict γ_e within 10%. Even then, the error in discomfort probability can be a factor 2 (due to the choice of TNO comfort criteria, this applies to the data of this chapter only). This is because discomfort is very sensitive to γ (figure 6.2).
Because of this sensitivity to γ, it is of great importance that wind experts agree on the climate statistics, far field linkage methods, and on the turntable roughness which is to be used.

The present (simple) desk estimates must be considered as too inaccurate, as the relative error in γ_e is typically about 20%. Fortunately, the desk estimates tend to be conservative, at least near high rise buildings. Data of chapter 4 can be used to improve desk estimates for high rise buildings. However, this can only be done at the expense of convenience.

Expert models are expected to be much more accurate. Stathopoulos et al (1991) reported that their expert model could estimate γ for a building complex with a typical relative error of 8%. However, they considered only one wind direction (perpendicular flow).

The present improved estimates yield a relative error of 12%. This figure may be somewhat higher if turntable roughness is accounted for in the correct way. Still, this 12% (or a slightly larger error) is considered to be the most realistic for an urban environment. Table 6.8 shows that the errors are still on the high side, particularly in complex geometry, and in low rise building groups.

The errors can be reduced if the following can be modelled (in a better way):
> -influence of local ground surface (turntable) roughness
> -influence of scattered trees, and of trees near building corners
> -flow in low rise building groups
> -flow around non rectangular (groups of) buildings

An expert model with a suitable flow field database, and a number of routines which can deal with the above given issues, will be much more accurate than a 'simple' desk estimate.

Even then, the complexity of the built environment remains a significant error source. In complex geometries, a relative error in γ of 20% (for given wind direction) may be the best that can be achieved.

Up till now, we have not discussed the accuracy of design rules. Wind climate at a specific location can not be predicted with the present design rules (chapter 7). In the present design rules, only the worst affected location near a building (or in a street) is considered.

The accuracy of the present design rules is expected to be significantly better than the accuracy of desk estimates. This is because wind speed maxima (e.g. close to building corners) are relatively insensitive to the complexity of the built environment.

6.4 Summary and conclusions

The main issues of this chapter are:
-early cooperation between wind expert and architect
-validation of early wind comfort advice by means of a wind tunnel test

During cooperation between the author and the architect (prof. R. Uytenhaak), the following issues have been considered (table 6.1):
-planned human activities; required shelter
-available shelter at undeveloped site; shelter to be offered by buildings
-sketch design
-evaluation; finishing touches

The considered site (where e.g. houses, shops and a park are planned) is the Java-island in the river IJ in Amsterdam (figure 6.1). Wind climate on the

174

undeveloped site is just tolerable for 'walking fast' activities (table 6.2, fig. 6.3). Locations which are intended for 'sitting/standing' activities require 50% wind speed reduction, other locations ('strolling') about 20%.

A low rise building development has been chosen for various reasons, including wind comfort. Figure 6.4 - 6.6 give an impression of the advice given: No direct connections across the island (short circuiting), short and narrow streets in the interior of the island, and trees for shelter at the quays.

Wind climate for the final design has been evaluated by means of a desk estimate, based on literature data. Wind climate in the interior of the island will be suitable for 'strolling' activities (fig. 6.7, table 6.2). At the quays, wind climate will be suitable for 'walking fast'. Comfort requirements for 'sitting / standing' activities (table 6.2) are not met because:
-very short streets were not preferred because of accessability and social control
-quays are difficult to shelter
-the width of the island was only 132 m (easy wind penetration)
Wind tunnel data show that the interior of the Java-island still has a better wind climate (fig. 6.9) than the interior of the neighbouring KNSM-island. This may be caused by the dense building structure on the Java-island.

The other main issue of this chapter is validation of early advice by means of a wind tunnel test. It turns out to be of great importance to use the same starting points in desk estimate and wind tunnel test.
In section 6.3, corrections are made for the influence of:
-differing climate data (table 6.4)
-different estimates of terrain roughness (z_0) and differing methods to link local wind speed to wind speed at a meteorological site at which climate data are available (fig. 6.10)
-local ground surface roughness at the considered site (p. 166)

The error in the present desk estimates (i.e. the difference between wind tunnel data and desk estimates) could be determined after correction for the above starting points. Figure 6.11 and table 6.8 show a comparison between the present desk estimates and wind tunnel data. The relative error in wind speeds is about 20%, whereas an error of 10% would just be acceptable.
Table 6.6 suggests how the desk estimates can be improved, e.g. by directly using the present numerical data. Then, the relative error reduces to about 12%. It is expected that expert models can achieve about the same accuracy. Future research (p. 174) may yield still better accuracy. However, in very complex geometries, an accuracy of 20% may be the best that can be achieved.

Finally, it is noted that the design rules of chapter 7 are expected to be more accurate than the present desk estimates. This is because the design rules are based on wind speed maxima (e.g. near building corners), which are relatively insensitive to the complexity of the built environment.

7   Rules of thumb for design

Wind climate is dependent on surrounding terrain and on building geometry. This chapter gives a number of graphs and statements which allow the architect to judge whether wind climate will be acceptable on all locations in a street or near a building.

Section 7.2 and 7.3 give rules of thumb for design of streets (low rise building groups), and for design of high rise buildings. The main points are summarized in section 7.4.

The design rules are set up in the following way:
-illustration of flow patterns
-basic graphs for wind climate evaluation
-application and extension of basic graphs
-remedial action

7.1   Definitions

High rise buildings are defined as buildings with a height **H** which is at least 50% higher than the average height h of surrounding buildings. Details such as small penthouses do not contribute to H. Building width is indicated as **W**, building length (or thickness) as **L**.

high rise buildings: at least 50% higher than surroundings

site and surrounding terrain:

building

within 500 m: site

beyond 500 m: surrounding terrain

177
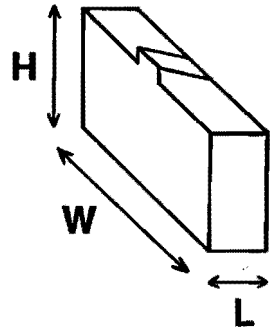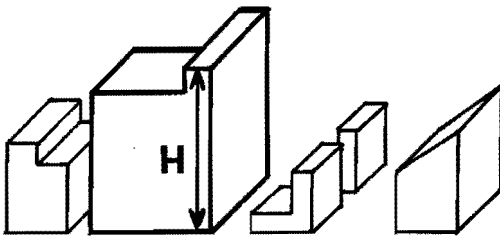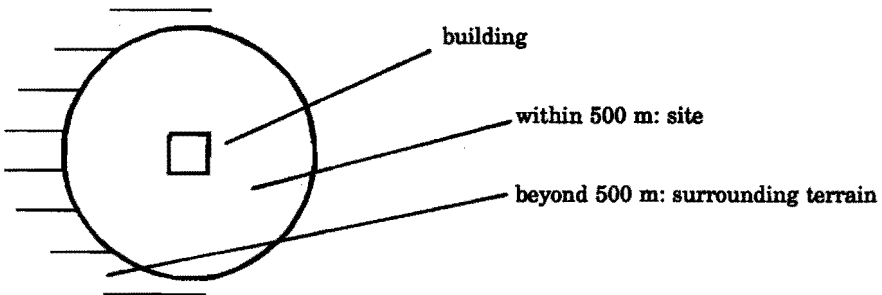
regular building groups:

at least 9 buildings or 3x3 rows   street length $\dot{S}_x$ and street width S_y
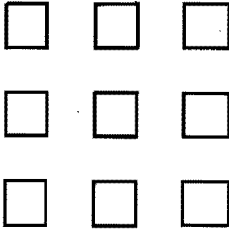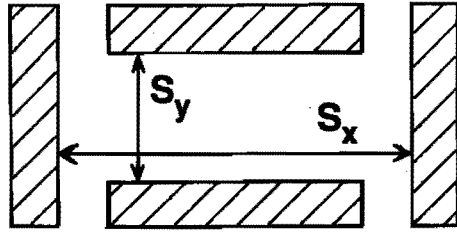

Low rise (or regular) building groups are defined as groups with at least 3 building rows in each direction, and a typical height **h** of up to 20 (typically 10) meter). Maximum building height is less than 1.5 times the average building height. Street length S_x and street width S_y are defined as clear spacing between two opposite building faces, street length being the larger of the two. Surrounding terrain is defined as the dominating terrain at distances of 0.5-20 km from the considered street. Table 7.1 gives a classification of terrain types.

1	Open water	Open sea, large lake, tidal flat, tarmac, concrete, all with free fetch of several kilometres
2	Open field	Level country with low vegetation (grass), obstacles with separations of at least 50 obstacle heights. Typical for some locations near Dutch coast and IJsselmeer.
3	Farmland	Landscape with high crops or crops of varying height. Scattered obstacles (dense shelterbelts, vineyards) at spacings of about 15 obstacle heights. Typical for farmlands in most parts of the Netherlands.
4	Suburb	Built up areas with average building height of 2 storeys or less. Also bush land, orchards, young and densely planted forests, park landscape with many large obstacles (e.g. clumps of forest).
5	city	Village or town with average building height up to about 7 storeys; no Manhattan like structures. Also mature, regular forests.

Table 7.1:   Classification of surrounding terrain as used in this chapter.

Judgement of wind climate starts by stating which class of human activities is allowed. Table 7.2 gives a description of each class. The percentage of hours for which uncomfortable conditions are allowed is 2% for class A, 10% for class B and 15% for class C (table 5.1). For all classes (D included), wind conditions should be *safe*: dangerous conditions are only allowed for a few (3.5) hours per year.

178

A	Long stay	Sufficient shelter for all human activities, including locations with 'long stay' activities such as terrace, swimming pool, open air theatre, and locations which are used daily by elderly people.
B	Short stay	Sufficient shelter for 'short stay' activities: sitting or standing. To be applied for shop centres, squares, bus stops or playgrounds. Insufficient shelter for typical 'long stay' activities.
C	Strolling	Sufficient shelter for locations with 'strolling' activities: park, shop centre, footpath, building entrance, park. Cycle tracks may belong to class C or class D. Insufficient shelter for typical 'short stay' and 'long stay' activities.
D	Walking fast	Only sufficient shelter for locations with 'walking fast' activities: car park, side walk, road.

Table 7.2:   Classification of human activities and related outdoor areas in terms of sensitivity to wind.

7.2   Regular building groups; streets and squares
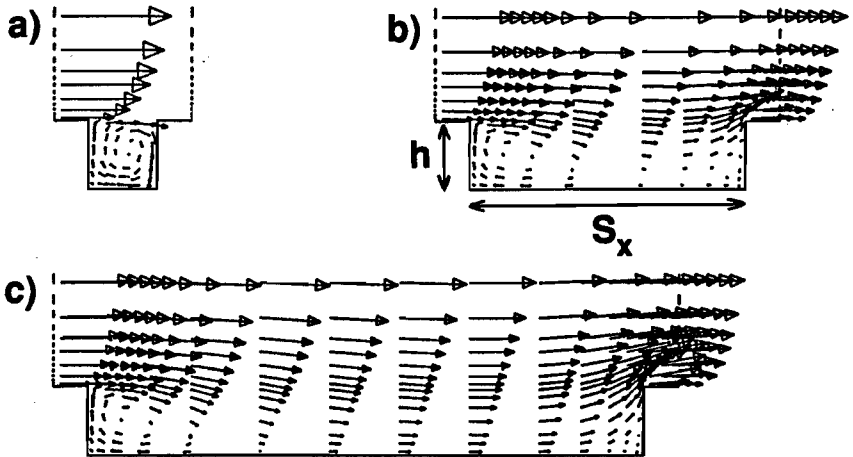
Wind climate in streets; flow patterns

Figure 7.1:   Flow regimes in regular building groups. Note that the flow regime is determined by the ratio of street length over building height (S_x/h).
a) $S_x/h = 1$ skimming flow
b) $S_x/h = 4$ wake interference flow
c) $S_x/h = 8$ isolated roughness flow

179

Wind climate in streets is primarily determined by the ratio of street length and building height. Figure 7.1 shows a 'skimming flow' regime where wind flows smoothly over the roofs, an intermediate 'wake interference' regime and an 'isolated roughness' regime where wind flow enters the street.

Wake interference flow and isolated roughness flow are most favourable for removal of air pollutants from streets. Skimming flow will result in insufficient air pollutant removal as flow only 'skims' over the building roofs. Street width in streets with much traffic should be at least 4 building heights.

For wind comfort, short streets ($S_x/h < 4$) are most favourable. For longer streets, wind 'falls' into the streets, and shelter decreases. Figure 7.2 and 7.3 show which street lengths are allowed for different terrains and different human activities. Applications and extensions of these graphs will be discussed.

Wind climate in streets; basic graphs

street length and terrain type

Figure 7.2: Relative street length (street length divided by building height: S_x/h) for which wind climate is acceptable. The x-axis gives 5 terrain types as given in table 7.1. Street orientation is SW-NE. A, B, C, D indicate allowed types of activities: long stay, short stay, strolling, walking fast (table 7.2).

Figure 7.2 is only valid if the considered building group (size up to 500 m) is surrounded by at least 10-20 km of uniform terrain. We can use figure 7.2 either for small villages (use terrain class of surroundings) or for very large cities (terrain class 5). In the Netherlands, distance to the town edge is generally important, and figure 7.3 should be used.
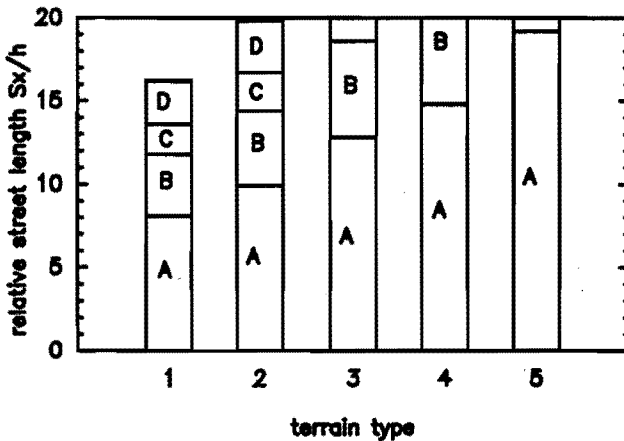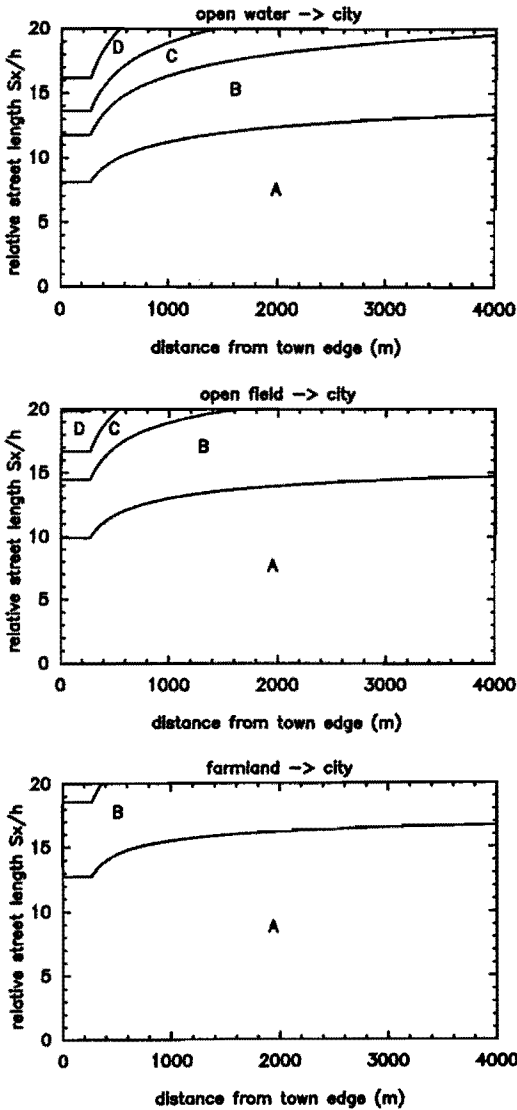
Figure 7.3: *Relative street length (street length divided by building height: S_x/h) for which wind climate is acceptable. The x-axis gives distance to town edge in metres. Street orientation is SW-NE. A, B, C, D indicate allowed types of activities: long stay, short stay, strolling, walking fast (table 7.2).*

a)   *City (terrain class 5) surrounded by open water (class 1)*
b)   *City (terrain class 5) surrounded by open field (class 2)*
c)   *City (terrain class 5) surrounded by farmland (class 3)*

Wind climate in streets; application

General; Interpretation of basic graphs:
The estimates of figure 7.2 and 7.3 are primarily meant for streets *within* a regular building group. Street lengths greater than 20 building heights are not shown as longer streets may be considered as 'infinite'. All estimates are valid for locations near Amsterdam. Other locations are discussed under 'regional design'.
Figure 7.2 shows significant increase in maximum street length as surrounding terrain becomes rougher. Typical 'long stay' activities require a maximum street length of 8 building heights if the site is near open water. In a very large city, street length may be 19 building heights. 'Walking fast' activities do only require street length reduction (to 16h) near open water. Figure 7.3 shows strong dependence of maximum street length on distance to the town edge, especially in the first kilometre. At larger distances, allowed street length increases rather slowly.
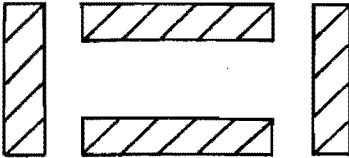
Application to crossings:
Figure 7.2 and 7.3 give a fair estimate if street length of the windiest (generally the longest) street is taken.

Application to large squares:
Figure 7.2 and 7.3 give a fair estimate, but a conservative estimate can be obtained by reducing allowed street lengths by 30%.

street within group   outward road
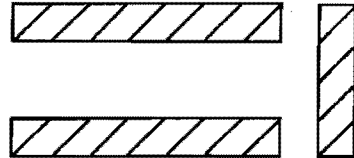
Application to outward roads:
Roads connecting the building group with the surrounding terrain should be considered as roads of 'infinite' length (i.e. $S_x/h = 20$).

Building height:
All graphs assume a uniform building height of 10 m. Changes in building height have little effect except at the edge of the building group. In cities, a twofold increase in building height requires 20% reduction in street length. Effects of slight variations in building height are expected to be small.
High rise buildings however, may destroy all shelter in streets. Wind sensitive activities should not be located near high rise buildings. Design rules for high rise buildings are given in section 7.3.

182

Street width:
If relative street width S_y/h is less than 6, streets may be about 15% longer than in base graph. Street width (or at least street length) should be more than 4 building heights if removal of air pollutants is important.

Narrow streets with perpendicular buildings

$$\nearrow S_y < 2h$$
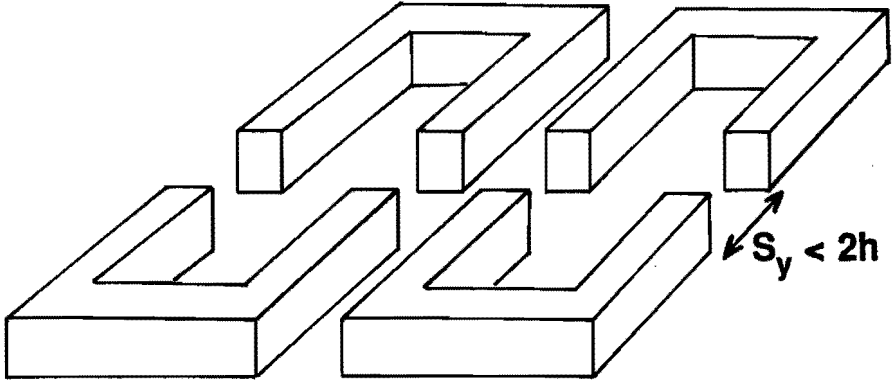
Building arrangement:
For narrow streets ($S_y/h < 2$), building arrangement can be very important. If buildings are placed perpendicular to a long but narrow street (see sketch above), wind climate may be the same as for a street with a length of 10 building heights h (i.e. the 'effective' street length is 10h).
At a larger scale level, building arrangement is a means of providing short streets. A network of T-crossings (see sketch below) is recommended for long islands, and for ribbon developments (in Dutch: lintbebouwing).

Network of T-crossings
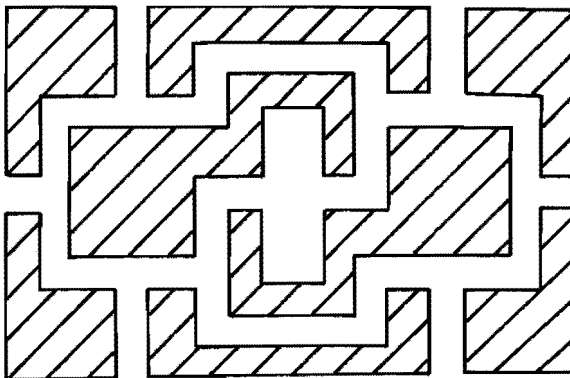
$$d > 2h$$

Effect of hills:
Hills may have a strong influence on wind climate. Street length should be reduced at the upper half of a hill. At the crest of a ridge, the street length reduction factor can be as large as $1 + 5*\tan(\alpha)$, where α is the average slope of the ridge (α less than 10°). For the crest of an escarpment, a reduction factor of $1 + 2.5*\tan(\alpha)$ applies.

Regional design:
The present estimates are valid for locations near Amsterdam. The influence of surrounding terrain (table 7.1) is accounted for in fig. 7.2 and 7.3. Climatic differences in the Netherlands result in ±13% variation in allowed street length. Differences are within 20% for a coastal zone of about 200 km width which extends from Brittany (France) to Denmark, and for England (not Ireland and Scotland). General guidelines for other (southern) parts of Europe can not be given as wind climate is often highly location dependent.

Wind climate in streets; remedial action

Street width:
It is already mentioned that narrow streets ($S_y/h < 2$) with perpendicular buildings reduce effective street length to 10 building heights.

Street orientation:
If relative street width S_y/h is less than 6, a NW-SE orientation of a street allows for 25% increase in street length, compared with a SW-NE oriented street (as in base graphs). A NW-SE orientation yields also more air pollutant removal in conditions with weak (southeasterly) winds, when background pollutant levels are often high.

Rows of trees:
The sketch below shows a section *across* a street. If clear spacing between tree crowns is written as S, street length may be increased by 25% if $S/h = 3$. For dense 'canopies', with $S/h < 0.4$, street length may be increased by a factor 2 or even more. The above reductions should only be applied if the distance between buildings and trees is small as well (less than distance between tree crowns).

Effect of tree rows in streets

Street length may be increased by:

25%   100%

3h   **0.4h**
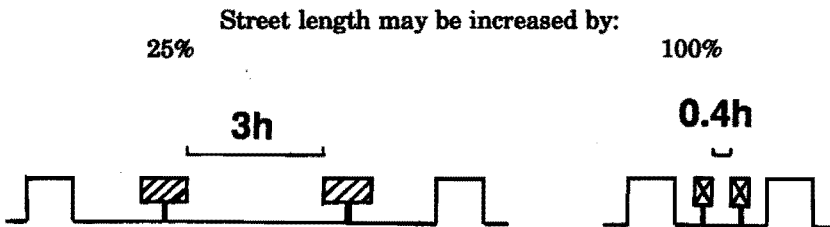
7.3   High rise buildings

This section discusses wind climate near (small groups of) high rise buildings. Wind climate is mainly determined by building height H by the surrounding terrain.
Wind climate in the interior of large skyscraper districts is not considered here. Suffice to say here that wind flow in large, homogeneous, skyscraper districts has some analogy with wind flow in streets (section 7.2).

Wind climate near high rise buildings; flow pattern

Figure 7.4 shows three typical time averaged flow patterns around buildings. Instantaneous flow patterns may look rather different as the flow is highly unsteady, especially in the wake.
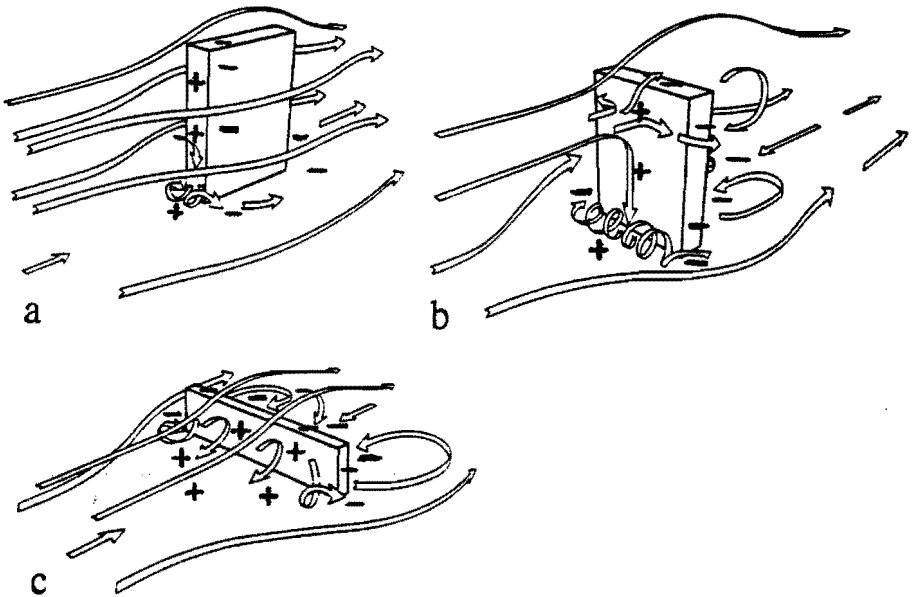
Figure 7.4:   Time averaged flow patterns around isolated high rise buildings (Beranek, 1984). Zones with positive and negative wind pressures are indicated with '+' and '-'.
a)   Tall building: flow mainly along the sides.
b)   Intermediate or transitional type: flow along sides and over roof.
c)   Wide building: flow mainly over roof.

Figure 7.4 may be helpful for a first estimate of air pollutant dispersion, but it does not show where high wind speeds occur. These high wind speeds are caused by short circuiting of positive wind pressures on the windward side of the building, and negative wind pressures at the leeward side.

185
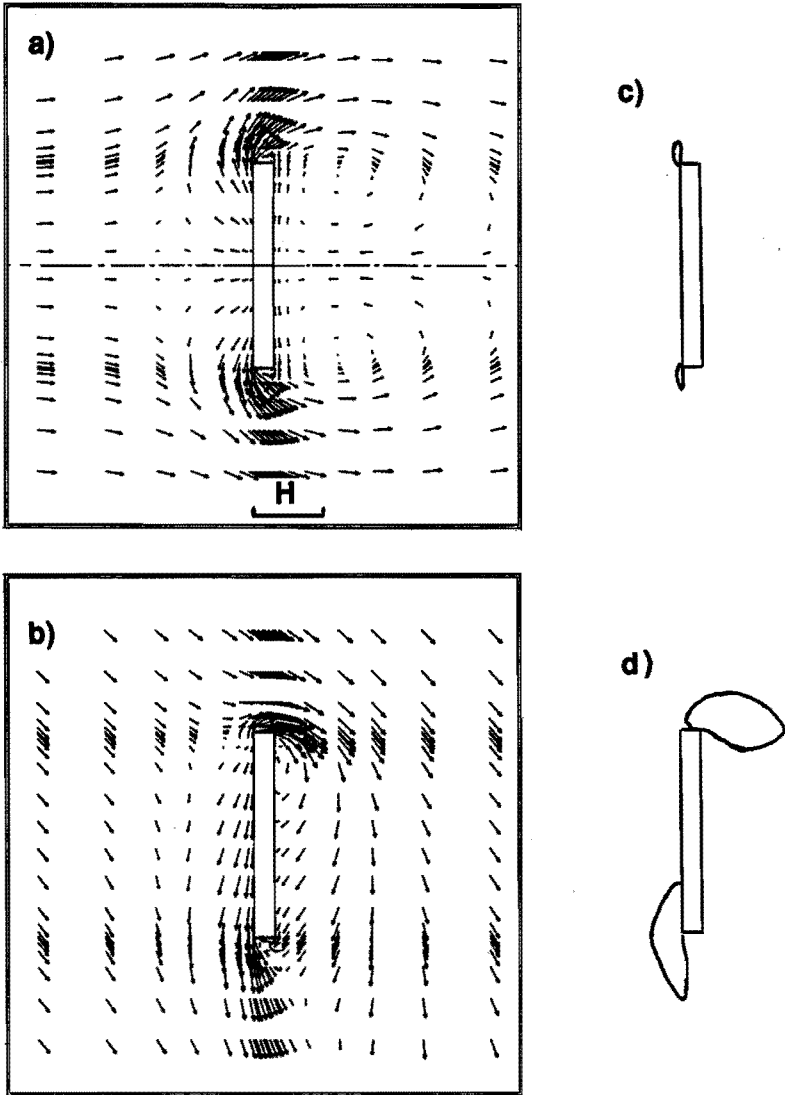
Figure 7.5: Time averaged pedestrian level flow pattern around a building of 15x150x50 m (thickness, width, height) together with location of high wind speed regions (corner streams).

a)   Flow pattern for normal flow (perpendicular to longer building face)
b)   Flow pattern for oblique flow (flow at angle of 45°)
c)   High wind regions (corner streams) for normal flow
d)   High wind regions (corner streams) for oblique flow

Figure 7.5 shows high wind speed regions near a high rise building. In the case of oblique flow (at an angle to the building faces), wind flows rather easily downstream along the windward building faces. This may be an explanation for the fact that oblique flow yields the highest wind speeds, even though pressure differences over the building are smaller.

High rise buildings do offer some shelter as well. The main shelter can be found in the recirculation zone behind the building, for normal flow.

Wind climate near high rise buildings; basic graphs

The main issue is whether wind climate is acceptable or not. Figure 7.6 shows maximum building height for a number of human activities. As in figure 7.2, surrounding terrain is uniform over at least 10-20 kilometres. Hence, figure 7.6 can only be used for small villages (use terrain class of surroundings), and for very large cities. Figure 7.7 shows maximum building height for towns of finite size.

building height and terrain type
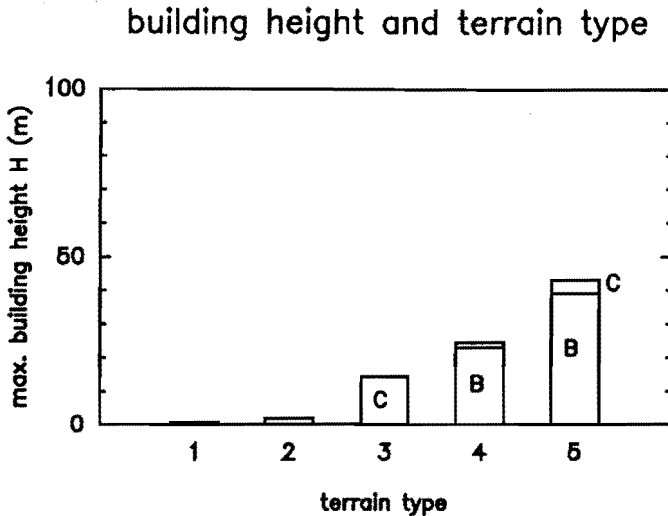
Figure 7.6:   *Maximum building height H for which wind climate is acceptable at all nearby locations. The x-axis gives 5 terrain types as given in table 7.1. 'B' and 'C' indicate allowed activities ('short stay' and 'strolling'; table 7.2). Valid for all building orientations.*

Comfort class 'A' is not indicated in figure 7.6 because in all cases, high rise buildings yield locations which are not suitable for 'long stay' activities (A). 'Walking fast' areas (D) coincide with 'strolling areas' (C) as the safety requirement turns out to be rather restrictive.

187
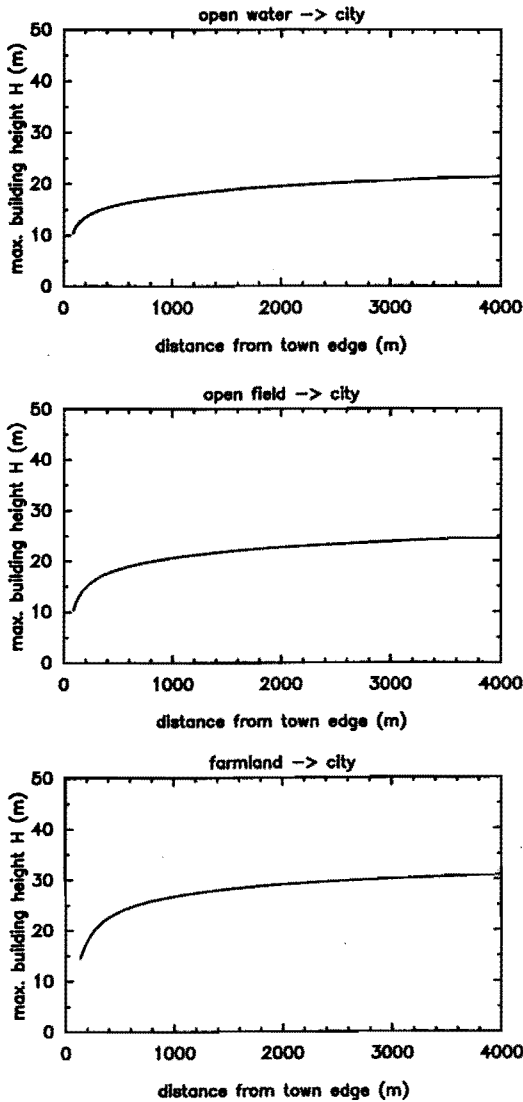
Figure 7.7: Maximum building height for which wind climate is acceptable at all nearby locations. The x-axis gives distance to town edge in metres. Area below solid line is acceptable for 'walking fast' and 'strolling' activities. Valid for all building orientations.

a)   City (terrain class 5) surrounded by open water (class 1)
b)   City (terrain class 5) surrounded by open field (class 2)
c)   City (terrain class 5) surrounded by farmland (class 3)

188

In the open field, and near open water, the safety requirement can not be satisfied. Allowed building height increases up to 43 m in (centres of) very large cities. The influence of the town edge is especially clear in the first kilometre. At one kilometre from the town edge, maximum building height varies between 16 and 26 m (town surrounded by open water and farmland respectively). At larger distances, maximum building height increases very slowly.

A maximum building height of 25-40 m may not be feasible in practice. However, twice the 'allowed' building height results in a factor 5 increase in danger probability (to 20 hours per year) and a factor 2 increase in discomfort probability (to more than 25% of time). Such high buildings yield areas near building corners which are unsuitable for human activities during part of the year. The unsuitable areas can be described by a danger circle at building corners (see sketch). Table 7.3 gives dimensions of the danger radius R_{dan}.
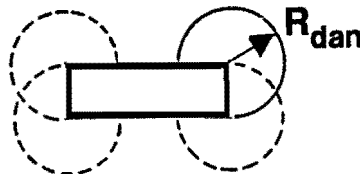
terrain class		danger radius R_{dan} is the lesser of:
2	open field	1.8*H and 3.0*(W*H)/50
3	farmland	1.0*H and 1.7*(W*H)/50
4	large suburb	0.6*H and 1.1*(W*H)/50
5	large city	0.4*H and 0.6*(W*H)/50

Table 7.3:   Order of magnitude estimate of danger radius R_{dan} if building height H is between 50 and 100 m. Building width W is between 15 and 150 m. Within a distance R_{dan} of building corners, danger probability is too large for the activities of table 7.1. Building orientation is assumed to be NW-SE.

It is important to note that the estimates of table 7.3 are overruled if the following design rules, and figure 7.6 and 7.7, yield an acceptable building height H, even if this H is greater than 50 m.

Wind climate near high rise buildings; application

General; Interpretation of basic graphs:
Figure 7.6 and 7.7 are meant for (groups of) high rise buildings as defined in section 7.1. Manhattan like districts should be investigated in a wind tunnel.
In very large cities, building height should not exceed 45 m in order to guarantee that all nearby locations are suitable for at least 'walking fast' activities. Downward revision is required for other activities and near a town edge. Table 7.3 shows dimensions of the area of increased danger near building corners if these requirements are not satisfied.

189

Building dimensions:
The main building dimensions are building height H and building width W. Figure 7.6 and 7.7 apply to wide buildings (W/H > 2). The allowed building height increases gradually with increasing slenderness. Building height may be increased by a factor 1.3 if W/H < 0.5.

Still, the best way of achieving a good wind climate is to reduce building height. Wind climate near building corners will improve (figure 7.6 and 7.7) and danger areas (if present) will reduce in size (table 7.3) or disappear. Sheltered areas at the longer building sides will increase in size as building width increases (assuming that building volume remains constant). However, additional measures are needed to maintain this shelter for W/H > 2.

Finally, closely spaced buildings may act as a single building mass (see sketch). In this way, a group of slender skyscrapers may still act as a very high and wide building. In the passages, wind climate will not be much better than at the corners of the building mass.

Building mass:

< 20% open
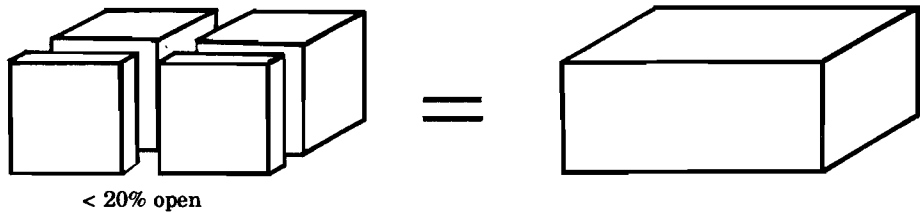
Urban context; nearby low rise buildings:
The main parameter is L_g/h where h is the low rise building height. L_g is the geometrical length scale, defined as the lesser of W and 2H. Allowed building heights change little, except for short stay activities (class B). These heights may be increased by 10% if $L_g/h = 3$ and by 30% if L_g/h is less than 1.5. Maximum building heights can not be relaxed for buildings at large open areas in cities. Building height should even be reduced by 25% in order to satisfy safety requirements.

type of building group:	correction factor:	'short stay'	'walking fast'
aligned buildings	(- -)	1.0	1.0
build. behind each other	(| |)	1.0	1.0
shifted buildings	(' ,)	0.8	0.9
cross arrangement	(+)	1.3	1.3
open square arrangement	(□)	2.0	1.7

Table 7.4: *Building arrangement and correction factors, to be applied on building heights of figure 7.6 and 7.7. Building arrangement is given in brackets, and in figure 4.18. Building orientation is SW-NE. See table 7.2 for typical 'short stay' and 'walking fast' locations.*

190

Building groups:
As a general guideline, enclosure (□: square arrangement) works beneficial, and pressure short circuiting effects (ˈ₁ : shifted buildings) are disadvantageous. Table 7.4 quantifies the effects for some typical building arrangements.
Wind climate in passages is good if buildings are placed behind each other, and bad for a passage between shifted buildings.
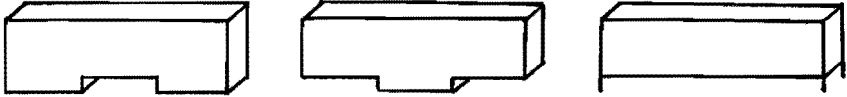
Buildings with gaps:
Pedestrian level gaps yield considerable deterioration of wind climate. This applies to all gap types. Wind climate is only acceptable if building heights in fig. 7.6 and 7.7 are reduced by 40%. If building height is too large, danger area is 50% larger than indicated by table 7.3 (except for centre gap). The 'length' of the affected area (perpendicular to longer building face) is of the order of 10 gap heights or gap widths, whichever is the less. The affected area can be made small by reducing gap dimensions. Remedial action for the gap itself is almost impossible; often a 'labyrinth' of screens is needed (Grand Arche in Paris).

Effects of hills:
High rise buildings should not be placed at the upper half of a hill. The allowed building height can be reduced by over 50%, even on hills with a slope of 5%.

Regional design:
The allowed building heights are about 30% lower at the North Sea coast, and about 50% higher in the southern part of Limburg. The influence of surrounding terrain is still larger (table 7.1; fig. 7.6 and 7.7).

Wind climate near high rise buildings; remedial action

Orientation of a building:
Building orientation has little effect on acceptability (safety) of wind climate near building corners. Wind climate in passages and in centre gaps in buildings improves considerably if the passage is oriented NW-SE instead of SW-NE.

Corner shape:
Rounded corners may allow for 30% increase in building height, except for very thin buildings (L << W). The effect of triangular, and other non-rectangular building shapes is not clear.

Podium shaped extensions:
Buildings with podium shaped extensions have generally a much better wind climate. A podium with size L_p (see sketch on next page) larger than either W or 2H generally yields a wind climate which is dominated by the podium. This applies to all given podium types.

Podium types, and definition of podium size L_p (plan view):
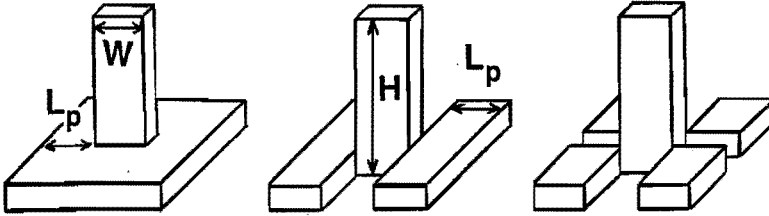
Building extensions for creating shelter at longer building faces (e.g at quay):
Hatched area denotes high rise building plan.

length > 2H

d < 2H
d < 8h
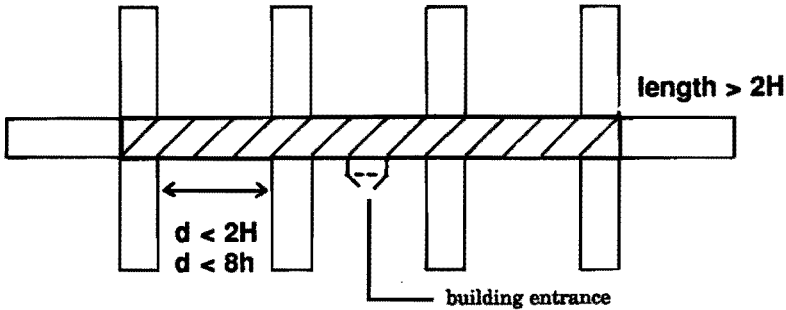
building entrance

Location of building entrances and pedestrian walkways:
Building entrances can best be located near the centre of the longer building face. Wind conditions near building corners and in building gaps are unfavourable, both for people and for doors. Entrances should be avoided here. The same applies for pedestrian walkways around the building. Entrances and walkways which are used by elderly people should be equipped with handrails. The will reduce probability on accidents.

Screens and trees:
Scattered trees will allow for 30% increase in building height. The effect of screens could not be quantified. The best arrangement is shown below:

Optimum location and orientation for wind screens near building corners:

7.4 Summarizing statements

General

1. These rules of thumb give maximum building and street dimensions for which wind climate is acceptable at all nearby locations.

2. Terrain within 10-20 km of the site has a significant influence on wind climate.

3. Hill tops have a particularly unpleasant wind climate.

4. Large water surfaces (lake, river) within a town may cancel all urban shelter; wind climate is comparable with wind climate at a town edge.

5. These design rules are meant for the information and sketch design stage. They should not replace afterwards (wind tunnel) testing.

Regular building groups; streets and squares

1. A maximum street length of 8-19 building heights (depending on surrounding terrain) is acceptable for all human activities. Outward roads at a town edge require further wind reducing measures.

2. Narrow streets (street width less than two building heights) with perpendicular buildings or irregular building faces yield much wind reduction and are generally acceptable from a wind comfort viewpoint. Tree rows yield much wind reduction if distance of tree crowns is less than one tree height (one tree crown width for slender tree).

3. If air pollutant removal is important, street length (and preferably street width as well) should be more than 4 building heights.

4. A NW-SE street orientation of streets yields slightly better conditions, both for wind comfort and for air pollutant removal.

High rise buildings:

1. High rise buildings (with height at least 50% larger than surroundings) tend to bring roof height wind speeds down to pedestrian level.

2. Long stay activities should not be situated near high rise buildings, and high rise building should not be situated near existing long stay activities. Building entrances and pedestrian walkways should be located at the long sides of the building, and certainly not near building corners, or in building gaps.

3. Building heights over 20-45 m (depending on surrounding terrain and distance to town edge) result in violation of safety requirements, and in large areas of increased danger. The allowed building height may be larger if remedial measures are taken (6), or if building height is uniform (interior of large skyscraper districts such as Manhattan).

4. Climatic differences within the Netherlands have significant influence on allowed building height; building height near the North sea coast should be reduced by about 30%.

5. Buildings with pedestrian level gaps (e.g. buildings on columns) yield considerable deterioration of wind climate and require a 40% reduction in building height.

6. Wind climate may be improved by rounded corners, by trees, and by podium shaped extensions. Both rounded corners and trees (preferably at building corners) may allow for 30% increase in maximum building heights. Podia (against building corners) will dominate wind climate if the size of the (podium) extension is one building width, or two building heights.

7. In groups of high rise buildings, building arrangement has little influence on allowed building height. Exceptions are shifted ($^|_|$) buildings which are disadvantageous (pressure short circuiting) and square (□) arrangements which are beneficial (enclosure).

8. Building orientation is only significant for wind climate in passages between buildings, and for (centred) gaps in buildings. The best orientation of passages and gaps is NW-SE.

8   Conclusions and future work

8.1   Conclusions

The aims of this study are given in section 1.3. Chapter 2 - 6 give the results of re-evaluation and extension of the present wind comfort knowledge. Chapter 7 gives results of knowledge transfer as rules of thumb for the architect. The main conclusions for each chapter are given below.

Measuring and simulation techniques are discussed in *chapter 2*. Numerical simulations have led to a better understanding of obstacle flow (section 2.2). Validation of numerical results yielded the following conclusions:

2.1   -Hot wire measuring techniques may suffer from large systematic errors if measured turbulence intensity is greater than 30%. Laser Doppler techniques are needed for these large turbulence intensities.

2.2   -The present numerical model can predict mean and turbulent properties (U/U_{Ho}, C_{pHo} and K) within 10-20% of wind tunnel data. This applies to single buildings, and to small or regular groups of buildings (p. 41). Significant improvement is only expected if better modelling techniques are combined with a finer grid (factor 10 increase in grid points).

2.3   -An important limitation for all numerical models is the fact that the first grid node near the wall must be greater than $20z_0$. In practice, building height H should be larger than $50z_0$, and the urban canopy should be at least $20z_0$ above pedestrian level. If these requirements can not be satisfied, all individual roughness elements should be modelled, which is not feasible. Alternatively, too small a z_0 must be chosen in the proximity of the obstacle.

Wind comfort criteria (*chapter 3*) are the basis of any wind climate judgement. Criteria can be split into a discomfort threshold (mean wind speed or gust speed which is experienced as unpleasant) and a maximum percentage of time in which the threshold is exceeded (maximum discomfort probability).

3.1   -Existing models are not suitable for thermal comfort evaluation as turbulence effects are not accounted for. Incorporation of these effects is essential (Fanger et al, 1988). In may cases, people's activities (metabolism) and outdoor circumstances (sun/shade) are so variable (in space and time) that comfort modelling is not possible at all.

3.2   -Existing discomfort thresholds (due to mechanical wind effects) are based on intuition and on observed effects of peak gusts, not on comfort investigations. A suitable threshold ($U + \sigma_u < 6$ m/s) is chosen in section 3.2. Maximum discomfort probabilities are given in section 3.4.

3.3   -Discomfort and danger probability are sensitive to uncertainties in wind amplification factor γ. An uncertainty of 10% in γ results in a factor 1.4 uncertainty in discomfort probability, and about a factor 2 in danger probability.

Wind amplification factor γ (*chapter 4*) links local mean wind speed to mean wind speed at an ideal meteorological site. Wind amplification factor is determined by contributions on three different scale levels:
- topography and surrounding terrain
- building or building group
- details of site

The following conclusions can be drawn:

4.1 -Surrounding terrain (within 10-20 km) has a large influence on wind amplification factor γ. Hills may have a dominating influence on γ.

4.2 -It is not clear which wind profile formulas should be used for locations which are 2 - 20 km downstream of a change in terrain roughness. This results in errors in γ of up to 15%.

4.3 -Neglect of thermal effects (surface heat flux and also horizontal temperature gradients may result in up to 25% underestimation of γ over cities. Thermal effects on γ can generally not be corrected.

Note: The above mentioned errors are not so important in judgement of wind climate as maximum acceptable discomfort probability is also determined by using a γ in which thermal effects are neglected.

4.4 -Pedestrian winds are dependent on many parameters. The importance of the parameters is, in decreasing order: building height H, approach flow angle θ or building width W, local ground surface roughness $z_{0,loc}$ (smooth turntable in wind tunnel!), and building length L or approach flow roughness z_0. Many additional parameters are needed to describe the flow field. Incorporation of flow field data in expert models is only feasible if data analysis is automatized.

4.5 -A suitable presentation of data is essential to allow for linkage to climate data at a meteorological site. As building flow is governed by U_{Ho}, the approach flow wind speed at roof height, U/U_{Ho} is the appropriate wind speed parameter, not $U(z)/U_0(z)$. The same applies to the reference wind speed for the pressure coefficient C_p. Turbulence levels should be represented as K/K_0 (or its square root). Turbulence intensity T_u (σ_u/U) can only be used if wind speed is not close to zero.

4.6 -High wind speed regions near building corners (corners streams) yield an important contribution to discomfort. Oblique flow yields the largest corner streams. The so called Venturi effect for '>' shaped building arrangements is a wrong interpretation of corner stream maxima for oblique flow.

4.7 -Details of building and site (including local ground surface roughness $z_{0,loc}$) may have considerable influence on γ.

4.8 -The relative error in an estimate of γ can be over 20%. Errors in the z_0 estimate may result in up to 15% error. Systematic errors (statement 4.3 and numerical errors) may also contribute to the total error in γ. Consequences for wind climate judgement are discussed in chapter 5.

Estimates of local turbulence properties are needed for a translation of a discomfort threshold (including turbulence) into a local mean wind speed.

4.9 -A good estimate can be obtained by putting σ_u (not T_u) equal to the airport value ($\sigma_{u,pot}$). The standard relative error in this estimate is within 30%.

196

Chapter 5 shows how classification of building and terrain in terms of γ can be converted into a classification in terms of wind climate.

The main conclusions are:

5.1   -A method to judge wind climate should include the effects of surrounding terrain (roughness) and the effects of the building.

5.2   -Wind climate can generally not be judged by wind amplification factor γ alone; discomfort probability should be considered

5.3   -A combined building/terrain classification allows for judgement of the worst affected location in a street, or near a high rise building. Spatial distributions of discomfort probability are often difficult to model.

The first part of *chapter 6* describes cooperation between architect and wind expert in the development of a town plan. In the second part, accuracy of the advice is judged by comparison with wind tunnel measurements.

6.1   -Cooperation between architect and wind expert has led to an improved wind climate.

6.2   -Other factors in design, such as through sight (social control), traffic, and the required amount of dwellings make that requirements with respect to wind climate can not always be fully satisfied.

6.3   -Prediction of wind climate requires an uniform approach on:
　　　　　　　-climate statistics
　　　　　　　-methods to link local wind speeds to potential wind speed
　　　　　　　-turntable roughness
Different prediction methods may yield a factor 2 difference in discomfort probability (and a factor 5 in danger), even when only one of the above 'components' is non standard.

6.4   -Errors in the desk estimate are judged by comparison with wind tunnel data for the same geometry. Differences in discomfort probability are comparable with differences resulting from a 20% relative error in γ. The difference can be reduced to 10% if the present numerical data are used. Further improvement is possible if effects of trees, ground surface (roughness), and non rectangular building geometries can be accounted for.

Chapter 7 presents rules of thumb which may serve to transfer wind comfort knowledge to the architect. He must judge the applicability of this rules.

Some other conclusions are:

7.1   -Rules of thumb are most suitable for early design stages as they may generate ideas of suitable building geometries. Expert models often have a controlling function instead of a generating function.

7.3   -Differing wind climates may have significant consequences for design, even within the Netherlands (see also chapter 7).

8.2 Further research

Prediction of wind climate; criteria

1. Prediction of thermal comfort for long stay activities (outdoor restaurant or open air theatre) may be feasible if turbulence effects can be accounted for. However, extensive comfort investigations are needed as turbulence effects on comfort can only be determined by experiment.
2. Further investigations must lead to suitable discomfort thresholds for all types of human activities, and to suitable danger thresholds for cyclists.
3. The levels of maximum acceptable discomfort probability should be provided of a better experimental basis. Discomfort probability should be determined in such a way that systematic errors (as for conclusion 4.3) are minimized.
4. Habituation to wind needs further investigation.

Prediction of wind climate; wind amplification factor

5. Validity of wind profile formulas over very rough terrain ($z_0 > 1$ m).
6. Development of wind profile formulas which can be used at 2 - 20 km downstream of a roughness change.
7. Incorporation of thermal effects (horizontal gradients and surface heat flux) into estimation of γ.
8. Reliable measurements or simulations for oblique flow and flow parallel to streets (low rise building groups), including turbulence measurements.
9. Modelling of wind flow patterns close to building facades and roofs for predicting wind comfort on balconies etc., and for various other applications (energy losses of buildings, rain penetration, cladding design).

Prediction of wind climate; modelling

10. Further exploratory research on details of building and site (screens, trees, building podia, local ground surface roughness $z_{0,loc}$ etc.) is needed to improve design rules.
11. Expert models need a good and flexible method for classification of building geometries. Extensive parameter studies are needed on all kinds of building groups (low rise, high rise, mixed) and on details of building and site before expert models can predict wind climate on a specific location with acceptable accuracy.

Outdoor climate; general

There is a number of wind related topics which need further consideration:
-dispersion of air pollution in the built environment
-prediction of pressure fluctuations and peak pressures on buildings
-driving rain, and rain penetration into buildings

In a later stage, when all 'basic' research on outdoor climate has been done, it is worthwhile to consider the issue of integration of all environmental aspects. A handbook or an expert model may indicate which way(s) of building yield an optimum outdoor climate.

198

SUMMARY

Wind climate should be considered in the early design stages, where most important design decisions are made. The present day practice of wind tunnel testing at the end of the design process does not allow for this. Rules of thumb for design do exist, but they do not allow the architect to judge whether future wind climate will be acceptable or not.
The aim of this study is to analyze and to supplement existing knowledge of the prediction of wind comfort, and to communicate the results to the architect by means of verbal or graphical design rules. These rules should be applicable in the first stages of design, and they should allow for an early judgement of wind climate.

Chapter 1 discusses outdoor climate and its incorporation into the design process. The state of the art on the prediction of wind comfort is briefly described, and the aim of the present work is formulated.

Chapter 2 presents theories of boundary layer meteorology and obstacle aerodynamics, the fields which are used most frequently in this study. Measuring and numerical simulation techniques are discussed as well. Validation of numerical results made clear which accuracy and limitations are to be expected, not only of the numerical simulations (relative error within 10-20%), but also of the measuring techniques (fig. 2.11 and 2.13).

The issue of wind comfort is discussed in chapter 3. Evaluation of outdoor thermal comfort is not feasible (p. 193, conclusion 3.1). Therefore, only mechanical effects of wind, and their consequences for comfort, are considered. Section 3.3 discusses the relation between discomfort (and danger) probability, shelter and climate (fig. 3.5-3.6). Both probabilities are rather sensitive to uncertainties in wind amplification factor γ, where γ is the ratio of local mean wind speed and wind speed at 10 m height over a grass plain. A 10% increase in γ (for all wind directions) yields a factor 1.4 increase in discomfort probability, and a factor 2 increase in danger probability. Section 3.4 gives an overview of existing comfort criteria (mean or gust speed threshold together with maximum exceedance probability). Criteria are compared by the concept of 'required shelter' (table 3.8). Finally, 'good' criteria are selected.

Wind climate at the considered site is mainly dependent on wind amplification factor γ, with contributions on three different scale levels (fig. 4.30):
     -surrounding terrain
     -building and building group
     -details of site
Each scale level yields an important contribution to γ. Chapter 4 discusses these contributions in detail.
Numerical errors in γ can be up to 10-20%. Linkage of local wind speeds to wind speeds at a meteorological site may result in additional errors over 20%

(conclusion 4.8, p. 196). Routine wind tunnel predictions of wind comfort are affected by the latter error as well.

A good turbulence estimate can be obtained by putting the standard deviation σ_u equal to the airport value. The standard relative error of this estimate is within 30%.

The data of chapter 4 can be summarized in a combined building and terrain classification. Wind climate can generally not be judged by wind amplification factor γ alone. Chapter 5 presents distributions of discomfort probability around buildings. This leads to an improved building and terrain classification for the worst affected location in streets or near high rise buildings (fig. 5.12). Spatial distributions of discomfort probability are often difficult to model.

Chapter 6 gives an example of wind comfort evaluation. Development of a town plan at a windy location in Amsterdam has been described, as well as cooperation between the architect and wind expert. The cooperation led to an improved wind climate. Wind climate could not be fully optimized due to other factors in design such as traffic, through sight (social control), and the required amount of dwellings.

The second part of chapter 6 discusses the accuracy of the advice. Discomfort probabilities, which are estimated during the advice, are compared with results of a routine wind tunnel test. Differing starting-points (e.g. climate data) caused major differences between estimate and wind tunnel result and hampered comparison. After correction for these starting points, it was found that it is feasible to reduce differences (estimate vs. wind tunnel) in wind climate to a level which corresponds to about 10% difference in γ.

Finally, chapter 7 presents rules of thumb for design. For a number of human activities and surrounding terrain types, maximum street lengths and maximum building heights are given. They will allow the architect to choose building and street dimensions with the desired degree of comfort. They may also serve as a first check for whether a design yields an acceptable wind climate.

SAMENVATTING

Windhinder moet worden aangepakt in een vroeg stadium van ontwerp, wanneer de belangrijkste ontwerpbeslissingen worden genomen. De huidige praktijk, met uitsluitend windtunnelproeven aan het eind van het ontwerpproces, laat dit niet toe. Vuistregels voor ontwerp bestaan, maar ze zijn niet geschikt om te beoordelen of het windklimaat wel of niet acceptabel zal worden. Het doel van het huidige onderzoek is het analyseren en aanvullen van de huidige kennis van het voorspellen van windhinder, en om de resultaten aan architecten te presenteren in de vorm van verbale of grafische ontwerpregels. Deze ontwerpregels moeten bruikbaar zijn vanaf de eerste stadia van ontwerp, en ze moeten een vroege beoordeling van het windklimaat mogelijk maken.

Hoofdstuk 1 gaat in op het buitenklimaat, en de integratie daarvan in het ontwerpproces. De huidige kennis van (het voorspellen van) windhinder wordt samengevat, en het doel van het huidige onderzoek wordt omschreven.

Hoofdstuk 2 geeft theorieën uit de grenslaagmeteorologie, en gebouw-aërodynamica, de gebieden die het meest gebruikt zijn in dit onderzoek. Ook worden meettechnieken en methoden voor numerieke simulatie besproken. Door validatie van numerieke simulaties werd duidelijk met welke nauwkeurigheid en beperkingen we hadden te maken, zowel in de berekeningen (relatieve fout binnen 10-20%) als in de meettechnieken (fig. 2.11 en 2.13).

In hoofdstuk 3 wordt nader ingegaan op het begrip windhinder. Het bepalen van thermisch comfort buiten blijkt niet mogelijk te zijn (conclusie 3.1 op pag. 193). Daarom zijn alleen de mechanische effecten van wind, en hun effecten op comfort, in beschouwing genomen. Paragraaf 3.3 gaat in op de relatie tussen de kans op hinder (en gevaar) door wind enerzijds, en beschutting en klimaat anderzijds (fig. 3.5-3.6). Beide kansen zijn nogal gevoelig voor de windfactor (of windversterkingsfactor) γ, waarbij γ de verhouding tussen de locale uurgemiddelde windsnelheid en de windsnelheid op 10 m hoogte boven een grote grasvlakte is. Een toename van 10% in γ (voor alle windrichtingen) leidt tot een factor 1.4 toename in de windhinderkans, en een factor 2 toename in de kans op gevaar. In paragraaf 3.4 tenslotte wordt een overzicht gegeven van bestaande windhindercriteria (drempelwaarde bestaande uit een gemiddelde of vlaagsnelheid, en een maximale overschrijdingskans daarvan). De criteria worden vergeleken met behulp van het begrip "vereiste beschutting" (tabel 3.8). Uiteindelijk is een aantal "goede" criteria geselecteerd.

Het windklimaat op de beschouwde locatie is in de eerste plaats afhankelijk van de windfactor γ, die wordt bepaald door bijdragen op drie schaalnivo's (fig. 4.30):
- -de omgeving; terreintype
- -gebouw en gebouwgroep
- -kenmerken (details) van de locatie

Elk schaalnivo levert een belangrijke bijdrage tot γ. Hoofdstuk 4 gaat op deze bijdragen in detail in.

De relatieve fout in γ ten gevolge van numerieke modellering is maximaal 10-20%. Koppeling van locale windsnelheden aan windsnelheden op een weerstation kan nog eens ruim 20% fout veroorzaken (conclusie 4.8, pag. 196). Laatstgenoemde fout heeft ook effect op routinematige voorspellingen van windhinder met behulp van een windtunnel.

De turbulentie-nivo's kunnen goed geschat worden door de locale standaard-deviatie σ_u gelijk te stellen aan de waarde op het weerstation. De standaard relatieve fout in deze schatting is minder dan 30%.

De gegevens van hoofdstuk kunnen worden samengevat met een gecombineerde classificatie van gebouw en terrein. Het windklimaat kan meestal niet beoordeeld worden door uitsluitend de windfactor γ te beschouwen. Hoofdstuk 5 geeft verdelingen van de windhinderkans rond gebouwen. Dit leidt tot een verbeterde classificatie van gebouw en terrein (fig. 5.12), die gebruikt kan worden voor de meest winderige locaties in straten, of bij hoge gebouwen. Ruimtelijke verdelingen van de windhinderkans blijken vaak moeilijk te modelleren.

Hoofdstuk 6 geeft een praktijkvoorbeeld van de vroege beoordeling van windhinder. De eerste paragraaf gaat in op de ontwikkeling van een stedebouwkundig plan voor een winderige locatie in Amsterdam, en op de samenwerking tussen architect en (windhinder-)adviseur. Deze samenwerking heeft tot een verbeterd windklimaat geleid. Optimale beschutting bleek niet haalbaar vanwege andere factoren, zoals verkeer, doorzicht (sociale controle), en de vereiste hoeveelheid woningen.

Het tweede deel van hoofdstuk 6 gaat in op de nauwkeurigheid van het advies. De bij het adviseren geschatte windhinderkansen zijn vergeleken met resultaten van een windtunneltest. Verschillende uitgangspunten (bijv. klimaatgegevens) zorgden voor aanzienlijke verschillen en bemoeilijkten de vergelijking. Na correctie voor de uitgangspunten bleek dat het mogelijk is verschillen tussen de vroege voorspelling en de windtunneltest terug te brengen tot een nivo dat overeenkomt met 10% verschil in γ.

Hoofdstuk 7 tenslotte, geeft vuistregels voor ontwerp. Voor een aantal menselijke activiteiten en terreintypes (van het omringende terrein) zijn maximale straatlengte en maximale gebouwhoogte gegeven. Hiermee kan de architect gebouw- en straatafmetingen kiezen met de gewenste hoeveelheid comfort. De vuistregels kunnen ook gebruikt worden als eerste controlemiddel, om na te gaan of het gewenste ontwerp in een acceptabel windklimaat zal resulteren.

LITERATURE

E. Arens, 1982, On considering pedestrian winds during building design, in: (Reinhold, 1982), p. 8-26

R.E. Akins, J.A. Peterka, J.E. Cermak, 1980, Averaged pressure coefficients over rectangular buildings, in: (Cermak, 1980), p. 369-380

W. Alberts, 1981, De faktor wind in het stedelijk klimaat (in Dutch), report 81/01416, Planologische Studiecentrum TNO, Delft, 100 pp.

R.M. Aynsley, W. Melbourne, B.J. Vickery, 1977, Architectural aerodynamics, Applied Science Publishers, LTD, London, 254 pp.

A. Baskaran, T. Stathopoulos, 1989, Computational evaluation of wind effects on buildings, Building and Environment 24-4, p. 325-333

W.J. Beranek, 1980, General rules for the determination of wind environment, in: (Cermak, 1980), p. 225-234

W.J. Beranek, 1982, Beperken van windhinder om gebouwen (in Dutch), Stichting Bouwresearch, Kluwer Technische Boeken BV, Deventer, 148 pp.

W.J. Beranek, 1984a, Wind environment around single buildings of rectangular shape, Heron 29-1, p. 3-31

W.J. Beranek, 1984b, Wind environment around building configurations, Heron 29-1, p. 33-70

M. Bottema, 1990, Wind flow around buildings; experimental results, Eindhoven University of Technology, FAGO-report 90.16.K

M. Bottema, J.A. Leene, J.A. Wisse, 1991a, Towards forecasting of wind comfort, Eindhoven University of Technology, FAGO-report 91.17.K; to be publ. in Proc. 8th Int. Conf. on Wind Engineering, London, Ontarion, Canada.

M. Bottema, J.G.M. Eggels, J.A. Wisse, 1991b, Numerical simulation of wind in a built-up environment and experimental verification, J. of Wind. Engng. and Ind. Aerodyn. 38, p. 141-149

M. Bottema, 1992, Windhinder op het Java-eiland (in Dutch), Eindhoven Univeristy of Technology, FAGO-Report 92.01.K

A. Bowen, 1977, A wind-tunnel investigation of the wind speed and turbulence chracteristics close to the ground over various escarpment shapes, Boundary-Layer Meteorology 12, p. 259-277

R.E. Britter, J.C.R. Hunt, 1979, Velocity measurements and order of magnitude estimates of the flow between two buildings in a simulated atmospheric boundary layer, J. of Ind. Aerodyn. 4, p. 165-182

P. Builtjes, P. Vermeulen, 1980, Atmospheric boundary layer simulation in the "PIA" and "MIA" windtunnel of TNO-Apeldoorn, Report 80-0290, IMET-TNO, Apeldoorn, NL.

P. Carpenter, 1990, Wind speeds in city streets - full scale measurements and comparison with wind tunnel tests, in: (Sun, 1989) p. 845-852

I.P. Castro, 1980, The relaxation and steadiness of wakes behind obstacles in boundary layers, in: (Cermak, 1980), p. 299-307

J.E. Cermak (ed.), 1980, Wind Engineering (Proc. 5th Int. Conf. on Wind Engineering), Fort Collins, Colorado, 1400 pp.

J.M. Cimbala, W.J. Park, 1989, Elimination of temperature stratification in a low-speed open-return wind tunnel, AIAA Journal 27-6, p. 823-825

R.H. Clarke, G.D. Hess, 1974, Geostrophic departure and the functions A and B of Rossby-number similarity theory, Boundary-Layer Meteorology 7, p. 267-287

M. Claussen, 1989, Neutral surface-layer flow over isolated roughness strips, Boundary-Layer Meteorol. 48 (1989), p. 431-442

N.J. Cook, 1982, Simulation techniques for short test-section wind tunnels: Roughness, barrier and mixing device method, in: (T.A. Reinhold, 1982), p. 126-136

N.J. Cook, 1990, The designers guide to wind loading, part 2: Static structures, Butterworths, 585 p.

Creare.x, 1990, FLUENT Version 3.0 Users Manual, Hanover, New Hampshire

F.T. DePaul, C.M. Sheih, 1986, Measurements of wind velocity in a street canyon, Atm. Env. 20-3, p. 455-459

H.W. Detering, D. Etling, 1985, Application of the E-ϵ turbulence model to the atmospheric boundary layer, Boundary-Layer Meteorol. 33, p. 113-113

F.H. Durgin, 1991, Pedestrian level wind studies at the Wright Brothers Facility, Proc. 8th Int. Conf. on Wind Engineering, London, Ontario, Canada.

P.O. Fanger, 1972, Thermal comfort, Danish Technical press, Copenhagen, 245 p.

P.O. Fanger, A.K. Melikov, H. Hanzawa, J. Ring, 1988, Air turbulence and sensation of draught, Energy and Buildings 12-1, p. 21-39

J.L. Ferziger, 1990, Approaches to turbulent flow computation: Applications to flow over obstacles, J. of Wind Engng. and Ind. Aerodyn. 35, p. 1-19

J. Gandemer, 1975, Wind environment around buildings: aerodynamic concepts, Proc. 4th Int. Conf. on Buildings and Structures, Heathrow, UK, p. 423-432

J. Gandemer, 1978, Aerodynamic studies of built-up areas made by C.S.T.B. at Nantes, France, J. of Ind. Aerodyn. 3, p. 227-240

J. Gandemer, 1981, La protection contre le vent, Centre Scientifique et Technique du Batiment, Paris, 132 pp.

J.R. Garratt, 1990, The internal boundary layer - a review, Boundary-Layer Meteorology 50, 171-202

M. Glaumann, U. Westerberg, 1988, Klimatplanering vind (in Swedish), Svensk Byggtjanst, Stockholm, 158 pp.

A.M. Goliger, J.L. Waldeck, R.V. Milford, 1991, A topographical study to investigate wind nuisance, preprints 8th Int. Conf. on Wind Engineering, London, Ontario, Canada, paper 9-2

G. Gross, 1987, A numerical study of the air flow within and around a single tree, Boundary-Layer Meteorology 40, p. 311-327

C. van der Harst, 1990, Windklimaatonderzoek in de windtunnel aan een maquette van het projekt KNSM-eiland te Amsterdam (in Dutch), Report 90-073, IMET-TNO, Apeldoorn, NL.

C. van der Harst, 1992, Windklimaatonderzoek in de windtunnel aan een maquette van het projekt Java-eiland te Amsterdam (in Dutch), Report 92-172, IMET-TNO, Apeldoorn, NL.

D.A. Haugen (ed.), 1972, Workshop on Micrometeorology, American Meteorological Society, 390 pp.

N.C. Helliwell, 1971, Wind over London, Proc. 3rd Int. Conf. on Buildings and Structures, Tokyo, p. 22-32

A. Holtslag, 1987, Surface fluxes and boundary layer scaling, PhD Thesis, Agricultural University Wageningen, NL; also available as Scientific Report WR-87-2, KNMI, De Bilt, 173 pp.

R.P. Hosker, 1985, Flow around isolated structures and building clusters; a review, ASHRAE Transactions 91, 2B, p. 1672-1692

R. Hoxey, A.P. Robertson, P.J. Richards, 1989, Full-scale, model-scale and computational comparison of wind loads on the Silsoe structures building, in: (Sun, 1989), p. 477-484

205

J.C.R. Hunt, E.C. Poulton, 1972, Some effects of wind on people, Proc. Symp. on external flows, Bristol, p. k1-k9

J.C.R. Hunt, 1975, Turbulent velocities near and pressure fluctuations on structures in turbulent winds, Proc. 4th Int. Conf. on Buildings and Structures, Heathrow, UK, p. 309-320

J.C.R. Hunt, E.C. Poulton, J.C. Mumford, 1976, The effects of wind on people; New criteria based on wind tunnel experiments, Building and Environment 11, p. 15-28

J.C.R. Hunt, J.E. Simpson, Atmospheric boundary layers over non-homogeneous terrain, in: (Plate, 1982b), p. 269-318

M. Hussain, 1978, A study of the wind forces on low rise buildings and their application to natural ventilation methods, PhD Thesis, Dept. of Build. Sc. Univ. of Sheffield, 325 pp.

D. Hutchinson, 1978, Wind - a planners view, Journal of industrial aerodynamics 3, p. 117-127

K. Häggkvist, R. Taesler, 1987, Wind pressure distributions around single family houses (in Swedish), Byggforskningsrådet, Stockholm, Rapport R7:1987, 30 pp.

R. McIlveen, 1992, Fundamentals of weather and climate, Chapman and Hall, London, 500 pp.

N. Isyumov and A.G. Davenport, 1975, The ground level wind environment in built-up areas, Proc. 4th Int. Conf. on Build. and Struct., Heathrow, p. 403-422

P.S. Jackson, 1978, The evaluation of windy environments, Building and environment 13, p. 251-260

A.F.G. Jacobs, 1983, Flow around a line obstacle, PhD Thesis, Agricultural Univ. Wageningen, NL, 104 pp.

N. Jamieson, 1991, The effect of architectural detailing on pedestrian level wind speeds, to be publ. in Proc. 8th Int. Conf. on Wind Engineering, London, Ontarion, Canada.

N.O. Jensen, 1978, Change of roughness and the planetary boundary layer, Quart. J. R. Met. Soc. 104, p. 351-356

N.O. Jensen, N.E. Busch, 1982, Atmospheric Turbulence, in: (Plate, 1982b), p. 179-232

N.O. Jensen, E.L. Petersen, I. Troen, 1984, Extrapolation of mean wind statistics with special regard to wind energy applications, WMO World Climate Applications Programme TD-No. 15, 85 pp.

A.T. Kenworthy, 1985, Wind as a influential factor in the orientation of the orthogonal street grid, Building and Environment 20-1, p. 33-38

W. Kollmann, 1980, Prediction methods for turbulent flows, Hemisphere Publ. Corp. London, 465 pp.

Kondo, 1975, Air-sea bulk transfer coefficients in diabatic conditions, Boundary-Layer Meterol. 9, p. 91-112

A. Laneville, I.S. Gartshore, G.V. Parkinson, 1975, An explanation of some effects of turbulence on bluff bodies, Proc. 4th Int. Conf. on Wind Effects on Build. and Struct., Heathrow, p. 333-341

B.E. Launder, D.B. Spalding, 1974, The numerical computation of turbulent flows, Computer mothods in applied mechanics and engineering 3, p. 269-289

T.V. Lawson, A.D. Penwarden, 1975, The effects of wind on people in the vicinity of buildings, Proc. 4th Int. Conf. on Buildings and Structures, Heathrow, UK, p. 605-622

T.V. Lawson, 1978, The wind content of the built environment, J. of Ind. Aerodyn. 3, p. 93-105

T.V. Lawson, 1980, Wind effects on buildings, Applied Science Publ. London, 318 pp.

J.A. Leene, D. Delaunay, A.G. Jensen, 1990, Handbook on obstacle wake effects related to wind turbine siting, Report 90-117, IMET-TNO, Apeldoorn, NL

J.A. Leene, 1991, Building wake effects in complex situations, to be publ. in Proc. 8th Int. Conf. on Wind Engineering, London, Ontarion, Canada.

D.R. Lemelin, D. Surry, A.G. Davenport, 1988, Simple approximations for wind speed-up over hills, J. of Wind Engng. and Ind. Aerodyn. 28, p. 117-127

F. Livesey, D. Inculet, N. Isyumov, A.G. Davenport, 1990, A scour technique for the evaluation of pedestrian winds, J. of Wind Engng. and Ind. Aerodyn. 36, p. 779-789

C.G. Logan, 1986, Fundamentals of hot wire anemometry, Cambridge Univ. Press, New York, 150 pp.

S. Majumdar, W. Rodi, 1989, Three-dimensional computation of flow past cylindrical structures and model cooling towers, Building and Environment 24-1, p. 3-22

207

E. Maruta, 1984, The study of high wind regions around tall buildings (in Japanese; translation available at BRE, Watford, UK), PhD Thesis, Nihon University, Tokyo, 200 pp.

W.H. Melbourne, P.N. Joubert, 1971, Problems of wind flow at the base of tall buildings, Proc. 3rd Int. Conf. on Build. and Struct., Tokyo, p. 105-114

W.H. Melbourne, 1978, Criteria for environmental wind conditions, J. of Ind. Aerodyn. 3, 241-249

R.N. Meroney, 1980, Wind-tunnel modeling of the flow about bluff bodies, Proc. 4th Coll. on Ind. Aerodyn., Aachen, Germany, p. 61-80

Mulhearn, 1978, A wind-tunnel boundary-layer study of the effects of a surface roughness change: rough to smooth, Boundary-Layer Meteorol. 15, p. 3-30

S. Murakami, K. Uehara, K. Deguchi, 1980, Wind effects on pedestrians: New criteria based on outdoor observation of over 2000 persons, in: (Cermak, 1980), p. 277-288

S. Murakami, 1982, Wind tunnel modelling applied to pedestrian comfort, in: Reinhold, 1982), p. 486-503

S. Murakami, K. Fujii, 1983, Turbulence characteristics of wind flow at ground level in built-up area, J. Wind Engng. Ind. Aerodyn. 15 p. 133-144

S. Murakami, Y. Iwasa, Y. Morikawa, 1986, Study on acceptable criteria for assessing wind environment on ground level based on residents' diaries, J. of Wind Engng. and Ind. Aerodyn. 24, p. 1-18

S. Murakami, A. Mochida, 1988, 3-D Numerical simulation of airflow around a cubic model by means of the K-ε model, J. of Wind Engng. and Ind. Aerodyn. 31, p. 283-303

S. Murakami, 1990a, Numerical simulation of turbulent flowfield around cubic model; Current status and applications of K-ε model and LES, J. of Wind Engng. and Ind. Aerodyn. 33, p. 139-152

S. Murakami, A. Mochida, Y. Hayashi, 1990b, Examining the K-ε model by means of a wind tunnel test and large-eddy simulation of the turbulence structure around a cube, J. of Wind Engng. and Ind. Aerodyn. 35, p. 87-100

Y. Nakamura, T.R. Oke, 1988, Wind, temperature and stability conditions in an East-West oriented street canyon, Atm. Env. 22-12, p. 2691-2700

T.R. Oke, 1987, Boundary Layer Climates, Methuen and co, London, UK, 372 p.

T.R. Oke, 1988, Street design and urban canopy layer climate, Energy and building 11, p. 103-111

H.A. Panofsky, 1972, Tower micrometeorology, in (Haugen, 1972), p. 151-176

H.A. Panofsky, J.A. Dutton, 1984, Atmospheric turbulence, John Wiley and sons, New, York, 397 p.

S.V. Patankar, 1980, Numerical heat transfer and fluid flow, Hemisphere Publ. Corp., 198 pp.

D.A. Paterson, 1986, Computation of wind flows over three-dimensional buildings, PhD Thesis, Dept. Civil Engineering, Univ. of Queensland, 295 pp.

D.A. Paterson, C.J. Apelt, 1989, Simulation of wind flow around three-dimensional buildings, Building and Environment 24-1, p. 39-50

A.D. Penwarden, 1973, Acceptable wind speeds in towns, Build. Sci. 8, p. 259-267

A.D. Penwarden, P.F. Grigg, R. Rayment, 1978, Measurements of wind drag on people standing in a wind tunnel, Building and environment 13, p. 75-84

M.D.A.E.S. Perera, 1980, Shelter behind two-dimensional solid and porous fences, Proc. 4th Coll. on Ind. Aerodyn. Aachen, Germany, p. 255-273

J.A. Peterka, J.E. Cermak, 1975, Turbulence in building wakes, Proc. 4th Int. Conf. on Buildings and Structures, Heathrow, UK, p. 447-463

J.A. Peterka, R.N. Meroney, K.M. Kothari, 1985, Wind flow patterns about buildings, J. Wind. Engng. Ind. Aerodyn. 21, p. 21-38

E.L. Petersen, I. Troen, J. Wieringa, 1984, Development of a method for wind climate analysis for non-mountainous terrain in Europe, Proc. Europ. Wind Energy Conf., Hamburg, p. 6-12

E.J. Plate, 1982a, Wind tunnel modelling of wind effects in engineering, in: (Plate, 1982b), p. 573-640

E.J. Plate (ed.), 1982b, Engineering meteorlogy, Elsevier Sc. Publ. Comp., Amsterdam, NL, 740 pp.

J.K. Raine, D.C. Stevenson, 1977, Wind protection by model fences in a simulated atmospheric boundary layer, J. of Wind Engng. and Ind. Aerodyn. 2, p. 159-180

M.A. Ratcliff, J.A. Peterka, 1990, Comparison of pedestrian wind acceptability criteria, J. of Wind. Engng. and Ind. Aerodyn. 36, p. 791-800

D.A. Reed, 1990, Expert systems in wind engineering, J. of Wind Engng. and Ind. Aerodyn. 33, p. 487-494

T.A. Reinhold (ed.), 1982, Wind tunnel modelling for civil engineering applications, Cambridge Univ. press, New York, 688 pp.

W. Rodi, 1980, Turbulence models for environmental flows, in: (Kollmann, 1980), p. 259-350

E. Simiu, R.H. Scanlan, 1986, Wind effects on structures, John Wiley and sons, New York, 590 p.

T.F. Sun (ed.), 1989, Recent advances in wind engineering (proc. 2nd Asia-Pacific Symp. on Wind Engineering), Pergamon Press, 1200 pp.

T. Stathopoulos, 1985, Wind environmental conditions around tall buildings with chamfered corners, J. Wind Engng. and Ind. Aerodyn. 21 (1985), p. 71-87

T. Stathopoulos, R. Storms, 1986, Wind environmental conditions in passages between buildings, J. Wind. Engng. and Ind. Aerodyn. 24, p. 19-31

T. Stathopoulos, H. Wu, C. Bédard, 1991, Wind environment around buildings: A knowledge-based approach, to be publ. in Proc. 8th Int. Conf. on Wind Engineering, London, Ontario, Canada

H. Tennekes, 1972, Similarity laws and scale relations in planetary boundary layers, in (Haugen, 1972), p. 177-216

H. Tennekes and J.L. Lumley, 1972, A first course in turbulence, MIT Press Cambridge, Mass., 300 pp.

I. Troen, E.L. Petersen, 1989, European Wind Atlas, Risø National Laboratory, Denmark, 656 pp.

N.K. Tutu, R. Chevray, 1975, Cross-wire anemometry in high intensity turbulence, J. Fluid Mech. 71-4, p. 785-800

Y. Uematsu, M. Yamada, H. Higashiyama, T. Orimo, 1991, Effects of the corner shape of high-rise buildings on the pedestrian-level wind environment with consideration for mean and fluctuating wind speeds, preprints 8th Int. Conf. on Wind Engineering, London, Ontario, Canada, paper 15-12

R. Uytenhaak, 1991, Studieopdracht Java eiland (in Dutch), Architektenbureau Ir. Rudy Uytenhaak, Amsterdam

P. Vermeulen, P. Hooftman, 1980, Methode ter bepaling van het verband tussen de windsnelheid bij een weerstation en de locale windsnelheden zoals gemeten bij een maquette in de windtunnel (in Dutch), Report 80-02760, IMET-TNO, Apeldoorn, NL.

Vermeulen, 1986a, Experimenteel onderzoek ten behoeve van de modelbeschrijving van driedimensional ruwheidsovergangen (in Dutch), Report 86-201, IMET-TNO, Apeldoorn, NL

Vermeulen, 1986b, Windkaart Den Haag (in Dutch), Report 86-330, IMET-TNO, Apeldoorn, NL

G. Th. Visser, 1980, Windhindercriteria: Een literatuuronderzoek naar en voorstellen voor het hanteren van uniforme TNO-windhindercriteria (in Dutch), Report 80-02746, IMET-TNO, Apeldoorn, NL

G. Th. Visser, 1987, Onderzoek naar de bruikbaarheid van het "Winstek" rapport voor de voorspelling van het windklimaat in de openbare ruimte (in Dutch), Report 87-180, IMET-TNO, Apeldoorn, NL

U. Westerberg, M. Glaumann, 1990, Design criteria for solar access amd wind shelter in the outdoor environment, Energy and Buildings 15, p. 425-431

J. Wieringa, 1991, Updating the Davenport roughness classification, to be publ. in Proc. 8th Int. Conf. on Wind Engineering, London, Ontario, Canada

J. Wieringa, 1992, Representative roughness parameters for homogeneous terrain, submitted to Boundary-Layer Meteorology

A.J.M. van Wijk, A.C.M. Beljaars, A.A.M. Holtslag, W.C. Turkenburg, 1990, Diabatic wind speed profiles in coastal regions: Comparison of an internal boundary layer (IBL) model with observations, Boundary-Layer Meteorology 51, p. 49-75

C.J. Williams, M.J. Soligo, 1991, A discussion of the components for a comprehensive pedestrian level comfort criteria, Proc. 8th Int. Conf. on Wind Engineering, London, Ontario, Canada.

D.J. Wilson, 1989, Airflow around buildings, ASHRAE Handbook of fundamentals, p. 14.1-14.18

J.A. Wisse, 1988, A philosophy for teaching wind in the built environment, Energy and Buildings 11, p. 157-161

J.A. Wisse, M. Bottema, 1991, Urban geometry and wind, Proc. Symp. on planning aplications of urban and building climatology, Berlin. Also available at Eindhoven University of Technology (NL) as FAGO-Report 91.40.K

D.H. Wood, 1982, Internal boundary-layer growth following a step change in surface roughness, Boundary-Layer Meteorol. 22, p. 241-244

Stellingen

1. Windhinder behoort aandacht te krijgen in een vroeg stadium van ontwerp, voordat de belangrijkste ontwerpbeslissingen zijn genomen.
(Dit proefschrift, hoofdstuk 1)

2. Hoge gebouwen vangen veel wind

3. Straten die korter zijn dan 8 gebouwhoogtes zullen zelden aanleiding geven tot windhinder.
(Dit proefschrift, hoofdstuk 7)

4. Openingen onder een hoog gebouw geven vaak aanleiding tot een zodanig slecht windklimaat, dat het doorzicht door de opening zelden door mensen belemmerd wordt.

5. Een windhinder-expert-systeem is alleen bruikbaar voor niet-specialisten, als het expert systeem (en niet de gebruiker) voorziet in gegevens met betrekking tot:
-terreinruwheid in de regio
-bebouwing in de directe omgeving van de gewenste locatie.

6. Het percentage van de tijd met hinder of schade door luchtverontreiniging in de gebouwde omgeving, is vaak een stuk moeilijker te bepalen dan het percentage van de tijd met windhinder.

7. De zegswijze "meten is weten" gaat alleen op als de beperkingen van de meetmethode bekend en onderkend zijn.

8. In de zomer is voldoende beschaduwing even belangrijk als voldoende bezonning.

9. Democratie gaat niet samen met de filosofie "ieder voor zich, God voor ons allen".

10. Het gebruik van een aantal natuurkundige begrippen in de psychologie betekent niet dat psychologie altijd op een natuurkundige manier moet worden aangepakt.

11. Artikel 17.3 van het promotiereglement van de Technische Universiteit Eindhoven stimuleert de promovendus niet tot het maken van eigen, originele stellingen.
Artikel 17.3 van het TUE promotiereglement 1990: "De stellingen zijn zo mogelijk voorzien van literatuurverwijzingen of bronvermelding".